Understanding how targeting zinc transporters prevents the development of aggressive cancer

A thesis submitted in accordance with the conditions governing candidates for the degree of:

Philosophiae Doctor in Cardiff University

by

Silvia Ziliotto

December 2018

Breast Cancer Molecular Pharmacology Group
Cardiff School of Pharmacy and Pharmaceutical Sciences
Cardiff University
Cardiff, Wales

Statements and declaration

STATEMENT 1

This thesis is being submitted in partial fulfilment of the requirements for the degree of PhD.

Signed ..... Silvia Liletto ..... Date ..... 17/12/2018 .....

STATEMENT 2

This work has not been submitted in substance for any other degree or award at this or any other university or place of learning, nor is it being submitted concurrently for any other degree or award (outside of any formal collaboration agreement between the University and a partner organisation).

Signed ..... Silvia Liletto ..... Date ..... 17/12/2018 .....

STATEMENT 3

I hereby give consent for my thesis, if accepted, to be available in the University's Open Access repository (or, where approved, to be available in the University's library and for inter-library loan), and for the title and summary to be made available to outside organisations, subject to the expiry of a University-approved bar on access if applicable.

Signed ..... Silvia Liletto ..... Date ..... 17/12/2018 .....

DECLARATION

This thesis is the result of my own independent work, except where otherwise stated, and the views expressed are my own. Other sources are acknowledged by explicit references. The thesis has not been edited by a third party beyond what is permitted by Cardiff University's Use of Third Party Editors by Research Degree Students Procedure.

Signed ..... Silvia Liletto ..... Date ..... 17/12/2018 .....

WORD COUNT 58,836

(Excluding summary, acknowledgments, declarations, contents pages, appendices, tables, diagrams and figures, references, bibliography, footnotes and endnotes)

Summary

Zinc is one of the most abundant trace elements in the human body. Cellular zinc homeostasis is primarily controlled by zinc transporters, including the ZIP family of zinc importers. Since zinc homeostasis needs to be tightly controlled, dysregulation of these zinc transporters is associated with multiple diseases including cancer. ZIP7, a zinc transporter residing on the endoplasmic reticulum membrane, was discovered to be involved in driving endocrine resistant breast cancer. Findings within this project support the hypothesis that tamoxifen-resistant breast cancer cells are driven by the increased activation of ZIP7 which, together with ZIP6, drives the invasive behaviour of this more aggressive breast cancer phenotype. This study confirmed the suitability of activated ZIP7 as a good biomarker of acquired resistance to anti-hormone treatment in breast cancer, a current clinical unmet need.

Zinc is also important in cell cycle progression and, in particular, is essential for progression of cells through the G2 phase and mitosis. Our group have discovered that ZIP6 forms a heteromer with ZIP10 on the plasma membrane which influxes zinc into cells to trigger mitosis. This study demonstrated that treatment of different cancer cell lines with specific N-terminal ZIP6 or ZIP10 antibodies was able to inhibit mitosis by preventing the zinc influx necessary at this stage of the cell cycle. These agents were also shown to be effective at reducing the growth of different cancer cell lines. Using a model of ZIP6 CRISPR/Cas9 knockout cells it was discovered that ZIP6 downregulation induces upregulation of ZIP10, as a compensatory mechanism to counteract the lack of ZIP6. This study revealed novel targets for proliferative diseases such as cancer, which is manifested by uncontrolled growth. Additionally, this project brought new insight into the regulation of ZIP6 and discovered the potential for CK2 phosphorylation as well as proteolytic cleavage for proper function.

Publications and presentations

Journal articles

- Nimmanon T*, **Ziliotto S***, Morris S, Flanagan L, Taylor KM. Phosphorylation of zinc channel ZIP7 drives MAPK, PI3K and mTOR growth and proliferation signalling. *Metallomics*. 2017; **9**(5):471-481. *(*: equally contributed as first authors*).
- Taylor KM, Muraina I, Brethour D, Schmitt-Ulms G, Nimmanon T, **Ziliotto S**, Kille P, Hogstrand C. Zinc transporter ZIP10 forms a heteromer with ZIP6 which regulates embryonic development and cell migration. *Biochem J*. 2016;**10**:2531–44.
- **Ziliotto S**, Gee JMW, Taylor KM. Activated zinc transporter ZIP7 as an indicator of anti-hormone resistance in breast cancer. (*Manuscript in preparation*).
- Nimmanon T, Burt A, **Ziliotto S**, Gee JMW, Andrews GP, Ogle O, Kille P, Hogstrand C, Maret W, Taylor KM. Inhibition of zinc importer ZIP6/ZIP10 heteromer prevents mitosis confirming zinc influx as a prerequisite to trigger mitosis. *(Manuscript in preparation*).

Book chapters

- **Ziliotto S**, Ogle O, Taylor KM. Targeting Zinc(II) Signalling to Prevent Cancer. Metal Ions in Life Sciences. 2018 Feb 5,18.

Oral presentations

- Postgraduate Research Day, Cardiff School of Pharmacy and Pharmaceutical Sciences, Cardiff (UK), March 2018. “Understanding how targeting zinc signalling prevents cell division in cancer”. Winner of the prize for the talk presentation.
- Zinc-UK/Zinc-Net Meeting, Belfast (UK), November 2016. “Phosphorylated ZIP7 as a biomarker for anti-hormone resistant breast cancer”.

Poster presentations

- UK Interdisciplinary Breast Cancer Symposium, Manchester (UK), January 2018. “ZIP7-mediated zinc signalling drives anti-hormone resistance in breast cancer”.

- ISZB/Zinc-Net Meeting, Pyla (Cyprus), June 2017. “Understanding how targeting zinc signalling prevents cell division in cancer”. Winner of the prize for the poster presentation.
- Postgraduate Research Day, Cardiff School of Pharmacy and Pharmaceutical Sciences, Cardiff (UK), April 2017. “Understanding how targeting zinc signalling prevents cell division in cancer”.
- Zinc-UK/Zinc-Net Meeting, Belfast (UK), November 2016. “Phosphorylated ZIP7 as a biomarker for anti-hormone resistant breast cancer”. Winner of the 1st prize for the poster presentation.
- Zinc-UK/Zinc-Net Meeting, London (UK), December 2015. “Phosphorylated zinc channel ZIP7 as a biomarker for anti-hormone resistant breast cancer”.

Acknowledgments

I would like to express my deepest gratitude to Dr Kathryn Taylor for being such an insightful guide throughout my PhD. I would also like to thank my second supervisor Dr Julia Gee for her support throughout the project, in particular for her help with the immunohistochemistry data. In this regard, I would like to thank Ian Ellis and Andrew Green of Nottingham City Hospital for providing the clinical breast samples used in this project and Anna Gobbato for the preparation of the slides. Thanks to Thirayost Nimmanon for his contribution to various domains, especially at the beginning of my PhD. I am very thankful to Tenovus Cancer Care for funding this project. I have been so grateful to participate in many public engagements for Tenovus because it is so important to share science with the people the science is directed to.

A big thank you goes to all the members of the Breast Cancer Molecular Pharmacology Group for their support and help. In particular, thanks to Olivia, my favourite zinc colleague and friend. Since she started her PhD in my group, she brought a ray of sunshine to my Cardiff life. Thanks to Mike and Sam for all the fun in the lab and for the great friendship that we have. Thanks to Sara for being such a lovely colleague to be around. Thanks to all the amazing friends I made in Redwood Building and thanks to all the crazy Redwood parties that have made my PhD much more fun too. In particular, I would like to mention: Birgit, Mike, Matt, Sean and Helen. Without them I would have never enjoyed my PhD as much as I did.

Thanks to all of the other friends I met in Cardiff. Thanks to Laura who has been sharing with me basically all of my Cardiff experience, since that day we first met each other outside that house in Colum Road during our Erasmus. Her friendship was invaluable for me, especially during the toughest times of my PhD. Thanks to Chantelle, my lovely housemate for the strong friendship we built. Thanks to John for being such a good friend to me. It would be impossible to mention all of the amazing people I met throughout these 3 years, but they all know how much they mean to me. I would also like to thank all my friends back in Italy for their support and for all the funny moments we shared when they came to visit me in Cardiff during my PhD. Last, but not least, I would like to thank my family for having my back at all times and for being so proud of me. Living abroad had its ups and down, and this experience would have never been possible without knowing that I will always have them to support me.

Table of Contents

List of figures

List of tables

Abbreviations

Ab: antibody

ADC: antibody drug conjugate

ATM/ATR: ataxia telangiectasia and Rad3-related protein kinases

AKT: protein Kinase B

BSA: bovine Serum Albumin

CDK: cyclin-dependant kinase

CK2: casein kinase II

CON: control

CRISPR: clustered regularly interspaced short palindromic repeats

DAPI: 4,6-diamino-2-phenylindol

DAPK: death-associated protein kinase

DMPK: myotonin-protein kinase

DNAPK: DNA-dependent protein kinase

DTT: dithiothreitol

ECL: enhanced chemiluminescence

EGF: epidermal growth factor

EGFR: epidermal growth factor receptor

EGTA: ethylene glycol tetraacetic acid

EDTA: ethylenediaminotetraacetic acid

EMT: epithelial-mesenchymal transition

ER: oestrogen receptor

ER+: oestrogen receptor positive

ER-: oestrogen receptor negative

ERK 1/2: extracellular signal-regulated kinases

FAK: focal adhesion kinase

FasR: Faslodex® resistant MCF-7 derived cell line

FasRL: Faslodex®-resistant long-term MCF-7 derived cell line

FBS: foetal bovine serum

GRK: G protein-coupled receptor kinase

GSK3β: glycogen synthase kinase 3 beta

HER2: human epidermal growth factor receptor 2

HER2+: human epidermal growth factor receptor 2 positive

HER2-: human epidermal growth factor receptor 2 negative

HRP: horseradish peroxidase

IF: immunofluorescence

IGFR: insulin-like growth factor receptor

INSR: insulin receptor kinase

IP3R: inositol 1,4,5-Trisphosphate receptor

JNK1: c-Jun N-terminal kinase

Ko: knockout cells

MAPK: mitogen-activated protein kinase

MCF-7: human breast adenocarcinoma cell line

MEK1: meiosis-specific serine/threonine-protein kinase

mTOR: mammalian target of rapamycin

MTT: 3-(4,5-dimethylthiazol-2-yl)-2-5-diphenyltetrazolium bromide

NCAM1: neural cell adhesion molecule

NOC: nocodazole treated cells

PAK: p21-activated kinases

pAKT: phospho-S^{473}AKT

PBS: phosphate buffered saline

PDHK: pyruvate dehydrogenase kinase

PI3K: phosphoinositide 3-kinase

PIM1: proto-oncogene serine/tyrosine protein kinase

PKC: protein kinase C

PLA: proximity ligation assay

PLK1: polo-like kinase 1

PR: progesterone receptor

PrP^c: cellular prion protein

pZIP7: phosphoS^{275}-phosphoS^{276}ZIP7

pS^{10}Histone H3: phospho-Histone H3 (S^{10})

rpm: revolutions per minute

S: serine residue

SDS-PAGE: sodium dodecylsulfate polyacrylamide gel electrophoresis

SERM: selective estrogen-receptor modulator

Src: proto-oncogene tyrosine-protein kinase Src

STAT3: signal transducer and activator of transcription 3

pTyr^{705}STAT3: phospho-STAT3 (Y705)

pSer^{727}STAT3: phospho-STAT3 (S727)

T: threonine residue

TAMR: tamoxifen-resistant MCF-7 derived cell line

TAMRL: tamoxifen- resistant long-term MCF-7 derived cell line

TBS: tris-buffered saline

TGFB1: transforming growth factor beta 1

TM: transmembrane domain

Wt: wild type

Y: tyrosine residue

ZIP: Zrt-/Irt-like protein (SLC39A)

ZnT: zinc Transporter (SLC30A)

1 GENERAL INTRODUCTION

1.1 The role of zinc in human health

1.1.1 Zinc in the diet and body

Zinc is one of the most important and essential trace elements in humans. The first evidence of its importance in human development was in 1869, when it was first identified as an essential element for the growth of *Aspergillus niger* (Raulin, 1869). However, it was not until the mid 20th century that its role in humans was fully discovered (Prasad *et al.*, 1963). The amount of zinc in the human body is normally 2-3 g, varying between tissues. Zinc is referred to as a trace element as its content in the plasma is in the order of micromolar (Rink & Gabriel, 2000). It is mainly found in the muscle and bones (Wastney *et al.*, 1986) but also in the liver and skin, with the highest concentration seen in the prostate and eye (John *et al.*, 2010). Zinc intake comes from the diet with a recommended intake of 8 mg/day for women and 11 mg/day for men. This amount decreases for infants (2-3 mg/day) and children (5-9 mg/day) (Trumbo *et al.*, 2001). Zinc is absorbed in the small intestine and it is then distributed in the body via the serum (Scott & Bradwell, 1983). As zinc is an essential dietary nutrient, the body counteracts any reduction in zinc uptake by reducing its excretion (King, 2011). In fact, it was seen both in animals and humans that reducing the zinc intake led to a significant reduction of zinc excretion in order to preserve zinc in the body (Baer & King, 1984). Furthermore, zinc deficiency is followed by an increase of tissue metabolism such as muscle catabolism.

Dietary zinc comes from a variety of food; oysters, for example, contain more zinc than any other type of food. Other sources include meat, nuts, beans, seafood, whole grains and dietary products (Figure 1.1). However, phytates contained in most plant food and grains bind zinc and reduce its absorption, therefore its availability from food is significantly decreased in comparison to animal foods, if eaten in the presence of phytates (Trumbo *et al.*, 2001). Despite its proven importance in human health, many people around the world suffer from zinc deficiency.

Figure 1.1 ***Zinc in the diet****.*
Zinc is one of the most important trace elements in the human body and it is absorbed from food in the gut. The Figure above illustrates the main sources of zinc in the diet.

1.1.2 Molecular aspects of zinc signals

Two different types of zinc can be found in the body: labile zinc and protein-bound zinc. The predominance of zinc in the human body is bound to proteins; in fact almost 10% of proteins encoded in the human genome have potential zinc-binding motifs (Andreini *et al.*, 2006). The amount of labile zinc is very low and is estimated to be in the order of nanomolar (Maret, 2011). Zinc acts as a cofactor for more than 300 enzymes and is essential for their function, ranging from the synthesis to the degradation of metabolites (Vallee & Auld, 1990). An enzyme is defined as a zinc metalloenzyme when its activity is significantly decreased after zinc removal (King, 2011). Zinc is indispensable for RNA transcription, DNA synthesis, cell division and molecular signalling activation (Prasad, 1998). The importance of zinc in gene expression is highlighted by the fact that more than 2000 transcription factors bind zinc in order for them to bind DNA. Furthermore, zinc also plays an essential role in cell proliferation (Li & Maret, 2009) as well as in cell death through its involvement in apoptosis (Wätjen *et al.*, 2002). Any change in intracellular labile zinc concentration can also affect cell signal transduction because zinc not only regulates the activity of transcription factors but also several signalling molecules, such as kinases (Kim *et al.*, 2000; Samet *et al.*, 1998) and phosphatases (Haase & Maret, 2003). Manipulation of the zinc level in cells by either adding extracellular zinc or by withdrawing it through the use of chelating agents can

influence several signalling pathways which require zinc in order to be activated (Beyersmann & Haase, 2001).

1.1.3 Cellular zinc homeostasis

Zinc cannot pass through cell membranes, therefore, zinc homeostasis requires the involvement of two families of zinc transporters (Figure 1.2). The ZIP family (Zrt-/Irt-like protein, termed SLC39A) of zinc importers transports zinc from the outside of the cell or from intracellular stores to the cytosol, whereas the ZnT family (termed SLC30A) of zinc exporters transports zinc either out of the cell or into stores (reviewed by Kambe et al. 2015). While the ZnT transporters are known to be Zn^{2+}/H^{+} exchanger (Ohana *et al.*, 2009; Shusterman *et al.*, 2014), the ZIP members are generally referred to as transporters in the literature, despite some evidence that they may act in a channel-like manner (Taylor *et al.*, 2012). Another important mechanism involved in zinc homeostasis is due to the action of zinc-binding proteins such as metallothioneins and glutathione which bind most of intracellular zinc (Maret & Vallee, 1998; Jiang, Maret & Vallee, 1998) (Figure 1.2-C).

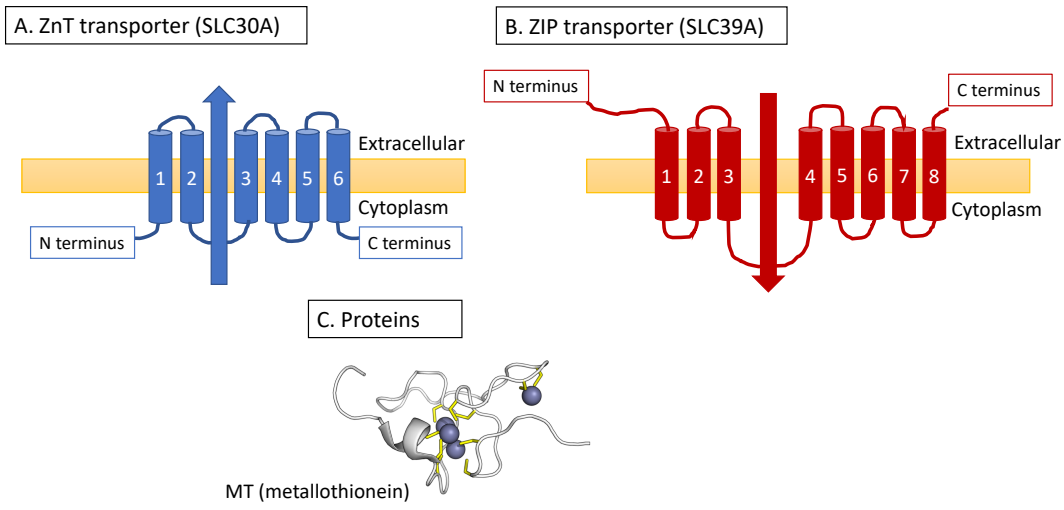

Figure 1.2 ***Zinc homeostasis is mainly controlled by two families of zinc transporters.***
A. The ZnT transporters are zinc exporters, characterised by 6 transmembrane domains.
B. The ZIP transporters are zinc importers, characterised by 8 transmembrane domains with a long intracellular loop between TM III and TM IV.
C. The amount of labile zinc in the cytoplasm is in the order of nanomolar as most of the cytoplasmic zinc is bound to proteins, such as metallothionein and glutathione.

The human ZnT family of zinc transporters consists of ten members in total. ZnT transporters are all predicted to contain six transmembrane (TM) domains with both the N and C-terminal domains on the intracellular side of the membrane (reviewed by Kambe et al. 2015) (Figure 1.2-A). Furthermore, they have a long C-terminus and they have been shown to be specific to the transport of zinc and no other metal (Palmiter & Huang, 2004). ZnT transporters function as a Zn^{2+}/H^{+} exchanger (Ohana *et al.*, 2009; Shusterman *et al.*, 2014) where the two conserved aspartic acids of TM II and two histidines of TM V are thought to create an intramembranous cavity for the zinc transport. The importance of these residues has been confirmed by the fact that mutation at these sites suppressed the transport activity (Wei & Fu, 2006). Most interestingly, the ZnT transporters form homodimers in order to transport zinc, with the exception of ZnT5 and ZnT6 which form a heterodimer together (Fukunaka *et al.*, 2009). One common characteristic of all the members of the ZnT family is the histidine rich loop between TM IV and V, which is thought to act as a sensor of cytosolic zinc and be involved in the regulation of zinc entry (Podar *et al.*, 2012; Kawachi *et al.*, 2012).

In contrast, the human ZIP family contains 14 members that can be divided into four different subfamilies (Gaither & Eide, 2001) (Figure 1.3). They each have eight transmembrane domains with a long cytoplasmic loop between TM III and TM IV (Figure 1.2-B). Differently from the ZnT transporters, they do not transport zinc exclusively, as they also transport manganese, iron, and cadmium (Gao *et al.*, 2008; Fujishiro *et al.*, 2012). The phylogenetic tree obtained from the alignment of the amino acid sequences of the human ZIP transporters confirms the classification into four subfamilies: GufA, subfamily I, subfamily II and the LIV-1 subfamily (Figure 1.3). The horizontal lines on the phylogenetic tree show the change of the evolutionary lineages over time. When two members are in the same branch, it means that they share a common ancestor and that they are more related to each other. Furthermore, a longer length of the branch represents a large change that has taken place. The phylogenetic tree shows that the human ZIP transporters descend from the same ancestor; however, they have all undertaken different changes with time. According to the phylogenetic tree, the members of the LIV-1 subfamily derive from a more recent ancestor than the other members of the ZIP family and they have also undergone more changes (Figure 1.3).

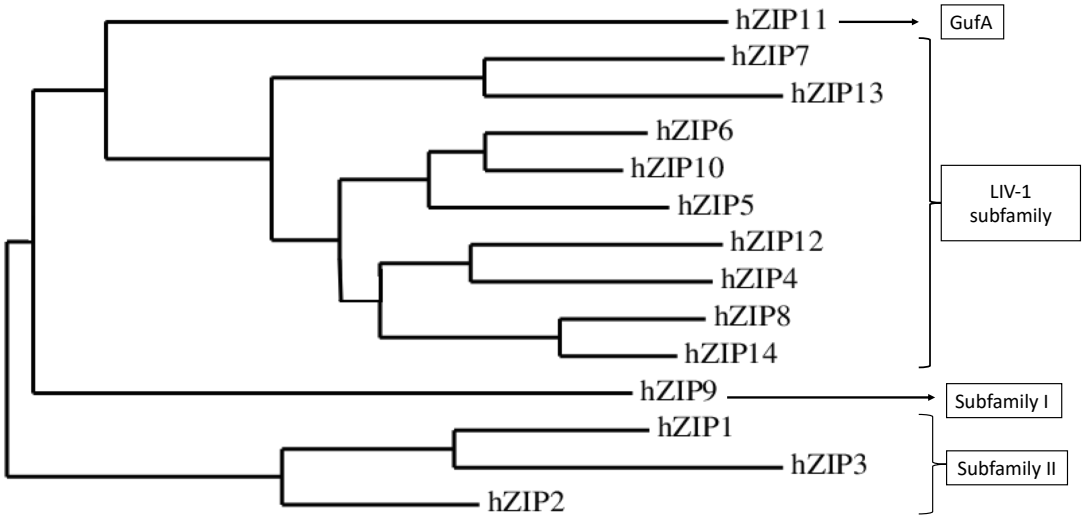

Figure 1.3 ***Phylogenetic tree of the ZIP family of zinc transporters.***
The human sequences of the ZIP family members were retrieved using the NCBI database in FASTA format and aligned using the ClustalW tool (Swiss Institute of Bioinformatics) (Larkin *et al.*, 2007). *The phylogenetic tree was obtained using the Phylogeny.fr web service* (Dereeper *et al.*, 2008). *The ZIP family can be divided into 4 main subfamilies according to the similarities existing between the different members: GufA (ZIP11), the LIV-1 subfamily (ZIP4-ZIP8, ZIP10, ZIP12-ZIP14), subfamily I (ZIP9) and subfamily II (ZIP1-ZIP3).*

ZIP7 and ZIP13 are in the same branch, meaning that they are related to each other. This is confirmed by the fact these two zinc transporters are the only two members that reside on the membrane of intracellular stores, rather than the plasma membrane. Similarly, ZIP6 and ZIP10 are in the same branch, indicating that they are related to each other as well. ZIP5 is not known to be directly related to ZIP6 and ZIP10, nevertheless it comes from a more recent ancestor and it may have a closer relationship to those two than to the other members of the family. The alignment of the sequences of the ZIP family members indicates the similarities between them and reveals that they are characterised by eight transmembrane domains (TM) (Taylor & Nicholson, 2003) (Figures 1.4-1.5). These regions are easily distinguished in the alignment because they correspond to the regions with the highest similarities, which suggest how these domains are structurally conserved in all the family members. The ZIP family members are characterised by a long N-terminal domain and a short C-terminal domain. Interestingly, they all reveal a long intracellular loop between TM III and TM IV. The long intracellular loop contains a large number of histidine residues (Manning *et al.*, 1995; Guerinot, 2000), which are predicted to be involved in the metal binding region as they

bind zinc and, thus are involved in zinc ion transport (Guerinot, 2000; Gaither & Eide, 2001). Nevertheless, this intracellular loop does not show many similarities between the different transporters, suggesting that each zinc transporter of the family may undergo different regulation in order to be activated. The LIV-1 subfamily is the largest of the ZIP family (Figure 1.3). In addition to the characteristics that they share with the entire family, the members of the LIV-1 subfamily also contain a CPALLY motif and the consensus HEXPHEXGD motif (Taylor & Nicholson, 2003) (Figures 1.4-1.5), which is similar to the zinc binding site of the zinc metalloproteinases zincins (Hooper, 1994). The role of the CPALLY motif has not been defined yet; however, it contains three conserved cysteines that can create disulphide bonds between each other and are thought to be involved in the regulation of the zinc transport (Taylor *et al.*, 2007). This leaves a spare cysteine, but as seen in Figure 1.5 prior to the HEXPHEXGD motif there is an additional adjacent cysteine which is conserved between most members, which could make a further disulphide bond with the third cysteine present in the CPALLY motif and therefore create the pore for zinc transport (Taylor *et al.*, 2007). Most of the LIV-1 family members are situated on the plasma membrane (Taylor *et al.*, 2004), but two of them (ZIP7 and ZIP13) are predicted to be located in intracellular membranes: the endoplasmic reticulum (Taylor *et al.*, 2004) and Golgi (Huang *et al.*, 2005) respectively, enabling them to transport zinc from intracellular stores to the cytosol (Taylor, 2008). ZIP7 and ZIP13 are included in a subgroup of the LIV-1 subfamily, which was initially called KE4 (Taylor *et al.*, 2004). One characteristic that distinguishes the member of the LIV-1 subfamily from the other ZIP transporters is the incidence of histidine-rich repeats throughout their sequence. In particular, the long N-terminus of ZIP6 contains 317 residues of the total 749 in the entire sequence, 27 of which are histidine residues (Taylor & Nicholson, 2003). The presence of many histidine residues is key to zinc transport since histidine is known to bind zinc. High abundance of histidine residues are seen on the long cytoplasmic loop between TM III and TM IV, on the extracellular loop between TM II and TM III and on the extracellular N terminus (Taylor, 2000) (Figure 1.6).

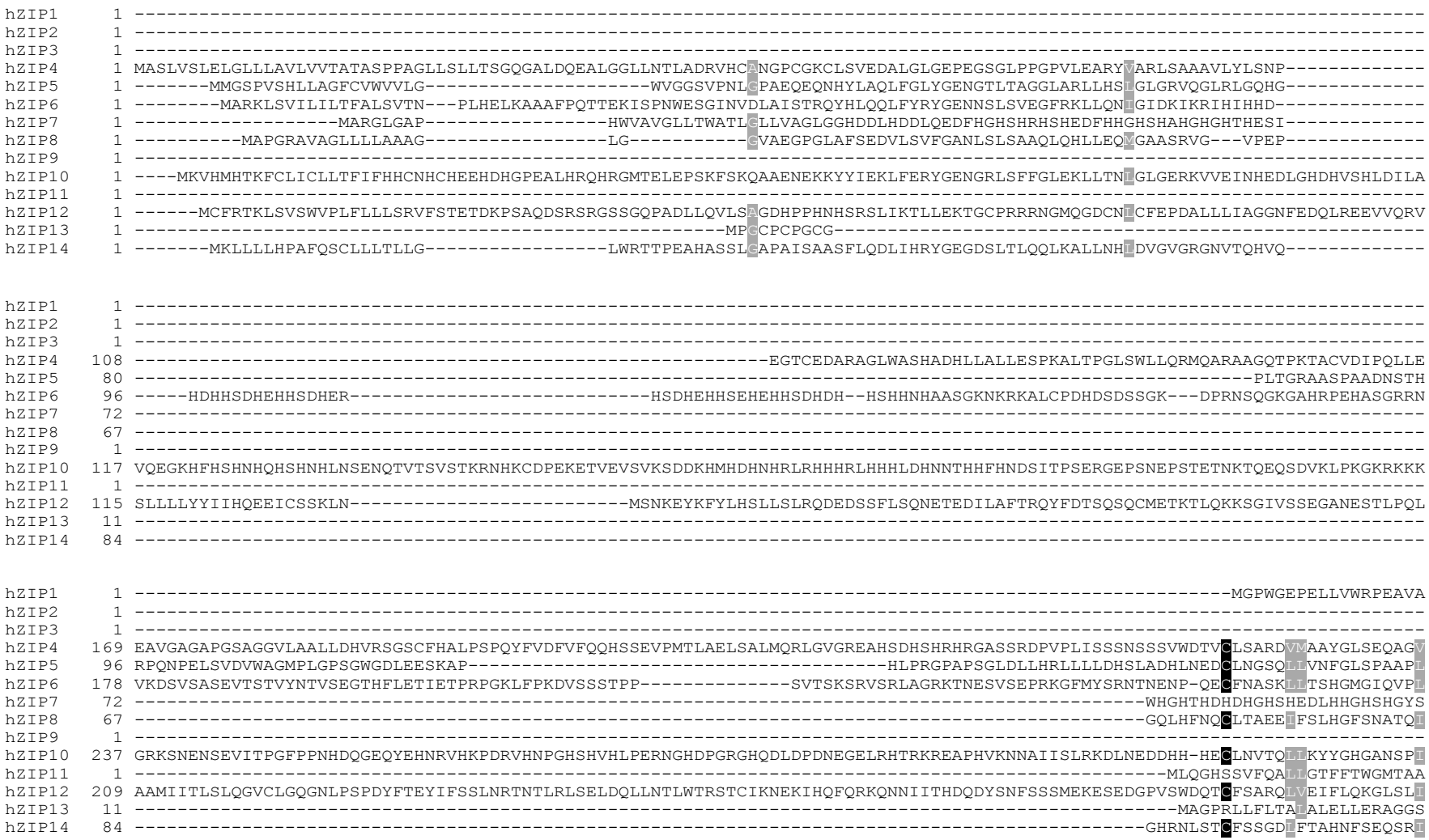
hZIP1 1
hZIP2 1
hZIP3 1
hZIP4 1 MASLVSLELGLLLAVLVVTATASPPAGLLSLLTSGQGALDQEALGGLLNTLADRVHCANGPCGKCLSVEDALGLGEPEGSGLPPGPVLEARYVARLSAAAVLYLSNP
hZIP5 1 -------MMGSPVSHLLAGFCVWVVLG----------WVGGSVPNLGPAEQEQNHYLAQLFGLYGENGTLTAGGLARLLHSLGLGRVQGLRLGQHG
hZIP6 1 --------MARKLSVILILTFALSVTN---PLHELKAAAFPQTTEKISPNWESGINVDLAISTRQYHLQQLFYRYGENNSLSVEGFRKLLQNLGIDKIKRIHIHHD
hZIP7 1 ------------------MARGLGAP----------HWVAVGLLTWATLGLLVAGLGGHDDLHDDLQEDFHGHSHRHSHEDFHHGHSHAHGHGHTHESI
hZIP8 1 ----------MAPGRAVAGLLLLAAAG----------LG----------GVAEGPGLAFSEDVLSVFGANLSLSAAQLQHLLEQVGAASRVG---VPEP
hZIP9 1
hZIP10 1 ----MKVHMHTKFCLICLLTFIFHHCNHCHEEHDHGPEALHRQHRGMTELEPSKFSKQAAENEKKYYIEKLFERYGENGRLSFFGLEKLLTNLGLGERKVVEINHEDLGHDHVSHLDILA
hZIP11 1
hZIP12 1 ------MCFRTKLSVSWVPLFLLLSRVFSTETDKPSAQDSRSRGSSGQPADLLQVLSAGDHPPHNHSRSLIKTLLEKTGCPRRRNGMQGDCNLCFEPDALLLIAGGNFEDQLREEVVQRV
hZIP13 1 ----------MP-CPCPGCG----------
hZIP14 1 -------MKLLLLHPAFQSCLLLTLLG----------LWRTTPEAHASSLGAPAISAASFLQDLIHRYGEGDSLTLQQLKALLNHLDVGVGRGNVTQHVQ
hZIP1 1
hZIP2 1
hZIP3 1
hZIP4 108 ----------EGTCEDARAGLWASHADHLLALLESPKALTPGLSWLLQRMQARAAGQTPKTACVDIPQLLE
hZIP5 80 ----------PLTGRAASPAADNSTH
hZIP6 96 -----HDHHSDHEHHSDHER----------HSDHEHHSEHEHHSDHDH--HSHHNHAASGKNKRKALCPDHDSDSSGK---DPRNSQGKGAHRPEHASGRRN
hZIP7 72
hZIP8 67
hZIP9 1
hZIP10 117 VQEGKHFHSHNHQHSHNHLNSENQTVTSVSTKRNHKCDPEKETVEVSVKSDDKHMHDHNHRLRHHHRLHHHLDHNNTHHFHNDSITPSERGEPSNEPSTETNKTQEQSDVKLPKGKRKKK
hZIP11 1
hZIP12 115 SLLLLYYIIHQEEICSSKLN----------MSNKEYKFYLHSLLSLRQDEDSSFLSQNETEDILAFTRQYFDTSQSQCMETKTLQKKSGIVSSEGANESTLPQL
hZIP13 11
hZIP14 84
hZIP1 1 ----------MGPWGEPELLVWRPEAVA
hZIP2 1
hZIP3 1
hZIP4 169 EAVGAGAPGSAGGVLAALLDHVRSGSCFHALPSPQYFVDFVFQQHSSEVPMTLAELSALMQRLGVGREAHSDHSHRHRGASSRDPVPLISSSNSSSVWDTVCLSARDVMAAYGLSEQAGV
hZIP5 96 RPQNPELSVDVWAGMPLGPSGWGDLEESKAP----------HLPRGPAPSGLDLLHRLLLLDHSLADHLNEDCLNGSQLLVNFGLSPAAPL
hZIP6 178 VKDSVSASEVTSTVYNTVSEGTHFLETIETPRPGKLFPKDVSSSTPP----------SVTSKSRVSRLAGRKTNESVSEPRKGFMYSRNTNENP-QECFNASKLLTSHGMGIQVPL
hZIP7 72 ----------WHGHTHDHDHGHSHEDLHHGHSHGYS
hZIP8 67 ----------GQLHFNQCLTAEEIFSLHGFSNATQI
hZIP9 1
hZIP10 237 GRKSNENSEVITPGFPPNHDQGEQYEHNRVHKPDRVHNPGHSHVHLPERNGHDPGRGHQDLDPDNEGELRHTRKREAPHVKNNAIISLRKDLNEDDHH-HECLNVTQLLKYYGHGANSPI
hZIP11 1 ----------MLQGHSSVFQALLGTFFTWGMTAA
hZIP12 209 AAMIITLSLQGVCLGQGNLPSPDYFTEYIFSSLNRTNTLRLSELDQLLNTLWTRSTCIKNEKIHQFQRKQNNIITHDQDYSNFSSSMEKESEDGPVSWDQTCFSARQLVEIFLQKGLSLI
hZIP13 11 ----------MAGPRLLLFLTALALELLERAGGS
hZIP14 84 ----------GHRNLSTCFSSGDLFTAHNFSEQSRI

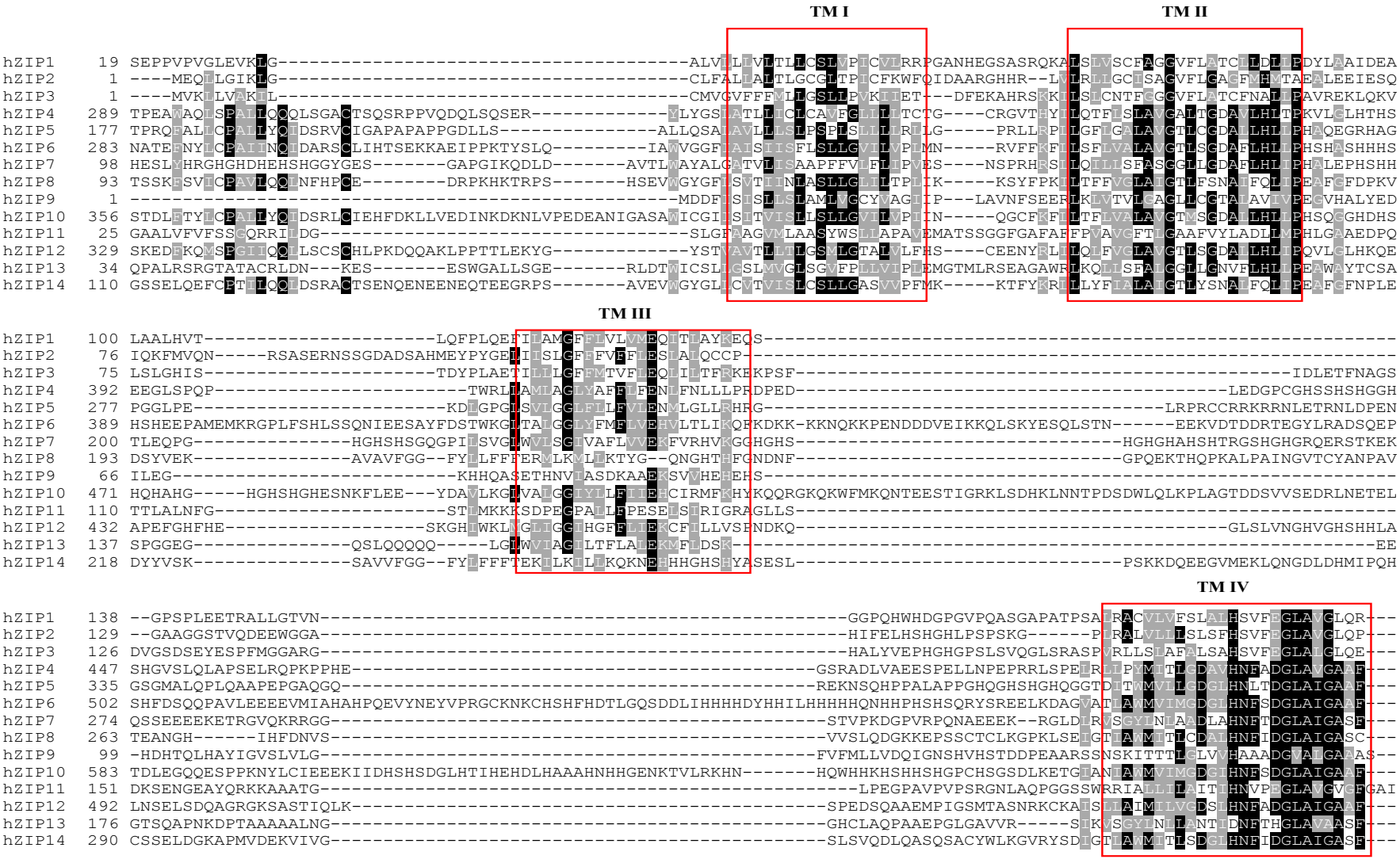
TM I
TM II
TM III
TM IV

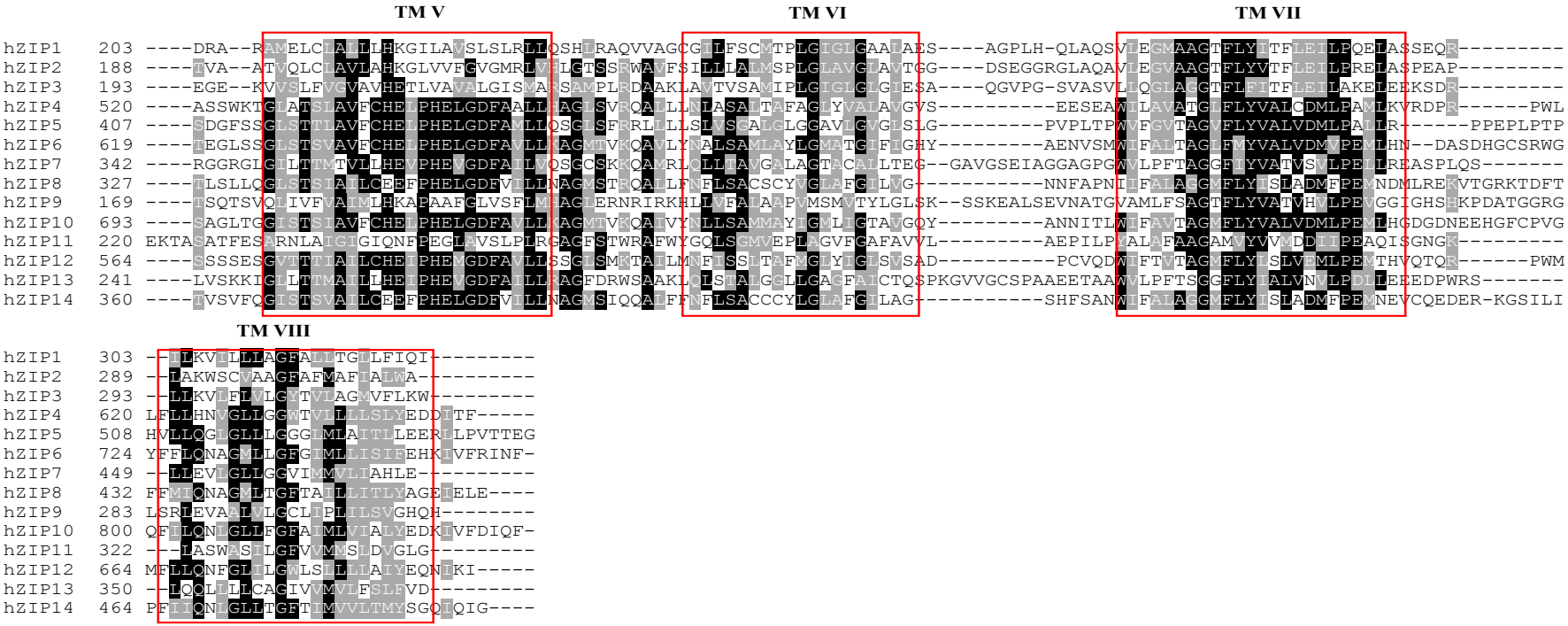

Figure 1.4 ***Alignment of the human sequences of the ZIP family of zinc transporters.***
The human sequences of the ZIP transporters were retrieved from the NCBI database with FASTA format and aligned using the ClustalW alignment tool (Swiss Institute of Bioinformatics) (Larkin *et al.*, 2007). *The aligned sequences were shaded using the BoxShade program (Swiss Institute of Bioinformatics) (available https://embnet.vital-it.ch/software/BOX_form.html). The black and grey colours show the presence of at least 70% identical or complementary residues, respectively.*

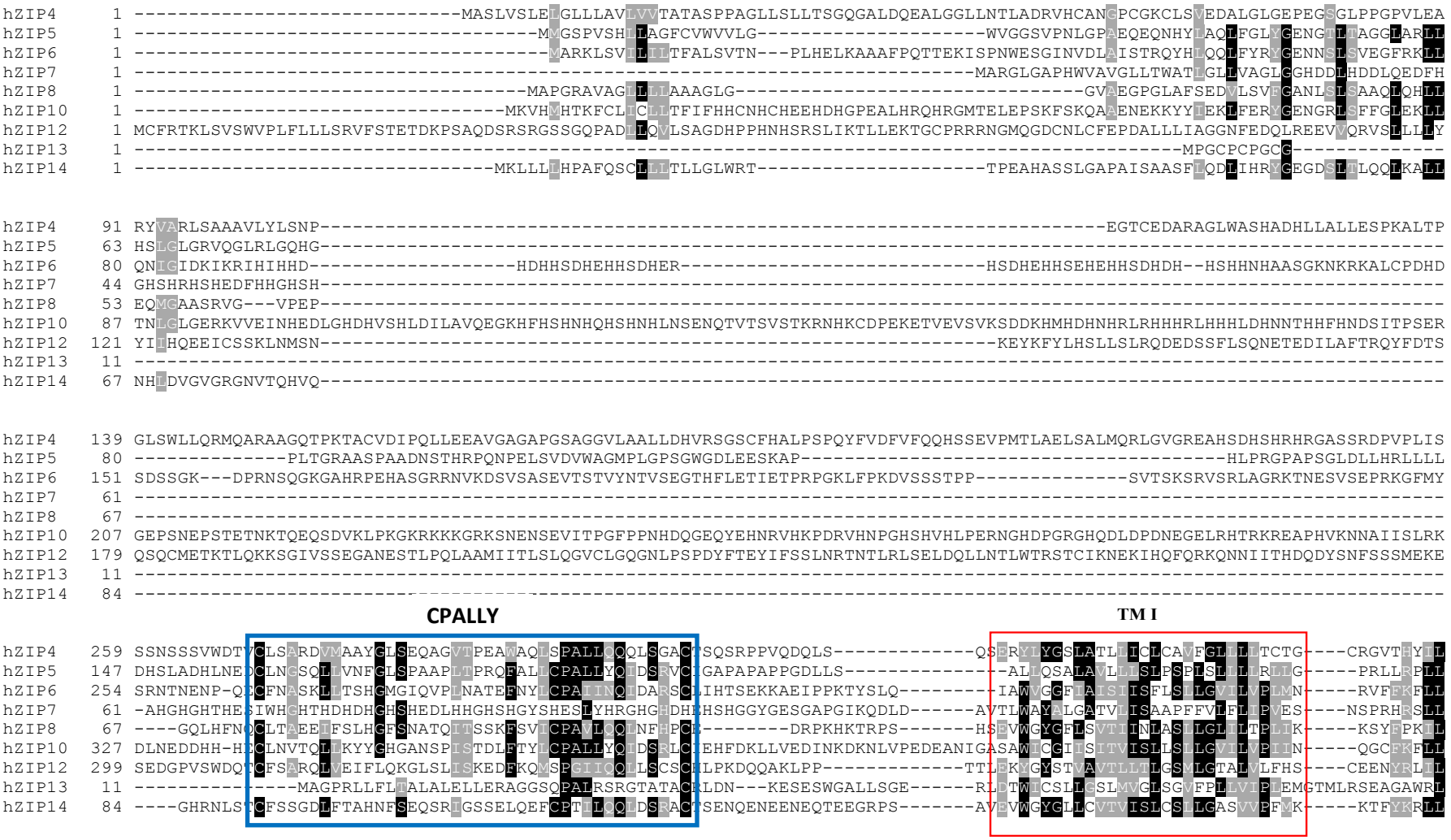
CPALLY
TM I

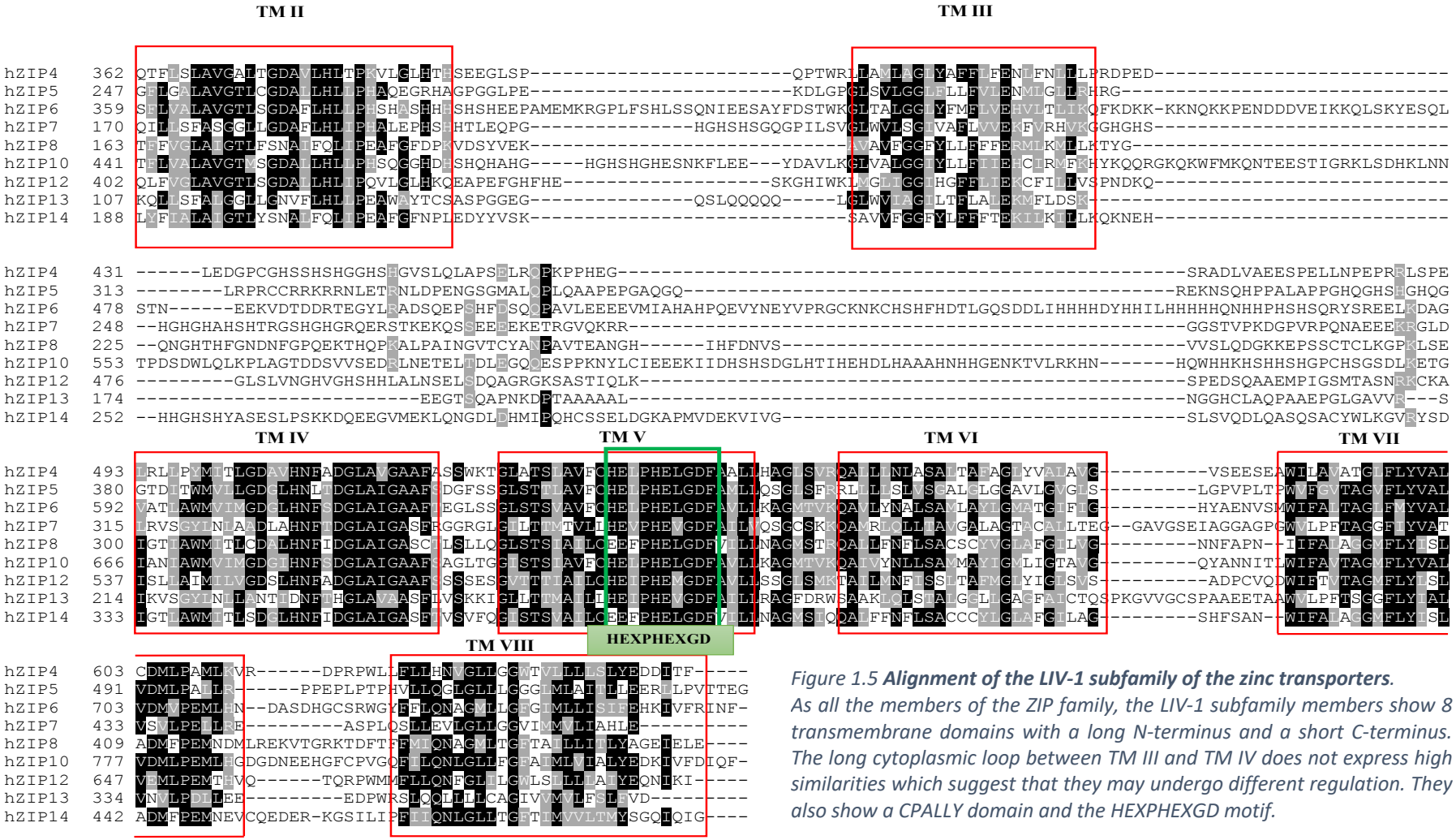

Figure 1.5 ***Alignment of the LIV-1 subfamily of the zinc transporters.*** *As all the members of the ZIP family, the LIV-1 subfamily members show 8 transmembrane domains with a long N-terminus and a short C-terminus. The long cytoplasmic loop between TM III and TM IV does not express high similarities which suggest that they may undergo different regulation. They also show a CPALLY domain and the HEXPHEXGD motif.*

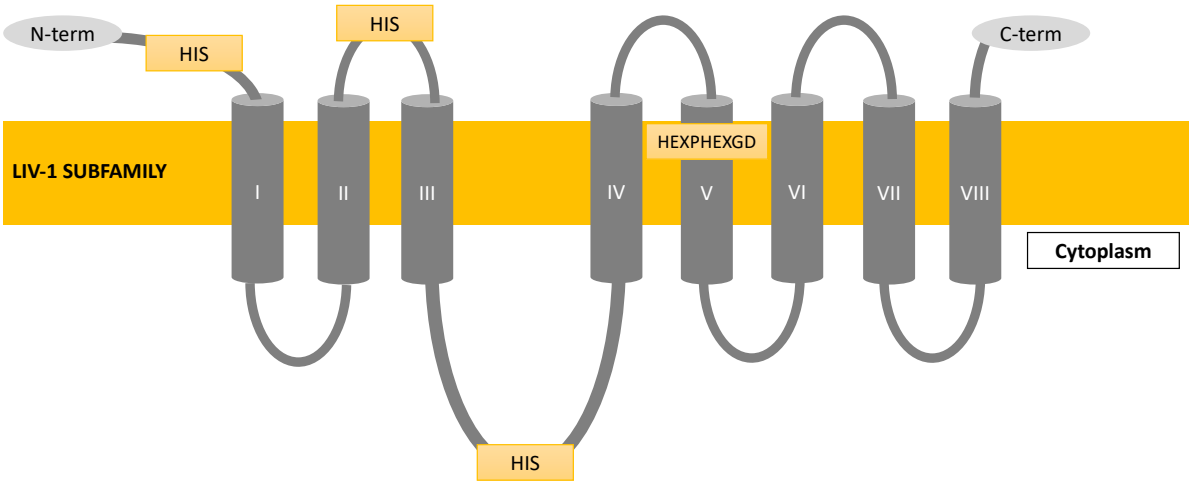

Figure 1.6 ***Schematic of predicted membrane topology of the LIV-1 subfamily members.*** *Most of the members of the LIV-1 subfamily of ZIP transporters have a long N- terminal domain and a short C-terminal domain. They all have a long cytoplasmic loop between the third and fourth transmembrane domain and most of them are rich in histidine residues, which have a potential role in zinc transport. In TM V domain there is the consensus motif HEXPHEXGD which is similar to the zinc binding site of the metalloproteinases zincins* (Hooper, 1994).

1.1.4 Zinc handling in cells

Intracellular zinc signalling is often classified into fast or early signalling and late signalling. Fast signalling does not require the synthesis of proteins, whereas the late signalling needs the transcription of genes such as zinc transporters and can take place within hours (Taiho, 2014). Since the amount of labile cytoplasmic zinc is very low, the binding of zinc to proteins is critical for its role in human biology. Cytoplasmic zinc needs to be tightly controlled to sustain proper zinc signalling. The availability of labile zinc is governed by buffering reactions which control the overall level of zinc in the cytoplasm (Colvin *et al.*, 2010). In fact, in steady state conditions, the role of a zinc-binding protein is to buffer the amount of zinc ions to a picomolar cytoplasmic leve l. In contrast, in non-steady state conditions, proteins and transporters cooperate in order to maintain the proper zinc level in response to a change of intracellular zinc. This process is called muffling (Colvin *et al.*, 2010). Zinc entering the cells was predicted by a “muffler” hypothesis which suggests that when zinc enters the cell, it is immediately buffered in a zinc “muffler” before being sequestered inside the intracellular stores, possibly by a ZnT transporter (Colvin *et al.*, 2008). These buffering agents, acting as a zinc “muffler”, are thought to be metallothionein or glutathione which bind zinc tightly (Krężel, Hao & Maret, 2007). Muffling allows the restoration of a correct steady state zinc

concentration (Colvin *et al.*, 2010). This process classifies zinc as a second messenger in a manner which is likely to be akin to calcium, whereby within minutes of an extracellular stimulus there is a change of zinc gradient across the membranes which leads to the activation of intracellular signalling events (Yamasaki *et al.*, 2007).

1.1.5 Zinc in human health and diseases

The role played by zinc in the control of several mechanisms which are necessary for human health, highlights its importance in the body. It is well established that imbalance of zinc in the body can be detrimental for both humans and animals.

Zinc deficiency has been associated with several dysfunctions such as skin changes, slowed growth, brain development disorders, hypogonadism, human lethargy and impaired immunity (Todd, Elvehjem & Hart, 1933; Prasad, Halsted & Nadimi, 1961; Prasad, 1995) (Figure 1.7). However, these conditions can be overcome by increasing zinc intake. Zinc deficiency is involved in several aspects of adaptive and innate immunity, which include lymphopenia, thymic atrophy and altered thymic hormones that can cause increased duration of infection (reviewed by Fukada et al. 2011). Moreover, zinc is known for its importance in the healing process, as zinc deficiency is associated with a delayed wound healing process (Lansdown *et al.*, 2007). Another disease associated with zinc deficiency is called acrodermatitis enteropathica, which is a rare disease due to downregulation or mutation of ZIP4, a zinc transporter involved in zinc absorption in the intestine (Dufner-Beattie *et al.*, 2007). This disease can be lethal if not treated with zinc supplementation. Conversely, an excess of zinc can also be detrimental and toxic for health, leading to increased migration and exaggerated cell growth (Hogstrand *et al.*, 2009). Zinc excess is also associated with nausea, vomiting and diarrhoea (Brown *et al.*, 1964). Moreover, high supplementation of zinc can induce copper deficiency long term, due to the competition of zinc and copper absorption mediated by metallothioneins (Van Campen, 1969; Ogiso, Ogawa & Miura, 1978) (Figure 1.7).

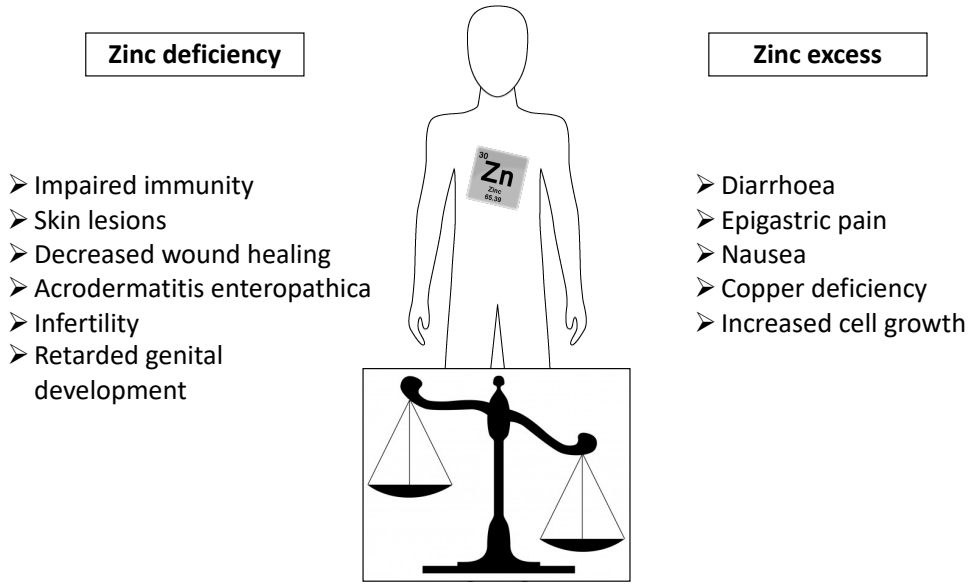

Figure 1.7 ***Zinc imbalance can be detrimental for human health****.*
Both zinc deficiency and zinc excess can be harmful to humans, as associated with different conditions (Plum, Rink & Haase, 2010)*. For this reason, it is important that zinc homeostasis is tightly controlled.*

Zinc dysregulation has been observed in several important diseases such as neurodegeneration (Frederickson & Bush, 2001), diabetes (Chimienti, Favier & Seve, 2005; Wenzlau *et al.*, 2007; Mocchegiani, Giacconi & Malavolta, 2008) and cancer (Franklin *et al.*, 2005; Taylor *et al.*, 2007). Zinc in the brain is known to be important as a neuromodulator in synaptic transmission (Sensi *et al.*, 2009) and it was observed that high level of zinc can induce neuronal death (Kim & Koh, 2002). Moreover, zinc has been associated to Alzheimer's disease, as zinc was found to be present in the amyloid plaques (Bush *et al.*, 1994; Garai *et al.*, 2006), typical hallmark of this disorder. Zinc is also important in the control of insulin-receptor signalling transduction (Haase & Maret, 2005b) and of insulin storage and secretion (Figlewicz *et al.*, 1984). This evidence would explain why a previous study had revealed the possibility that abnormal zinc metabolism may predispose to diabetes mellitus (Kinlaw *et al.*, 1983). The role of zinc in cancer can be explained by its important requirement for gene expression, signal transduction and cell survival. Zinc is also related to cell cycle progression (G1 and G2 phases) (Chesters & Petrie, 1999; Li & Maret, 2009) and it is important for the function of several cyclins, so it is possible that cancer cells use more zinc than usual during their uncontrolled growth. Moreover, zinc inhibits tyrosine phosphatases (Haase & Maret, 2003), preventing the dephosphorylation and deactivation of an extensive number of tyrosine kinase receptors that are normally overexpressed and activated in cancer (Taylor *et al.*, 2008).

Tyrosine phosphatase inhibition would explain the widespread activation of tyrosine kinases seen in cells with elevated levels of zinc (Taylor *et al.*, 2012). In this respect, it was discovered that the protein tyrosine phosphatase PTP1B, a phosphatase which is known to be overexpressed in breast cancer (Wiener *et al.*, 1994) and associated with tumorigenesis (Julien *et al.*, 2007), is inhibited by zinc (Bellomo *et al.*, 2014). Zinc is also involved in the activation of the widely active EGF receptor and MAPK molecules that both have a key role in breast cancer (Wu *et al.*, 1999). Zinc levels were discovered to be altered in serum and cancer tissues of different varieties of cancer (Mulay *et al.*, 1971). Although serum zinc appears to be low in most cancers, breast and lung cancer tissues show higher levels of zinc (Schwartz & Schwartz, 1975; Margalioth, Schenker & Chevion, 1983) with almost a double amount of zinc in breast cancer when compared to benign breast tissue (Jin *et al.*, 1999). Despite the fact that zinc measurements are still controversial between the amount of zinc measured in the serum and its level in tissues, the increase of zinc in breast cancer tissue is significant (Margalioth, Schenker & Chevion, 1983; Jin *et al.*, 1999). Furthermore, the difference observed between serum and tissue zinc level can be explained by the fact that zinc binds albumin in the serum (Stewart *et al.*, 2003), making it less available.

1.1.6 Zinc and apoptosis

Apoptosis is a programmed cell death that allows for the safe removal of cells that are damaged or superfluous without affecting neighbouring cells. The mechanism involves several processes such as cell shrinkage, DNA fragmentation, condensation of the cytoplasm and changes in the phospholipid composition, resulting in apoptotic bodies that are normally removed by macrophage-mediated efferocytosis (Kerr, 2002). Failure of this system can lead to accumulation of apoptotic bodies that can eventually culminate in the activation of pro-inflammatory reactions (Zalewski, 2011). The involvement of zinc in apoptosis has been controversial in the last decades as both zinc deficiency and zinc excess have been associated with apoptosis (Kim *et al.*, 1999; Fraker, 2005). This controversial data may be due to the different type of cells or tissue used in each study. Most of the investigations showing zinc as a potent inducer of apoptosis involved neuronal cells (Kim *et al.*, 1999). However, other studies have seen the same effect on mouse dendritic cells and pancreatic cancer cells (Shumilina *et al.*, 2010; Jayaraman & Jayaraman, 2011). On the other hand, zinc deficiency was reported to

induce programmed cell death in hepatocytes, glioma, kidney, fibroblast and testicular cells (Nodera, Yanagisawa & Wada, 2001; Ho, Courtemanche & Ames, 2003; Verstraeten *et al.*, 2004; Fraker, 2005). Therefore, it is difficult to conclude whether a cell is protected or not by a rise in intracellular zinc as it may vary in each cell compartment. The actual level of zinc will depend on the presence or absence of zinc transporters and also of zinc-binding proteins such as metallothioneins (Zalewski, 2011).

1.1.7 Zinc transporters and cancer

The discovery of the implications of zinc transporters in multiple diseases has shined new light on zinc investigations, in particular its involvement in cancer and cell cycle signalling (Beyersmann & Haase, 2001; Pan *et al.*, 2017; Ziliotto, Ogle & Taylor, 2018). Table 1.1 shows the involvement of different ZnT and ZIP transporters in a variety of different cancer types (reviewed by Pan *et al.*, 2017). The first evidence of the involvement of the LIV-1 subfamily of zinc transporters in cancer was reported in breast cancer, where dysregulation of ZIP6 was observed (Manning *et al.*, 1995). Other evidence of zinc involvement in cancer was reported in prostate cancer, where dysregulation of zinc transporters includes ZIP1-3 and ZnT4 (Jong & McKeage, 2014). Zinc levels in prostate cancer decrease, in contrast with normal prostate tissue where zinc levels are high (Costello & Franklin, 1998). This finding was a result of down-regulation of the ZIP transporters, in particular of ZIP1 (Franklin *et al.*, 2005) and alteration of the zinc efflux transporter ZnT4 (Henshall *et al.*, 2003). ZIP4, another member of the LIV-1 subfamily, has been associated with the development and growth of pancreatic cancer (Li *et al.*, 2007). Its expression was reported to be more than five times increased in cancer compared to normal tissue (Li *et al.*, 2007) and associated with repression of apoptosis, increased migration and enhancement of the cell cycle (Weaver *et al.*, 2010). This was demonstrated by the fact that silencing ZIP4 expression led to decreased proliferation, migration and tumour volume in several pancreatic cancer cell lines (Li *et al.*, 2009).

Recent studies have also associated ZIP14 with cancer (Jenkitkasemwong *et al.*, 2012). In particular, downregulation of ZIP14 was associated with hepatocellular cancer, where intracellular zinc levels were observed to be significantly decreased in both the early and advanced stages of the malignancy when compared to normal tissue (Franklin

et al., 2012). Conversely, other studies have seen enriched expression of an alternatively spliced gene of ZIP14 in colorectal cancer (Thorsen *et al.*, 2011). Samples of renal cell carcinoma have been associated with increased expression of ZIP10 mRNA, suggesting the possibility of its use as a marker of aggressiveness in renal carcinoma (Pal *et al.*, 2014).

Cancer type	Zinc transporters
Prostate cancer	ZnT1, ZnT3, ZnT4, ZIP1, ZIP2, ZIP3, ZIP4, ZIP6, ZIP9
Breast cancer	ZnT2, ZIP6, ZIP7, ZIP9, ZIP10
Oesophageal cancer	ZnT7, ZIP5, ZIP6
Lymphoblastic leukaemia	ZnT1
Pancreatic cancer	ZIP3, ZIP4, ZIP6
Hepatocellular cancer	ZIP4, ZIP14
Glioma	ZIP4, ZIP11
Cervical cancer	ZIP6
Hepatic cancer	ZIP6
Kidney cancer	ZIP10, ZIP11
Bladder cancer	ZIP11

Table 1.1 ***Zinc transporters and cancer.***
The table shows the involvement of different ZnT and ZIP transporters in a variety of different cancer types (reviewed by Pan *et al.*, 2017).

Furthermore, many studies have associated ZIP7, ZIP6 and ZIP10 with breast cancer (Manning *et al.*, 1995; Mcclelland *et al.*, 1998; Kagara *et al.*, 2007; Taylor, 2008). The involvement of individual zinc transporters in breast cancer will be discussed in detail in the next sections.

1.2 Zinc transporters and breast cancer

1.2.1 Breast cancer and endocrine resistance

Breast cancer is a severe malignancy that develops from breast cells and it is considered to be one of the main health issues around the world (Bray *et al.*, 2018), even though mortality rates have started to decrease in the last decades, in particular in European countries (Levi *et al.*, 2004). The decrease in mortality is certainly due to more

widespread early screening, more precise diagnosis and improvements in treatment (Carioli *et al.*, 2018). However, breast cancer still remains one of the most common cancers among women (Bray *et al.*, 2018). There are several factors that are associated with a higher risk of breast cancer: having a relative with a previous history of breast cancer, late age at first pregnancy, absence or short term of breastfeeding, use of contraceptives, long menstrual history and nulliparity or use of postmenopausal therapy (Veronesi *et al.*, 2005; Sun *et al.*, 2017). Breast tumours are phenotypically very different from each other and Perou *et al.* showed that this heterogeneity was accompanied by a huge diversity in gene expression (Perou *et al.*, 2000). Typical immunohistochemical biomarkers of breast cancer are: PR (progesterone receptor), ER (oestrogen receptor) and HER2 (human epidermal growth factor receptor 2) (Vallejos *et al.*, 2010) along with different clinicopathological parameters such as tumour size, grade and nodal involvement (Dai *et al.*, 2015). The evaluation of these parameters is necessary in order to establish the proper therapy to be undertaken.

Breast cancer at its first stage is usually removed by surgery, followed by postoperative radiotherapy and systematic control through hormonal therapy and/or chemotherapy (Veronesi *et al.*, 2005).

Almost 70% of breast carcinomas express the oestrogen receptor (ER), so initial breast cancer characterisation tests for ER are performed to discover whether the cancer is ER-positive or negative (Hanstein *et al.*, 2004). There are two different types of oestrogen receptor: ERα and ERβ (Nilsson *et al.*, 2001). While the implication of ERα in breast cancer has been known for a long time, the role of ERβ has only been elucidated in recent years (Kuiper *et al.*, 1996; Mosselman, Polman & Dijkema, 1996; Paternia *et al.*, 2015). ERβ exhibits its effect mainly on the prostate and immune system and can counteract the hyperproliferative effect of ERα. In contrast, ERα exerts its function mainly on the mammary gland and uterus, hence its crucial role in breast cancer (Paternia *et al.*, 2015). Oestrogens, the ligand of this receptor, play a pivotal role in the growth and development of breast cancer (Johnston, 2004). The discovery of the involvement of oestrogen in breast cancer led to the use of endocrine therapy. Oestrogen receptors are the main target for ER-positive breast cancer which involves the use of selective receptor modulators named SERMs (selective estrogen receptor

modulators), pure antagonist or aromatase inhibitors to block the action or production of oestrogens (Williams & Lin, 2013). Oestrogens stimulate gene expression and the production of proteins which are important for the growth and function of breast cells, but they are also implicated in cancer growth and metastasis. Indeed, the main role of anti-oestrogens is indeed to compete with the endogenous ligand to bind ER, causing inhibitory effects on responsive breast cancer (Williams & Lin, 2013). However, these agents differ from each other in the way they act towards the ER. SERMs represent a class of drugs used in breast cancer therapy that show a partial agonist and antagonist response on the oestrogen receptor (Dutertre & Smith, 2000). Tamoxifen, the most common SERM drug used in breast cancer therapy, is used as a first-line endocrine therapy (Johnston, 2004). Its partial oestrogen receptor agonist activity and its metabolites were hypothesised to be involved in the acquisition of tamoxifen-induced growth, which can be reversed by the use of other agents with no agonist activity (Johnston, 2004).

An alternative therapy to tamoxifen is the use of a pure antagonist of the oestrogen receptor called fulvestrant (Faslodex®), a steroidal drug that blocks receptor activity and also leads to the degradation of ER proteins (Williams & Lin, 2013). However, this drug is normally used as a second-line treatment when the tumour starts to develop resistance to tamoxifen treatment (Robertson *et al.*, 2014). The other possible strategy to target ER-positive breast cancer is the use of an aromatase inhibitor. Aromatase is an enzyme involved in the conversion of androgens into oestrogens, thus indirectly targeting the activity of the ER (Williams & Lin, 2013). The most common aromatase inhibitors used in therapy are anastrozole, letrozole and exemestane and they are commonly used in post-menopausal women (Miller, 2004). Aromatase inhibitors are now considered the first adjuvant standard care in the treatment of oestrogen positive breast cancer in post-menopausal women (Robertson *et al.*, 2014). Nevertheless, since both aromatase inhibitors and fulvestrant have a high toxicity in the treatment of women with functional ovaries, these drugs have not yet replaced the efficacy and use of tamoxifen in the treatment of pre-menopausal women with ER-positive breast cancer (Clarke, Tyson & Dixon, 2015).

Other new promising drugs in the treatment of breast cancer are CDK4 and CDK6 inhibitors, which act as downregulators of the cell cycle and aim at reducing the size and proliferation of the tumour. These drugs are now under investigation in several clinical trials having shown the ability of inducing an immune response that can be helpful in combination with new therapies for the treatment of breast cancer (Goel *et al.*, 2017). Despite these promising new studies, the development of endocrine resistance remains one of the main burdens in clinics, especially in the management of ER-positive breast cancer (Clarke, Tyson & Dixon, 2015). New targets and biomarkers of resistance need to be discovered in order to help dissect the development of resistance.

1.2.2 Zinc transporter ZIP7

The "muffler" hypothesis, whereby zinc entering the cell is deposited in intracellular stores, increases the importance of the role of ZIP7, residing on the endoplasmic reticulum store membrane (Taylor *et al.*, 2004), and uniquely responsible for releasing zinc into the cytoplasm (Taylor, 2008) (Figure 1.8). Recent investigations demonstrated that ZIP7 is unable to release zinc from stores until it is activated by protein kinase CK2 phosphorylation on two serine residues (S275 and S726), situated in the long intracellular loop between TM III and TM IV (Taylor *et al.*, 2012).

Our group have produced a mouse monoclonal antibody which was confirmed to bind ZIP7 only when phosphorylated on these two residues (Nimmanon *et al.*, 2017). Moreover, our group have recently investigated two other potential phosphorylation sites of ZIP7 (S293 and T294) and have surprisingly discovered that they can contribute partially to the maximal activation of ZIP7. However, this mechanism could be due to hierarchal phosphorylation induced by CK2, which is yet to be fully deciphered (Nimmanon *et al.*, 2017). In any event, the activation induced by CK2 leads to the release of zinc from the endoplasmic reticulum store to the cytoplasm (Taylor *et al.*, 2012). This mechanism explains how zinc was classified as a second messenger, being released from stores within minutes of an extracellular stimulus, resulting in increased cytosolic zinc leading to multiple downstream effects on cell signalling pathways (Yamasaki *et al.*, 2007). In mast cells, it was seen that increase of calcium concentration resulted in zinc release from the endoplasmic reticulum, also called "zinc wave" (Yamasaki *et al.*, 2007). One of the downstream effects induced by zinc release is the inhibition of tyrosine

phosphatases which can play a significant role in maintaining activated pathways that are important in diseases such as cancer (Taylor *et al.*, 2012). It was recently discovered that pathways such as MAPK, mTOR, PI3K-AKT, pathways that are involved in cell survival and normally hyperactivated in cancer, are directly downstream of ZIP7-mediated zinc release (Nimmanon *et al.*, 2017) (Figure 1.8).

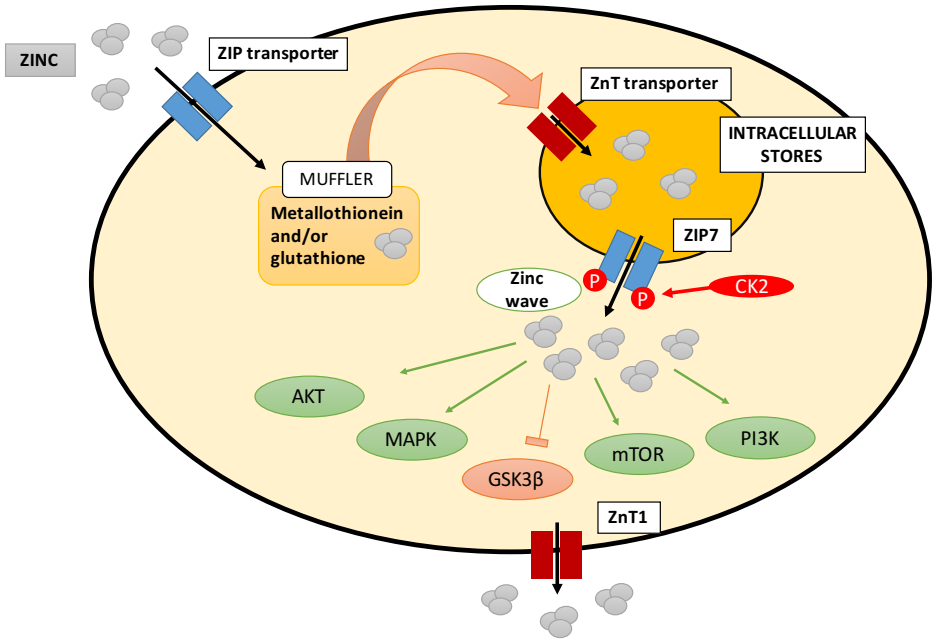

Figure 1.8 ***Schematic model of zinc mobilisation in cells mediated by ZIP7.***
When zinc enters the cell, potentially by a ZIP transporter, it is immediately buffered in the zinc "muffler" before being sequestered inside intracellular stores. After the activation of ZIP7, mediated by CK2, the zinc is released from the store. ZIP7-mediated zinc release is involved in the activation of downstream pathways such as MAPK, AKT and mTOR (Nimmanon *et al.*, 2017).

Evidence of ZIP7 abundance in tumours showed it to be one of the top 10% genes overexpressed in many poor prognostic cancer states (Hogstrand *et al.*, 2009). This placed ZIP7 at a hub for the regulation of cell growth and suggested it as a potential target in a number of diseases in which the prevention of downstream pathways induced by tyrosine kinase activation would be therapeutically important (Hogstrand *et al.*, 2009). Moreover, the requirements of CK2 for the activation of ZIP7 suggested that these two molecules collaborate to mediate zinc signalling, assuming also an important role in cell survival (Taylor *et al.*, 2012).

1.2.3 ZIP7 and breast cancer

Our group have been investigating endocrine resistance in breast cancer for many years, and it was surprising to discover the implication of ZIP7 in this mechanism.

Having the availability in our group of a model of tamoxifen-resistance, it was found that this resistant model exhibited a significant increase in the expression of ZIP7 (Taylor *et al.*, 2007), together with an increase in intracellular zinc (Taylor *et al.*, 2008). It was demonstrated that silencing ZIP7 in this model of tamoxifen resistance prevented activation of EGFR, IGF-1R and Src signalling, all hallmarks of aggressive cancer, which was accompanied by a significant reduction of intracellular zinc (Taylor *et al.*, 2008). This could stem from the capability of zinc to inhibit tyrosine phosphatases (Haase & Maret, 2003), highlighting the important role played by ZIP7 in the mobilisation of zinc in the cytoplasm. Moreover, expression of ZIP7 was shown to be associated with the antigen Ki67, a breast cancer proliferation marker, and to those cancers with high grade lymph nodes spread (Taylor *et al.*, 2007), suggesting its association with aggressive phenotypes of breast cancer. Furthermore, ZIP7 also showed a significant association with STAT3 (signal transducer and activator of transcription 3) (Taylor *et al.*, 2007), a protein which is known for its role as an oncogene (Bromberg *et al.*, 1999).

This evidence together with our recent discovery of the mechanism of ZIP7 activation and associated downstream pathways (Taylor *et al.*, 2012; Nimmanon *et al.*, 2017), paves the way for further analyses in order to understand the correlation between ZIP7 and the development of more aggressive phenotypes in breast cancer.

1.2.4 Zinc transporter ZIP6

ZIP6 (also termed SLC39A6, LIV-1) was the first member of the LIV-1 subfamily to be described. ZIP6 is an oestrogen-regulated gene (Mcclelland *et al.*, 1998) that has been linked to oestrogen receptor-positive breast cancer (Manning *et al.*, 1995), especially those with the capability to spread to the lymph nodes (Mcclelland *et al.*, 1998). In fact, the highest expression of ZIP6 mRNA was seen in the prostate, mammary gland and placenta, which are all controlled and regulated by sex steroid hormones (Taylor *et al.*, 2004).

Moreover, ZIP6 has been demonstrated to cause EMT (epithelial-mesenchymal transition), a crucial event in embryonic development, in a mechanism involving transcription factor STAT3 (Hogstrand *et al.*, 2013). The key event of EMT is the loss of intracellular adhesion together with the required remodelling of the cytoskeleton,

creating a higher predisposition to migration (Kalluri & Weinberg, 2009). The loss of intracellular adhesion is mainly due to the loss of E-cadherin, the main component of adherens junctions, which establishes intracellular adhesion through a mechanism involving Ca^{2+}-dependent homophilic binding (Kalluri & Weinberg, 2009). The expression of E-cadherin is an essential event in tissue organisation and development with alterations of its expression occurring as a consequence of transcriptional repression and often seen during embryogenesis and carcinogenesis (Kalluri & Weinberg, 2009). In particular, in carcinogenesis the loss of E-cadherin can lead to tumour cell migration and invasion, crucial events in tumour progression (Onder *et al.*, 2008). The main transcriptional regulator of E-cadherin is Snail which is implicated in many processes taking place during embryonic development, such as morphogenesis, cell division and mesoderm differentiation (Leptin & Grunenwald, 1990). Snail binds DNA-binding sequences involved within the E-cadherin promoter, leading to the repression of E-cadherin (Cano *et al.*, 2000; Batlle *et al.*, 2000).

ZIP6 is expressed as a pro-protein in the endoplasmic reticulum and it undergoes N-terminal cleavage at a predicted PEST cleavage site (Taylor *et al.*, 2003) before its relocation to the plasma membrane where it can finally mediate zinc transport (Hogstrand *et al.*, 2013) (Figure 1.9). A PEST sequence is a region in the peptide sequence which is rich in proline (P), glutamic acid (E), serine (S) and threonine (T), hence the name PEST. This characteristic is important as it is associated with a protein having a short half-life (Rechsteiner & Rogers, 1996). ZIP6 was demonstrated to drive EMT in a mechanism which involves both the transcription factor STAT3 and Snail (Hogstrand *et al.*, 2013). STAT3 was shown to transactivate the expression of ZIP6 during gastrulation in zebrafish, and ZIP6 was shown to be essential for the nuclear localisation of Snail leading to the repression of E-cadherin (Yamashita *et al.*, 2004). STAT3 is known to have a crucial role in cancer formation and progression (Bromberg *et al.*, 1999; Bromberg, 2002). Many human malignancies have indeed shown increased activation of STAT3, including breast cancer and breast-cancer-derived cell lines (Taylor, Hiscox & Nicholson, 2004). Activation of STAT3 results in the activation of several genes involved in cell proliferation, cell invasion, angiogenesis, metastasis and immune function (Haura, Turkson & Jove, 2005).

Furthermore, the activation of ZIP6 was shown to induce the phosphorylation of GSK3β through a direct mechanism (Ilouz *et al.*, 2002) or through the action of AKT, another kinase activated in response to zinc (Lee *et al.*, 2009). The phosphorylation of GSK3β triggers its inactivation, making it unable to phosphorylate Snail, which remains in the nucleus acting as an E-cadherin transcriptional repressor (Hogstrand *et al.*, 2013) (Figure 1.9). This ability of ZIP6 to cause cell detachment was confirmed in breast cancer cell lines showing an increased population of non-adherent cells which had higher expression of ZIP6 (Hogstrand *et al.*, 2013). All this evidence together suggests how ZIP6 could be an important link between cancer and normal development.

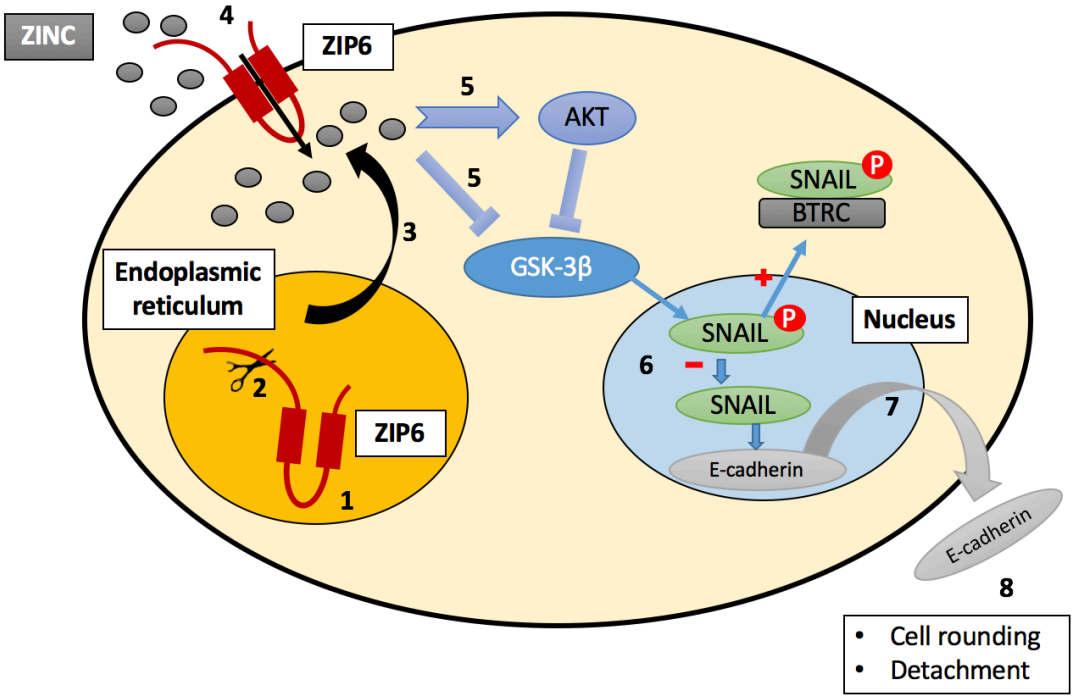

Figure 1.9 ***Schematic of the role of ZIP6 in EMT.***
ZIP6 is expressed as a pro-protein in the endoplasmic reticulum [1] where it undergoes a proteolytic cleavage [2] before being relocated on the plasma membrane [3-4]. The ZIP6-mediated zinc transport leads to the inhibition of GSK-3β, either by a direct mechanism or with the help of AKT, which is activated by zinc as well [5]. The inhibition of GSK-3β leads to the retention of Snail in the nucleus [6] where it acts as a repressor of E-cadherin [7], resulting in cell rounding and detachment [8] (Hogstrand *et al.*, 2013).

1.2.5 Zinc transporter ZIP10

ZIP10 is the most similar homologue to ZIP6 within the LIV-1 subfamily of ZIP transporters, and it resides mainly on the plasma membrane (Lichten *et al.*, 2011). This zinc transporter is known to have an important role in B cell maturation and survival, as a model of a ZIP10 knockout showed a decreased humoral immune response (Hojyo *et*

al., 2014). Moreover, it promotes survival by inhibition of caspase activation, proteins which are essential in the regulation of apoptosis (Miyai *et al.*, 2014). ZIP10 was also found to be involved in skin development via upregulation of p63, a regulator of epidermal progenitor and modulation of zinc intake (Bin *et al.*, 2017).

ZIP10, similarly to ZIP6, was also associated with invasive breast cancer and its metastasis to lymph nodes (Kagara *et al.*, 2007). The expression of ZIP10 and its role in zinc homeostasis involves a STAT3-dependent mechanism, as was also seen for ZIP6. This mechanism involves cytokine stimulation which acts as the first signal for the activation of the JAK-STAT proteins, resulting in zinc mobilisation through the action of ZIP10 (Miyai *et al.*, 2014). ZIP10 was recently found to form a heteromer with ZIP6, which is involved in EMT in breast cancer cells via GSK3β inactivation and downregulation of E-cadherin (Taylor *et al.*, 2016). Moreover, analysis of renal cell carcinoma in comparison to associated normal tissue has revealed a significant increase of ZIP10 expression in the high grade tumour (Pal *et al.*, 2014), highlighting its importance in driving the aggressiveness of renal carcinoma. Considering the involvement of the STAT3 signalling pathway in oncogenesis and the higher levels of ZIP10 expression seen in various types of cancer, it suggests a potentially important role for ZIP10 in cancer (Miyai *et al.*, 2014). ZIP10 expression is upregulated in zinc deficient cells, and downregulated in zinc excess conditions (Lichten *et al.*, 2011). Similar to ZIP6, ZIP10 undergoes a proteolytic cleavage which is essential for its function and which will be discussed in further detail later in this chapter.

1.3 The involvement of zinc transporters in the regulation of the cell cycle

1.3.1 Cell cycle

The cell cycle comprises all those events that prepare a cell for its cell division, also called mitosis. It is divided into four stages called: G1, S, G2 and M phase (Figure 1.10) (Sisken & Morasca, 1965). When a cell is not growing but resting, cells are said to be in G0 phase, also called quiescence (Pardee, 1974). The G1 phase is characterised by cell growth in preparation for DNA synthesis, which happens during S phase. Cell growth is regulated by growth factors which regulate the entry from G0 to G1 (Schafer, 1998). During S phase, the DNA is replicated. This is an important step of the cell cycle, as abnormalities occurring during S phase are one of the main causes of cancer

development (Myung & Kolodner, 2002). The S phase is followed by the G2 phase, which is another step characterised by cellular growth, where cells prepare and synthesise all the molecules necessary for mitosis. Interestingly, the G1 and G2 are so-called "gap phases" to indicate the cellular growth which happens between the DNA replication and the actual cell division (Bohnsack & Hirschi, 2004).

The main protagonists of the regulation of the cell cycle are proteins called cyclins and their correspondent kinases called CDKs (cyclin-dependant kinase), which are essential for cyclin activation (Malumbres, 2011). Other molecules are involved in cell cycle regulation, including CDK inhibitors, transcription factors and kinases involved in the checkpoint of mitosis progression. Each cyclin binds to a specific CDK and their association is essential for the progression of each phase of the cell cycle (Lim & Kaldis, 2013). Cyclins are good indicators of cell cycle progression, as they are required during different phases, and their expression fluctuates throughout the entire cell cycle (Evans *et al.*, 1983) (Figure 1.10). As cyclins do not have any enzymatic activity, they require a kinase to function. Each cyclin and CDK form a complex which has different functions (Lim & Kaldis, 2013). Cyclins D are essential for the regulation of events which happen during the G1 phase and are mainly activated by the CDK4 or CDK6 (Sherr, 1994). These kinases are constitutively expressed, but they only become active when the expression of cyclin D raises during the G1 phase (Matsushime *et al.*, 1994). Cyclin E is mainly expressed at the end of G1 (Lew, Dulić & Reed, 1991) and its main role is to control the progression of cells through G1 and regulate DNA synthesis. Cyclin E is bound to CDK2 (Koff *et al.*, 1991) and this complex is required to phosphorylate and inactivate p27, which is a major inhibitor of the cell cycle (Sheaff *et al.*, 1997). Cyclin A binds both CDK2 and CDK1, and therefore it is essential at two stages of the cell cycle: during the S phase it interacts with specific factors necessary during DNA replication, and during the G2/M transition it activates the complex between cyclin B1 and CDK1 (also known as cdc-2) (Pagano *et al.*, 1992). Cyclin B is the mitotic cyclin which functions in a complex with CDK1. This complex is kept inactive during interphase by phosphorylation of two tyrosine residues. When mitosis is occurring, the cyclin B1/CDK1 complex is activated by the dephosphorylation of CDK1 by phosphatase Cdc25C (Roshak *et al.*, 2000). Activation of the phosphatase Cdc25C is regulated by CDK1 and PLK1, but also by the action of the

kinase Aurora A (Seki *et al.*, 2008; Schmucker & Sumara, 2014). The B1/CDK1 complex is activated before nuclear membrane breakdown and controls the mitotic events in conjunction with PLK1 (Gavet & Pines, 2010a, 2010b; Gheghiani *et al.*, 2017). PLK1 is involved in the maturation of the centrosome by phosphorylating many proteins and recruiting γ-tubulin (Petronczki, Lénárt & Peters, 2008).

The inactivation of cyclins is normally mediated by ubiquitination, which happens as soon as the cyclin-CDK complex is no longer required (Glotzer, Murray & Kirschner, 1991). Moreover, all these mechanisms are tightly controlled by CDK inhibitors which intervene when abnormalities occur. For example, when DNA is damaged the protein p53 is activated, which consequently activates p21 to inhibit cell cycle progression (Bohnsack & Hirschi, 2004).

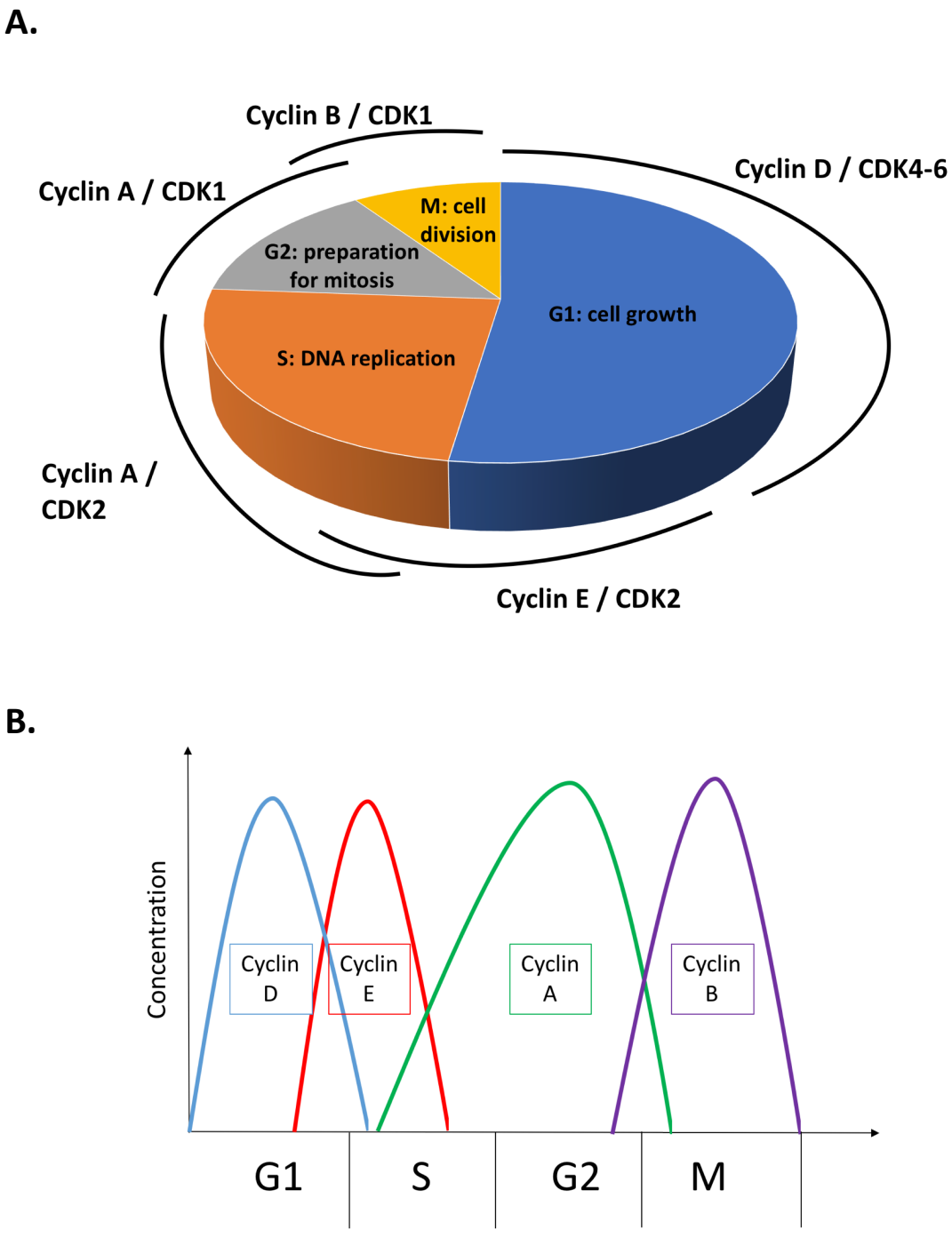

Figure 1.10 ***Cell cycle schematic and cyclins expression.***
A. The cell cycle is divided into 4 phases: G1, S, G2 and M phase. Each phase is regulated by different cyclin-CDK complexes.
B. The expression of the cyclins changes throughout the cell cycle, and each cyclins is synthesised at a specific stage of the cell cycle.

1.3.2 Mitosis

Cell division or mitosis is the culmination of the cell cycle. It occurs when a cell divides into two daughter cells, which is a common feature of development and proliferation. Mitosis is divided into several stages: prophase, prometaphase, metaphase, anaphase and telophase, and ends with cytokinesis (Figure 1.11). During prophase the chromatids condense into chromosomes and this is accompanied by histone phosphorylation (Gurley *et al.*, 1978). The nuclear membrane starts to break down at this point. This series of events is regulated by the complex between cyclin B1/CDK1 and PLK1 (Gavet & Pines, 2010a). The nuclear membrane is completely disrupted during prometaphase, where spindles begin to assemble and it sees the formation of a protein structure called kinetochore that keeps the sister chromatids together (Cleveland, Mao & Sullivan, 2003). The next step is metaphase, where the chromosomes align on one plain. The microtubules create tension, by trying to pull each chromatid to one pole. This event only happens during anaphase, after the spindle checkpoint is passed to make sure that the segregation will not continue until all the chromatids are perfectly aligned (Nasmyth, 2002). Before the final cleavage, the nuclear membrane begins to assemble again around the two groups of chromosomes. This phase is called telophase. The last step of mitosis sees the actual formation of two daughter cells, in a process called cytokinesis (Fededa & Gerlich, 2012).

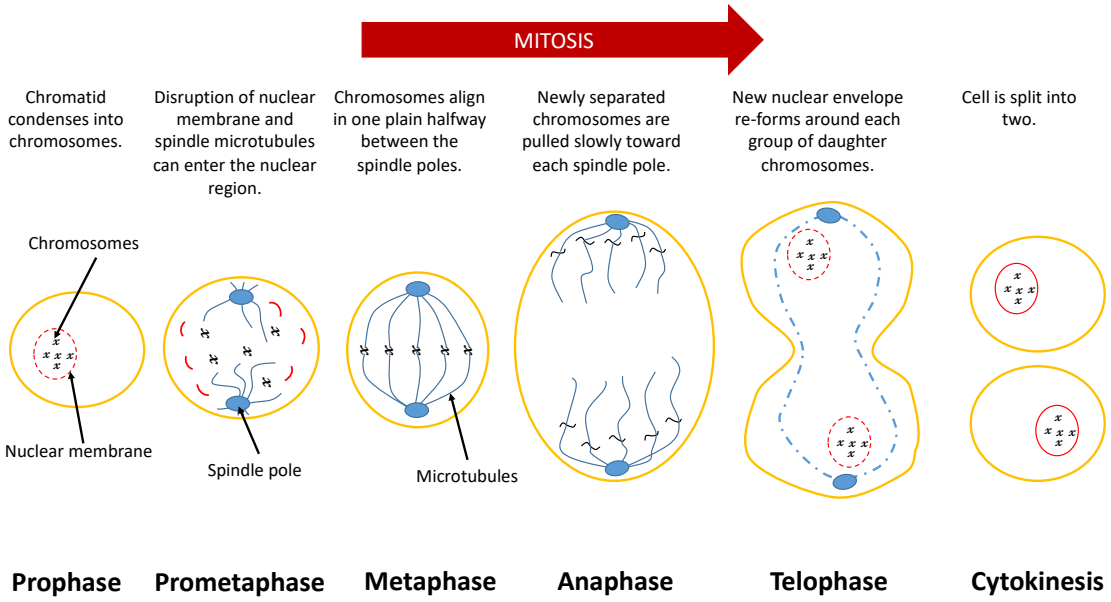

Figure 1.11 ***Mitosis schematic.***
Mitosis is divided into several phases which begins with the breakdown of the nuclear membrane and the separation of the chromosomes, and culminates with the actual separation of the two daughter cells, containing the right chromosomes that were replicated during the S phase.

1.3.3 Requirement of zinc during the cell cycle

The regulation of the cell cycle is dependent on the availability of several nutrients that are required for the progression of the cell cycle. Many vitamins are involved in the regulation of the cell cycle, such as vitamin A, important during embryogenesis (Zile, 1998), or vitamin D, required for the differentiation of certain cells such as keratinocytes or osteoblasts (Bikle, 2011; Van Leeuwen *et al.*, 2011). Other important nutrients include vitamin B12 and folic acid, both required for DNA synthesis (Rotherham *et al.*, 1971), iron, necessary for oxygen transport (Bohnsack & Hirschi, 2004), and glucose, essential for the production of energy in the form of ATP (Newcomb *et al.*, 2003). Another essential nutrient in the regulation of the cell cycle is zinc (Li & Maret, 2009).

The first evidence of zinc requirement during the cell cycle comes from the mid-sixties where studies on rat kidney cortex treated with a metal ion chelator showed that DNA synthesis was suppressed completely and that this mechanism was only reversed by addition of zinc but no other metals (Fujioka & Lieberman, 1964). Moreover, further studies performed with lymphocytes showed that zinc is required during mid-G1 prior to DNA synthesis (Chesters, 1972). The role played by zinc during the G1 phase is to allow the gene expression of cyclin D, thymidine kinase and all of the proteins required for DNA synthesis (Zalewski, 2011). Another important cell cycle stage that requires zinc is during late S phase, as an essential step for cells to progress into G2 (Chesters, Petrie & Vint, 1989). Nevertheless, it is important that the amount of zinc is tightly controlled during this stage, as both an excess of zinc and insufficient zinc can stop cells in G2 at the G2/M checkpoint (Zalewski, 2011). Studies on bronchial epithelial cultures showed that when cells were treated with a high amount of extracellular zinc (32 μM, which corresponds to double the amount of normal human plasma zinc level), they were blocked at the G2/M transition due to the zinc-mediated expression of p53, up-regulation of p21 and consequent inhibition of the complex CDK1/cyclin B (Wong *et al.*, 2008). Furthermore, zinc is necessary for the transcription of cyclins. In fact, it was observed that the expression of cyclins was significantly decreased in zinc-deficient cells, but when zinc was replenished, their expression reverted to normal (Chesters & Petrie, 1999). In particular, in the case of cyclin B, a cyclin essential for the progression of cells in mitosis, adding zinc over normal levels significantly increased cyclin B expression

(Chesters & Petrie, 1999). The specific role of zinc during mitosis is yet to be fully understood, and this project will attempt to provide some insight into this.

1.3.4 The role of ZIP6 and ZIP10 in mitosis

Zinc is essential for the function of several cyclins as it is involved in cell cycle progression (G1 and G2 phases) and essential for progress of cells through G2 and mitosis (Chesters & Petrie, 1999). During the cell cycle, two different peaks of zinc concentration have been observed: a zinc influx from outside the cell occurs at early G1, whereas in the late G1/S phase zinc is released from stores, suggesting the importance of zinc in the control of the cell cycle (Li & Maret, 2009). Most recently, ZIP10 together with ZIP6 were also found to control the zinc uptake during the oocyte to egg transition, which is an essential step in meiosis progression (Kong *et al.*, 2014). This evidence has shined new light into the role of these two zinc transporters in the regulation of cell division.

A recent study in our group has identified zinc in the switch of pTyr^{705}STAT3 to Ser^{727}STAT3, mediated by zinc influx from the plasma membrane (*Taylor et al, unpublished*). Zinc binds STAT3 and it alters its tertiary structure, resulting in disruption of the binding of STAT3 to the JAK2 kinase which stops the Y705 phosphorylation of STAT3 (Kitabayashi *et al.*, 2010). Moreover, our group have demonstrated that ZIP6 and ZIP10 form a heteromer (Taylor *et al.*, 2016), and that the presence of this heteromer increases on the plasma membrane at the beginning of mitosis, leading to the zinc influx responsible for the conversion of STAT3 to pSer^{727}STAT3 (*Taylor et al, unpublished*). This event is followed by the binding of pSer^{727}STAT3 to pStathmin, a regulatory protein which is required for microtubule reorganisation. Most importantly, pSer^{727}STAT3 binds to this heteromer in mitotic cells only, implying that these two zinc transporters are important in the regulation of mitosis. This evidence was observed in breast cancer cell lines, breast cancer tissue and in normal mouse intestine (*Taylor et al, unpublished*), suggesting that this could be a general mechanism that does not only happen in cancer. This new discovery provides a major focus area for much of the investigations within this current project.

1.4 Post translational modification of zinc transporters

1.4.1 Role of phosphorylation

Existing data recognises the importance of phosphorylation in the regulation of the function of several proteins and in particular of zinc transporters (Taylor *et al.*, 2012). Protein phosphorylation is considered the most important post-translational modification. This mechanism involves the addition of a phosphate group to a molecule which is followed by its conformational change in order to interact with other substrates (Ardito *et al.*, 2017). Phosphorylation is mainly used as a trigger for the activation of downstream pathways in cells, hence its crucial role in the body. Phosphorylation is mediated by kinases which act as mediators in the exchange of the phosphate group (Li *et al.*, 2013). Most proteins are phosphorylated on serine, threonine or tyrosine residues, with serine residues having the highest percentage of phosphorylation in the human genome (Nishi, Hashimoto & Panchenko, 2011). Despite tyrosine phosphorylation counts for less than 2% in proteins, it still plays an important role in cell biology (Olsen *et al.*, 2006). Phosphorylation is essential in cells to regulate events such as development, aging, cell cycle, protein synthesis and signal transduction. This mechanism is possible thanks to the combined action of kinases and phosphatases (Ardito et al. 2017). While kinases transfer the phosphate group to a protein, the role of the phosphatase is opposite, removing the phosphate group via hydrolyzation (Johnson, 2009). The human genome contains over 586 kinases and 156 protein phosphatases. The availability of different database tools have predicted that almost 90% of human proteins undergo phosphorylation (Ardito et al. 2017). The activation of this post-translational modification acts as a molecular switch and dysfunction of this mechanism can lead to aberrant activation or dysregulation of several signalling pathways that can result in oncogenesis and cancer development (Harsha & Pandey, 2010). The cell cycle is an important event in human biology which is driven by phosphorylation (Fisher *et al.*, 2012) and, as a consequence of this, any abnormalities in the regulation of this mechanism can lead to abnormal cell growth, one of the hallmarks of cancer.

The discovery of the CK2-mediated phosphorylation of ZIP7 as an essential requirement for its activation (Taylor *et al.*, 2012) has shined a new light on a new area of study in zinc biology which could help decipher how these zinc transporters are regulated. As stated in this chapter, the mechanism by which the ZIP transporters are

activated is not clear yet, and despite the fact that they are normally referred to as transporters, the discovery of ZIP7 activation by phosphorylation suggests that they may in fact act as channels (Taylor *et al.*, 2012). ZnT6, a member of the ZnT family, was found to have a serine in the cytoplasmic C-terminal domain with the potential to be phosphorylated. This phosphorylation is predicted to be essential in the regulation of the zinc transport mediated by the ZnT5-ZnT6 heteromer (Hogstrand *et al.*, 2009; Fukunaka *et al.*, 2009). Beyond ZIP7, no other ZIP member has been confirmed to be activated by phosphorylation yet. However, since ZIP6 and ZIP10 were found to be essential at the onset of mitosis (*Taylor et al, unpublished)*, and since mitosis is driven by phosphorylation (Dephoure *et al.*, 2008), there is a high chance that these two zinc transporters are regulated in mitosis by phosphorylation as well. Part of this project aims to decipher this.

1.4.2 Role of protein cleavage

Protein cleavage is a ubiquitous event which occurs in proteins, and results in the breakdown of proteins in smaller pieces leading to the formation of new proteins with a new C-terminus and/or N-terminus. This mechanism leads to activation, deactivation or acquisition of a completely different function of the protein, which is often used as a regulatory mechanism (Barret, Rawlings & Woessner, 1998). This is another important post-translational modification which takes place in cells for the regulation of important processes such as cell cycle, cell death, cell proliferation or even cancer and inflammation (Rogers & Overall, 2013). For example, the degradation of cyclins during the cell cycle is mediated by ubiquitin-mediated proteolysis (Glotzer, Murray & Kirschner, 1991). Moreover, the removal of certain domains, such as nuclear localisation signal, or ectodomain-shedding regulate localisation of proteins or convert them into their active form (Klein *et al.*, 2018). In fact, many proteins are initially synthesised as inactive pro-proteins which are then cleaved in order to generate the active and mature molecule (Duckert, Brunak & Blom, 2004). This mechanism is mediated by proteases which comprise a wide number of proteins in humans (Puente *et al.*, 2003) and many drugs targeting these proteins are available in therapy (Turk, 2006).

A good example of a protein which requires cleavage in order to be activated is ZIP6. Hogstrand *et al* showed that ZIP6 is expressed as a pro-protein in the endoplasmic reticulum, before it undergoes a proteolytic cleavage which leads to its relocation to the plasma membrane. This proteolytic cleavage is essential for its active function (Hogstrand *et al.*, 2013). Prior to that, it was discovered that ZIP4, another member of the LIV-1 subfamily of zinc transporters, was proteolytically cleaved on its N-terminal domain in zinc deficiency conditions (Kambe & Andrews, 2009). Moreover, in this conditions, ZIP4 is accumulated on the apical surface of epithelial cells while it is internalised and degraded in normal conditions. This is an example of how proteolytic cleavage manages protein localisation and function (Kambe & Andrews, 2009).

ZIP6 contains a PEST cleavage site on its N-terminal domain which is a peptide sequence associated with proteins undergoing proteolytic cleavages and having a short half-life (Rechsteiner & Rogers, 1996). ZIP10 is the only other member of the LIV-1 family to contain a PEST cleavage site in the N-terminus (Hogstrand *et al.*, 2013), suggesting that it also undergoes a cleavage process which has been confirmed by Ehsani et al (Ehsani *et al.*, 2012). Interestingly the prion protein, a protein involved in neurodegenerative diseases of humans and animals, was shown to have descended from the LIV-1 subfamily of ZIP transporters and to have similarities especially with the amino acid sequences of ZIP6 and ZIP10 (Schmitt-Ulms *et al.*, 2009). It is known that the prion protein undergoes several endoproteolytic cleavages on its ectodomain (Vincent *et al.*, 2001; McMahon *et al.*, 2001; Altmeppen *et al.*, 2012) and recent studies have demonstrated that the prion protein undergoes N-terminal ectodomain shedding in zinc-depleted conditions, similar to that observed for ZIP10 (Ehsani *et al.*, 2012). The similarities of this protein to members of the LIV-1 subfamily of zinc transporters suggests that their N-terminal cleavage can be essential for their functional control. Interestingly, ZIP6 and ZIP10 are found in the same branch of the phylogenetic tree as shown in Figure 1.3, suggesting a similar function and regulation. This, together with the importance of proteolytic cleavage in the regulation of cell cycle progression (Rogers & Overall, 2013), suggests the possibility that ZIP6 and ZIP10 require this proteolytic cleavage in order to translocate to the plasma membrane and to provide the zinc necessary to trigger mitosis.

The importance of both phosphorylation and proteolytic cleavage in the regulation of mitosis (Glotzer, Murray & Kirschner, 1991; Dephoure *et al.*, 2008) provides an area of investigation that will be discussed in this project with the aim of deciphering the mechanism by which ZIP6 and ZIP10 are regulated in mitosis.

1.5 Hypotheses, aims and objectives of this project

Our group have been investigating the role of zinc signalling in breast cancer for many years and, in particular, it was discovered that three zinc transporters belonging to the LIV-1 subfamily were overexpressed in breast cancer: ZIP7, ZIP6 and ZIP10 (Taylor *et al.*, 2003, 2008; Kagara *et al.*, 2007). However, it still remains elusive how these transporters are responsible for the development of an aggressive phenotype of breast cancer or whether targeting these could be beneficial in breast cancer therapy. This project started from few recent discoveries in our group by trying to address these questions and has expanded this investigation beyond breast cancer.

1.5.1 Hypotheses

The hypotheses of the current project were:

1. Activated ZIP7 can be used as a biomarker of acquired endocrine resistance in breast cancer;
2. Inhibition of the ZIP6-ZIP10 heteromer on the plasma membrane is able to block the zinc influx necessary for mitosis and stop cell division;
3. ZIP6 and ZIP10 require phosphorylation and proteolytic cleavage in order to be activated during mitosis.

1.5.2 Aims

The overall aims of this project were:

1. To characterise the activation of ZIP7 in anti-hormone resistant breast cancer and investigate whether its activation changed with prolonged exposure to endocrine therapy;
2. To analyse the effectiveness of ZIP6 and ZIP10 antibodies at preventing cell division and to dissect the mechanism involved;
3. To investigate predicted phosphorylation and cleavage sites for ZIP6 and ZIP10 and to test whether these transporters require phosphorylation in order to influx zinc and trigger mitosis.

1.5.3 Objectives

The hypotheses and aims of this project were explored by setting the following objectives:

1. To investigate activated ZIP7 by using the group's unique anti-pZIP7 antibody (Nimmanon *et al.*, 2017) and to expand this study to endocrine resistant breast cancer cell models and breast cancer clinical samples;
2. To inhibit the ZIP6-ZIP10 heteromer by using specific antibodies towards the N-terminal domain of ZIP6 and ZIP10 and to expand this analysis to different cancer cell lines while analysing the fate of cells when treated with these antibodies;
3. To use different website database tools along with specific kinase and protease inhibitors to be tested on specific recombinant zinc transporter mutants in order to check and analyse potential phosphorylation sites for ZIP6 and ZIP10, and to discover the protease involved in ZIP6 cleavage.

2 MATERIALS AND METHODS

2.1 Cell growth and tissue culture

MCF-7 cells (human breast adenocarcinoma cells), a gift from AstraZeneca (Macclesfield, UK), and MDA-468 cells (triple negative breast cancer cell line) were cultured in RPMI (Roswell Park Memorial Institute) (Gibco, UK) with 5% foetal calf serum (FCS), 200 mM L-glutamine, antibiotics (10 IU/ml penicillin, 10 µg/ml streptomycin) and fungizone (2.5 µg/ml amphotericin B) (Gibco). All the anti-hormone resistant cell lines were cultured in phenol-red-free RPMI medium (Gibco) with 5% stripped steroid-depleted FCS, 200 mM L-glutamine and antibiotics (10 IU/ml penicillin, 10 µg/ml streptomycin and 2.5 µg/ml amphotericin B). They were grown in phenol-red free medium as phenol-red has been reported to have an oestrogenic effect. Stripped serum was added to the medium to remove any hormones that might alter the results. Tamoxifen-resistant MCF-7 derived cells (TamR) and long-term tamoxifen-resistant MCF-derived cells (TamRL) were cultured in the presence of 10^{-7} M 4-OH-tamoxifen, whereas Faslodex®-resistant MCF-7-derived cells (FasR) and long-term Faslodex®-resistant MCF-7-derived cells (FasRL) were cultured in the presence of 10^{-7} M Faslodex®.

CaCO-2 (colorectal adenocarcinoma) and NMuMg (mouse breast glandular) cells, were grown in Dulbecco's Modified Eagle's Medium (DMEM) (Gibco) containing 4.5 g/L glucose supplemented with 10% foetal calf serum (FCS), 200 mM L-glutamine, antibiotics (10 IU/ml penicillin, 10 µg/ml streptomycin) and fungizone (2.5 µg/ml amphotericin B) (Gibco). The NMuMg ZIP6 knockout cells have ZIP6 removed using the CRISPR/Cas9 technique (Brethour *et al.*, 2017).

All cells were kept at 37 °C in a 5% $C0_2$ atmosphere and the medium was changed every 3-4 days. A summary of all the different cell lines used in this project and their corresponding medium is found in Table 2.1. For western blot or immunofluorescence 1 or 3x 10^5 cells were seeded into 35 and/or 60 mm dishes, respectively. Furthermore, when the cells were required for immunofluorescence, a 22x22 mm 0.17 mm thick glass coverslip was placed in the dish or they were seeded into an 8 well chamber slide (Nunc, Denmark) adding 1.5x 10^4 cells per well. Briefly, cells in a T25 flask were trypsinised for a couple of minutes, then the same amount of medium was added to stop the lysis reaction. Cells were spun down and resuspended in appropriate medium after counting using a cell Coulter counter.

Cell line	*Growth medium*	*FCS*	*Antibiotics and antifungals*	*Other supplements*
MCF-7	RPMI 1640	5%	penicillin, streptomycin, amphotericin B	L-glutamine
TamR/TamRL	WRPMI	5% stripped serum	penicillin, streptomycin, amphotericin B	L-glutamine + tamoxifen
FasR/FasRL	WRPMI	5% stripped serum	penicillin, streptomycin, amphotericin B	L-glutamine + Faslodex®
MDA-468	RPMI 1640	5%	penicillin, streptomycin, amphotericin B	L-glutamine
CaCO-2	DMEM	10%	penicillin, streptomycin, amphotericin B	Glucose + L-glutamine
NMuMg (wild type and ZIP6 ko)	DMEM	10%	penicillin, streptomycin, amphotericin B	Glucose + L-glutamine

Table 2.1 ***Cell lines used in this project and their corresponding medium.***

2.1.1 Development of TamR (Tamoxifen-resistant MCF-7 derived cell line)

The MCF-7 monolayers were grown in phenol-red-free RPMI medium containing 5% charcoal-stripped steroid-depleted foetal calf serum, antibiotics, fungizone, glutamine (200 mM) and 4-hydroxytamoxifen (10^{-7} M in ethanol) (see Table 1). The cells were continually exposed to this treatment for six months. The medium was continually replaced every 3-4 days. Cell growth analysis revealed that wild type MCF-7 had a 60% reduced growth after 2 weeks of treatment with 100 nM of 4-hydroxytamoxifen. The cell growth of this cell line remained static for the next 2 months after which time the cell growth started to increase to a level similar to the wild type MCF-7 cells grown in the absence of 4-hydroxytamoxifen. This was the point at which the cells started to develop resistance to tamoxifen and were renamed TamR (Knowlden *et al.*, 2003). The cellular morphology of these cells was remarkably changed in comparison to wild type MCF-7 cells, showing angular shapes and a more disorganised growth. Before further investigation, this new cell line was cultured for a further four months in the presence of 4-hydroxytamoxifen (Knowlden *et al.*, 2003). Confirmation of the resistant phenotype was performed by assessment of the proliferation of MCF-7 and TamR cells grown in the

presence of 4-hydroxytamoxifen by comparison of growth curves. This investigation revealed that in the presence of 4-hydroxytamoxifen the growth rate of TamR cells was significantly higher than MCF-7 cells, up to 200% after 13 days of proliferation. Moreover, while the wild type MCF-7 grown in the presence of the antioestrogen showed a decreased growth rate in a concentration-dependent manner, TamR cells showed no reduction of cell growth even at highest concentration of 1 μM 4-hydroxytamoxifen (Knowlden *et al.*, 2003). Additionally, a long-term resistant model called TamRL was developed from TamR cells, following a prolonged exposure (36 months) to tamoxifen (Gee *et al.*, 2015).

2.1.2 Development of FasR (Faslodex®-resistant MCF-7 derived cell line)

Similar to the development of the TamR cells, MCF-7 cells were continuously exposed to fulvestrant (Faslodex®, ICI 182,780; a gift from Dr Alan Wakeling, AstraZeneca Pharmaceuticals, Macclesfield, UK) in phenol-red-free RPMI medium containing 5% charcoal stripped steroid-depleted foetal calf serum supplemented with glutamine, antibiotics, fungizone and Faslodex® (10^{-7} M in ethanol). Initially the cell growth of this cell line was static and there was no requirement to passage flasks when confluent. The medium was continually replaced every 3-4 days. After 3 months these cells started to grow, reaching a growth rate similar to that of MCF-7 cells grown in the absence of Faslodex®. Cells were cultured for further 3 months with fulvestrant, eventually leading to the establishment of a new resistant cell line renamed FasR (McClelland *et al.*, 2001). Characterisation of the resistant cell line was performed by comparison of growth curves of FasR cells and wild type MCF-7 grown in the presence of Faslodex®, which showed that the FasR cells had a sustained increased growth rate in comparison to MCF- 7 cells. Moreover, basal growth of FasR cells was sustained even in the presence of the highest concentration of Faslodex® (10^{-5} M), whereas MCF-7 cell growth was significantly affected by the presence of the antioestrogen ($p<0.001$). In fact, the sensitivity of wild type MCF-7 cells to the antiproliferative effect of Faslodex® was detectable even at concentration of 10^{-9} M, exhibiting a 50% reduction after 7 days of treatment in comparison to non-treated control cells. On the contrary, FasR cell growth was insensitive to the reagent (McClelland *et al.*, 2001). Additionally, a long-term resistant model called FasRL was developed from FasR cells, following a prolonged

exposure (36 months) to Faslodex® (Gee *et al.*, 2015).

2.1.3 Development of NMuMg ZIP6 knockout cells

The development of the NMuMg ZIP6 knockout cells was performed by Schmitt *et al* in Canada and they have been fully characterised for the loss of ZIP6. Briefly, wild type NMuMg cells (mouse mammary gland) were transfected with a construct which coded for a Cas9-D10A nickase with a pair of RNAs that guided the nickase to off-set target sites on opposite DNA strands within Exon-2 of the ZIP6 gene (Brethour *et al.*, 2017). This resulted in the generation of a double-strand break on the gene which was followed by a non-homologues end-joining program. The clones were isolated by the dilution method and presence of ZIP6 was detected by western blotting following TGFβ1 treatment. Characterisation of the ZIP6 knockout clone in comparison to NMuMg wild type cells by western blotting revealed that wild type cells induced by TGFβ1 had a significant increase of ZIP6 protein levels, whereas no ZIP6 was found on the ZIP6 knockout clone. Further characterisation by PCR and sequencing of the NMuMg ZIP6 knockout clone revealed a two nucleotide deletion in both ZIP6 alleles which had generated the formation of the STOP codons due to the shift of the open reading frame (Brethour *et al.*, 2017).

2.2 Cell treatments

A. For cell cycle synchronisation, three different methods were used:
    i) Nocodazole: cells were treated with 150 nM nocodazole (Sigma Aldrich, USA) for 20 hours to synchronise cells into mitosis. Nocodazole is an anti-neoplastic agent that interferes with the polymerisation of microtubules (Blajeski *et al.*, 2002). Cells treated with it arrested at M phase and so they entered mitosis but they arrested in prometaphase (phase after interphase, before metaphase) (see Figure 1.11) because the microtubules were not able to polymerise (Blajeski *et al.*, 2002).
    ii) Double thymidine block: cells at 25-30% confluence were washed twice with 1X PBS and added of medium (RPMI + 5% FCS + 1% pen-strep) containing 2 mM thymidine (Sigma Aldrich) for 18 hours. After this time, cells were released from the first thymidine block by replacing the treatment with fresh medium (RPMI + 5% FCS + 1% pen-strep) for 9 hours, after which 2 mM

thymidine was re-added for another 17 hours. Cells were washed with 1X PBS and left in fresh medium to progress through the cell cycle (Whitfield *et al.*, 2000). After the two thymidine blocks, the cells progressed synchronously through G2 and M phase. A double thymidine block allowed cells to arrest at the beginning of S phase and were then allowed to proceed through the cell cycle. After the second thymidine block, cells were harvested at different times: between 5 to 10 hours.

iii) CDK1 inhibition: cells were synchronised in G2 by treatment with 9 μM RO-3306 (Sigma Aldrich), a CDK1 inhibitor, for 18 hours. Cells treated with this agent stopped at the G2 phase of the cell cycle as RO-3306 inhibits the complex between cyclin B1 and CDK1 (also known as cdc2) which is necessary for the progression of cells into mitosis (Vassilev *et al.*, 2006). After being released from this agent, cells were either left to progress naturally through M phase for 2 hours, or treated with nocodazole (150 nM) for 2 hours to increase the number of mitotic cells.

B. To induce cells into apoptosis, cells were treated with 5 μM camptothecin (Sigma Aldrich) for 20 hours before harvesting. Camptothecin is a topoisomerase I inhibitor which binds DNA and prevents the reassociation of DNA after the cleavage induced by topoisomerase I (Wall & Wani, 1996). Treatment with camptothecin stopped cells in S phase and induced most cells into apoptosis.

C. Cells were also treated with ZIP6 Y3/Y1 (mouse monoclonal antibody, in house) or ZIP10 R (rabbit polyclonal antibody, in house) (see Table 2.4) for 20 hours at different concentrations in order to detect whether these extracellular N-terminal domain antibodies were able to block mitosis. Additionally, cells were treated with ZIP6 Y3/Y1 after 24 hours from seeding (day 0) and counted for 4 days using an automated cell counter (Beckman Coulter™) in order to assess the effect of this treatment on cell growth. Treatment of cells with 4 μg/ml of normal mouse IgG or 10.5 μg/ml normal rabbit IgG with 150 nM nocodazole was used as a negative control.

D. For the investigation of potential phosphorylation of ZIP6 at different residues on the long intracellular loop domain (more details in Chapter 6), cells were treated with 10 μM of CX-4945 (Silmitasertib, CK2 inhibitor, Abcam) or 1 μM AZD0530 (Saracatinib, Src inhibitor, Sigma Aldrich) for 1 hour prior to harvesting after 17 hours of cell transfection.

E. To analyse ZIP6 proteolytic cleavage, cells were treated with DAPT, a presenilin inhibitor (Morohashi *et al.*, 2006), at 10 μM for 20 hours and compared to cells that had been synchronised with nocodazole alone. Moreover, in order to see whether cells that were synchronised in mitosis were affected by the presenilin inhibitor treatment, cells were treated with both 150 nM nocodazole and 10 μM DAPT for 20 hours.

2.3 Immunofluorescence

Cells at 70-80% confluence on 22x22-mm glass coverslips with 0.17 mm thickness, or on the 8 well chamber coverslide, were moved into racks and fixed with 3.7% formaldehyde (Sigma Aldrich) in PBS for 15 minutes. The fixing was necessary to preserve the structures and to immobilise antigens. The coverslips were then washed twice with PBS for 5 minutes and incubated for 15 minutes with permeabilisation buffer made of PBS with 1% BSA (Sigma Aldrich) and 0.4% saponin (Sigma Aldrich). The coverslips were then blocked with 10% normal goat serum (DAKO, UK) in permeabilisation buffer for 15 minutes to prevent non-specific binding of the secondary antibodies. After having been probed with primary antibodies for an hour in a wet chamber, coverslips were incubated for 30 minutes with secondary antibodies, consisting of goat anti-mouse and/or goat anti-rabbit antibodies conjugated with Alexa Fluor 488 or 594 (Molecular Probes, Invitrogen, USA) and protected from light. The coverslips were mounted on microscope slides with Vectorshield mounting medium with DAPI (Vector Laboratories, USA) and sealed with nail polish. Cells were visualised on a Leica RPE automatic microscope using a 63x oil immersion lens with a multiple bandpass filter for DAPI, Texas Red and fluorescein. The pictures were acquired and processed using Openlab software for Macintosh operating system with one-level of deconvolution. Image processing and cell counting were performed using ImageJ

software.

2.4 Immunohistochemistry

Cell pellets of the different breast cancer resistant cells line were available from the Breast Cancer Molecular Pharmacology Group. For the clinical samples, 93 breast cancer samples from patients were used, which were obtained from Nottingham University (NRES active, ethical approval C2020313/Nottingham city hospital, see Appendix 2). These clinical samples belong to the "Cell Signalling Series". The clinical samples and cell pellets corresponded to pre-cut 4 μm sections. The cell pellets or clinical samples were formalin-fixed, embedded in paraffin and mounted onto slides, then washed in xylene and different concentrations of ethanol (from 100% to 70%) in order to rehydrate the sample. The first retrieval condition which was attempted (pH 6 Sodium Citrate buffer and pressure cooking microwave at 950 W for a minute followed by 9 minutes at 560 W) was not reliable as it did not show any significant staining across the different cell lines, resulting in negative staining. After trying different retrieval conditions, the optimal condition for phospho-ZIP7 (pZIP7) assay was pH 8 EDTA and a pressure cooking microwave at 950W for 2 minutes using the pZIP7 antibody (Table 2.4). Following the establishment of the right retrieval condition, the best antibody dilution was then sought. This was an essential step in order to have the best and reliable assessment of pZIP7 across the cell pellets and clinical samples, but also to reduce the background signal which could alter the final results. Similar to the establishment of the optimal retrieval condition, many dilutions were tried before eventually finding the most appropriate. The optimal dilution found for pZIP7 on cells pellets was 1/8000 and 1/800 dilution for breast cancer tissue. It is noticeable that the concentration of pZIP7 was higher in the clinical samples due to the more complex structure of the tissue and therefore the difficulty to unmask the epitope. The samples were washed with PBS/Tween 0.02% and covered with 0.18% hydrogen peroxidase before blocking with a drop of goat serum blocking reagent (DAKO, UK) for 20 minutes. The pZIP7 antibody incubation was carried out for an hour at room temperature for the cell pellets, whereas the tissue samples were left overnight at 23°C. The slides were then washed twice with PBS/Tween 0.02% and probed with secondary antibody (Mouse Envision labelled polymer-HPR #K4001, DAKO) for 30-60 minutes followed by another two washes with TBS/Tween 0.05%. The protein of interest was visualised using DAB (3'-3'-

diamobenzidine, DAKO) while nuclei were counterstained with methyl green 0.05%. The slides were then fixed with coverslips using DPX Mountant for histology and visualised on an Olympus BH-2 microscope at 20x magnification. As the "Cell Signalling series" is a historical series, clinicopathological and biomarker data was available in an SPSS database.

The immunostaining of the specimens was evaluated by consensus of two personnel viewing the slide at the same time through a dual-visual attachment to the microscope and by using a scoring system of 0, 1, 2 and 3 which corresponds to negative, weak, intermediate and strong staining, respectively. The HScore was evaluated using the following equation, which gives a value on a scale from 0 to 300 (Nicholson *et al.*, 1994):

$$HScore = [(\%\ cells\ showing\ an\ intesity\ value\ 1 \times 1) + (\%\ cells\ showing\ an\ intesity\ value\ 2 \times 2) + (\%\ cells\ showing\ an\ intensity\ value\ 3 \times 3)]/100$$

2.5 SDS-PAGE and Western Blot

Cells at 70-80% confluence, seeded in 35 or 60 mm dishes, were harvested using 100 or 200 µl of lysis buffer, respectively. Lysis buffer consists of 50 mM Trizma Base [pH7.6], 150 mM sodium chloride, 5 mM EGTA and 1% Triton X−100 containing a 1/10 dilution of a protease-inhibitor cocktail (Sigma Aldrich), 2 mM sodium orthovanadate and 50 mM sodium fluoride. The samples were left on ice for an hour with periodic agitation and centrifuged at 12000 rpm (13684 g) at 4°C. The supernatant was collected in a new clean tube and the pellet was discarded. The concentration of the lysates was determined with a BioRad Microassay procedure based on the Bradford protein assay. This method consists of the binding of a dye, Coomassie Brilliant Blue G-250, to the proteins forming a complex which is revealed at a wavelength of 595 nm with a UV spectrophotometer (Bio 35 Spectrometer). The lysate protein concentration was determined against a standard solution (solution of BSA, 1 mg/ml stock). The lysates were diluted with loading buffer containing 0.2 M DTT (Roche, Switzerland) to a final concentration of 1 µg/µl and were denaturated by heating at 100°C for 5 minutes, followed by a brief spin at 12000 rpm (13684 g) to deposit the condensate and insoluble material that formed during heating. The samples were used immediately or stored at

- 20°C until use. The concentration of the gels used for SDS-PAGE depended on the molecular range of the proteins of interest. In this project either a 7.5%, 10% or 14% resolving gel with either a 15 or 10 well comb (Table 2.2-2.3) was used.

Table 2.2 ***Recipes for resolving gel.***

Reagent (resolving gel)	units	7.5%	10%	14%
Distilled H_20	ml	9.6	8	5
TRIS-HCl buffer, pH 8.8	ml	5	5	5
30% Acrylamide	ml	5	6.8	9.52
10% SDS	µl	200	200	200
10% APS	µl	200	200	200
TEMED	µl	12	12	12

Table 2.3 ***Recipe for stacking gel.***

Reagent (stacking gel)	units	5% (3 x 1.5 mm gel)
Distilled H_20	ml	6.1
TRIS-HCl buffer, pH 6.8	ml	2.5
30% Acrylamide	ml	1.3
10% SDS	µl	100
10% APS	µl	50
TEMED	µl	10

The samples (20 or 40 µg each) were loaded into the wells and the gel electrophoresis was run at 120 V for 90 minutes. The proteins were transferred by electrophoresis to a 0.45 µm nitrocellulose membrane (GE Healthcare Life Sciences, UK) at 100 V for 60 minutes. For the transfer, a "sandwich" was made following the scheme shown in Figure 2.1. Following the transfer, the nitrocellulose membrane was stained with 1% Ponceau S (Sigma Aldrich) in 5% acetic acid to check if the transfer was successful and whether each lane was evenly loaded. Furthermore, it was possible to see if there were any bubbles or imperfections on the transfer that may alter the final results. The Ponceau S was easily removed later with TBS-Tween 1X on a rocking platform.

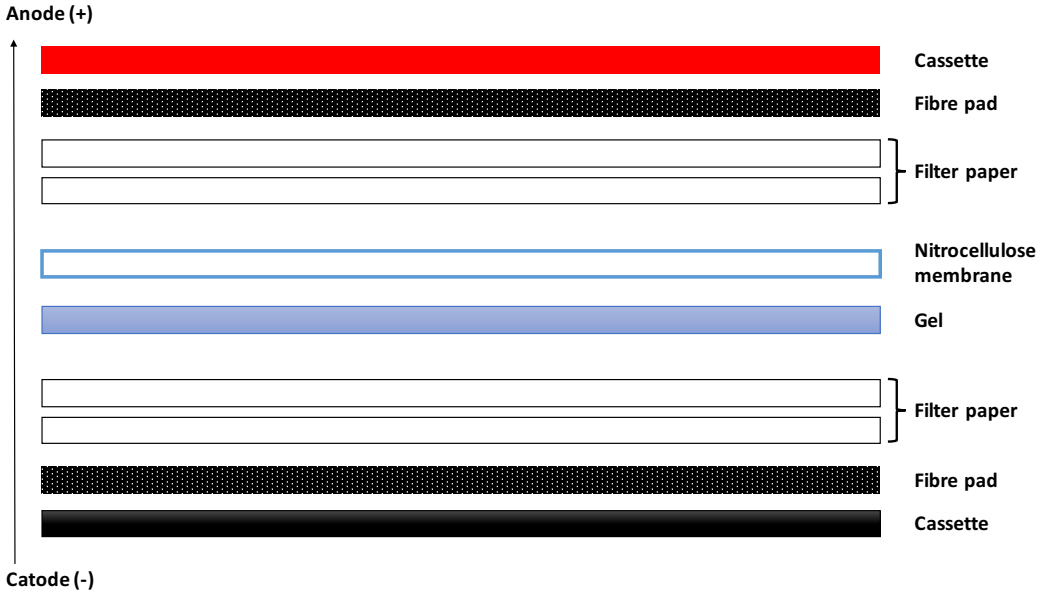

Figure 2.1 ***Diagram showing the transfer blotting "sandwich".***

Following the Ponceau S stain, the membrane was incubated for 1 hour with 5% non-fat dried milk (Marvel, Premier Internationals Foods, UK) in TBS-Tween 1X at room temperature to prevent non-specific binding of antibodies to proteins and to the membrane during the assay. The Marvel was washed away with TBS-Tween 1X on a rocking platform, then the membrane was transferred into a Falcon tube containing the solution of primary antibody. The solution was made with TBS-Tween 1X containing 5% Western Blocking reagent (Roche), 1 mM sodium azide (NaN_3) and the primary antibody at the required concentration (Table 2.4-5). The membrane was incubated with primary antibody overnight at 4°C on a roller-bed, followed by washing and incubation with secondary antibodies conjugated with horse-radish peroxidase (HRP) (Table 2.6), according to the species from which the primary antibody was made. Incubation with secondary antibodies was carried out for an hour at room temperature on a roller-bed. The secondary antibody solution was made up with 1% Marvel in TBS-Tween 1X.

For the apoptosis evaluation experiment, cells were probed with an apoptosis kit of antibodies which allowed the detection of apoptosis markers simultaneously, including cleaved PARP, pro-caspase 3 and cleaved caspase together with β-actin for normalisation.

The detection of the protein of interest was made using a chemiluminescent kit. This technique relied on the oxidation of the luminol substrate in the presence of the

enzyme HRP, which was conjugated to the secondary antibody and hydrogen peroxidase. The reaction allowed the emission of photons of light which could be captured by exposure to the X-ray film in a dark room. ECL (Thermo Scientific, USA), Clarity (Bio-Rad, USA) and Femto (Thermo Scientific, USA) chemiluminescent reagents were used for the immunodetection. The bands obtained were then analysed by densitometric analysis using Alpha DigiDoc software version 4.10 or ImageJ. Results were analysed with the Microsoft Excel 2016 programme for Macintosh OS and normalised to the results of β-actin or GAPDH level, obtained using a β-actin or GAPDH-HRP-conjugated antibody (Science Signaling, USA). The measurement of β-actin or GAPDH was required as a control to determine whether the samples have been loaded equally in all the wells. It is common to use β-actin or GAPDH because they are equally expressed in human cells and they are less affected by any cell treatments.

Table 2.4 ***ZIP antibodies.***

ANTIBODY	Species	Source	WB	IF	Other
pZIP7[a]	mouse	Biogenes (in house)	1:1000	1:100	
ZIP7[b]	rabbit	ProteinTech 19429-1-AP	1:1000		
ZIP7 B[c]	rabbit	Biogenes (in house)	1:1000		
ZIP10 R[d]	rabbit	Biogenes (in house)	1:1000	1:100	1:10-1:100 (cell treatment)
ZIP6 Y3/Y1[e]	mouse	Biogenes (in house)	1:1000		1:10-1:100 (cell treatment)
ZIP10[f]	rabbit	Abcam ab83947	1:1000		
ZIP10[g]	mouse	Sigma Aldrich SAB1401780	1:1000		
LIV-1 (E-20)[h]	rabbit	sc-84875, Santa Cruz Biotechnology, INC	1:500	1:100	1:50 (PLA)
ZIP4[i]	rabbit	ProteinTech 20625-1-AP		1:100	

The table indicates the species, the dilution used for the different techniques and the supplier. Additional information for the antibodies epitopes:

a) *pZIP7: the epitope is pS275-pS276 (TM III-TM IV)*

b) *ZIP7 ProteinTech™: the epitope is between the residues 236-383 (TM III-TM IV)*

c) *ZIP7 B: the epitope is between the residues 264-277 (TM III-TM IV)*

d) *ZIP10 R: the epitope is LEPSKFSKQAAENE (residues 46-59) at the N-terminus (Figure 2.2B)*

e) *ZIP6 Y3/Y1: the epitope is VSEPRKGFMYSRNTNEN (residues 238–254) at the N-terminus (Figure 2.2A)*

f) *ZIP10: the epitope is between the residues 514-530 (TM III-TM IV) (Figure 2.2B)*

g) *ZIP10: the epitope is between the residues 515-622 (TM III-TM IV) (Figure 2.2B)*

h) *LIV-1 (E-20): the epitope is between the residues 500-550 (TM III-TM IV) (Figure 2.2A)*

i) *ZIP4: the epitope is between the residues 23-327 at the N-terminus*

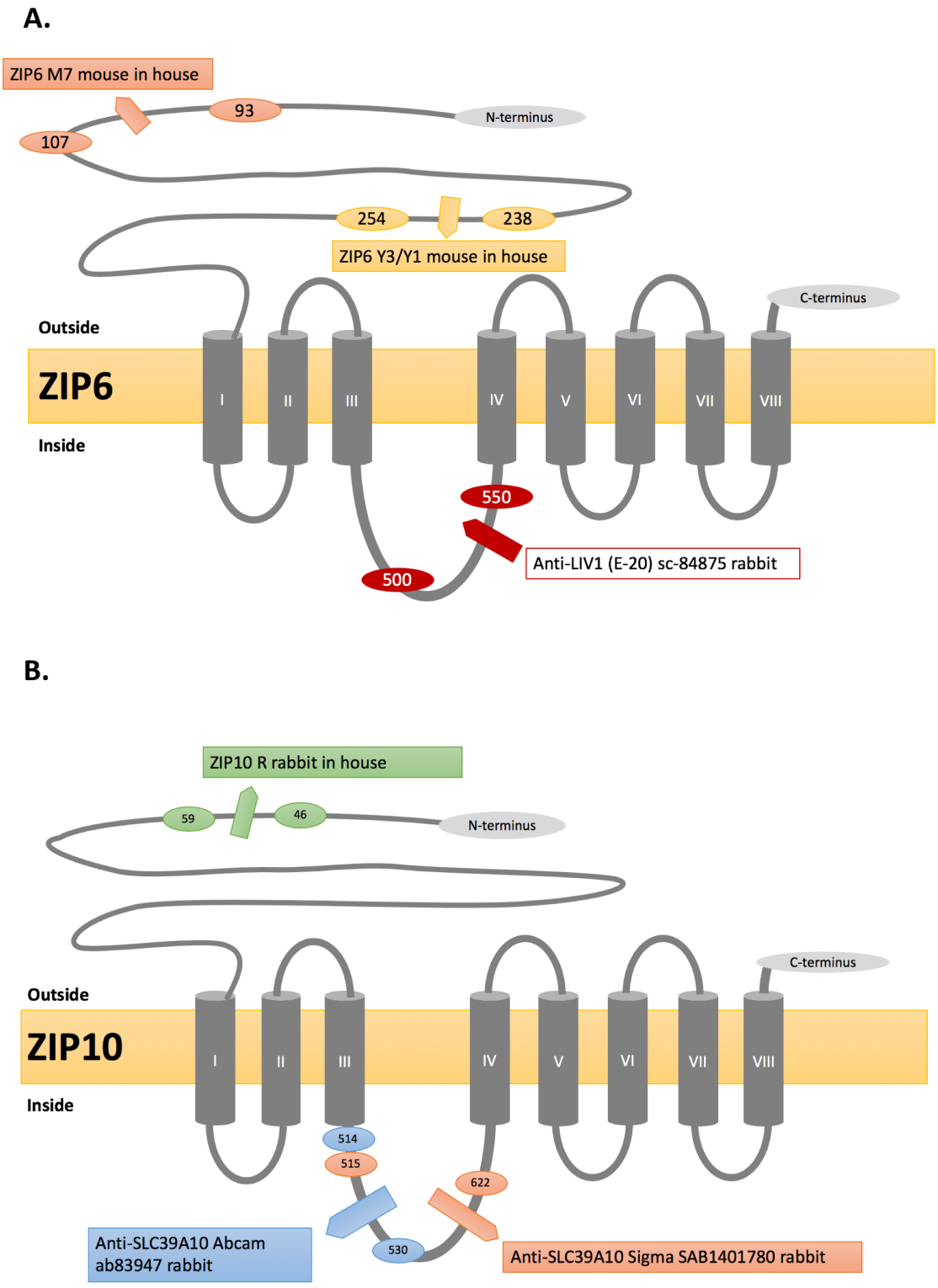

Figure 2.2 ***Schematic of ZIP6 and ZIP10 antibodies used throughout this project.***
The schematic indicates the name, the species and the epitope for both ZIP6 (Figure A) and ZIP10 (Figure B) antibodies.

Table 2.5 ***Primary antibodies.***

ANTIBODY	Species	Source	WB	IF	Other
pSer^{473}AKT	rabbit	Cell Signaling #9271	1:1000		
AKT	rabbit	Cell Signaling #9272	1:1000		
Phospho-p^{42}/p^{44} MAPK	rabbit	Cell Signaling #9101	1:1000		
p^{42}/p^{44} MAPK	rabbit	Cell Signaling #9102	1:1000		
pS^{10}Histone H3	mouse	Cell Signaling #9706	1:1000	1:200	
pS^{10}Histone H3	rabbit	Cell Signaling #3377	1:1000	1:200	
pSer^{727}STAT3	rabbit	sc-8001, Santa Cruz Biotechnology, INC	1:1000		
pTyr^{705}STAT3	rabbit	Cell Signaling #9145	1:1000		
Total STAT3	rabbit	Cell Signaling #4904	1:1000		
pSer	rabbit	Abcam, ab9332	1:1000		
pTyr (P-Y-1000 MultiMab)	rabbit mAb mix	Cell Signaling #8954	1:1000		
ZIP4	rabbit	ProteinTech 20625-1-AP		1:100	
CK2	mouse	sc-12738, Santa Cruz Biotechnology, INC	1:1000		1:50 (PLA)
Cyclin B1	mouse	sc-245, GNS1, Santa Cruz Biotechnology, INC	1:500	1:50	
Cyclin A	mouse	sc-271682, INC B-8, Santa Cruz Biotechnology	1:500	1:50	
Cyclin D1	mouse	sc-20044, DCS-6, Santa Cruz Biotechnology, INC	1:500		
Cyclin E	mouse	sc-481, M-20, Santa Cruz Biotechnology, INC	1:500		
p27^{kip1}	rabbit	Cell Signaling #2552	1:1000		
PLK1	mouse	Abcam, ab17056	1:1000		
V5 tag	rabbit	Abcam, ab15828	1:1000	1:1000	
V5 tag	mouse	Invitrogen R960-25	1:1000	1:1000	
GAPDH-HRP conjugated	rabbit	Sigma Aldrich G9295	1:50000		
β actin-HRP conjugated	mouse	Sigma Aldrich A3854	1:50000		
Apoptosis cocktail	mouse/ rabbit	Abcam, ab136812	1:100		

The table indicates the species, the dilution used for the different techniques and the supplier.

Table 2.6 ***Secondary antibodies.***

ANTIBODIES	Species	Source	WB	IF
Anti-mouse Alexa Fluor 594	goat	Invitrogen IgG A11032		1:1000
Anti-rabbit Alexa Fluor 594	goat	Invitrogen IgG A11072		1:1000
Anti-rabbit Alexa Fluor 488	goat	Invitrogen IgG A11034		1:1000
Anti-mouse Alexa Fluor 488	goat	Invitrogen IgG A10684		1:1000
Anti-mouse, HRP-conjugated	goat	GE Healthcare Uk limited NXA931	1:10000	
Anti-rabbit, HRP-conjugated	goat	Cell Signaling #7074	1:10000	
Anti-mouse IgG, HRP-conjugated	horse	Cell Signaling #7076	1:10000	
Apoptosis cocktail	goat	Abcam ab136812	1:250	

The table indicates the species, the dilution used for the different techniques and the supplier.

2.6 Site-directed mutagenesis

Site-directed mutagenesis was performed by Mutagenex (USA) and the mutations were checked by DNA sequencing. Serine or tyrosine residues were mutated to an alanine in order to provide a phosphoablative (null) mutant. In fact, serine and tyrosine residues are often phosphorylated in physiology due to the presence of a hydroxyl (–OH) group in their lateral chair. Hence, when this is mutated to an alanine, it cannot be phosphorylated anymore since the alanine only has a methyl group ($-CH_3$) that cannot be phosphorylated. The mutants that have been used in this project are listed in Table 2.7.

Construct	*Wild-type DNA sequence*	*Mutant DNA sequence*
ZIP6 S471A	CAGTTG**TCC**AAGTAT	CAGTTG**gCC**AAGTAT
ZIP6 S478A	CAACTT**TCA**ACAAAT	CAACTT**gCA**ACAAAT
ZIP6 Y528A	GAAGTC**TAC**AATGAA	GAAGTC**gcC**AATGAA
ZIP6 Y531A	AATGAA**TAT**GTACCC	AATGAA**gcT**GTACCC
ZIP6 Y528A/Y531A	GTC**TAC**AATGAA**TAT**	GTC**gcC**AATGAA**gcT**

Table 2.7 ***Sequences of mutants used in the project with their corresponding wild type sequence.*** *The letters in bold represent the wild type sequence of DNA bases that were mutated with the corresponding mutation on the right. The mutation is indicated on the right by a lower case letter in bold.*

2.7 Plasmid preparation

Transformation was performed by inserting recombinant ZIP6 or ZIP10 DNA constructs containing a C-terminal V5 tag into an ampicillin-resistant cDNA3.1/V5-His-TOPO plasmid vector and amplified by transformation in JM-109 E. coli competent cells. The transformed bacteria were grown overnight on agar plates containing 100 μg/ml ampicillin at 37°C. The correctly-orientated plasmids were then purified using EndoFree® Plasmid Maxi Kit (Qiagen, Germany) following the manufacturer's instructions (for buffers composition see Appendix 1). One colony from the selective plate was inoculated in 5 ml Lennox LB medium (Sigma Aldrich) containing 100 μg/ml ampicillin and incubated for 8 hours at 37°C with vigorous shaking. The starter culture was further diluted 1/500 in LB medium containing 100 μg/ml ampicillin for 16 hours at 37°C with vigorous shaking. The bacterial cells were harvested at 6000 x g for 15 minutes at 4°C and the pellet resuspended in 10 ml of Buffer P1 containing 100 μg/ml RNAse and 1x LyseBlue after which 10 ml of Buffer P2 and P3 was added. The lysate was filtered using the QIAfilter Cartridge and 2.5 ml of buffer ER was added to the filtered lysate

before incubation on ice for 30 minutes. The plasmid DNA was purified using a Qiagen resin and eluted with buffer QN. The DNA was precipitated with isopropanol, washed with endotoxin-free-room-temperature 70% ethanol and resuspended in the appropriate amount of endotoxin-free TE buffer. The DNA concentration and purity was calculated using UV spectrophotometry measuring the absorbance at 260 nm (OD260) and the ratio of the absorbance at 260 to the absorbance at 280 nm (OD260/OD280), respectively. Gel electrophoresis was performed to check the size of the plasmid by loading 5 μg of plasmid DNA and 0.25 μg of Quick-Load 1kb DNA ladder (New England Biolabs) and visualised with a UV transilluminator.

2.8 DNA transfection

MCF-7 cells or NMuMg cells with a 70% confluence were transfected with plasmid DNAs of recombinant human ZIP6 wild type or mutant constructs using Lipofectamine-3000 transfection reagent (Invitrogen), following the manufacturer's protocol. The recombinant DNA contained a C-terminal V5 tag which allowed visualisation with a V5 antibody by immunofluorescence. When used for immunofluorescence, cells were seeded into 35 mm dishes containing a 22x22-mm 0.17 mm thick glass coverslip. The transfection was performed for 16 to 18 hours in the presence of 3mM butyrate, which enhances the expression of recombinant DNA (Kyung *et al.*, 2005).

2.9 siRNA transfection

NMuMg wild type or NMuMg ZIP6 knockout cells were seeded onto 35 mm dishes until 70% confluent and transfected with 25 pmol of mouse ZIP10 siRNA (Dharmacon, USA) using Lipofectamine RNAiMAX reagent (Invitrogen), following the manufacturer's protocol in DMEM antibiotic free medium. The transfection was performed for 72 hours at 37°C. Cells were then harvested and used either for western Blot or MTT analysis. Details about the siRNA pool sequences are shown in Table 2.8.

siRNA target	*mZIP10*	*Non targeting control*
Product number	D-059712-00	D-001206-14-05
mRNA Target sequences	CAACACUACUCGUCACGUU	UAAGGCUAUGAAGAGAUAC
	CGAGAAGCACCACAUGUUA	AUGUAUUGGCCUGUAUUAG
	CAGCAGACUUUGUAUUGAA	AUGAACGUGAAUUGCUCAA
	GUGGAUCUGUGGCAUCAUA	UGGUUUACAUGUCGACUAA

Table 2.8 ***Summary of targeted siRNAs used throughout the project.***

2.10 Proximity ligation assay

Proximity ligation assay is a technique that allows the detection of interactions between proteins in close proximity by fluorescence. Cells are probed with two different antibodies from two different species and then coupled with secondary antibodies conjugated with specific oligonucleotides (PLA probe MINUS for rabbit and PLA probe PLUS for mouse). The cells are then exposed to a solution containing oligonucleotides and a ligase. If these probes are in proximity to each other, the oligonucleotides will hybridise with the probes. An amplification solution containing nucleotides and fluorescent oligonucleotides conjugated to Alexa Fluor 594 is added and the oligonucleotide arm of one of the PLA probes acts as a primer for the beginning of a rolling-circle amplification which generates a concatemeric product. If the two proteins are in close proximity, then the product is seen by fluorescence microscopy as a bright fluorescent red spot due to the conjugation of Alexa Fluor 594 to the reagent.

For the experiment, MCF-7 cells were seeded in an 8 well chamber coverslide (Nunc, Denmark) up to 70-80% confluence. After a 20 hours nocodazole treatment, cells were fixed with 3.7% formaldehyde (Sigma Aldrich, United States) for 15 minutes followed by several washes with PBS. The proximity ligation assay was made using the Duolink kit (Sigma Aldrich), following the manufacturer's protocol (Figure 2.3). After the wash with PBS, the sides of the wells were removed from the chamber slides leaving the gaskets behind, in order to minimise the amount of reagent to be used. Cells were permeabilised and blocked for 15 minutes with a 50/50 mixture of Duolink blocking solution and permeabilisation buffer made of 1% BSA (Sigma Aldrich) and 0.4% saponin (Sigma Aldrich), followed by an hour of incubation at room temperature with a solution

of primary antibodies made up in permeabilisation buffer. Cells were then incubated in a preheated humidity chamber for an hour at 37°C with a solution of MINUS (rabbit) and PLUS (mouse) probes, followed by a 30 minute incubation with a ligation-ligase solution. The subsequent step was performed in the dark because the reagents were light sensitive and cells were incubated for 100 minutes with an amplification solution containing a polymerase. All the solutions were made up in permeabilisation buffer. After the removal of the gaskets, a coverslip was mounted onto the slide with vectorshield containing DAPI and sealed with nail polish. Cells were visualised on a Leica RPE automatic microscope using a 63x oil immersion lens with a multiple bandpass filter for DAPI and Texas Red, taking at least 6 pictures per well with 25 stacks 0.3 μm apart for each red image. The counting of the number of dots per cell was made using ImageJ software. A schematic of the PLA procedure can be found in Figure 2.3.

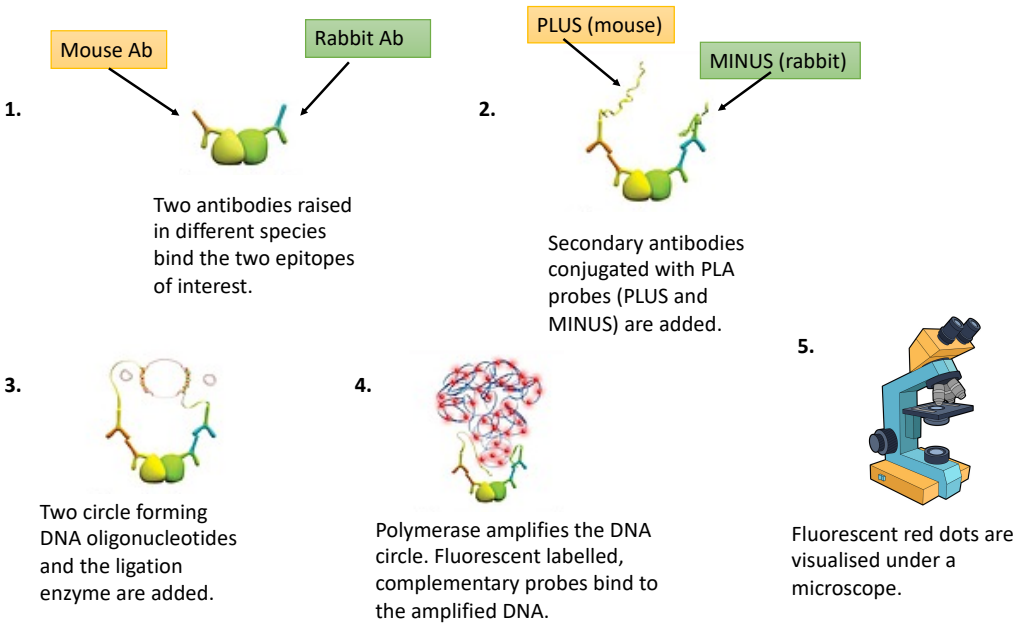

Figure 2.3 ***PLA schematic****.*
Briefly, two antibodies raised in different species are used in order to detect the proteins of interest. After primary antibody incubation, cells are incubated with a solution of secondary antibodies conjugated with specific oligonucleotide probes. Further incubation with a ligase solution containing DNA oligonucleotides and a polymerase solution which amplifies the DNA circle generates a rolling circle amplification reaction. Pictures were captured under a microscope with 25 stacks 0.3 μm apart for each image and results were visualised as red spots and counted with ImageJ.

2.11 Fluorescence-activated cell sorting (FACS analysis)

Cell cycle analysis was performed by flow cytometry. Briefly, cells seeded in 35 mm dishes were trypsinised, washed in PBS and fixed overnight in 70% ethanol at -20°C. The next day fixed cells were centrifugated at 2000 rpm and incubated with a staining solution of 20 μg/ml propidium iodide, 0.2 μg/ml DNase-free RNase A and 0.01% Triton X-100 at 37°C for 20 minutes. The cell suspension was passed through a cell strainer and fluorescence was measured with BD FACSVerse Flow Cytometer. Cell cycle analysis was carried out with FlowJo software version 10.

The amount of zinc in the different resistant cell lines was measured through a zinc assay using a BD FACSVerse Flow Cytometer. Cells were seeded on 35 mm dishes until 70-80% confluent, trypsinised and incubated with 5 μM Fluozin-3 dye (Invitrogen) for 30 minutes at 37°C, followed by a 30 minute recovery in dye-free medium at 37°C. Cells were then washed with PBS and kept on ice until analysis. FACS analysis results were analysed using FlowJo software version 10.

2.12 MTT assay

Cell viability/toxicity was measured using an MTT assay, testing the ability of a mitochondrial dehydrogenase enzyme from viable cells to cleave the tetrazolium ring of the pale yellow MTT [3-(4,5-dimethylthiazol-2-yl)-2-5-diphenyltetrazolium bromide] to form a purple formazan crystal which is impermeable to cell membranes, thus resulting in its accumulation in healthy cells.

6-9 x 10^3 cells previously transfected with siRNA for 72 hours in 35 mm dishes, were seeded onto a 96 well plate and allowed to grow for 2-3 days. Cells were washed with 200 μl warm PBS and incubated with 150 μl of MTT (0.5 mg/ml) at 37°C for 4 hours. The MTT was then removed from the plate and cells were lysated with 100 μl Tritox X-100 (10% in PBS) (Sigma Aldrich) and left overnight at 4°C. The colour was quantified using a colorimetric assay and measured on a scanning spectrophotometer (ELISA reader) which measures OD at 540 nm. Similarly, cells treated with nocodazole ± ZIP6 or ZIP10 antibody, at 4 μg/ml or 10.5 μg/ml respectively for 20 hours, were washed with PBS and incubated with 800 μl of MTT (0.5 mg/ml) but only transferred to a 96 well plate after the lysis with Triton X-100 for the colorimetric reading.

2.13 Immunoprecipitation

Cells were seeded on 60 or 35 mm dishes and lysed at 70% confluence (see western blot method). 500 μg of lysate was incubated for 2 hours at 4°C on a rotator with 2 μg of the antibody directed against the protein to be immunoprecipitated and taken to a volume of 1 ml with lysis buffer. In the meantime, 30 μl of the EZview Red Protein Affinity Gel Beads (Sigma) were equilibrated in lysis buffer. Following the 2 hours' incubation, the lysate, antigen and antibody were mixed with the appropriate immunoprecipitation beads according to the species the antibody was raised in (EZview Red Protein Affinity Gel Beads, Sigma Aldrich) and incubated for a further 2 to 3 hours at 4°C on a rotator to allow the complex of antigen/antibody to bind to the beads. The supernatant was discarded, and the beads were washed three times with lysis buffer. After the final wash, 25 μl of 2X loading buffer and 25 μl of lysis buffer were added to the beads containing the immunoprecipated protein and this mixture was denaturated at 100° C for 5 minutes in order to dissociate the antibody/antigen/bead complexes. The supernatant containing the protein of interest was collected and run on SDS-page followed by western blotting as described above.

2.14 ELISA (Enzyme-linked immunosorbent assay)

In order to measure the concentration of our customised ZIP6 antibody (mouse monoclonal) an immunoassay was performed using an IgG mouse uncoated ELISA kit (Invitrogen) following the manufacturer's protocol. In summary, a 96-well plate (provided with the kit) was coated with 100 μl/well of pre-titred purified anti-mouse IgG monoclonal antibody and incubated at 4°C overnight. The following morning the plate was washed twice with 400 μl/well of wash buffer, consisting of 1X PBS 0.05% Tween-20 (Sigma Aldrich). The wells were blocked with 250 μl/well of blocking solution (PBS with 1% Tween 20 and 10% BSA) and incubated at room temperature for 2 hours. After this time, wells were washed twice and the samples and standard solution were prepared as a 2-fold dilution series. The concentration of the initial standard was 100 ng/ml, and since our antibodies had an unknown concentration a dilution of 1/500 was performed. All wells had 50 μl/well of detection antibody (pre-titred HRP-conjugated anti-mouse IgG polyclonal antibody) added and were incubated at room temperature for 3 hours. After 4 washes, 100 μl/well of substrate solution was added and incubated at room temperature until the colour developed sufficiently (15-20 minutes). The

reaction was stopped by adding 100 μl/well of stop solution (2N H_2HSO_4, Sigma Aldrich) and the plate was read at 450 nm using a microplate spectrophotometer. The standard and interpolation curve for the standard and the unknown sample was performed using GraphPad. The concentration of our customised antibodies was calculated using Excel software for Mac OS.

2.15 Easy-Titer IgG assay

The concentration of the ZIP10 customised antibody (rabbit polyclonal) was evaluated using an easy-titer IgG assay kit from ThermoFisher Scientific (Catolog Number: 23305). This kit allowed for a quick and accurate determination of concentrations from 15-300 ng/ml of IgG, using monodispersed polystyrene beads that were coated with anti-IgG antibodies and absorbed light at 340 and 405 nm. This kit allows for the quantification of IgG in serum, ascites or cell culture supernatant. When the IgG binds to the beads, the beads aggregate and this leads to a decrease in light absorption which allows for the identification of the concentration by comparing the absorbance values to a standard curve of a known concentration. The standard used for the determination of the ZIP10 antibody concentration was a rabbit IgG isotype control from Invitrogen (#02-6102) at a known concentration of 5 mg/ml. Before starting the experiment, it was important to make sure that the beads were well mixed on a rotator for at least 10 minutes and vortexed for 60 seconds before use. The IgG standard was diluted to an initial concentration of 100 μg/ml and then additional dilutions were made with the supplied dilution buffer. Dilution buffer was added to the sample as the standard, but since the concentration of the sample was unknown, several starting dilutions were chosen from 1/50 to 1/5000. Only samples that fit on the curve were used for the final calculations. The first part of the assay required pipetting of 20 μl of mixed beads into the appropriate well of a 96 well plate. Following this, 20 μl of standard or sample was added to the wells containing beads. The 96 well plate was then mixed for 5 minutes on a plate mixer at a moderate speed before addition of 100 μl/well of the blocking buffer provided, and the plate was mixed again for 5 minutes on a plate mixer. The plate was then read at either 340 or 405 nm using a microplate spectrophotometer. Before reading the plate, any bubble was removed by using a needle, in order to prevent any misinterpretation of the data. Data was analysed using Excel software for Mac OS

and a standard curve was generated using GraphPad. The concentration of the sample was determined by interpolating between points on the curve.

2.16 Computational sequence analysis of ZIP transporters

The amino acid sequences of the ZIP family members were found on the NCBI database in text-based FASTA format and aligned using the ClustalW multiple sequences alignment program (Swiss Institute of Bioinformatics) (Larkin *et al.*, 2007). The aligned sequences were then analysed with the BoxShade program (Swiss Institute of Bioinformatics) (available https://embnet.vital-it.ch/software/BOX_form.html) to check similarities or identities between the different members of the family. Furthermore, the aligned sequences were used to generate a phylogenetic tree using the Phylogeny.fr free web service (Dereeper *et al.*, 2008).

The analysis and prediction of phosphorylation sites of ZIP6 and ZIP10 was performed using several online phosphorylation site databases: PHOSIDA (Max Planck Institute of Biochemistry) (Gnad, Gunawardena & Mann, 2011), PhosphoNET (Kinexus Bioinformatics Corporation), NetPhorest 2.1 (University of Copenhagen) (Horn *et al.*, 2014), NetPhos 3.1 (Blom *et al.*, 2004) and PhosphoSitePlus® (PSP) (Hornbeck *et al.*, 2015). Predicted sites without mass spectrometry confirmation were discarded. The analysis of potential cleavage sites was carried out using online databases such as epestfind (EMBOSS explorer) (Rogers, Wells & Rechsteiner, 1986) or ELM (Dinkel *et al.*, 2016).

2.17 Affymetrix analysis of gene expression

RNA samples for microarray analysis were extracted in triplicates from each different cell line and sent by the Breast Cancer Molecular Pharmacology Group to the Cardiff University Centre of Biotechnology Services (CBS) Affymetrix GeneChip® profiling service. Samples were checked by CBS for any DNA contamination or RNA degradation by initial quality control assessment before consequent microarraying using an Affymetrix-recommended procedure and kits (WT Human 1.0ST microarray platform) (Ertefai, 2016). During this procedure each sample was hybridized to a single Affymetrix 1.0ST GeneChip. Hybridised arrays were scanned using an Affymetrix GeneChip Scanner and pre-processed by correcting background, normalisation of data and providing

summary of gene expression level for each gene probeset. Comparative gene expression analysis was performed using an online software package called Genesifter (www.genesifter.net) by uploading the data for each model. Using this software, the gene of interest (SLC39A7/ZIP7): Probeset ID 8179525 and SLC30A1/ZnT1: Probeset ID 7924092) were visualised as a heatmap comparing the MCF-7 cells to the resistant cell lines and by using $\log_2$ intensity plots.

2.18 Statistical analysis

Statistical analysis was performed using t-test or analysis of variance (ANOVA) with Dunnet or Bonferroni post-hoc or Student t-test analysis. The difference was considered significant when $p<0.05$. The error bars show standard error of the mean (SEM) from at least 3 experiments for western blot and the cell growth analysis and 6 different visual fields for immunofluorescence from 3 different biological replicates. Statistical analysis of the immunohistochemical parameters was done through the "Cell Signalling Series" SPSS database available in the Breast Cancer Molecular Pharmacology Group. Non-parametric statistical analyses were performed using the pZIP7 HScore in correlation to several signalling pathways or endocrine markers using Spearman's correlation test. Mann-Whitney analysis was used to analyse pZIP7 level in relation to clinicopathological parameters such as tumour grade, size, age or menopausal status. Statistical analysis was performed using IBM SPSS or GraphPad software.

2.19 Materials

All the materials that have been used for the development of this project are listed in the following table (Table 2.9).

Reagent/material	Manufacturer	Catalogue number
Acrylamide/bis-acrylamide 30% solution, 37.5:1	Sigma Aldrich, USA	A3699
Agarose	Bioline Ltd, UK	BIO-41025
Ammonium persulfate	Sigma Aldrich, USA	A3678
Amphotericin B (fungizone)	Invitrogen, UK	15290
BD FACSVerse	Becton, Dickinson UK. Ltd	
Bio RAD Protein Assay Dye Reagent Concentrate	Bio-Rad, USA	#500-0006
Blue sensitive X-ray film	Photon Imaging Systems	FM024
Bovine Serum Albumin	Sigma Aldrich, USA	A7030
Bromophenol Blue	Merck, USA	L54971322
Cell scraper	Greiner Bio-one Ltd, UK	
Clarity™, Western ECL substrate	Bio-Rad, USA	#170-5061
DAB (Diaminobenzidine)	DAKO, UK	K3468
Dimethyl sulphoxide (DMSO)	Sigma Aldrich, USA	D8418
1.4-Dithiothreitol (DTT)	Sigma Aldrich, USA	10708984001
DAPT	Sigma Aldrich, USA	D5942
Dulbecco's Modified Eagle Medium (DMEM)	Fisher Scientific, UK	11960044
Dulbecco's Phosphate Buffered Saline	Life Technologies Europe Ltd, UK	14190-094
Duolink® In Situ Detection Reagents	Sigma Aldrich, USA	DUO92008
Duolink® PLA probe (Anti-mouse plus)	Sigma Aldrich, USA	DUO92001
Duolink® PLA probe (Anti-rabbit minus)	Sigma Aldrich, USA	DUO92006

EDTA (Ethylenediaminetetraacetic acid)	Sigma Aldrich, USA	E5134
EGTA (Ethylen Glycol Tetra-acetic acid)	Sigma Aldrich, USA	E3889
Ethanol	Fisher, UK	E/0650DF/17
Ethidium bromide	Sigma Aldrich, USA	E8751
EZview Red Protein A Affinity Gel	Sigma Aldrich, USA	P6486
EZview Red Protein G Affinity Gel	Sigma Aldrich, USA	E3403
Fluozin-3	Invitrogen, UK	F24195
Foetal bovine serum (FBS)	Invitrogen, UK	26140
Formaldehyde 37-41%	Fisher Scientific, UK	10041040
Glycerol	Sigma Aldrich, USA	G5516
Glycine	Fisher Scientific, UK	CAS 56-40-6
Hydrochoric acid 5M	Fisher, UK	J/4310/17
Immersol™ oil	Carl Zeiss, Germany	150925
Isopropanol	Fisher Scientific, UK	10723124
Isoton azide-free balanced electrolyte solution	Beckman, UK	8448011
L-glutamine 200 mM (100X)	Life Technologies Europe Ltd, UK	25030-024
Lipofectamine RNAiMAX	Life Technologies Europe Ltd, UK	13778-075
Lipofectamine 3000	Life Technologies Europe Ltd, UK	L3000001
Marvel Dried Skimmed Milk	Premier Internationals Foods, UK	3023034
Methanol	Fisher Chemical, UK	10284580
Methyl Green	Sigma Aldrich, USA	D2376
Mounting Medium with DAPI	Sigma Aldrich, USA	DUO82040
Nitrocellulose membrane	GE Healthcare Life Siences, UK	10600002

Nocodazole	Sigma Aldrich, USA	M1404
Paraplast plus, wax	Sigma Aldrich, USA	P3683
Penicillin/Streptomycin	Invitrogen, UK	15140
Pierce ECL Western Blotting Substrate	Thermo Scientific, USA	#32209
Ponceau S	Sigma Aldrich, USA	P-3504
di-Potassium hydrogen orthophosphate anhydrous	Fisher Scientific, UK	10375760
Potassium dihydrogen orthophosphate	Fisher Scientific, UK	10783611
Precision plus Protein™ All-Blue Standards	Bio-Rad, USA	#161-0373
Propidium iodide solution	Sigma Aldrich, USA	P4864
Protease Inhibitor Cocktail, animal component free in DMSO	Sigma Aldrich, USA	P8340-5ml
Resolving gel buffer, 1.5 M Tris-HCl pH 8.8	Bio-Rad, USA	#161-0798
RPMI (Roswell Park Memorial Institute)	Life Technologies Europe Ltd, UK	21875-034
Saponin from quillaja bark (sapogenin content $\geq$ 10%)	Sigma Aldrich, USA	S7900
Serum-Free Protein Block reagent	Dako, UK	X0909
Sodium azide (NaN_3)	Sigma Aldrich, USA	S-8032
Sodium butyrate	Sigma Aldrich, USA	B5887
Sodium chloride (NaCl)	Sigma Aldrich, USA	S6191
Sodium chloride (NaCl) 99.5%	Fisher, UK	S/3161/60
Sodium citrate tribasic dihydrate	Sigma Aldrich, USA	S4641
Sodium dodecylsulfate (SDS)	Sigma Aldrich, USA	L4390
Sodium fluoride (NaF)	Sigma Aldrich, USA	S-1504
Sodium orthovanadate (Na_3VO_4)	Sigma Aldrich, USA	S5608

Restore ™ PLUS Western Blot Stripping Buffer	Thermo Scientific, USA	#46430
SuperSignal™ West Femto Maximum Sensitivity Substrate	Thermo Scientific, USA	#34095
Tetramethylethylendiamine (TEMED)	Fisher Scientific, UK	10549960
Thiazolyl Blue Tetrazolium Bromide	Sigma Aldrich, USA	M5655
Thymidine	Sigma Aldrich, USA	T1895
Tris Base	Fisher Scientific, UK	10103203
Triton X-100	Sigma Aldrich, USA	X100-500ML
Trypsin-EDTA 0.5% (10X)	Life Technologies Europe Ltd, UK	15400-054
Tween 20	Sigma Aldrich, USA	P2287
Whatman filter paper	GE Healthcare Life Sciences, UK	3030-917
Western Blocking reagent	Roche, Germany	11921673001
Vectashield® Hard Set™ Mounting Medium with DAPI	Vector Laboratories, Inc, UK	H-1500
Vectashield® with DAPI	Vector Laboratories, Inc, UK	H-1200

Table 2.9 ***Table of all the materials used throughout the entire project.***

3 ACTIVATED ZIP7 AS A BIOMARKER OF ANTI-HORMONE RESISTANCE IN BREAST CANCER

3.1 Introduction

As described in Chapter 1, the development of endocrine resistance is a major burden in the treatment of breast cancer. Despite the new therapies that have been introduced recently and that are currently under clinical trials, the use of endocrine therapy is still the mainstay in the management of oestrogen receptor-positive (ER+) breast cancer, especially in pre-menopausal women (Clarke, Tyson & Dixon, 2015). For this reason, our group, the Breast Cancer Molecular Pharmacology Group of the Cardiff School of Pharmacy and Pharmaceutical Sciences, developed cell models of anti-hormone-resistant breast cancer from MCF-7 (human breast adenocarcinoma cells) which reflect the development of resistance in therapy. These cell lines are called TamR and FasR, due to their acquired resistance to tamoxifen and Faslodex®, respectively (Knowlden *et al.*, 2003; McClelland *et al.*, 2001). Interestingly, it was seen that a prolonged exposure to endocrine therapy led to ER loss, indeed further investigations on these resistant cell lines have reported that TamR cells were ER+, whereas FasR cells were ER- (Nicholson *et al.*, 2005). Furthermore, these models were expanded to produce long term resistant cell models for both the TamR and FasR cells, called TamRL and FasRL respectively, developed after a longer exposure (36 months) to tamoxifen and Faslodex®, which better mimic the clinical situation (Gee *et al.*, 2015).

Since the first evidence of a correlation between increased zinc and ZIP7 to breast cancer (Taylor *et al.*, 2008, 2007), this area has become an aspect that needs to be further explored in order to help decipher the mechanism that leads breast cancer to acquire resistance and fail to respond to endocrine treatment. This chapter expanded the first discovery that ZIP7 drives TamR cells to a model of Faslodex® resistance, and additionally examined any changes in the longer term resistance which better mimics the clinical situation. Moreover, since that first discovery, it has been demonstrated that the activation of ZIP7 relies on CK2 phosphorylation of two serine residues in the long intracellular loop of ZIP7 (Taylor *et al.*, 2012). This has enabled us to use a pZIP7 antibody (Nimmanon *et al.*, 2017) as a useful tool to better understand the role of ZIP7 in the development of drug resistance.

3.1.1 Aims and objectives

The aim of this chapter was to analyse the activation of ZIP7 in anti-hormone resistant breast cancer models and investigate whether its activation changed when the cells had prolonged exposure to endocrine therapy. Additionally, this investigation assessed whether pZIP7 can be used as a biomarker of endocrine resistance considering the well-established role of ZIP7 in cancer breast (see Chapter 1). This was performed by evaluating its presence not only in anti-hormone resistant cell models but also in samples belonging to a small clinical series. Therefore, the objectives of this chapter were:

1. To analyse the activation of ZIP7 in anti-hormone resistant breast cancer cell lines by using a combination of different molecular biological techniques such as western blotting, immunofluorescence and zinc assays;
2. To develop an immunohistochemical assay for activated ZIP7 to be tested on cell pellets of the different resistant cell lines;
3. To assess ZIP7 activation in a small breast cancer clinical samples series.

3.2 Methods

Knowing that ZIP7 is activated by CK2 phosphorylation on two serine residues (S275/S276) in the long intracellular cytoplasmic loop (Taylor *et al.*, 2012), the pZIP7 antibody (Table 2.4) developed in our group was used to assess the activation of ZIP7 (Nimmanon *et al.*, 2017) in comparison to its inactive state. This antibody was tested for the first time in our anti-hormone resistant breast cancer models. This antibody was used in comparison to a commercial ZIP7 antibody (Table 2.4) and to a customised ZIP7 antibody (Table 2.4), which both recognise an epitope on the long intracellular loop between TM III and TM IV. Western blotting was used to assess activation of ZIP7 in comparison to the total level of ZIP7 and to test activation of MAPK and AKT, both downstream pathways of ZIP7 (Nimmanon *et al.*, 2017). Activation of ZIP7 was also assessed using immunofluorescence and by immunohistochemistry on both cell pellets of the resistant cell lines and on a small series of breast cancer clinical samples (NRES active, ethical approval C2020313/Nottingham city hospital). Affymetrix and Kaplan-Meier analyses were used to compare the results of ZIP7 activation to its overall expression. Determining the difference in zinc levels between the different anti-hormone resistant models was performed by using a Fluozin-3 zinc assay.

3.2.1 The characterisation of ZIP7 antibodies

Three ZIP7 antibodies were first characterised for their ability to recognise the active and inactive form of ZIP7. The current analysis was performed using a total ZIP7 polyclonal antibody (ProteinTech™) which has the ability to bind both the active and inactive form of ZIP7. As seen in Figure 3.1-B, this antibody recognises a long epitope situated between TM III and IV (residues 236-383) which includes the two serine residues S275 and S276, which are phosphorylated by CK2 (Taylor *et al.*, 2012). The western blot carried out with this antibody showed two different bands: one at 35 kDa and another at 48 kDa (Figure 3.1-A). The 48 kDa band is at the same size as that obtained with our anti-pZIP7 antibody (Figure 3.1-A). Surprisingly, the 35 kDa band was consistent with the band seen using another customised total ZIP7 B polyclonal antibody (Figure 3.1-A) that has its epitope in a region of the cytoplasmic loop containing the residues S275 and S276 (residues 264-277) (Figure 3.1-B). The ZIP7 B antibody normally showed two bands on western blotting at 35 and 40 kDa (Figure 3.1). Therefore, it was assumed that the 40 kDa band was unspecific. The epitope of this antibody was smaller than the one of the ProteinTech™ total ZIP7, suggesting that it could have been unable to recognise the phosphorylated form of ZIP7, despite the fact that the epitope contained the residues 275-276. Additionally, since there was evidence that the ZIP7 B antibody became deteriorated, its use for the current investigation was discarded. Furthermore, the molecular size of ZIP7 is predicted to be around 50 kDa (Taylor & Nicholson, 2003), and there is currently no evidence that ZIP7 undergoes any proteolytic cleavage. Hence, it remained elusive whether the 35 kDa band was corresponding to ZIP7. For this reason and for the purpose of this project only the 48 kDa band was considered for the following analyses. The presence of a 35 kDa band on western blotting is still unclear and therefore could be subject of future investigations.

Conversely, the pZIP7 antibody allows the detection of the active form of ZIP7, regardless of its inactive state, since it is only specific to ZIP7 when phosphorylated on S275 and S276 (Nimmanon *et al.*, 2017) (Figure 3.1). The evaluation of its active state is important as the release of zinc mediated by ZIP7 activation is implicated in several downstream pathways which have a significant impact on cancer prognosis. Some of these include MAPK, mTOR and PI3K, which are all involved in cell survival and cell proliferation (Nimmanon *et al.*, 2017).

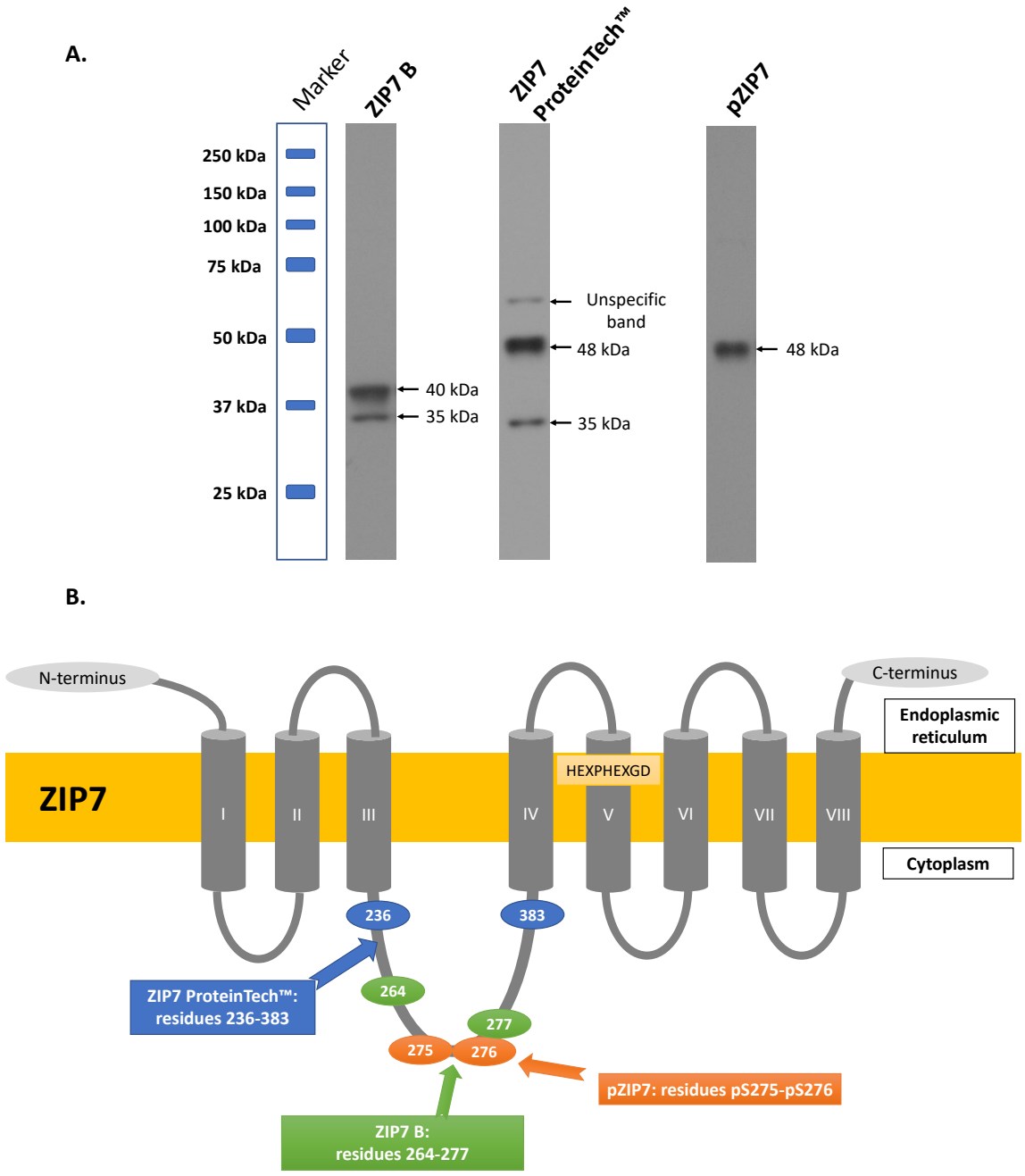

Figure 3.1 ***Comparison of ZIP7 antibodies****.*
A. MCF-7 cells were harvested and probed for three ZIP7 antibodies. The customised ZIP7 B antibody shows two bands at 35 and 40 kDa. The total ZIP7 antibody (ProteinTech ™) detects two bands, one at 35 and one at 48 kDa. The 35 kDa band is consistent with the band seen using the ZIP7 B antibody. The pZIP7 antibody shows a unique band at 48 kDa.
B. Schematic showing the epitopes of the different ZIP7 antibodies used for the investigation of ZIP7 in anti-hormone resistant cell lines. All the three antibodies have their epitope in the long cytoplasmic loop between TM III and TM IV.

3.3 Results

3.3.1 Investigation of zinc channel ZIP7 in anti-hormone resistant breast cancer cell models

The level of ZIP7 activation was assessed first using biological tests. The experiments were carried out by western blot and immunofluorescence, using our unique anti-pZIP7 monoclonal antibody (Nimmanon *et al.*, 2017) to evaluate the activation of the channel. This analysis compared phosphorylated ZIP7 in MCF-7 cells to our unique anti-hormone-resistant cell models of tamoxifen-resistance, both short-term (TamR) and long-term (TamRL), and Faslodex®-resistance, both short-term (FasR) and long-term (FasRL).

3.3.1.1 ZIP7 in anti-hormone resistant breast cancer

Previous studies have identified ZIP7 as a major driver of poor prognostic cancer (Hogstrand *et al.*, 2009) and highlighted its potential role in driving anti-hormone resistance in breast cancer. In fact, Taylor *et al* discovered that ZIP7 was highly expressed in our TamR cell line (Taylor *et al.*, 2007) and that this cell line had an increased level of zinc compared to the non-responsive MCF-7 (Taylor *et al.*, 2008). However, these studies were unable to analyse the state of ZIP7 activation, since no antibody was available. It was interesting to notice that Kaplan-Meier plotter analysis between relapse-free survival in a cohort of breast cancer patients (ER+, HER2-) following endocrine therapy or chemotherapy and ZIP7 expression revealed that increased expression of ZIP7 is associated with decreased relapse-free survival up to 10 years, suggesting the role of ZIP7 in driving cancer growth and aggressiveness (Figure 3.2-A). Therefore, before starting any analysis, the expression of the SLC39A7 gene (ZIP7) was checked in the different anti-hormone resistant cell lines. The data retrieved with Affymetrix analysis of ZIP7 gene expression showed that ZIP7 expression was increased in all the resistant cell lines when compared to MCF-7 and, in particular, the highest expression is observed in the TamR and FasRL cells (Figure 3.2-B).

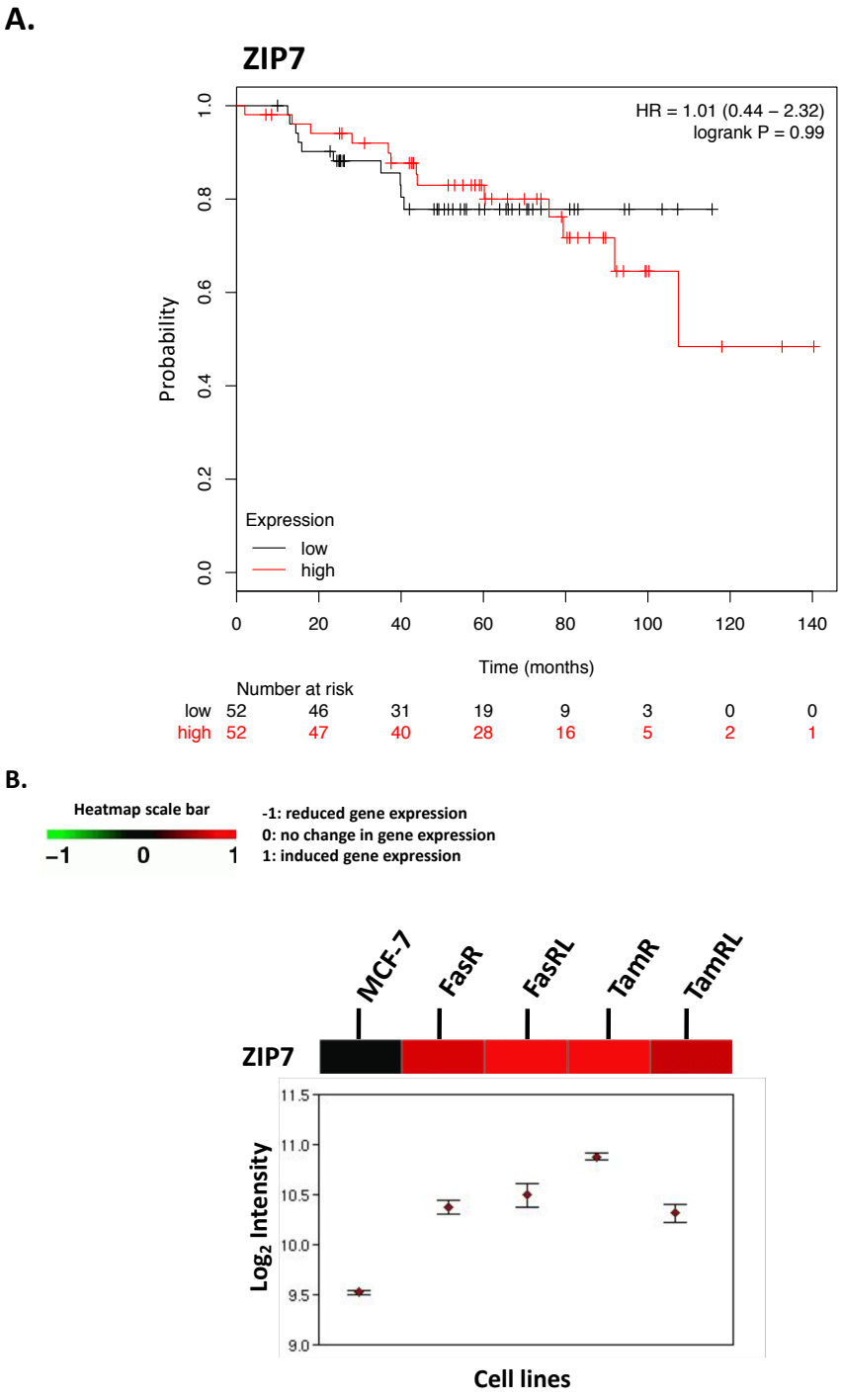

Figure 3.2 ***Kaplan-Meier plotter analysis and Affymetrix data****.*
A. Kaplan-Meier plotter analysis of relationship between relapse-free survival in a cohort of ER+/HER2- breast cancer patients following endocrine treatment or chemotherapy, and ZIP7 expression. Increased ZIP7 decreases relapse-free survival up to 10 years.
B. Affymetrix data showing the gene expression level of ZIP7 in a group of different anti-hormone resistant cell lines in comparison to MCF-7 cells is viewed as heatmap and a log_2 intensity plot generated using Genesifter. The log_2 intensity plot shows the mean value of three independent microarray (±SEM) for ZIP7 mRNA expression. The colours of the heatmap represent an arbitrary legend that goes from green to red, indicating with red [1] induced gene expression, black [0] no changes of gene expression and green [-1] reduced gene expression.

3.3.1.2 Use of pZIP7 antibody to investigate ZIP7 in anti-hormone resistant breast cancer

Next, the level of ZIP7 in the resistant cell line was assessed by western blot. Probing with the ProteinTech™ antibody showed a significant increase of the total amount of ZIP7 protein in both TamR (*p<0.001*) and FasRL cells (*p<0.5*) when compared to MCF-7 (Figure 3.3-A), confirming that seen with the Affymetrix data (Figure 3.2-B). The level of total ZIP7 protein was higher in the FasR cells in comparison to the parental MCF-7, although not significant. Similarly, the analysis did not reveal any significant increase of total ZIP7 protein in the TamRL, suggesting a change in ZIP7 in the long-term phenotype (Figure 3.3-A).

On the other hand, the results gained with our pZIP7 antibody showed a significant increase of activated ZIP7 protein in the TamR cells (*p<0.001*) in comparison to the MCF-7 cells (Figure 3.3-B). Interestingly, activation of ZIP7 in the TamRL cells was decreased in comparison to the TamR cells, yet significant when compared to MCF-7 (*p<0.05*). In contrast, while FasRL cells showed more activated ZIP7 compared to FasR cells, neither had a significantly increased level of pZIP7 in comparison to MCF-7 (Figure 3.3-B). Nevertheless, the western blotting data allowed measurement of the ratio between activated ZIP7 and total ZIP7 and, despite showing an overall increase of pZIP7 in the tamoxifen-resistant cell lines, showed a significant increase in the TamR cells (*p<0.01*) (Figure 3.3C), suggesting that TamR cells actively utilise zinc signalling, which may change with resistance duration.

While the analysis with the total ZIP7 antibody provided information regarding the overall level of ZIP7 protein, which was comparable to data obtained from Affymetrix analysis (Figure 3.2-B), the pZIP7 antibody was a valuable tool to assess the status of activation of ZIP7 and, as a consequence of that, the cascade of signalling pathways that are downstream of its activation. For this reason, this analysis suggested that pZIP7 could potentially be a more useful indicator of acquired anti-hormone resistance in breast cancer providing evidence not only of anti-hormone resistance but also changes over time.

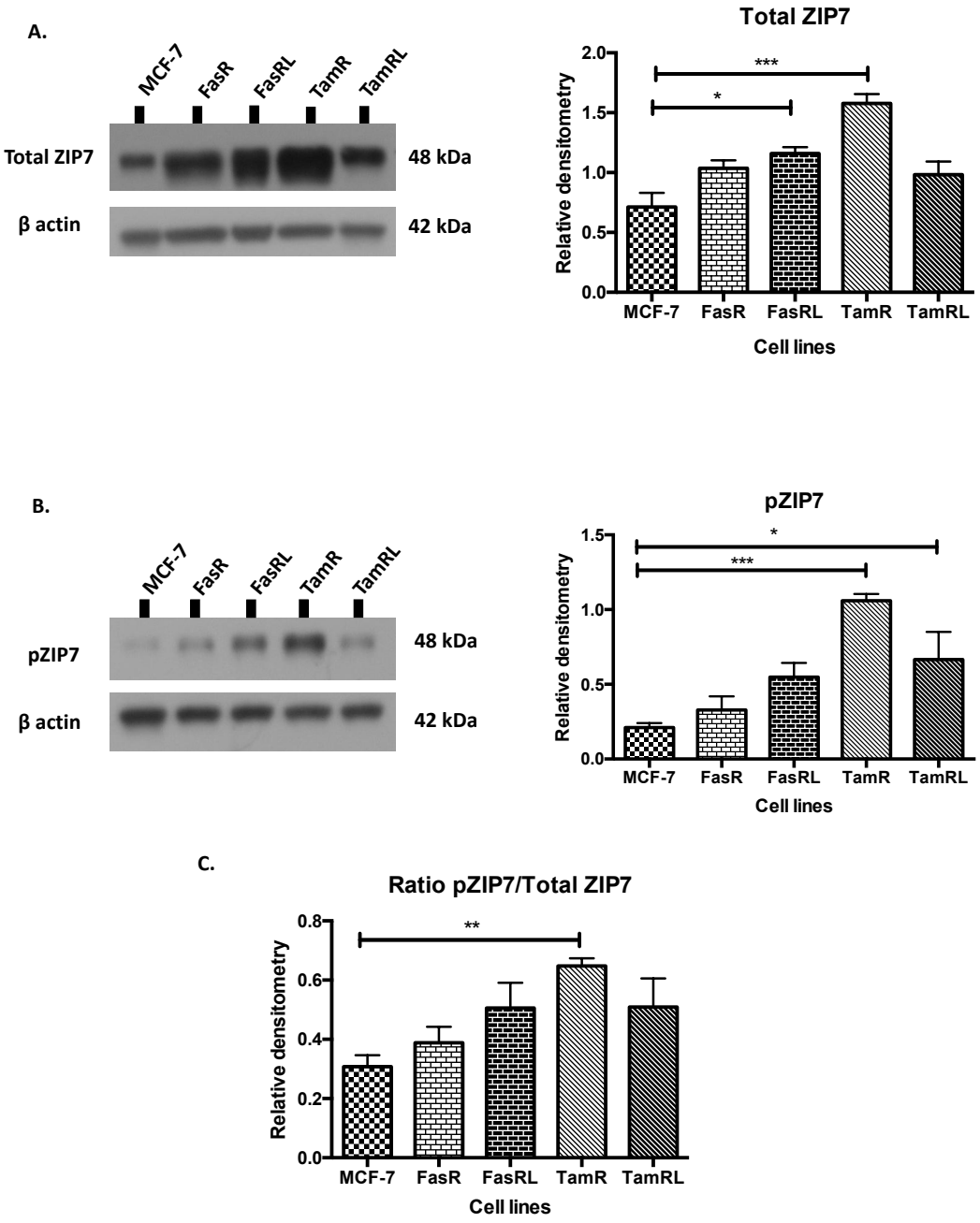

Figure 3.3. ***Study of ZIP7 in anti-hormone resistant breast cancer****.*
*MCF-7 and the anti-hormone resistant cell lines were seeded in 60 mm dishes, and harvested at 70% confluence. Samples for western blot were prepared and probed with different ZIP7 antibodies. The experiment was performed using four biological replicates and the densitometric data was normalised to β-actin. The bar graphs show the mean values of n= 4 ± SEM (standard error of mean). Statistical analysis was performed and statistical significance is shown as *** (p<0.001), ** (p<0.01) and *(p<0.05).*
A. The total ZIP7 antibody (ProteinTech™) detects one band at 48 kDa which corresponds to both the inactive and active form of ZIP7.
B. The pZIP7 antibody detects a unique band at 48 kDa, which corresponds to the active form of ZIP7 when phosphorylated on residues S275 and S276.
C. Ratio between pZIP7 and total ZIP7 densitometry is expressed as a bar graph.

3.3.1.3 Tamoxifen-resistant models show increased ZIP7 activation

The analysis of activated ZIP7 was performed with immunofluorescence using the pZIP7 antibody (red fluorescence) along with DAPI (blue fluorescence) staining (Figure 3.4). DAPI allowed the detection of the total number of cells per field of view. Therefore, when looking at the overlay picture it was possible to assess the amount of cells that were positive for pZIP7 and gain an estimation of the proportion of ZIP7 activation in the different cell lines. This analysis confirmed the western blot data for the level of ZIP7 activation, as it was evident that the TamR cells had increased activation of ZIP7 compared to MCF-7 (Figure 3.4). Interestingly, TamRL cells also showed a similar raised activation of ZIP7 as seen in the TamR model (Figure 3.4). Both TamR and TamRL showed that almost all of the cells stained positively for pZIP7 in comparison to MCF-7. This was an interesting result consistent with the TamR phenotype being able to utilise ZIP7-mediated zinc signalling to drive its growth (Taylor *et al.*, 2008).

In contrast, the staining for FasR cells reflected what was seen with western blotting as there was no clear increase of activated ZIP7 when compared to MCF-7, despite a slight increase of pZIP7 in the FasRL (Figure 3.4). Interestingly, FasRL showed more staining for phospho-ZIP7 compared to FasR cells and also suggested the possibility of the presence of two different subclones in this long-term resistance cell line (Figure 3.4, white arrows). In fact, in a previous study it was discovered that our models of Faslodex® resistance were characterised by the presence of two different clones: EGFR positive and EGFR negative (Lewis, 2010). The double clonality of these cell lines could suggest that the cells that are EGFR positive may utilise more zinc than the other clone, hence the difference in ZIP7 activation observed.

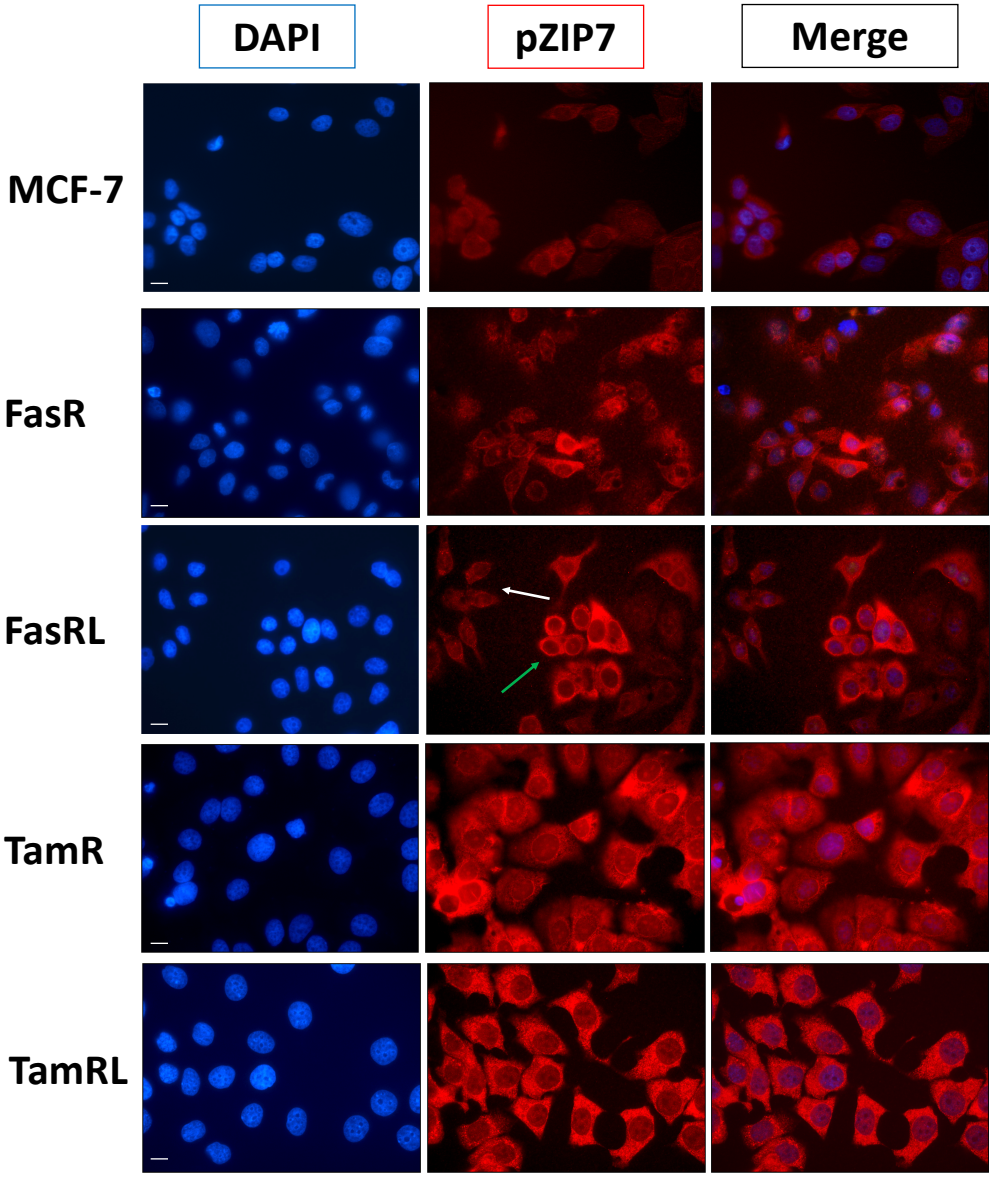

Figure 3.4 ***Activation of ZIP7 is increased in tamoxifen-resistant cell lines.***
Cells were seeded on coverslips, fixed with 3.7% formaldehyde and stained for pZIP7 antibody (red) and DAPI (blue). Pictures are representative of n=3 for each cell line model and were taken with a 63x oil lens using Leica DMIRE2 Microscope. The arrows indicates the potential dual clonality of cells found for the FasRL cell line: EGFR positive (green arrow) and EGFR negative (white arrow).
Scale bar: 10 μm.

The difference observed between the activation of ZIP7 in the two models of endocrine resistance (TamR + FasR) could be linked to the distinct phenotype of the two resistant cell lines. It was interesting to notice that the two resistant models have a different expression of the zinc transporter ZnT1 (Figure 3.5). The zinc transporter ZnT1 is another important player in the mobilisation of zinc, being the major zinc exporter, as it is the only SLC30A family member which resides on the plasma membrane (Palmiter & Findley, 1995). Affymetrix® data of the gene SLC30A1 (ZnT1) in the different resistant cell lines revealed that the highest expression of ZnT1 is observed in the FasR cells (Figure 3.3), raising the question whether this could have an effect on zinc homeostasis, considering both ZIP7 and ZnT1 play a pivotal role in transporting zinc in the opposite direction.

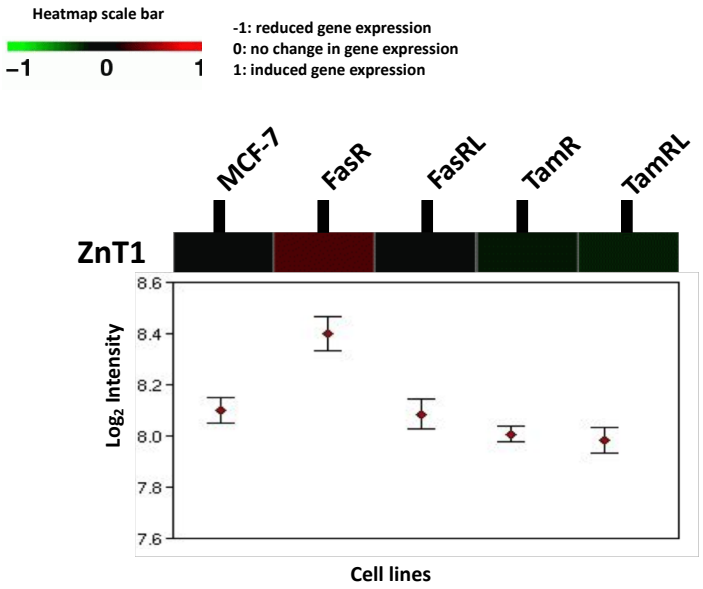

Figure 3.5 ***Affymetrix data regarding SLC30A1 (ZnT1) expression.***
Affymetrix data showing the gene expression level of ZnT1 in a group of different anti-hormone resistant cell lines in comparison to MCF-7 cells is viewed as a heatmap and a log_2 intensity plot generated using Genesifter. The log_2 intensity plot shows the mean value of three independent microarray (±SEM) for ZnT1 mRNA expression. The colours of the heatmap represent an arbitrary legend that goes from green to red, indicating with red [1] induced gene expression, black [0] no changes of gene expression and green [- 1] reduced gene expression.

3.3.2 Zinc measurement in anti-hormone resistant breast cancer

To try to understand whether ZIP7 and ZnT1 may play a role in zinc homeostasis in FasR cells, the content of zinc in each different resistant cell line was measured in comparison to MCF-7. Previous studies have shown that TamR cells have higher levels of intracellular zinc than MCF-7 cells (Taylor *et al.*, 2008). The content of zinc can influence the activation of all the downstream pathways which are related to and activated by zinc, such as AKT, PI3K, GSK3β, MAPK or mTOR (Nimmanon *et al.*, 2017). Its evaluation was a valuable tool to better understand what happens to cells when they acquired resistance to a specific drug and whether increased zinc signalling was part of this mechanism.

FACS analysis was performed using Fluozin-3, an indicator selective for the detection of zinc in the range of 1-100 nM (Taylor *et al.*, 2008). Despite a recent paper has suggested that Fluozin-3 may be more specific to measure vesicular zinc rather than labile zinc (Han *et al.*, 2018), Fluozin-3 was used in the following experiment to assess intracellular zinc. This dye was believed suitable to measure intracellular zinc in the different anti-hormone resistant cell lines, as previous investigations in our group have shown that TamR cells had a significant increase in intracellular zinc in comparison to MCF-7 when using Fluozin-3 as zinc dye. In particular, TamR cells treated with ZIP7 siRNA and loaded with Fluozin-3 had a significant reduction of intracellular zinc, whereas cells treated with 20 μM zinc + ionophore showed a significant increase of intracellular zinc, confirming that Fluozuin-3 was a suitable marker of intracellular zinc (Taylor *et al.*, 2008). Interestingly, results within this current project showed that FasR cells had increased levels of zinc in comparison to MCF-7 ($p<0.05$) (Figure 3.6). This data also confirmed a previous study demonstrating increased zinc in TamR cells (Taylor *et al.*, 2008). Nevertheless, both the two long-term resistant cells did not show the same significant increased intracellular zinc when compared to MCF-7, suggesting changes in zinc signalling use with resistance duration (Figure 3.6).

A.

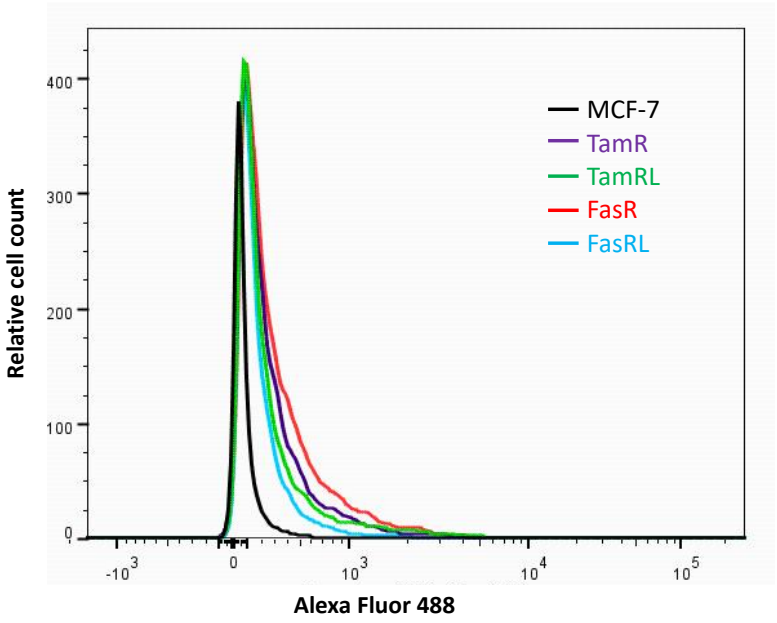

B.

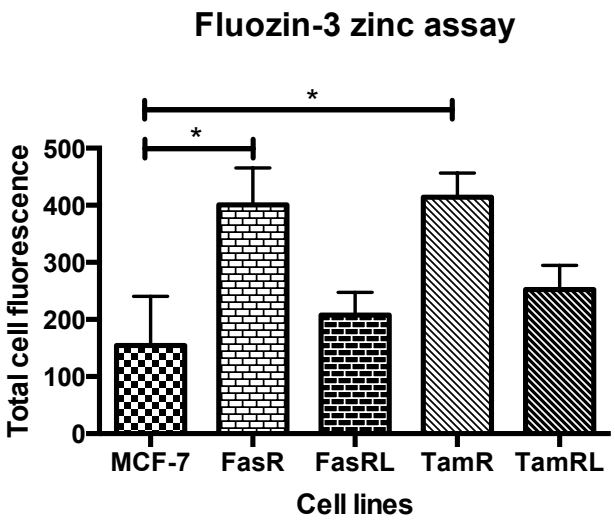

Figure 3.6 ***FasR and TamR cells have increased cytoplasmic zinc in comparison to the parental MCF-7 cells.***

A. Cells of the different cell lines were seeded on 60 mm dishes up to 70% confluence and loaded with Fluozin-3. FACS analysis was performed and the data is shown in an overlay histogram.

*B. Measurement of total cell fluorescence is shown in a bar graph as mean values of n=3 + ± SEM (standard error of mean). Statistical significance is shown as * ($p<0.05$).*

3.3.3 Examination of downstream signalling pathways of ZIP7

In a recent study in our group, it was demonstrated that ZIP7 is associated with the activation of downstream pathways such as MAPK, mTOR and PI3K-AKT (Nimmanon *et al.*, 2017) (Figure 3.7). In order to examine a relationship between ZIP7 activation and downstream signalling pathways, the activation of AKT and MAPK was examined in anti-hormone resistant breast cancer cell lines.

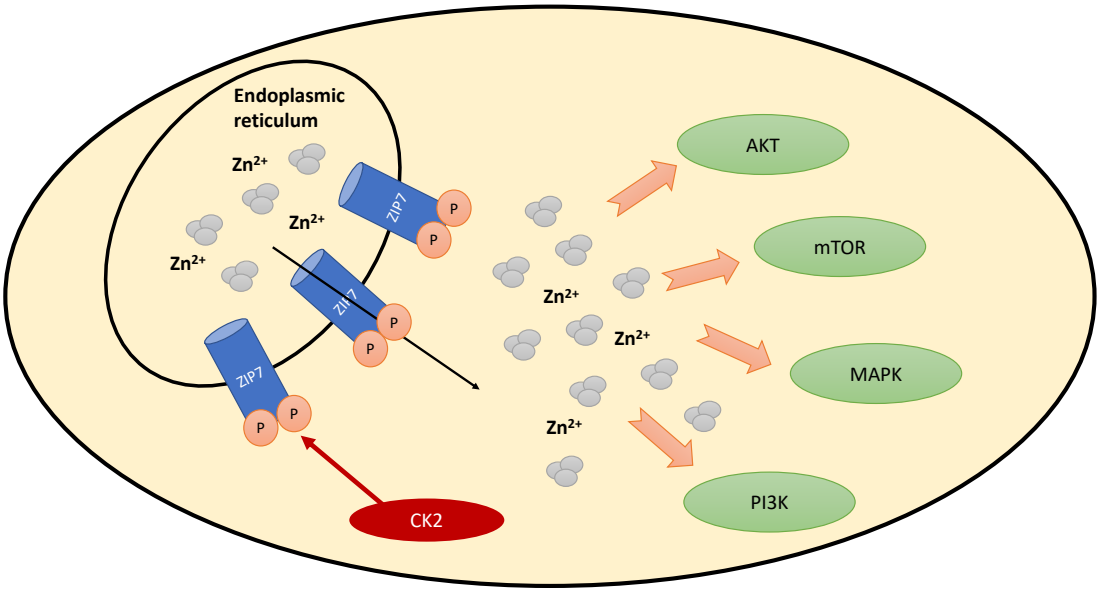

Figure 3.7 ***Downstream pathways of activated ZIP7.***
ZIP7 is activated by CK2-phosphorylation on two serine residues on the long intracellular loop between TM III and TM IV. Its activation is involved in the activation of several downstream pathways such as AKT, mTOR, MAPK and PI3K (Nimmanon *et al.*, 2017).

AKT is a widely known kinase which can be considered the mainstay of pathways leading to cell proliferation and oncogenesis (Chang *et al.*, 2003). Accordingly, the link between ZIP7 activation and this molecule may be crucial in the development of aggressiveness in cancer and in particular the development of endocrine resistance. The analysis of AKT activation was performed by evaluating the ratio between the active form of AKT phosphorylated on serine residue 473 to the total AKT protein level. AKT is activated via phosphorylation on two residues: serine 473 and threonine 308, which are both required for maximal activation of the molecule (Alessi *et al.*, 1996). However, AKT phosphorylation on S473 residue is the most common site used for investigation of active AKT, as being extensively studied in cancer (Vivanco & Sawyers, 2002; Bjornsti &

Houghton, 2004). Analysis of activated AKT in our resistant cell lines in comparison to MCF-7 showed increased AKT activation ($pSer^{473}$) in the TamR cells (*p<0.05*) and TamRL (*p<0.01*) (Figure 3.8-A). The increased activation of AKT in tamoxifen-resistant cell lines was consistent with activated ZIP7, as AKT is a direct downstream of the zinc release induced by ZIP7 activation (Nimmanon *et al.*, 2017). The same investigation on Faslodex®-resistant MCF-7-derived cells did not show any significant activation of AKT, which mirrored the previous results seen for the activation of ZIP7 in these cell lines (Figure 3.3 B). This result highlighted the requirement for ZIP7 activation in the onset of AKT cascade signalling in the tamoxifen-resistant cell line.

Further to the analysis of activated AKT, MAPK activation was also analysed. The MAPK signalling pathway is widely known for its implication in cancer survival, which is the reason why it is often used as a target for cancer treatment (Hayes & Der, 2007). Since MAPK was seen as a downstream pathway of ZIP7 activation (Nimmanon *et al.*, 2017), its activation in the anti-hormone resistant cell lines could help us to understand the mechanism behind drug resistance. Similarly to other kinases, MAPK is activated by phosphorylation and, in particular, the p42/p44 MAPK (ERK1/2) is phosphorylated on residues T202/Y204 and T185/Y187 respectively (reviewed by Chen et al. 2001). Similar to the analysis of AKT, the level of active MAPK was measured in comparison to the total p42/p44 MAPK kinase protein. The analysis of activated p42/p44 MAPK performed on MCF-7 in comparison to the tamoxifen and Faslodex® resistant cell lines revealed a significant decrease of activated MAPK in the FasR and FasRL cell lines (*p<0.05*) in comparison to MCF-7 (Figure 3.8-B). In contrast, there was no significant difference of activated MAPK when comparing the tamoxifen resistant cell lines to MCF-7 (Figure 3.8 B).

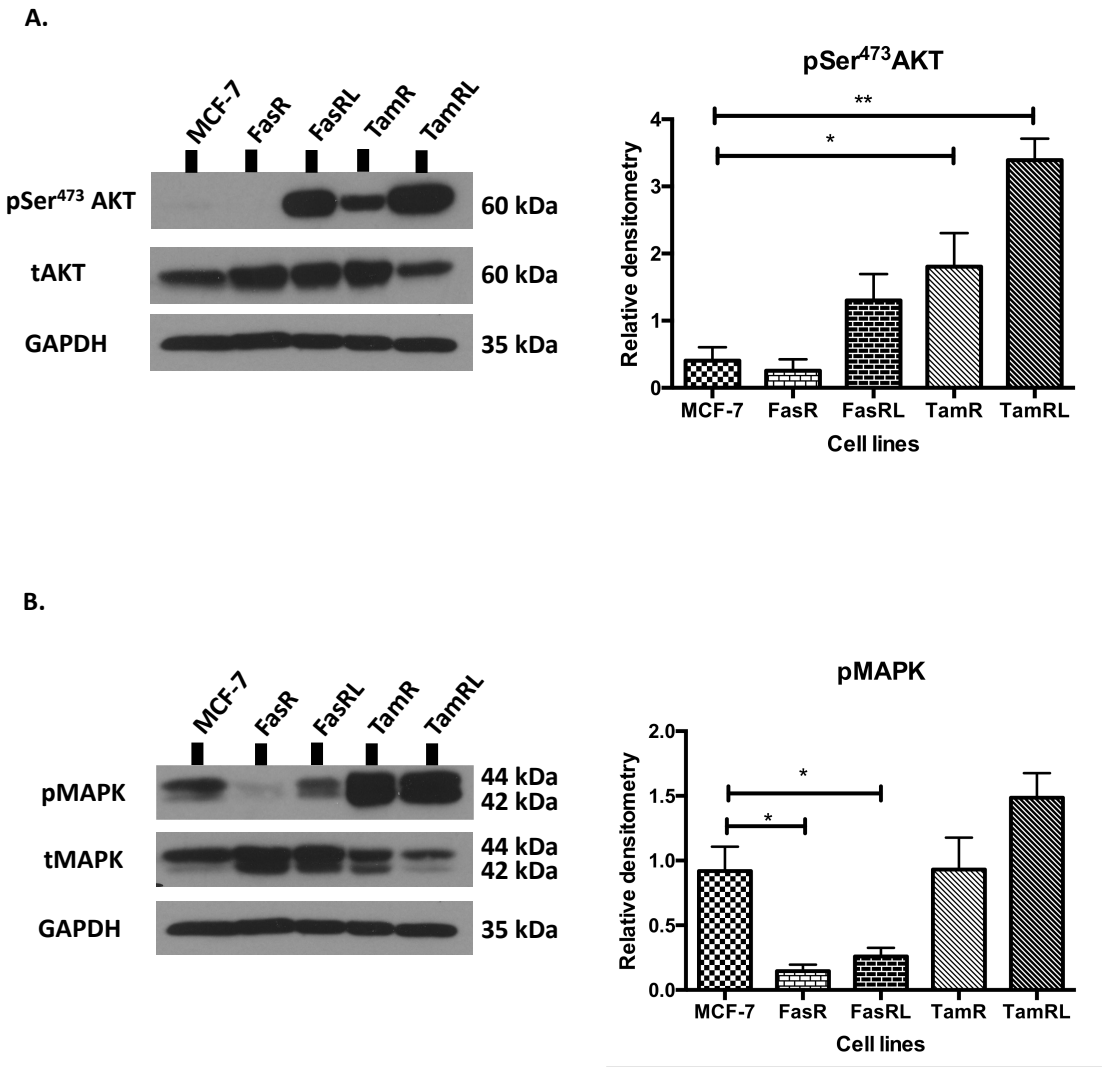

Figure 3.8 ***Activation of ZIP7- downstream pathways in anti-hormone resistant breast cancer.*** *MCF-7 cells and the anti-hormone resistance cell lines were probed for pSer^{473} AKT and phospho-p^{42}/p^{44} MAPK (Figure A-B). The experiment was performed using four different batches of cells and the densitometric data were normalised to the total level of AKT and MAPK (Figure A+B). The level of GAPDH is also shown (Figure A-B). The bar graph show the mean values of n=4 ± SEM (standard error of mean). Statistical analysis was performed and statistical significance is shown as ** (p<0.01) or * (p<0.05).*

3.3.4 Developing an immunohistochemistry assay for pZIP7

In our Breast Cancer Molecular Pharmacology group we had several resistant cell line pellets that could be utilised for an immunohistochemistry investigation. In addition, we had the privilege of having samples which belong to a small clinical series (Cell Signalling Series) that could be used for further research analysis. The immunohistochemical evaluation of pZIP7 was important in order to confirm the suitability of pZIP7 as a biomarker of endocrine resistance and to validate what was discovered *in vitro*. Therefore, in order to test our pZIP7 antibody in this clinical series, an immunohistochemistry assay had to be developed first. A new protocol for the use of pZIP7 antibody for immunohistochemistry was developed by Anna Gobbato, a master student working in our group under my supervision.

3.3.4.1 First immunohistochemical evaluation of pZIP7 in breast cancer cell pellets

Having established the best immunohistochemical protocol for the pZIP7 antibody, cell pellets of the different resistant cell lines were analysed as part of Anna Gobbato's Master's project. Cell pellets of the resistant cell lines were compared to both MCF-7 grown in stripped serum and also those grown in full serum. All the previous analyses with western blotting and immunofluorescence have been carried out by comparing the resistant cell lines to the MCF-7 grown in stripped serum in order to compare the same growth conditions in all cell lines. Here, the resistant cell lines were compared to both, in order to analyse any change between the two serum conditions.

The assessment of the slides showed that the cells grown in full serum had a very weak 1+ signal and looked almost completely negative for pZIP7, whereas the cells grown in stripped serum had a much stronger signal, although not as strong as the resistant cell lines (Figure 3.9). In fact, it was noticeable that the cell line with the strongest DAB signal for pZIP7 was TamR (Figure 3.9), confirming that previously discovered with the other techniques (Figure 3.3-B/Figure 3.4). In fact, TamR cells showed a strong 3+ DAB signal, with some areas of 1+ or 2+ staining. Immunohistochemical analysis revealed that almost 100% of TamR cells were positive for pZIP7, highlighting once again how this cell line was characterised by a significant ZIP7 activation. The long-term resistance model of TamR (TamRL) showed a slight decrease in DAB signal compared to TamR (Figure 3.9), confirming the results gained

with western blotting (Figure 3.3-B-C). TamRL cells generally exhibited a 1+ and 2+ signals, similar to FasRL (Figure 3.9). Interestingly, the long-term Faslodex®-resistant model had a stronger DAB signal for pZIP7, agreeing with previous results (Figure 3.3-B-C/Figure 3.4). In fact, while FasR cells displayed a heterogeneous staining similar to that seen for MCF-7 cells in stripped serum, the amount of activated ZIP7 increased in the corresponding long-term resistance model (Figure 3.9), suggesting that these cells had an increased use of zinc signalling mediated by the activation of ZIP7.

Table 3.1 showed the HScore of the cell pellets, confirming that the highest staining was revealed for the TamR cells, in accordance with that discovered with the previous biological analyses. While FasR cells showed only a slight increase of pZIP7 in comparison to MCF-7 grown in stripped serum, this level increased in the long-term resistance counter part of FasR (FasRL) (Table 3.1).

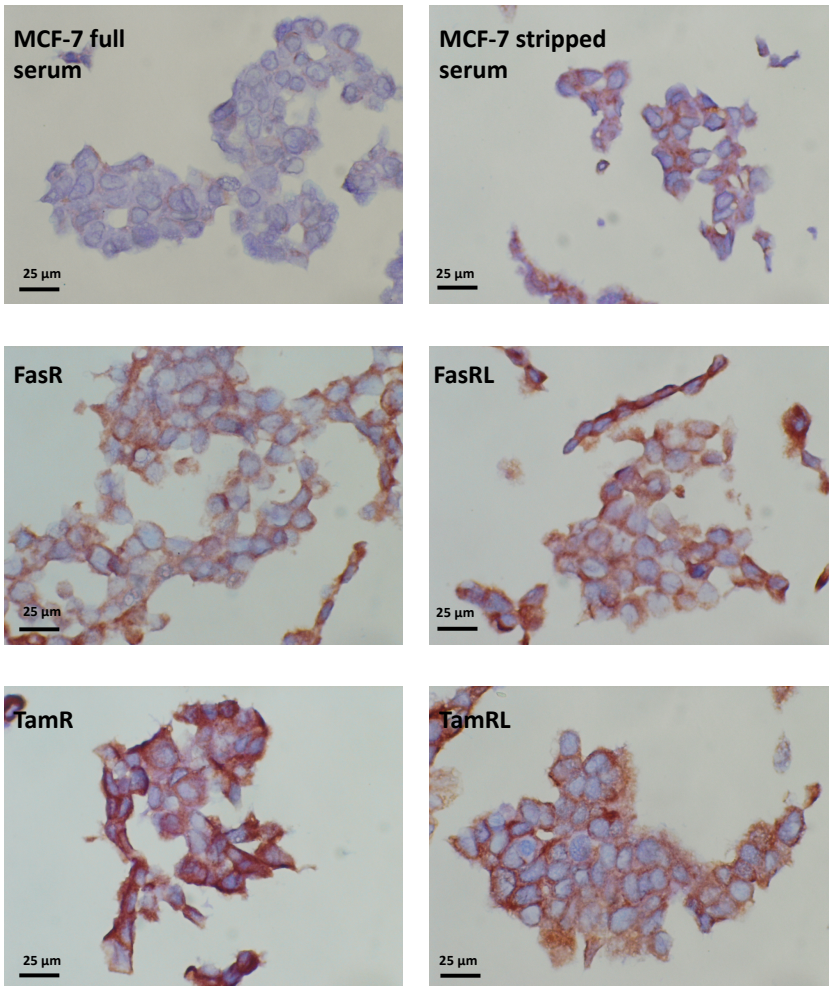

Figure 3.9 ***Immunohistochemistry analysis of pZIP7 in the different resistant cell lines****.*
Cell pellets were immunostained for pZIP7 (dilution 1/8000) using DAB (3'-3'-Diaminobenzidine) and methyl green for the nuclei. Magnification: 40x. The retrieval condition used for the protocol was pH 8 EDTA and pressure cooking microwave 950 W for 2 minutes. The resistant cell lines were compared to the MCF-7 pellets grown both in stripped and full fat serum. Scale bar: 25 µm. Courtesy of Anna Gobbato.

Cell line	HScore
MCF-7 full serum	20
MCF-7 stripped serum	95
FasR	115
FasRL	160
TamR	220
TamRL	175

Table 3.1 ***HScore of cell pellets.***
The table indicated the HScore of the cell pellets of the resistant cell lines in comparison to their parental MCF-7 grown in full fat serum or stripped serum. HScore is calculated as described in Chapter 2.4.

3.3.4.2 Analysis of pZIP7 in a small series of clinical samples

Following the evaluation of pZIP7 in cell pellets, the investigation analysed pZIP7 in breast cancer samples belonging to a series of 93 patients called "Cell Signalling Series" (NRES active, ethical approval C2020313/Nottingham city hospital). This was carried out in order to confirm the suitability of pZIP7 as a novel biomarker of breast cancer aggressiveness. After initial optimisation of the immunohistochemical protocol in the clinical material, the assay was extended to the full series of 93 patients. This assay revealed cytoplasmic staining typical of ZIP7, as consistent with a multi-transmembrane domains protein expressed in the endoplasmic reticulum. Overall, with this assay it was possible to see a remarkable pZIP7 staining in all the epithelial cells of the cancer tissues, as well as pZIP7 positivity across all samples in comparison to the low pZIP7 staining found in the tumour associated normal breast tissue (Figure 3.10). Overall the samples showed a heterogenous distribution of 1+, 2+ or 3+ DAB staining across the different sections (Figure 3.10). The range of HScores was 0-250 and the median HScore for the series was 117 (Table 3.2). The HScore of 0 was found in only one patient (Table 3.2), hence all but one patient showed evidence of some staining for pZIP7. The median HScore found for pZIP7 in this clinical series revealed that most of the samples had moderate staining, confirming that pZIP7 is evenly expressed in breast cancer and therefore it can be considered as a potential novel biomarker in the detection of breast cancer.

The "Cell Signalling Series" had been previously assessed for clinical parameters or biomarkers that are relevant to endocrine resistance. Therefore these were tested versus the level of pZIP7 (HScore). Comparison of pZIP7 to compiled data of other cancer markers revealed a significant direct association of pZIP7 with erbB2 ($p=0.028$), pMAPK ($p=0.019$), Fos ($p=0.007$) and CD71 ($p=0.015$), but weak or non-significant association with expression of ZIP7, PI3K or EGFR (Table 3.3). Spearman's analysis of pZIP7 in relation to steroid hormone receptors demonstrated a significant indirect association with the progesterone receptor ($p=0.036$), but non-significant association to the ER receptor (Table 3.3). Similar to the latter, proliferation (Ki67), tumour size and age were also found to be non-significant (Table 3.3). The only significant clinicopathological parameter which was linked to pZIP7 was high tumour grade ($p=0.046$), whereas there was no correlation between pZIP7 and menopausal status or tumour stage (Table 3.4).

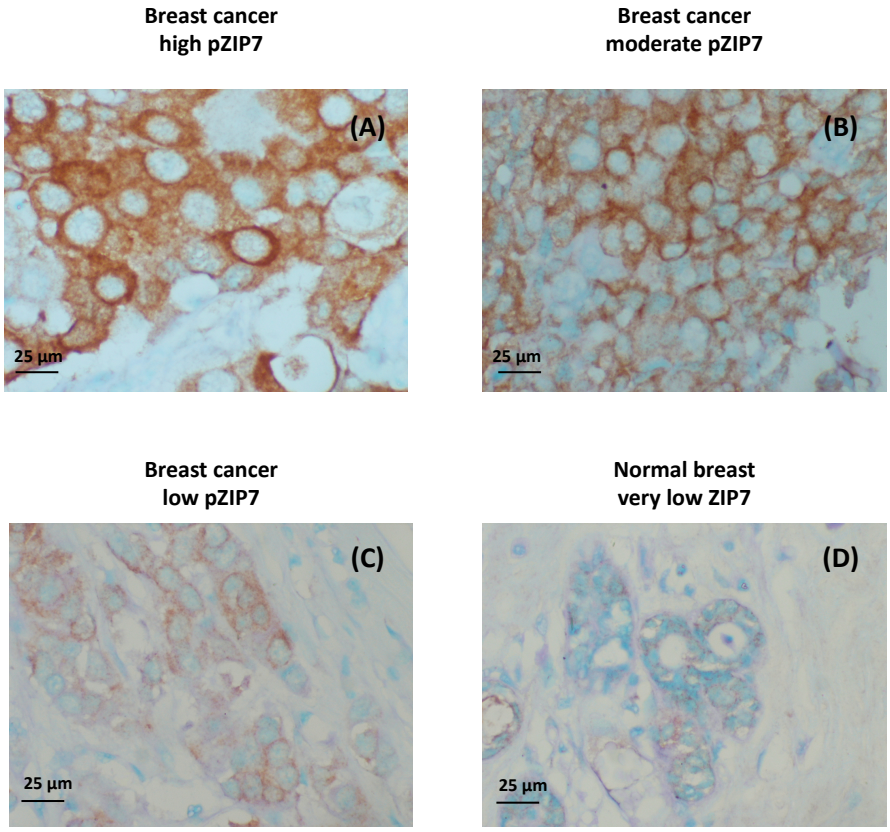

Figure 3.10 ***Immunohistochemistry analysis of pZIP7 in a small series of clinical samples****.*
Immunostaining of pZIP7 in breast cancer tissue samples from a clinical series (NRES active, ethical approval C2020313/Nottingham city hospital) compared to tumour associated normal breast tissue using the pZIP7 antibody at 1/800 dilution. pZIP7 was visualised using DAB (3'-3'-Diaminobenzidine) and methyl green for the nuclei. Magnification: 40x. Courtesy of Anna Gobbato and Pauline Finley.

Median HScore pZIP7	117	N=93
Min	0	
Max	250	

Table 3.2 ***HScore for pZIP7 in clinical breast cancer samples.***
The table indicated the median HScore from the 93 patients samples belonging to the "Cell Signalling Series" series (NRES active, ethical approval C2020313/Nottingham city hospital). The table also indicates the minimum and maximum score found for the analysis of this series.

Molecule	Test	Correlation	p and R values	Number	Comment
Steroid hormone receptors					
ER	protein	indirect	p=0.809 R=-0.025	n=92	non-significant
PR	protein	indirect	p=0.036 R=-0.234	n=81	significant
Growth factor receptors					
ErbB2	mRNA	direct	p=0.028 R=0.344	n=41	significant
EGFR	mRNA	indirect	p=0.488 R=-0.122	n=41	non-significant
CD71/transferrin receptor	protein	direct	p=0.015 R=0.252	n=93	significant
Transcription factors and other intracellular kinases					
pMAPK	phospho-protein	direct	p=0.019 R=0.244	n=93	significant
Fos	protein	direct	p=0.007 R=0.280	n=92	significant
PI3K	mRNA	direct	p=0.092 R=0.103	n=45	Weak association
Others					
ZIP7	mRNA	direct	p=0.109 R=0.199	n=66	weak association
Age	protein		p=0.460 R=-0.079	n=89	non-significant
Tumour size	protein		p=0.139 R=-0.170	n=77	non-significant
Proliferation (Ki67)	protein		p=0.383 R=-0.093	n=89	non-significant

Table 3.3 ***Spearman's correlation analysis between pZIP7 and different signalling pathways.***
This analysis was performed using the biomarkers data of the "Cell Signalling series" of breast cancer samples available on the SPSS database.

Clinicopathological parameters	Test	p value	Number of patients	Comment
Menopausal status	protein	p=0.522	n=82	non-significant
Tumour grade (1/2 low-moderate vs 3 high grade)	protein	p=0.046	n=91	significant
Tumour stage (Stage 1= lymph node negative disease vs 2/3= lymph node positive disease)	protein	p=0.331	n=73	non-significant

Table 3.4 ***Mann-Whitney tests examining pZIP7 in relation to clinicopathological parameters****.*
This analysis was performed using the clinicopathological parameters of the "Cell Signalling series" of breast cancer samples available on the SPSS database.

3.4 Discussion

Breast cancer is the most common malignancy among women (Bray *et al.*, 2018), and although several therapies are now available to tackle the illness, development of resistance is a considerable problem. Unfortunately, the mechanism of resistance is still unclear. When women are diagnosed with oestrogen-positive breast cancer, endocrine therapy is the mainstay of treatment. Despite the general success of this therapy, a large number of patients develop resistance (Dixon, 2014), making the treatment management a significant issue. The actual mechanism leading to developing resistance has been investigated for years, both *in vitro* and on clinical material (Clarke, Tyson & Dixon, 2015), but still displays several limitations, mainly due to the heterogeneity between different individuals and their cancers (Perou *et al.*, 2000). The lack of specific biomarkers to identify acquisition of resistance is another of these limitations (Larionov & Miller, 2009).

3.4.1 ZIP7 is highly expressed and activated in tamoxifen-resistant breast cancer

Many studies have linked zinc to breast cancer (Manning *et al.*, 1995; Mcclelland *et al.*, 1998; Kagara *et al.*, 2007; Taylor *et al.*, 2008) but in particular, studies on tamoxifen-resistant breast cancer cells have revealed a significant role for ZIP7, a member of the ZIP family of zinc transporters. Beyond being overexpressed in tamoxifen-resistant breast cancer cells (Taylor *et al.*, 2007), manipulation of ZIP7 has shown effects on both intracellular zinc content and in the aggressiveness of this different phenotype of breast cancer (Taylor *et al.*, 2008). Silencing ZIP7 expression in TamR cells by using siRNA reduces the activation of EGFR, Src and IGF-1R, as well as reducing cell motility, highlighting the importance of ZIP7 in driving the aggressiveness of the TamR breast cancer cell line (Taylor *et al.*, 2008). Moreover, a recent study in our group identified activated ZIP7 in driving downstream pathways such as PI3K, MAPK and mTOR, which are often hyperactivated in cancer and have implications with cancer survival and cell proliferation (Nimmanon *et al.*, 2017). Therefore, this project was focused on the study of ZIP7 in anti-hormone resistant breast cancer with the aim of addressing a potential role for ZIP7 as a biomarker of endocrine resistance in breast cancer. In order to achieve this, some unique models available from the Breast Cancer Molecular Pharmacology Group were used. These included tamoxifen and Faslodex®-resistant cells developed from MCF-7 cells and their long-term counter parts. These cell

models were tested for ZIP7 activation using our unique pZIP7 antibody (Nimmanon *et al.*, 2017). This study revealed that TamR cells had a significantly increased activation of ZIP7 (Figure 3.3-B) consistent with previous data of high gene expression of ZIP7 in this cell model (Taylor *et al.*, 2007), which was also confirmed by Affymetrix data (Figure 3.2-B). Increased activation of ZIP7 in conjunction with increased ZIP7 expression suggested that these resistant cells relied on ZIP7-mediated zinc signalling for growth. The current study also confirmed that TamR cells had increased cytoplasmic zinc in comparison to the parental MCF-7 cells (Figure 3.6), confirming that seen in a previous study (Taylor *et al.*, 2008). This finding suggested the likelihood of pZIP7 as a good biomarker and indicator of acquired resistance to tamoxifen in oestrogen receptor-positive breast cancer. Most importantly, immunofluorescence analysis showed that, although the total level of ZIP7 activation was decreased slightly in TamRL cells, it was still present in the same number of cells as the TamR (Figure 3.4), confirming that its use as a biomarker could be extended into prolonged treatment. The overexpression of ZIP7 in endocrine resistant breast cancer could be a cause of resistance that, as a consequence, led cells to utilise more zinc signalling to drive the activation of different downstream pathways associated with worsening of cancer, such as increased activation EGFR, IGR-1 and ERK signalling (Knowlden *et al.*, 2003, 2005; Frogne *et al.*, 2009; Nimmanon *et al.*, 2017). Therefore, the current study argued that increased activation of ZIP7 was responsible for the development of a more aggressive phenotype in the tamoxifen-resistant cell model as a consequence of increased use of ZIP7-mediated zinc signalling. The decrease of ZIP7 activation in the long-term model of TamR could be explained by the decrease of ZIP7 expression between the TamR and TamRL cells, as showed by Affymetrix data (Figure 3.2-B) and also by the decrease of total ZIP7 protein level seen with western blotting (Figure 3.3-A). Whether decrease of ZIP7 expression in the TamRL was a result of a longer exposure to tamoxifen is yet to be understood, but it still emphasised the importance of ZIP7 in driving the aggressiveness of this endocrine-resistant model. Taken together, this data confirmed the suitability of pZIP7 as a potential biomarker of acquired resistance to tamoxifen treatment, irrespective of additional exposure to the drug.

Moreover, TamR and TamRL had a significant increased activation of AKT when compared to MCF-7 (Figure 3.8-A). AKT, also known as protein kinase B, is a serine/threonine protein kinase participating in the control of apoptosis, cell growth and cell survival (Chang *et al.*, 2003). It is activated through phosphorylation on threonine residue 308 and serine 473 following an external stimulus such as growth factors and/or insulin (Alessi *et al.*, 1996). Activation of AKT is normally associated with cancer because of its involvement in mechanisms such as cell proliferation and cell survival (Chang *et al.*, 2003). Since previous studies discovered that activation of AKT was downstream of ZIP7 (Taylor *et al.*, 2008; Nimmanon *et al.*, 2017) and to the release of zinc (Taniguchi *et al.*, 2013), this evidence suggested that the increased activation of AKT observed in the tamoxifen-resistant cell lines could be a result of increased activation of ZIP7 in these cells. Interestingly, activation of AKT was higher in the long-term model of TamR (TamRL) than TamR cells (Figure 3.8 A), hinting that with additional exposure to tamoxifen, cells had increased use of ZIP7-mediated zinc signalling. This data confirmed the link between activated ZIP7 in driving activation of the AKT downstream pathway (Nimmanon *et al.*, 2017). Taken together this data implied that a longer exposure to tamoxifen led cells to acquire a more aggressive breast cancer phenotype.

3.4.2 The role of ZIP7 in Faslodex®-resistant breast cancer

No one has examined ZIP7 in FasR cells before, so it was intriguing to discover that FasR cells had a higher level of zinc when compared to MCF-7 cells (Figure 3.6). Nevertheless, FasR cells did not exhibit the same significant increase of ZIP7 activation as seen for TamR cells (Figure 3.3-B). Although ZIP7 phosphorylation increased in the long term FasR cells (FasRL) as suggested by immunofluorescence (Figure 3.4), this was not increased to the high level seen in the TamR cells. The slight increase of activated ZIP7 in FasRL cells could be explained by the fact that this long-term model of Faslodex® resistance had increased expression and protein level of ZIP7 (Figure 3.2-B/Figure 3.3-A), suggesting that with additional exposure to the drug the resistant cells utilised more ZIP7-mediated zing signalling. Moreover, our model of Faslodex® resistance were discovered to have two subpopulations of cells: EGFR positive and EGFR negative (Lewis, 2010), but it was not known whether the long-term model of FasR had a larger population of EGFR positive cells compared to the short-term model. However, since it

was previously discovered that the CK2-mediated activation of ZIP7 could be downstream of EGFR activation (Taylor *et al.*, 2008, 2012; Bafaro *et al.*, 2017), it could be that only the EGFR positive subpopulation actively used ZIP7-mediated zinc signalling. Furthermore, the discovery that the Faslodex®-resistant models did not have a significant level of activated ZIP7 in comparison to the tamoxifen-resistant models explained why activation of AKT was not significant in the former models, since AKT was discovered to be a direct downstream of ZIP7 (Nimmanon *et al.*, 2017). This implied that the Faslodex®-resistant cells relied on a different mechanism to grow other than ZIP7, which is yet to be fully understood.

3.4.2.1 FasR cells have increased expression of the ZnT1 transporter

Surprisingly, FasR cells were found to have significantly reduced activation of MAP kinase in comparison to MCF-7, which was observed also in their corresponding long-term cell line (Figure 3.8 B). This result was unexpected since activation of ZIP7 was discovered to be upstream of MAPK signalling pathway (Nimmanon *et al.*, 2017), and data from immunofluorescence and western blotting revealed that the overall activation of ZIP7 was slightly increased in the FasRL model, although not significant. However, MAP kinase is known to be associated with the activation of the ERα receptor (Kato *et al.*, 1995) and, as stated earlier, the Faslodex®-resistant-MCF-7 derived cells were discovered to be ER-negative (Nicholson *et al.*, 2005) due to the action of Faslodex®, an agent that induces the disruption of the oestrogen receptor. The correlation of the oestrogen receptor to the MAP kinase pathway could explain why the MAP kinase pathway was not activated in the FasR cell models. Additionally, FasR cells were shown by Affymetrix data to exhibit a higher expression of ZnT1 transporter (Figure 3.5). The zinc transporter ZnT1 is a zinc exporter involved in the transport of zinc from the cytoplasm to the extracellular space (Palmiter & Findley, 1995). The higher expression of ZnT1 transporter in the FasR cells could play a role in emptying the cytoplasm as soon as zinc is released from the endoplasmic reticulum by ZIP7 and could explain this reduced activation of MAPK. The overexpression of ZnT1 can also be a mechanism that this cell line acquired in order to overcome the highest level of zinc that was observed in the FasR cell line (Figure 3.6). The finding that both TamR and FasR cells had increased intracellular zinc (Figure 3.6) raised the question of whether other zinc transporters may be involved in this. The only zinc transporters that are known to be

dysregulated in breast cancer are ZnT2, ZIP6, ZIP7, ZIP9, and ZIP10 (reviewed by Pan *et al.*, 2017), but there is no current information about their expression in endocrine resistant cells, except for the know role of ZIP7 and the data provided within the current project on endocrine resistant breast cancer. In fact, the zinc transporter ZnT2 is known to accumulate zinc in the vesicles to prevent zinc toxicity (Lopez, Foolad & Kelleher, 2011) and it may act in coordination with ZnT1 to counteract the high level of intracellular zinc discovered in the FasR cell line (Figure 3.6). Assessment of these others zinc transporters in endocrine resistant breast cancer could help us decipher the mechanism by which FasR cells develop resistance as this model of resistance did not show the same increased activation of ZIP7 as observed in the TamR cells (Figure 3.3).

3.4.3 pZIP7 is evenly distributed in breast cancer clinical samples

This project was expanded to look at clinical breast cancer material to try to confirm these findings. In fact, a higher activation of ZIP7 would be expected to have severe consequences on cancer progression, considering the downstream pathways induced by zinc, such as inhibition of tyrosine phosphatases (Haase & Maret, 2003), activation of AKT and other pathways involved in cell migration (Taylor *et al.*, 2012; Nimmanon *et al.*, 2017). Here it was provided the first evidence that pZIP7 could be used as a good biomarker of tamoxifen-resistance. In fact, after having developed a pZIP7 assay for immunohistochemistry, it was possible to confirm that discovered with the biological tests. Once again, the tamoxifen-resistant cell pellets were found to have increased activation of ZIP7 (Figure 3.9), suggesting the increased use of zinc signalling and increased activation of signalling pathways that are downstream to the release of zinc in the cytoplasm. Hence, pZIP7 antibody was also tested on a small clinical sample series, revealing that pZIP7 was evenly expressed in the breast cancer tissue, in comparison to tumour associated normal breast tissue (Figure 3.10). This finding confirmed the suitability of pZIP7 as a novel biomarker of breast cancer diagnosis.

3.4.4 Activated ZIP7 is linked to a poor prognosis cohort of breast cancer patients

Analysis of clinical biomarkers in correlation with pZIP7 revealed the association of pZIP7 with activated MAPK (Table 3.3), confirming what was demonstrated in our recent paper which linked activation of ZIP7 to the MAPK signalling pathway, a hallmark of cancer (Nimmanon *et al.*, 2017). Moreover, the association of pZIP7 with receptor

protein tyrosine kinase erbB2 (Table 3.3), a well-known protein involved in endocrine resistance (Lupien *et al.*, 2010), reinforces the evidence of pZIP7 enrichment in a poor prognosis breast cancer cohort. Surprisingly, pZIP7 was found to be associated with the transferrin receptor (CD71) (Table 3.3). The transferrin receptor was initially discovered to transport iron, but it was also demonstrated to have a relative affinity to zinc (Charlwood, 1979). Considering that cells with increased expression and activation of ZIP7 were found to have increased cytoplasmic zinc, it implied that the transferrin receptor may cooperate with ZIP7 in transporting zinc in the cytosol and regulating its homeostasis. Additionally, Habashy *et al* discovered that the transferrin receptor was associated with cells having a high proliferation rate and it was also related to endocrine resistance, in particular to tamoxifen resistance (Habashy *et al.*, 2010). The correlation of CD71 to pZIP7 might imply a requirement of zinc in tissues with high cell proliferation rate which exhibit a more aggressive phenotype. Furthermore, this association fitted with the increased activation of ZIP7 seen in our model of tamoxifen resistance. Although Spearman's analysis between ki67, a marker of cell proliferation (Scholzen & Gerdes, 2000), and pZIP7 did not show any significant association (Table 3.3), it may indicate that pZIP7 could be involved with invasive, migration capacity more than cell proliferation or that pZIP7 could contribute to proliferation once the tumour had acquired resistance. Nevertheless, activated ZIP7 was significantly correlated to tumour grade (Table 3.4) with higher pZIP7 found in higher grade disease, typical of tumours that acquire poor differentiation and more disorganised nuclei. These types of tumours are indicator of poor prognosis and endocrine resistance, further suggesting a role for ZIP7 in this process. In this respect, it is interesting to notice that Kaplan-Meier plotter analysis has revealed that high ZIP7 gene expression is associated with decrease relapse-free survival (Figure 3.2). This indicates that increased ZIP7 expression and activated ZIP7 is not a good parameter to have in relation to endocrine outcome and further corroborates the direct association found between pZIP7 and tumour grade (Table 3.4).

Spearman's analysis also revealed the association of phospho-ZIP7 with the proto-oncogene c-Fos. Interestingly, this molecule is known to be associated to zinc status (Fanzo *et al.*, 2001) and endocrine resistance (Gee *et al.*, 1999). Fanzo *et al* have found that human epithelial bronchial cells supplemented with zinc had a two-fold

increase of c-Fos mRNA in comparison to cells with basal zinc status (Fanzo *et al.*, 2001). Therefore, the significant direct correlation of c-Fos to pZIP7 could be explained by the increased level of zinc induced by hyperactivation of ZIP7. Additionally, c-Fos was discovered to associate with the endoplasmic reticulum in order to activate lipid synthesis and it was found that its expression is increased in over 95% of biopsies of human ductal breast carcinoma (Motrich, Castro & Caputto, 2013), suggesting a link and a potential interaction between the two molecules in the development of aggressive breast cancer. All these findings contributed to strengthen the evidence that activation of ZIP7 was associated with the development of a more aggressive cancer phenotype and that pZIP7 may be an indicator of an endocrine resistance cohort. Moreover, the indirect association found between pZIP7 and the progesterone receptor (PR), an indicator of hormone responsiveness (Bartlett *et al.*, 2011) (Table 3.3), suggested that pZIP7 could be slightly enriched in tumours that are less likely to be hormone responsive and do acquire resistance. Since pZIP7 was also found to be directly associated with the ErbB2 receptor (Table 3.3), it implied that activation of ZIP7 could be higher in tumours that are HER2+ and PR-, both protein associated with increased endocrine resistance (Dunnwald, Rossing & Li, 2007; Lupien *et al.*, 2010). All this data was found on patients at diagnosis, therefore, now that this immunohistochemistry assay is available, this data needs to be followed-up with further analyses on different clinical series of breast cancer, which include samples of relapsed patients.

Taken together this data highlighted the involvement of zinc signalling in driving aggressiveness in breast cancer and added more information regarding the development of endocrine resistance, a clinical issue in breast cancer therapy that still needs to be fully understood. Activated ZIP7 could be used as a prognostic biomarker of acquired endocrine resistance that could have many therapeutic benefits. In fact, knowing that pZIP7 have been associated with downstream pathways such as MAPK and AKT, it suggests the possibility of using a combined targeted therapy to reduce the activation of pathways which are downstream of pZIP7 (Nimmanon *et al.*, 2017) by using MAPK, mTOR or AKT inhibitors in association with endocrine therapy. This strategy could provide a significant improvement to the outcome of the therapy. In fact, there is evidence of the use of an AKT inhibitor (AZD5363) on TamR cells which was shown to be

effective at resensitising cells to the antiproliferative effect of tamoxifen (Ribas *et al.*, 2015). These findings paved the way for further studies. In fact, as ZIP7 was demonstrated to require CK2 phosphorylation in order to be activated, tackling its activation could be a mechanism to prevent the downstream pathways responsible for the development of aggressive cancer. A CK2-inhibitor called CX-4945 is currently in clinical trials in combination with other chemotherapy drugs for its use in cancer treatment (ClinicalTrials.Gov Identifier: NCT02128282). Moreover, this drug was seen to enhance the antitumor effect of conventional chemotherapy drugs in different resistant cell lines (Zanin *et al.*, 2012). Since ZIP7 was discovered to be over-activated in our tamoxifen-resistant breast cancer model, this drug could be tested in these cells in order to assess any ability to reduce the activation of pathways that are downstream of ZIP7-mediated zinc signalling (Nimmanon *et al.*, 2017).

3.5 Chapter summary

This chapter has demonstrated that activation of ZIP7 can lead to the development of aggressive breast cancer. Using different biological techniques, it was possible to show that activation of ZIP7 was significantly increased in the tamoxifen-resistant cell lines, followed by increased activation of the protein kinase AKT. This investigation also showed that, despite a slight increase of pZIP7 in the Faslodex®-long term resistant model, this was not as significant as that observed in the tamoxifen-resistant cell lines. The distinct phenotype of the two different resistant models could be the reason beyond the outcome observed regarding the use of ZIP7 in these cell models.

Analysis of activated ZIP7 with different clinicopathological parameters and biomarkers also confirmed the association of pZIP7 with different molecular signalling pathways which play a pivotal role in driving cancer aggressiveness and are indicators of endocrine resistance. Now that an immunohistochemical assay for pZIP7 has been developed, this can be used in order to confirm its use as a novel biomarker of tamoxifen resistance in breast cancer, which is a current unmet need in therapy. In light of this, a new different approach to tackle the development of resistance can be investigated further by targeting the activation of ZIP7 with the use of CK2 inhibitors.

4 ZIP6 OR ZIP10 ANTIBODY TREATMENT INHIBITS CELL DIVISION IN MULTIPLE CANCERS

4.1 Introduction

It has been known since the 19th century that zinc is an essential requirement for cell growth (Raulin, 1869). Zinc was discovered to be necessary for DNA synthesis, required as a cofactor for DNA synthesis enzymes (Prasad & Oberleas, 1974; Chesters, Petrie & Vint, 1989; Chesters, Petrie & Travis, 1990), and also for the synthesis of new proteins which occurred during the cell cycle (Prasad, 1998). Most importantly, it was discovered that when cells were treated with metal chelating agents, cell growth was arrested and only reversed when zinc was supplied (Fujioka & Lieberman, 1964).

During the cell cycle two peaks of zinc concentration were reported: during the early G1 phase and at the G1/S transition (Li & Maret, 2009). However, another study revealed that zinc was also essential at the G2/M transition (Chesters & Petrie, 1999). More recently, it was also demonstrated that zinc is essential for meiotic maturation of oocyte (Bernhardt *et al.*, 2011, 2012), a type of cell division which occurs in gametes. However, the actual mechanism by which zinc regulates mitosis is yet to be fully discovered. Our group have discovered that two zinc transporters of the LIV-1 subfamily, called ZIP6 and ZIP10, form a heteromer on the plasma membrane (Taylor *et al.*, 2016) and that this heteromer provides the zinc necessary to trigger mitosis (*Taylor et al., unpublished*). Even though a crystal structure of these two zinc transporters is not yet available, a recent paper has predicted the crystal structure of the N-terminal domain of ZIP4, another ZIP transporter of the LIV-1 subfamily (Zhang, Sui & Hu, 2016). The N-terminal domain of ZIP4 was confirmed to be a dimer which is consistent with previous findings demonstrating that this feature is shared between ZIP transporters and necessary for zinc transport (reviewed by Kambe et al. 2015). The discovery of the first crystal structure of the extracellular domain of ZIP4 was extremely important as it provided the first predicted secondary structure of the ZIP6-ZIP10 heteromer (Zhang, Sui & Hu, 2016). This prediction led to the formulation of the hypothesis that by using specific ZIP6 and ZIP10 antibodies directed towards the extracellular domain of these zinc transporters it would be possible to block this heteromer and consequently to stop the zinc necessary to trigger mitosis. The current chapter provides insight into this matter.

4.1.1 Aims and objectives

The aim of this chapter was to confirm whether by treating different cancer cell lines with specific ZIP6 or ZIP10 antibodies it was possible to stop cell division. Consequently, the objectives of this chapter were:

1. To synchronise cells in mitosis and to treat cells with specific ZIP6 or ZIP10-directed antibodies;
2. To investigate the effect of ZIP6 and ZIP10 antibodies on cancer cell growth;
3. To investigate the fate of cancer cells when treated with these antibodies.

4.2 Methods

In order to investigate the potential of blocking mitosis by using specific customised antibodies directed against the N-terminal domain of both ZIP6 or ZIP10, cells were synchronised into mitosis by using different protocols. These consisted of nocodazole treatment, a double thymidine block and the use of a CDK1 inhibitor, called RO-3306. These methods will be explained in more detail in the next sections (Figure 4.1-3). After having established the protocol which gave the highest number of cells synchronised in mitosis, cells were treated with specific ZIP6 and ZIP10 antibodies (Figure 4.4) and tested for mitosis by probing cells for pS^{10}Histone H3, a marker of mitosis. The ability of these antibodies to stop mitosis was also investigated by measuring the rate of cell growth following a 4-day antibody cell treatment. Cells treated with these antibodies were assessed for cell viability by MTT assay. Moreover, the fate of the treated cells was analysed by measuring for apoptosis, cyclin levels and quiescence with western blot and immunofluorescence. For more details about the methods, refer to Chapter 2.

4.2.1 Cell synchronisation in mitosis

4.2.1.1 Nocodazole treatment

Cells were first treated with nocodazole for 20 hours. Nocodazole is an anti-neoplastic agent which interferes with the polymerisation of microtubules. Cells were treated for 20 hours with this agent which stopped cells in prometaphase as the microtubules could not polymerase (Blajeski *et al.*, 2002). After cells were fixed, cells were probed for pS^{10}Histone H3, a marker of mitosis and stained with DAPI, a marker of the nuclei. The slides were visualised under a microscope and assessed for the

percentage of cells in mitosis by comparing this result to the control (non-treated cells). Mitotic cells were counted by measuring the ratio between the cells positive for pS^{10}Histone H3 to the total number of cells per each field of view. Evaluation of MCF-7 cells treated with nocodazole revealed that an average of 34% of cells were mitotic when treated with this agent (Figure 4.1). In contrast, non-treated cells showed only 4% of mitotic cells (Figure 4.1).

4.2.1.2 Double thymidine block

The second method used to synchronise cells was a double thymidine block (2 mM) on MCF-7 cells (see section 2.2). The double thymidine block has been widely recognised to synchronise cells as thymidine blocks DNA synthesis. Cells were treated with this agent initially for 18 hours followed by a second treatment of 17 hours after 9 hours of release from the first thymidine block. This treatment blocked cells at the S phase of the cell cycle. After release from the second thymidine block, cells were left to proceed through the cell cycle without any further treatment (Whitfield *et al.*, 2002). Cells were monitored under the microscope until they rounded up, which is a characteristic typical of mitotic cells. Cells were harvested 5 hours after the removal from the second thymidine block and at different intervals, then imaged and probed for pS^{10}Histone H3. Nuclei were counterstained with DAPI. The highest number of mitotic cells was seen between 8.75 and 9 hours from release from the second thymidine block, showing an average of 15% of mitotic cells overall (Figure 4.2).

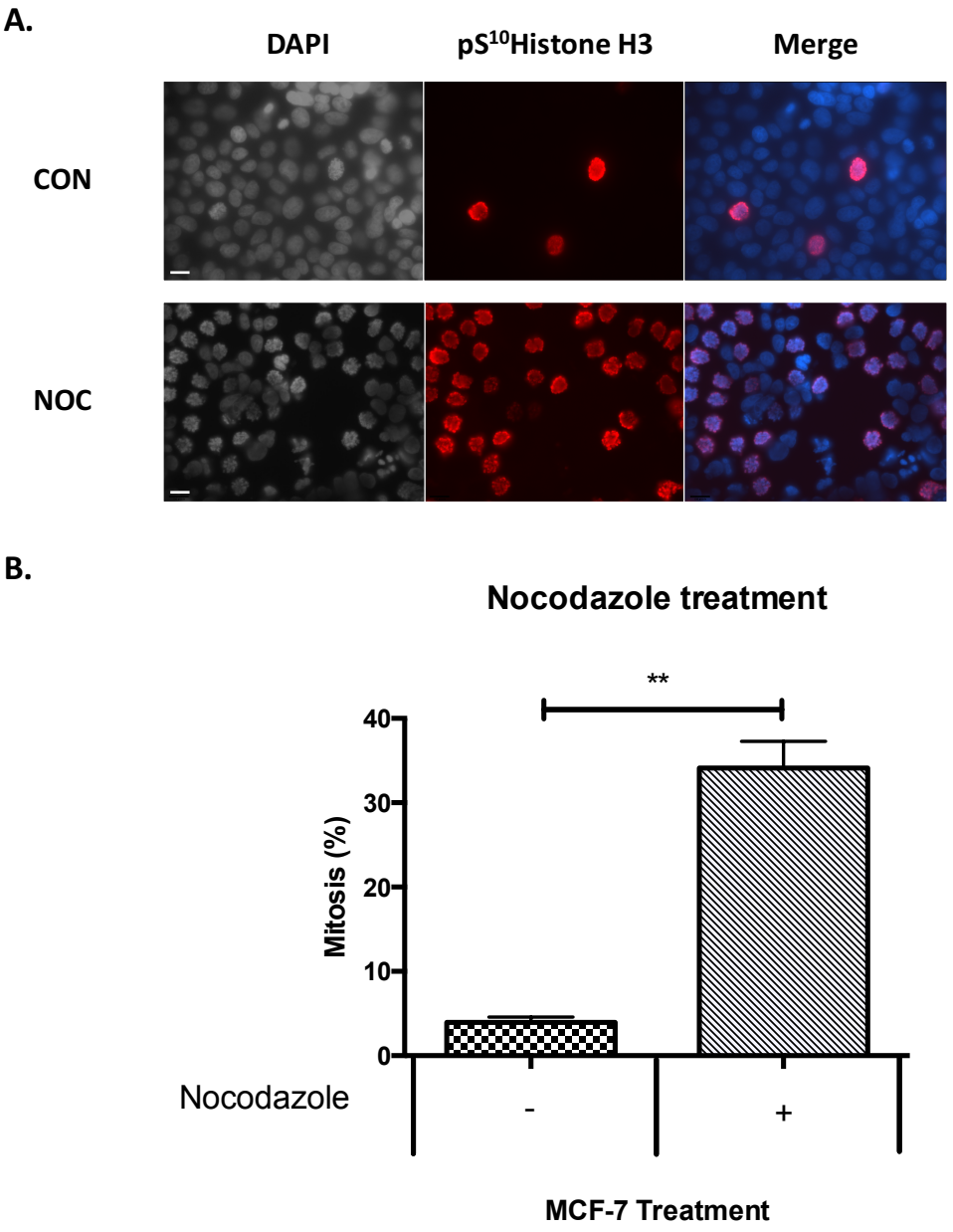

Figure 4.1 ***MCF-7 cells synchronisation in mitosis by nocodazole treatment****.*
Cells at 70-80% confluence were treated with 150 nM nocodazole (NOC) for 20 hours prior to harvesting.
A. Cell were fixed with 3.7% formaldehyde and probed for pS[10]Histone H3 (red) and the nuclei counterstained with DAPI (blue). Cells were visualised under a 63x oil Leica DMIRE2 microscope and pictures are representative of each treatment (n=3).
*B. Counting of the cells positive for mitosis per each field of view was performed by using ImageJ for Mac OS and at least 6 pictures were taken per each treatment. Statistical analysis is shown as n=3 + SEM (standard error of the mean) with **(p<0.01). Scale bar: 10 μm.*

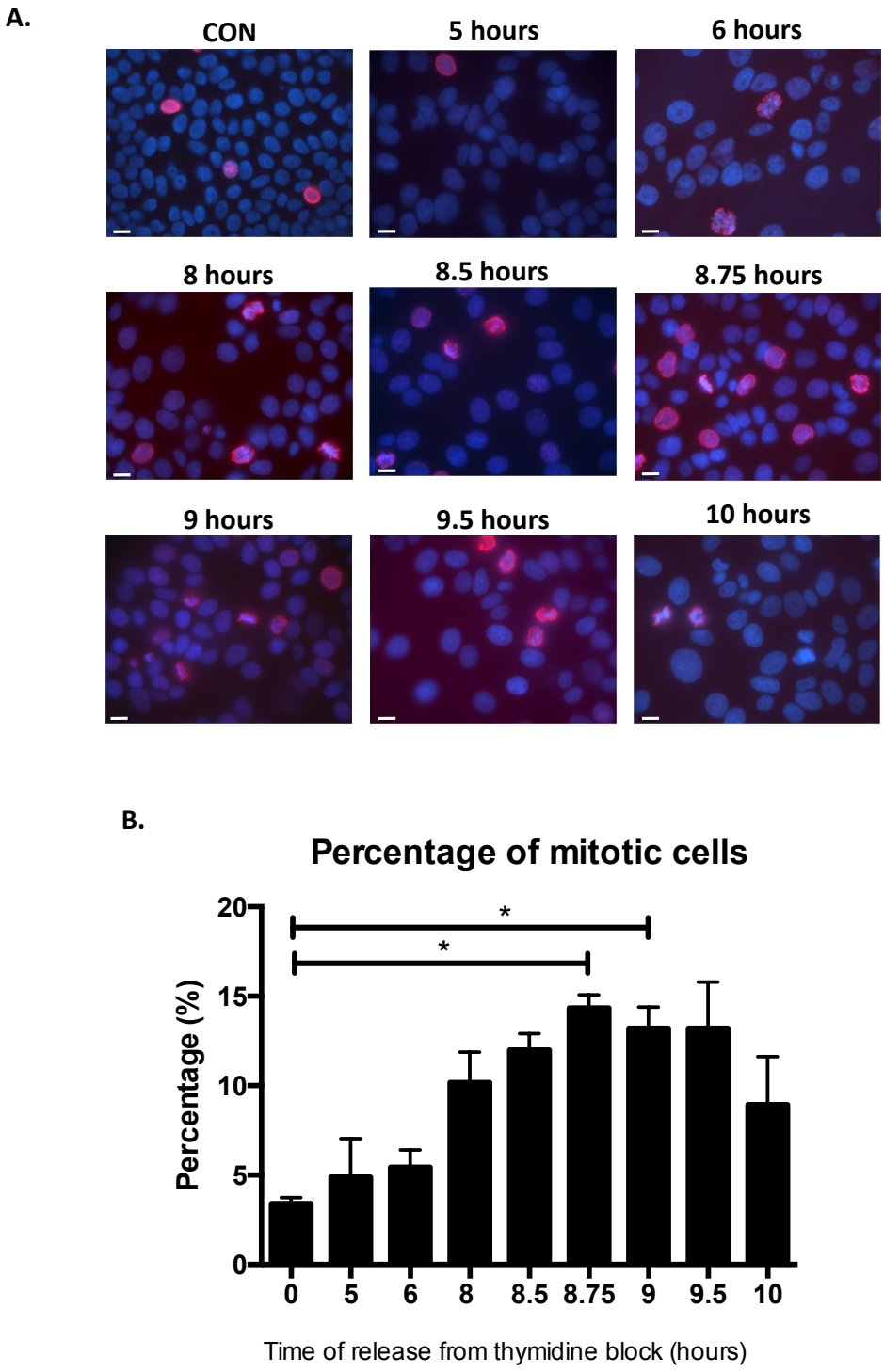

Figure 4.2 ***Percentage of mitotic cells following cell synchronisation with double thymidine block.***
MCF-7 cells at 30% confluence were treated with 2 mM thymidine for 18 hours. After this time cells were released from the treatment for 9 hours, followed by a second treatment with 2 mM thymidine for 17 hours. After this cells were left to proceed through the cell cycle before harvesting.
A. Cells were harvested at different times and fixed with 3.7% formaldehyde. Samples were probed for pS[10]Histone H3 (red) and nuclei counterstained with DAPI (blue). Slides were visualised under a 63x oil Leica DMIRE2 microscope and counted for the number of mitotic cells per each field of view. Pictures are representative of at least 6 different fields of view per each different harvest time.
*B. Statistical analysis is shown as n=3 + SEM (standard error of the mean) with *(p<0.05). Scale bar: 10 μm.*

4.2.1.3 Use of RO-3306, a CDK1 inhibitor

CDK1 (also known as cdc-2) is a molecule which regulates the progression of cells from the G2 phase to mitosis, as it forms a complex with cyclin B1 which is essential at the onset of mitosis (Gavet & Pines, 2010a, 2010b). For this reason, the third and last method used to investigate synchronisation of cells into mitosis was carried out by using a CDK1 inhibitor (RO-3306) to synchronise cells in G2 (Vassilev, 2006). MCF-7 cells were treated with 9 μM RO-3306 for 18 hours, in order to block cells at the G2 phase of the cell cycle. Following this, cells were either left to progress through the cell cycle or 150 nM nocodazole was added for 2 hours. Cells that were released from the RO-3306 treatment for 2 hours showed an average of 13% of mitotic cells (Figure 4.3) in comparison to the non-treated cells which displayed 4% of mitotic cells. On the contrary, cells that were treated with nocodazole for 2 hours after the release from the CDK1 inhibitor showed an average of 17% of mitotic cells (Figure 4.3). In order to test the efficacy of this treatment in comparison to other protocols, this experiment was performed comparing the use of the CDK1 inhibitor to nocodazole-only treated cells. In fact, when comparing the results obtained with the RO-3306 agent, it was noticeable that the highest percentage of mitotic cells was obtained with the 20 hours nocodazole-only treatment, which revealed that over 30% of cells were mitotic (Figure 4.3).

Pooling all this data together, treatment of cells with 150 nM nocodazole was determined to be the most effective method to generate sufficient cells in mitosis to enable a useful experiment. This method was used throughout the rest of this project in order to synchronise cells in mitosis.

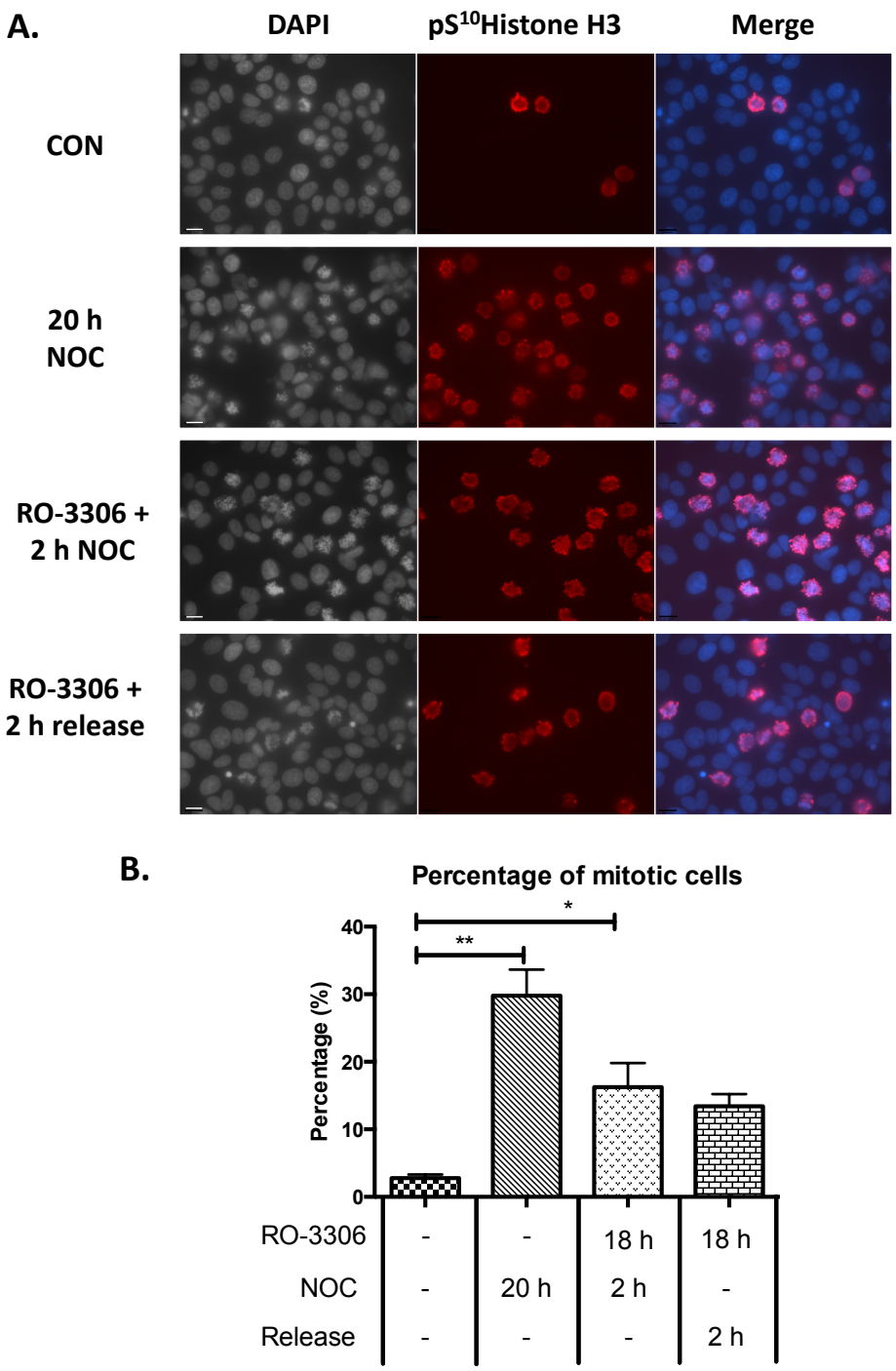

Figure 4.3 ***MCF-7 synchronised in mitosis by using a CDK1 inhibitor (RO-3306).***
MCF-7 cells at 70% confluence were treated with 150 nM nocodazole for 20 hours, or 9 μM RO-3306 for 18 hours followed either by 2 hours nocodazole or by medium replacement only.
A. Cells were harvested and fixed with 3.7% formaldehyde and probed for pS[10]Histone H3 (red) along with DAPI (blue). Cells were visualised under a 63x oil Leica DMIRE2 microscope and mitotic cells counted using ImageJ for Mac OS. Each picture is representative of at least 6 pictures per each treatment.
*B. Statistical analysis is shown as n=3 + SEM with ** ($p<0.01$) or * ($p<0.5$). Scale bar: 10 μm.*

4.2.2 Antibodies used for the mitosis inhibition experiment

Our group have unique ZIP6 and ZIP10 customised antibodies whose epitopes reside in their N-terminal domain. The N-terminal domain of ZIP6 and ZIP10 is located outside the cell when these are positioned on the plasma membrane. In particular, our customised ZIP6 Y antibody binds an epitope between residues 238-254 of the long N-terminal domain of ZIP6 (see Figure 4.4-A). This corresponds to an epitope after the potential PEST cleavage site, a post-translational modification that was confirmed for ZIP6 before its relocation to the plasma membrane (Hogstrand *et al.*, 2013). This cleavage has not yet been confirmed for ZIP10. However, ZIP6 and ZIP10 are the only two members of the LIV-1 subfamily to have potential PEST cleavage sites on their N-terminal domain (Taylor *et al.*, 2016) and therefore, it was believed that ZIP10 could also undergo a similar proteolytic cleavage. Nevertheless, the ZIP10 R antibody that was used for this project binds an epitope of ZIP10 in the early sequence of its N-terminal domain (residues 46-59) (see Figure 4.4-A). As soon as this PEST cleavage site is confirmed we will be able to generate a similar antibody for ZIP10 which could be used to assess whether ZIP10 is cleaved during mitosis.

Our group have recently discovered that the epitope recognised by the ZIP6 Y antibody is cleaved off during early mitosis and therefore this epitope is present on the plasma membrane only at the beginning of mitosis (Nimmanon, 2016). Whether this cleavage is used as a "switch-off" mechanism after mitosis starts is yet to be understood. Furthermore, our group have previously had another ZIP6 customised antibody made, called ZIP6 M, whose epitope resides at the beginning of the ZIP6 N-terminal domain (residues 93-107) (see Figure 2.2). The epitope of this antibody is prior to the PEST cleavage site which is cleaved off before ZIP6 relocates to the plasma membrane (Hogstrand *et al.*, 2013), thus prior to mitosis. This was further confirmed by the evidence that treatment of cells synchronised in mitosis by nocodazole and treated with the ZIP6 M antibody was not effective in stopping nocodazole-induced mitosis (Nimmanon, 2016). For this reason, for the mitosis inhibition experiments carried out in this study, the ZIP6 Y antibody was used. In order to test the hypothesis of the involvement of this heteromer in mitosis initiation, mitotic cells were incubated with the ZIP6 Y or ZIP10 R antibodies in an effort to block the required zinc influx (Figure 4.4-B).

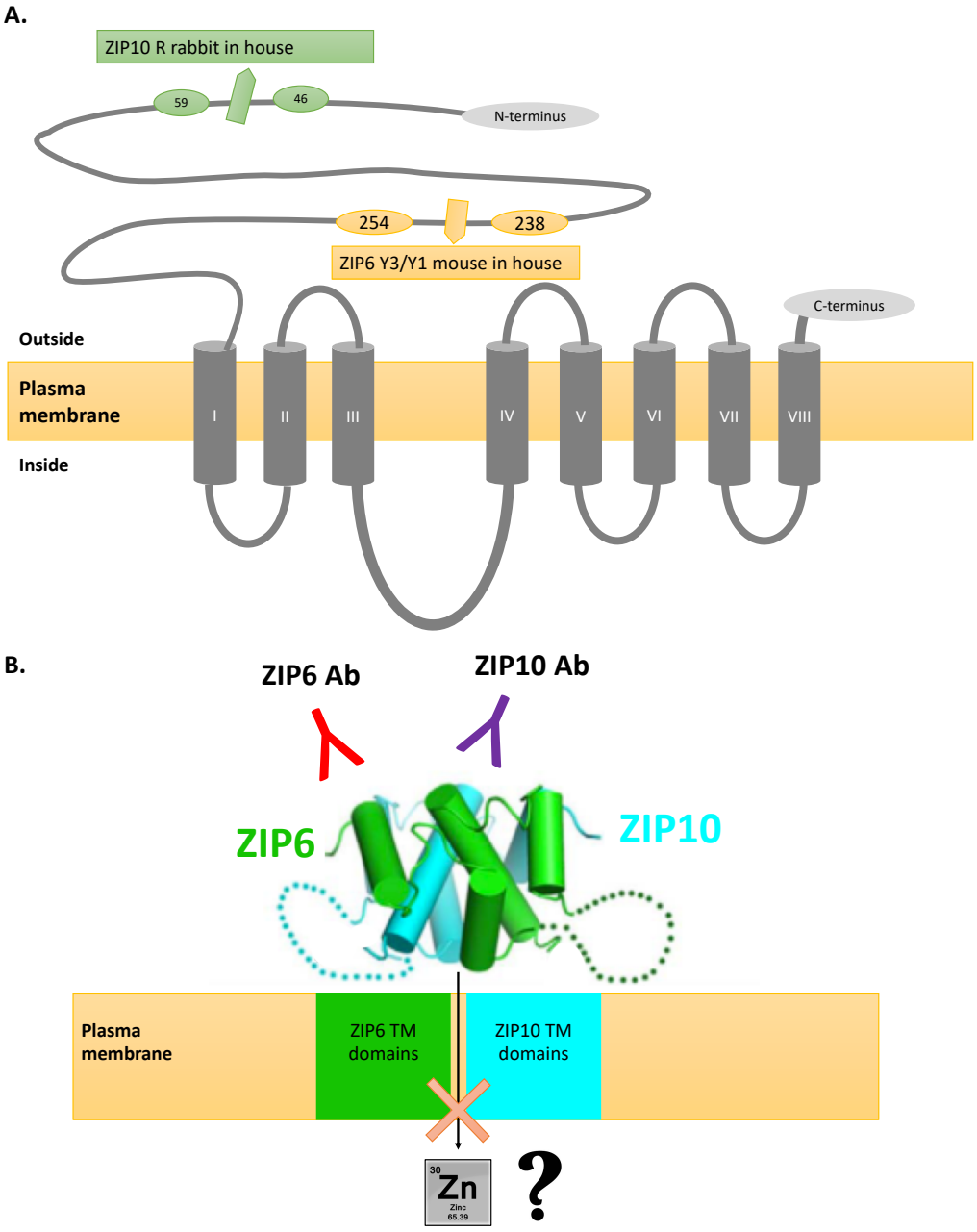

Figure 4.4 ***Inhibition of the ZIP6/ZIP10 heteromer****.*
A. Schematic showing the epitope of the ZIP6 Y and ZIP10 R antibodies used for the mitosis inhibition experiment.
B. Predicted crystal structure of the N-terminal domain of ZIP6 and ZIP10. These two zinc transporters form a heteromer (Taylor *et al.*, 2016) *and their N-terminal domain is intertwined with each other. This Figure suggests that either a ZIP6 or ZIP10-directed antibody to the extracellular region may be able to block this heteromer and the zinc influx to trigger mitosis. The picture was adapted from Zhang et al, 2016.*

4.2.2.1 Concentration of the ZIP6 and ZIP10 customised antibodies

Before starting any mitosis inhibition assessment, the concentration of the customised ZIP6 and ZIP10 antibodies was measured. This was achieved by ELISA for the ZIP6 Y antibody (mouse monoclonal) and using an easy-titer IgG assay for the ZIP10 R antibody (rabbit polyclonal). The method and protocol used for these assays can be found in Chapter 2. The concentration of the ZIP6 Y antibody is 40 μg/ml, whereas the concentration of the ZIP10 R antibody is 105 μg/ml (Table 4.1).

Antibody	Species	Epitope	Concentration
ZIP6 Y	Mouse	N-terminus Residue 238-254 VSEPRKGFMYSRNTNEN	40 μg/ml
ZIP10 R	Rabbit	N-terminus Residue 46-59 LEPSKFSKQAAENE	105 μg/ml

Table 4.1 ***Details of the antibodies used for the mitosis inhibition experiment.***
The table summarises the species, the epitope and the concentration of the antibodies used for the mitosis inhibition experiment within this current project.

4.3 Results

4.3.1 ZIP6 and ZIP10 antibody treatment to prevent cell division

4.3.1.1 ZIP6 and ZIP10 are overexpressed in mitosis

Our group have recently discovered that zinc transporters ZIP6 and ZIP10 form a heteromer on the plasma membrane (Taylor *et al.*, 2016) which influxes zinc into cells to trigger mitosis (*Taylor et al., unpublished*). Considering this recent discovery of a mechanism requiring zinc for the initiation of mitosis, the aim of this part of the project was to assess whether by treating cancer cell lines with antibodies targeting the extracellular N-terminal domain of ZIP6 or ZIP10, it was possible to prevent cell division. It was important to first show that ZIP6 and ZIP10 were increased in mitosis. In fact, a recent investigation in our group has already demonstrated that when MCF-7 cells were transfected with recombinant ZIP6 or ZIP10, FACS cell cycle analysis revealed a dramatic increase of the population of cells in the G2/M phase from 14 to 40%, in comparison to the control untransfected cells (Taylor *et al.*, 2016).

Here, MCF-7 cells were synchronised in mitosis with nocodazole and probed for ZIP6 or ZIP10. Cells were also probed for ZIP4, as a negative control. Results showed that while ZIP4 was evenly expressed on the plasma membrane of all the cells, ZIP6 and ZIP10 were only present on mitotic cells (Figure 4.5). Pictures in Figure 4.5 were taken on a confocal microscope. Therefore, it was interesting to notice that while staining for ZIP6 and ZIP10 showed a clear area on the plasma membrane only in mitotic cells which extended beyond the plasma membrane, ZIP4 staining showed a thin line on the plasma membrane of all cells whether mitotic or non-mitotic. The staining of ZIP6 and ZIP10 was indicative of a complex which corroborated the evidence that ZIP6 and ZIP10 was discovered to form a heteromer on the plasma membrane (Taylor *et al.*, 2016).

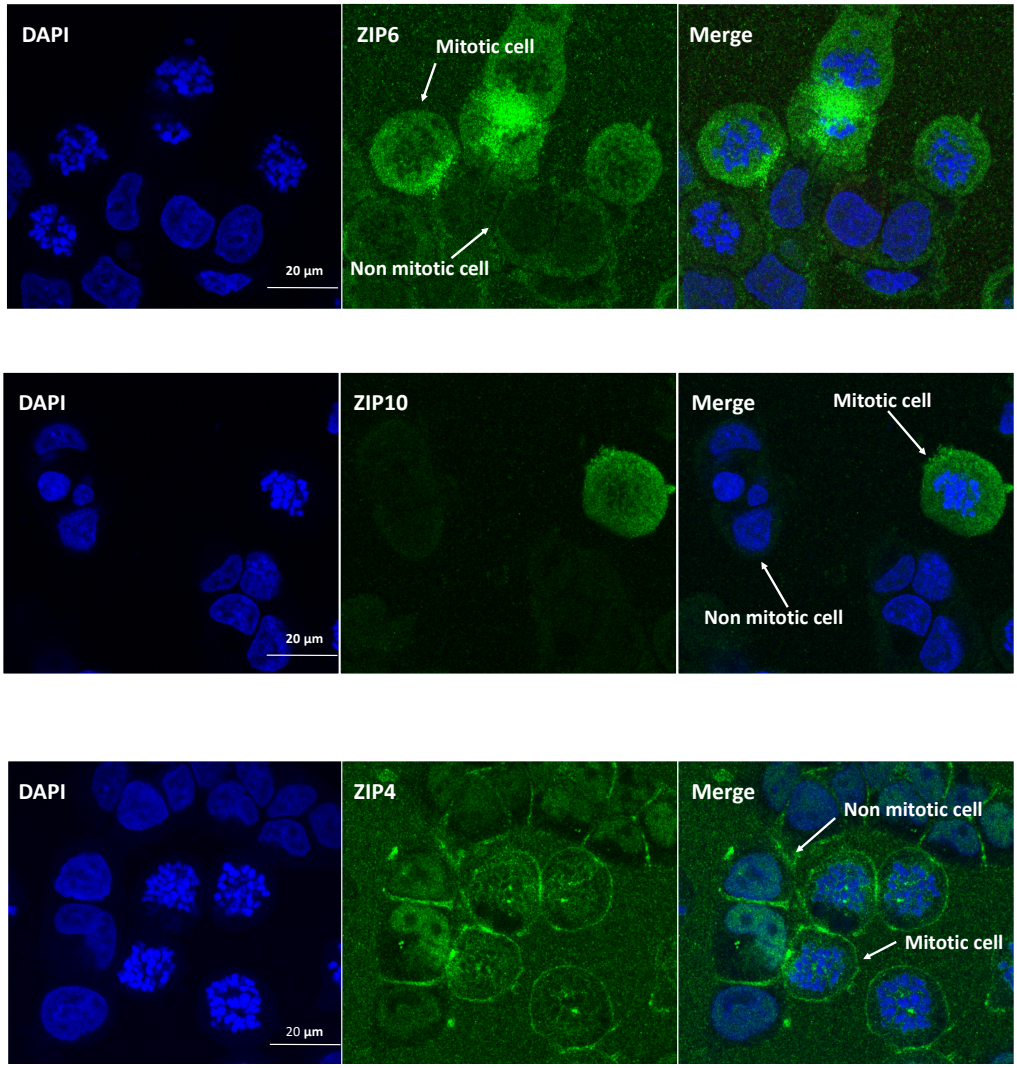

Figure 4.5 ***ZIP6 and ZIP10 are overexpressed in mitotic cells.***
MCF-7 cells at 70% confluence were treated with 150 nM nocodazole for 20 hours before harvesting. Cell were fixed with 3.7% formaldehyde and probed for ZIP6 (sc-84875)), ZIP10 (Biogenes, in house) or ZIP4 (20625-1-AP) (green fluorescence) and nuclei counterstained with DAPI (blue). Cells were visualised under a high resolution microscope Zeiss LSM 880 using a 63x oil immersion lens. Scale bar: 20 µM.

4.3.1.2 Using ZIP6 or ZIP10-directed antibodies to prevent cell division

Mitosis inhibition was assessed with immunofluorescence, probing cells for pS^{10}Histone H3 and nuclei counterstained with DAPI, both markers of mitosis (Figure 4.6-8). Cells treated with either the ZIP6 or ZIP10 antibody were compared to the non-treated cells (CON), to the cells treated only with nocodazole (NOC) and to the negative control which was normal mouse IgG for the ZIP6 antibody and normal rabbit IgG for the ZIP10 antibody. The experiment was performed first on MCF-7 cells. Counting of the untreated cells revealed 4% of the cells per field were mitotic judged by staining with both pS^{10}Histone H3 and DAPI, whereas nocodazole treatment increased this percentage to 30-40% (Figure 4.6-4.7). The inclusion of the ZIP6 antibody with nocodazole (Figure 4.6) was able to inhibit mitosis in an antibody concentration-dependent manner (Figure 4.6-B). In particular, treatment of MCF-7 cells with nocodazole and the ZIP6 antibody at 4 μg/ml reduced the percentage of mitotic cells to a percentage similar to control levels (Figure 4.6-B). This concentration was determined as the most effective at significantly preventing cell division. Therefore, a normal mouse IgG at the concentration of 4 μg/ml was used in comparison to our ZIP6 antibody at the same concentration. Since there is evidence that human IgG could bind zinc (Yamanaka *et al.*, 2016), a negative control was used in order to confirm that the ability to prevent cell division relied only on the binding of our antibody to ZIP6. The experiment confirmed that when cells were treated with nocodazole and the normal mouse IgG, the percentage of mitotic cells was around 30%, whereas when cells were treated with nocodazole and our ZIP6 antibody at the same concentration this percentage was down to 4-5% (Figure 4.6). This data confirmed the capability of the ZIP6 antibody to prevent cell division by stopping the zinc influx necessary to trigger mitosis.

The same experiment was performed with the ZIP10 R antibody, which binds an epitope at the beginning of the N-terminal domain of ZIP10. For this investigation a different concentration of the ZIP10 R antibody was used (10.5 μg/ml, 5.25, μg/ml, 2,1 μg/ml or 1.05 μg/ml), as preliminary results in our group have shown that this was required in order to have the same effect observed with the ZIP6 Y antibody. Whether this difference in concentration was due to the different nature of the antibody has not been confirmed yet. In fact, while the ZIP6 Y is a mouse monoclonal antibody, the ZIP10 R is a rabbit polyclonal, which may influence the effective concentration of the two

antibodies. Therefore, the concentration used for the IgG rabbit negative control was 10.5 μg/ml to fit with the amount of antibody used. The results obtained by using this antibody at preventing mitosis showed the same effect observed with the ZIP6 Y3 antibody. In fact, while untreated cells showed only 4% of mitotic cells in comparison to the 30% of nocodazole-treated cells (Figure 4.7), the inclusion of the ZIP10 R antibody decreased the percentage of mitosis in a concentration dependant manner, irrespective of the nocodazole synchronisation in mitosis (Figure 4.7). In particular, at the concentration of 10.5 μg/ml the percentage of mitotic cells was significantly decreased to 4%, similar to the control level (Figure 4.7). This experiment was previously performed with a commercial antibody in our group, showing that the most effective concentration at preventing cell division was 50 μg/ml (Nimmanon, 2016). However, the antibody used for that experiment was a commercial ZIP10 antibody (SAB 2102209) directed against a different epitope to the one recognised by the customised ZIP10 R. The commercial SAB 2102209 antibody binds ZIP10 on the N-terminal domain, but not on the same epitope as the ZIP10 R antibody. Different subfamilies of polyclonal antibody isotopes present different heavy chains and they differ in the capacity to activate the host immune system and complement or trigger antibody-dependant cell-mediated cytotoxicity (Vidarsson, Dekkers & Rispens, 2014). Moreover, as ZIP6 and ZIP10 forms a heteromer, it may be that the epitope recognised by the commercial antibody is masked by the intertwined N-terminal domains and not available for antibody binding, explaining the requirement for a different concentration of the antibodies in order to be effective at preventing mitosis. This could also explain why the concentration used for the ZIP6 antibody was lower than the one used for the ZIP10 antibody. Deciphering the nature of the ZIP6-ZIP10 heteromer would give us important information in this matter.

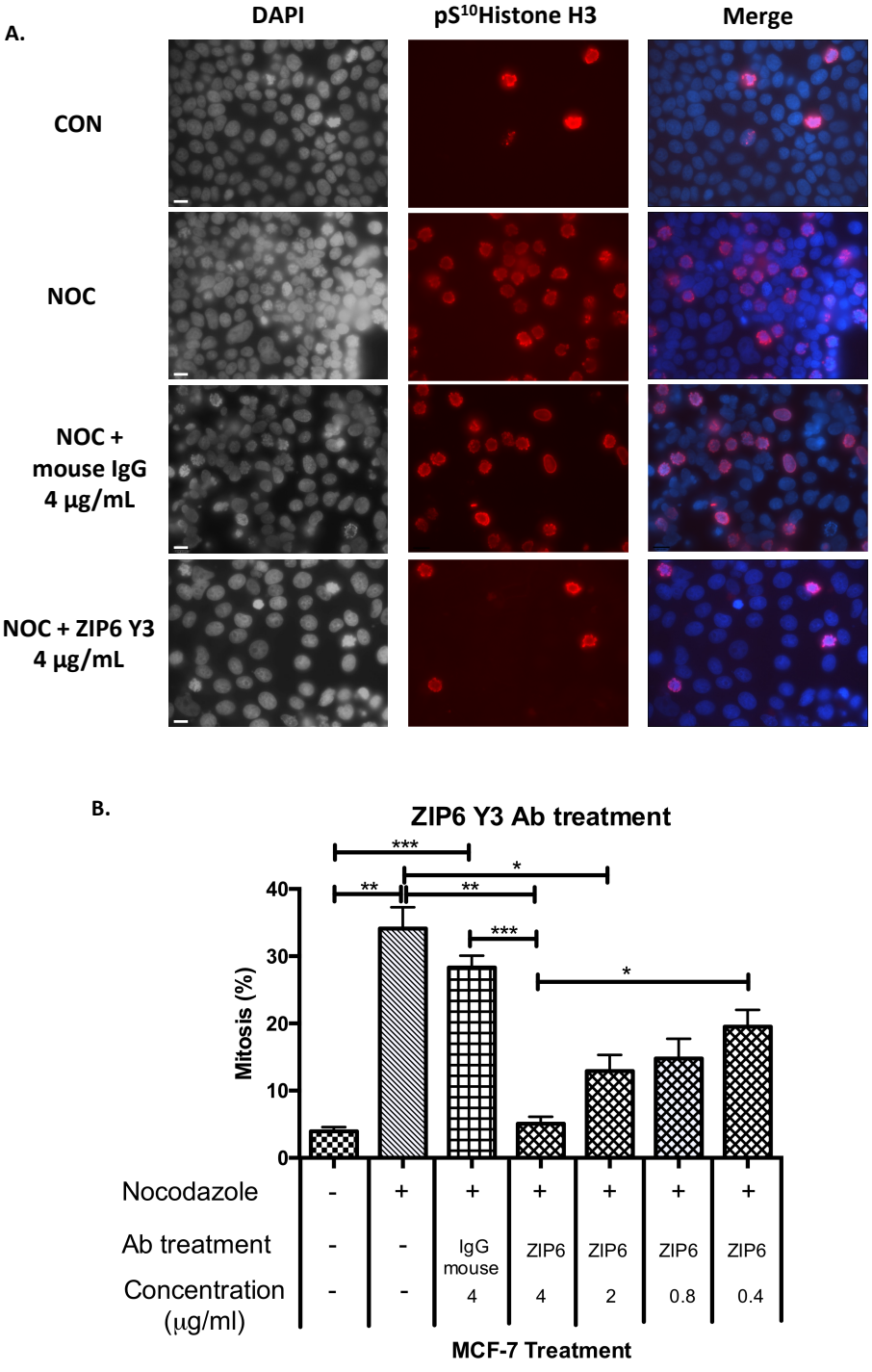

Figure 4.6 ***ZIP6 antibody treatment can prevent mitosis.***
MCF-7 cells were treated at 70% confluence with 150 nM nocodazole (NOC) with or without ZIP6 Y3 antibody at different concentrations. In addition, a normal mouse IgG at 4 µg/ml was used as a negative control.
A. After 20 hours treatment, cells were fixed and probed for pS[10]Histone H3 antibody (red) and nuclei counterstained with DAPI (blue). Each picture is representative of at least 6 pictures per each treatment (n=3).
*B. Total number of cells and mitotic cells were counted using ImageJ and the percentage of mitotic cells was plotted on a graph. The graph shows the mean of n=3 ± SEM (standard error of the mean). Statistical significance is indicated by *** (p<0.001),** (p<0.01) and * (p<0.05). Scale bar: 10 µm.*

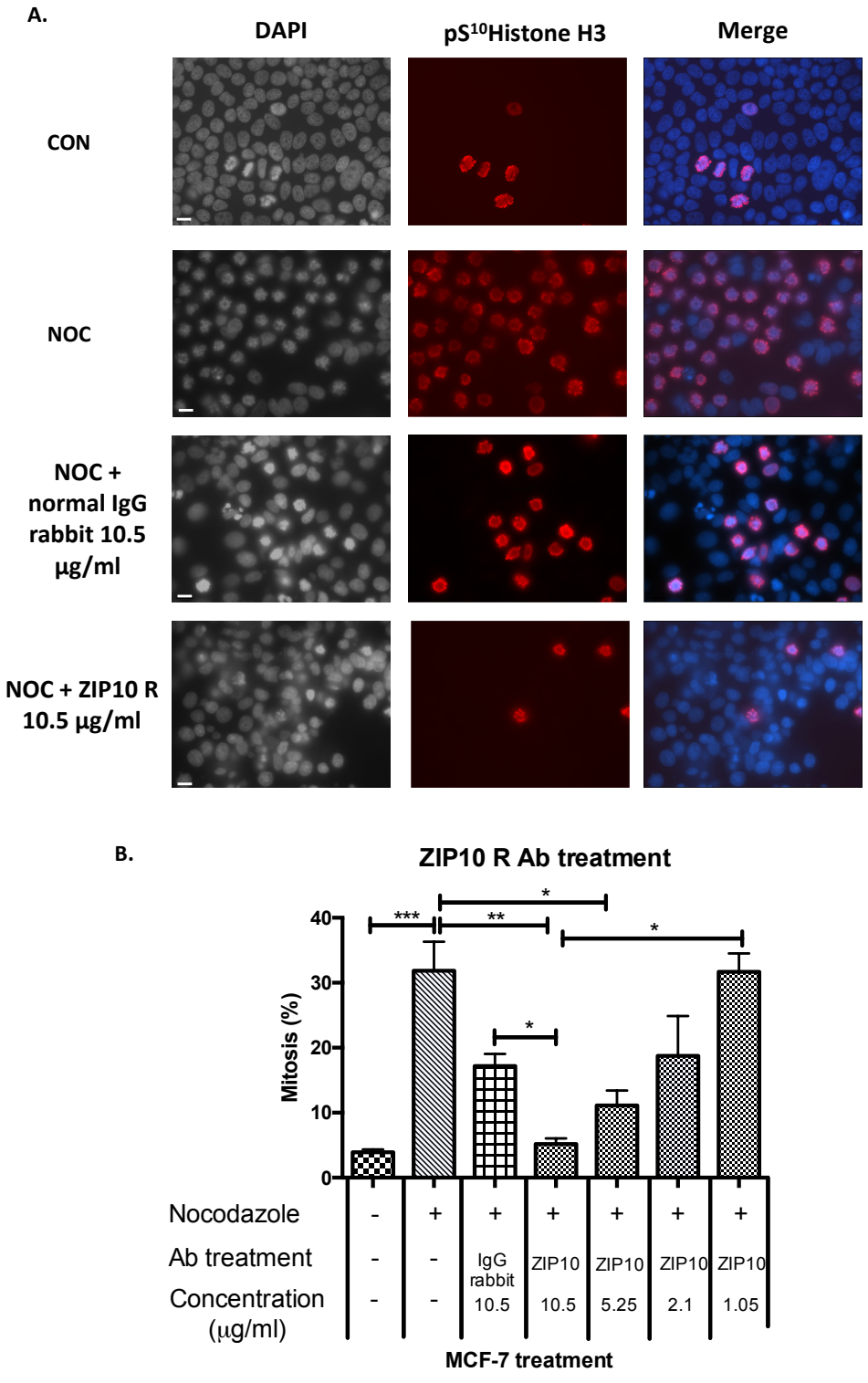

Figure 4.7 ***ZIP10 antibody treatment can prevent mitosis.***
MCF-7 cells were treated at 70% confluence with 150 nM nocodazole (NOC) with or without ZIP10 R antibody at different concentrations. In addition, a normal rabbit IgG at 10.5 µg/ml was used as a negative control.
A. After 20 hours treatment, cells were fixed and probed for pS[10]Histone H3 antibody (red) and nuclei counterstained with DAPI (blue). Each picture is representative of at least 6 pictures per each treatment (n=3).
*B. Total number of cells and mitotic cells were counted using ImageJ and the percentage of mitotic cells was plotted on a graph. The graph shows the mean of n=3 ± SEM (standard error of the mean). Statistical significance is shown as * (p<0.05), ** (p<0.01) and *** (p<0.001). Scale bar:10 µm.*

4.3.2 ZIP6 and ZIP10 antibodies treatment in a colorectal cancer cell line

Having demonstrated the efficacy of ZIP6 and ZIP10 antibody at preventing mitosis in MCF-7 cells, the same experiment was carried out in a different cancer cell line in order to demonstrate whether this ability was only restricted to breast cancer. In fact, when the SLC39A6 gene was first discovered, it was known as an oestrogen related gene (Mcclelland *et al.*, 1998) and both ZIP6 and ZIP10 have been associated with breast cancer for decades (Manning *et al.*, 1995; Kagara *et al.*, 2007). Therefore, the experiment was performed also on a cell line of colorectal cancer, called CaCO-2, as this ZIP6-ZIP10 heteromer mechanism could be a mechanism governing mitosis in all cells, regardless of their tissue origin.

The experiment was performed using the same condition previously used for MCF-7 cells by treating cells with 150 nM nocodazole for 20 hours in order to synchronise the cells in mitosis. Cells were also treated with the ZIP6 or ZIP10 antibody at the concentration of 4 μg/ml and 10.5 μg/ml, respectively. Only one concentration for both ZIP6 and ZIP10 was used this time and for the further experiments as these had been confirmed with the previous experiments to be the most effective concentration to inhibit mitosis. CaCO-2 cells treated with nocodazole showed a significant increase of mitotic cells up to 50-60% when compared to the control sample ($p<0.001$) (Figure 4.8). However, when cells were treated with nocodazole and either the ZIP6 or ZIP10 antibody at the concentration of 4 μg/ml and 10.5 μg/ml, respectively, the percentage of mitotic cells was significantly reduced to 4-5% when compared to the nocodazole-only treated cells ($p<0.001$) (Figure 4.8). The percentage of mitotic cells in the cells treated with either ZIP6 or ZIP10 antibody was similar to the control sample, even though these cells had been treated with nocodazole. These results confirmed the ability of ZIP6 or ZIP10-directed antibody to inhibit mitosis not only in breast cancer cells but also in colorectal cancer cells.

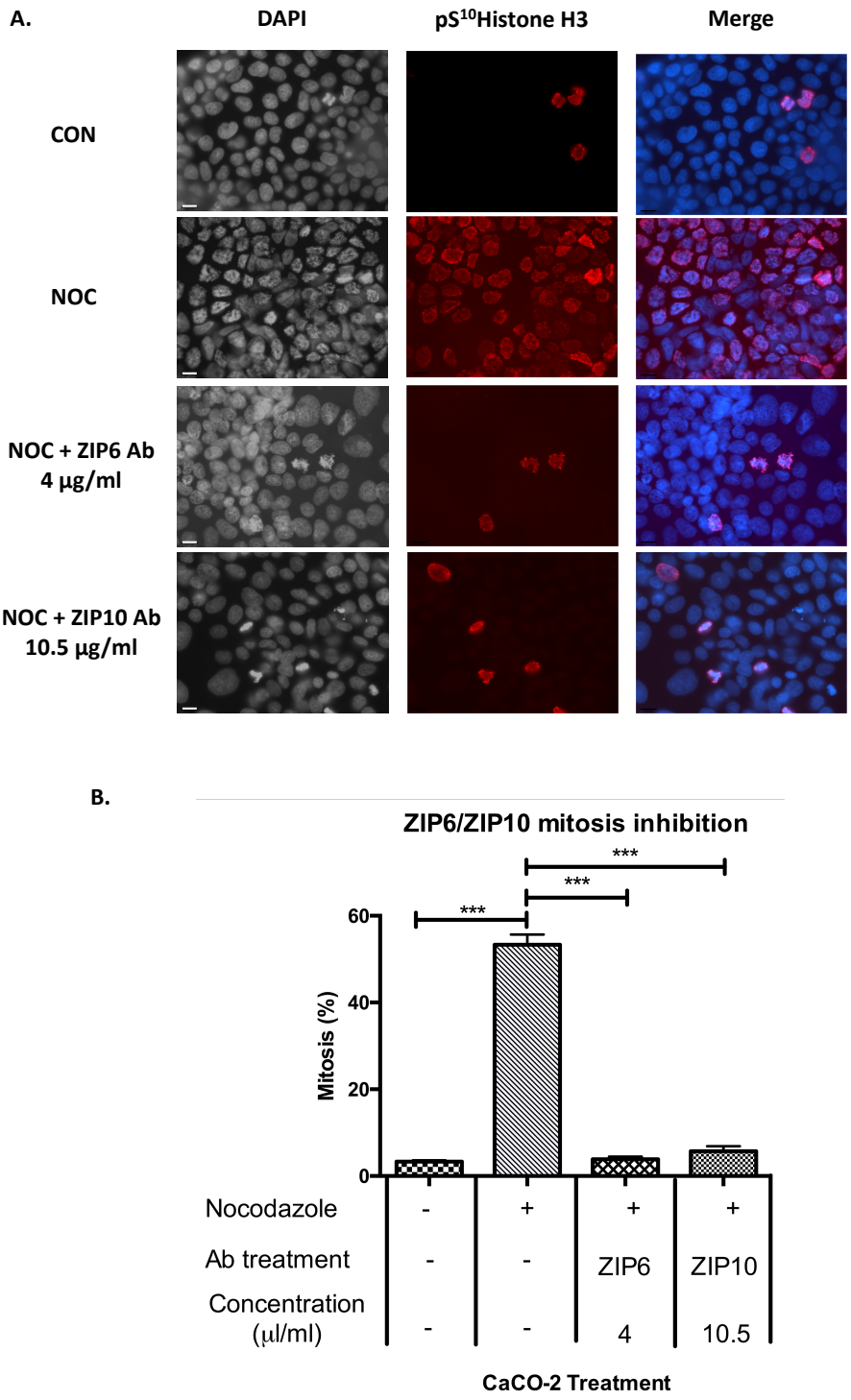

Figure 4.8 ***ZIP6 and ZIP10 antibody treatment prevents cell division of colorectal cancer cells.***
CaCO-2 cells were treated with nocodazole (NOC) (150 nM) at 70% confluence with or without ZIP6 or ZIP10 antibody at 4 µg/ml and 10.5 µg/ml, respectively.
A. After 20 hours treatment, cells were fixed and probed for pS[10]Histone H3 antibody (red) and nuclei counterstained with DAPI (blue). Each picture is representative of at least 6 pictures per each treatment (n=3).
*B. Total number of cells and mitotic cells were counted using ImageJ and plotted on a graph. The graph shows the mean of n=3 ± SEM (standard error of the mean). Statistical significance is shown as *** (p<0.001). Scale bar: 10 µm.*

4.3.3 Effect of ZIP6 antibody treatment on cancer cell growth

Having demonstrated that ZIP6-antibody treatment along with nocodazole was effective in preventing cell division in two different cancer cell lines, the antibody treatment investigation was extended from 20 hours to 4 days to investigate the ability of ZIP6 Y3 antibody to inhibit cell growth, this time in the absence of nocodazole. The same experiment could not be carried out with the ZIP10 antibody due to the lack of ZIP10 R stock, since this experiment required a considerable amount of antibody. A new stock of the ZIP10 R antibody was ordered from BioGenes GmbH (Germany), however it was not available until the end of this project.

MCF-7 cells were treated with ZIP6 Y3 antibody at 4 μg/ml and counted every 24 hours for 4 days after the treatment (Figure 4.9). A cell growth curve was constructed to compare the growth rate of treated cells with the control. Cells treated with the ZIP6 Y3 antibody showed significantly reduced cell growth rate compared to control untreated cells (Figure 4.9). Furthermore, cells treated with the ZIP6 Y3 antibody did not grow as much as the control. In particular, a significant decrease of cell growth was seen after 3 days ($p<0.01$) (Figure 4.9). This implied that the ZIP6 antibody treatment inhibited cell growth. However, it was interesting to notice that the cell growth was not completely arrested at the beginning with no significant difference detected until 2 days. Differently from the previous experiment these cells were not synchronised in mitosis by nocodazole treatment. This cell population would therefore comprise cells at different stages of the cell cycle, including those already moving into mitosis. The hypothesis of the current project would predict that cells that had already entered mitosis would not be inhibited by the antibody treatment. The evidence that the ZIP6 antibody treatment was effective at reducing cell growth even in the absence of nocodazole also ruled out the possibility that the previous results gained in this chapter were due to any potential interaction between nocodazole and the antibodies.

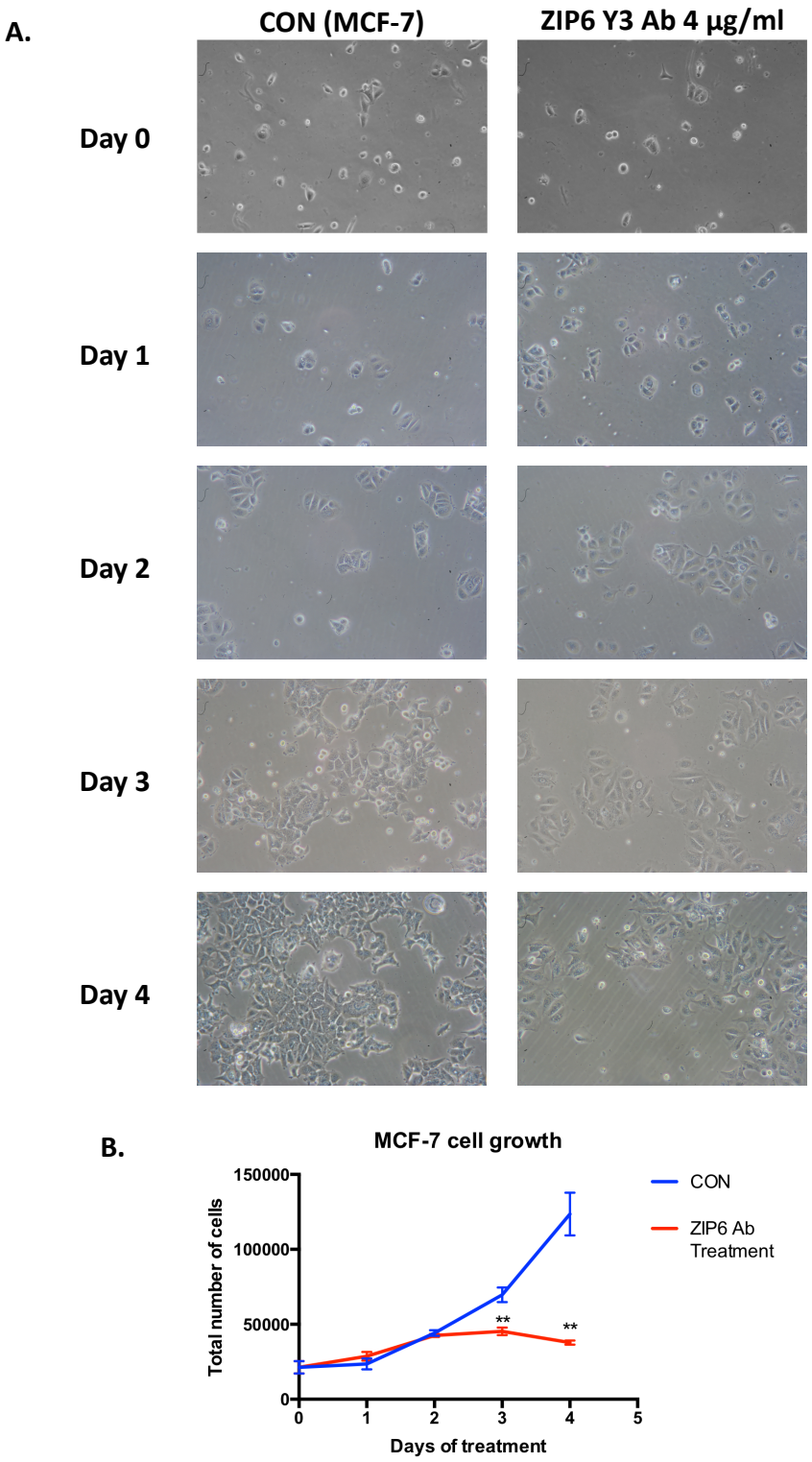

Figure 4.9 ***ZIP6 antibody treatment reduces cell growth of MCF-7 cells.***
MCF-7 cells were seeded in a 24 well plate and treated at 24 hours (day 0) with ZIP6 Y3 antibody (4 µg/ml).
A. Cells were counted every 24 hours for 4 days.
*B. The total number of cells were plotted in a line graph. The graph shows the mean of n=3 ± SEM (standard error of the mean) and the statistical significance of ZIP6-treated cells compared to non-treated (CON) is shown by ** ($p<0.01$).*

4.3.3.1 Use of a different ZIP6 Y antibody clone

Due to the reduction of our ZIP6 Y3 antibody stock, for the rest of the following investigation a different clone of ZIP6 Y antibody was used, called ZIP6 Y1. This clone binds the same peptide of the ZIP6 Y3, but it is a different IgG isoform. While the ZIP6 Y3 is an IgG_{2b}, the ZIP6 Y1 is an IgG_1. The main difference between the two IgG isoforms stems from the structure of the heavy chain and in the extent to which they are able to activate the host immune system. IgG_2 has four interchange-disulphide bonds in the hinge region, whereas the IgG_1 has only two (Vidarsson, Dekkers & Rispens, 2014). For this reason, the MCF-7 cell growth experiment with ZIP6 antibody treatment was repeated in order to check whether the different clone and isoform of ZIP6 antibody was as effective as the previous one. Results showed the same effect as seen for the ZIP6 Y3 with a significant decrease of the cell growth at day 3 and 4 ($p<0.01$) (Figure 4.10-A), confirming that the treatment with the ZIP6 Y antibody was effective at preventing cell division irrespective of the different isoforms of the antibody.

Next, this was expanded to test the effect of ZIP6 antibody treatment on MDA-468 cells, a cell line representative of triple negative breast cancer. The aim of this experiment was to confirm whether this treatment was able to stop cell division even in this different type of breast cancer. MDA-468 breast cancer cells represent a more aggressive phenotype of breast cancer. Triple negative breast cancer lacks the expression of all the common biomarkers of breast cancer which are normally used as a target for therapy. As a consequence of that, triple negative breast cancer is more difficult to tackle and treat. However, treatment with ZIP6 Y1 antibody at 4 μg/ml for 4 days was able to reduce the cell growth of the MDA-468 cells and their cell growth was significantly decreased at day 3 and 4 in comparison to non-treated cells ($p<0.01$) (Figure 4.10-B) similar to that seen with MCF-7 cells.

To summarise, this investigation confirmed the ability of ZIP6-directed antibodies to prevent cell division by blocking the zinc influx necessary to trigger mitosis (*Taylor et al, unpublished*).

A.

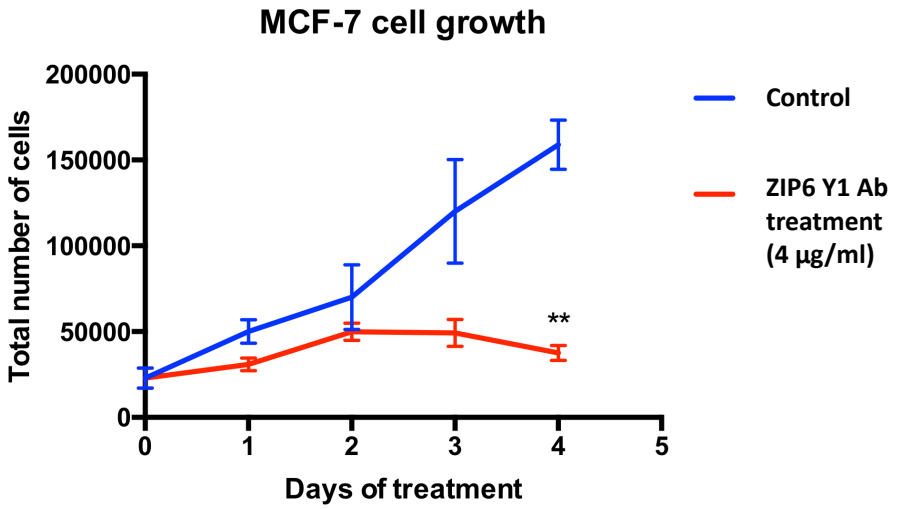

B.

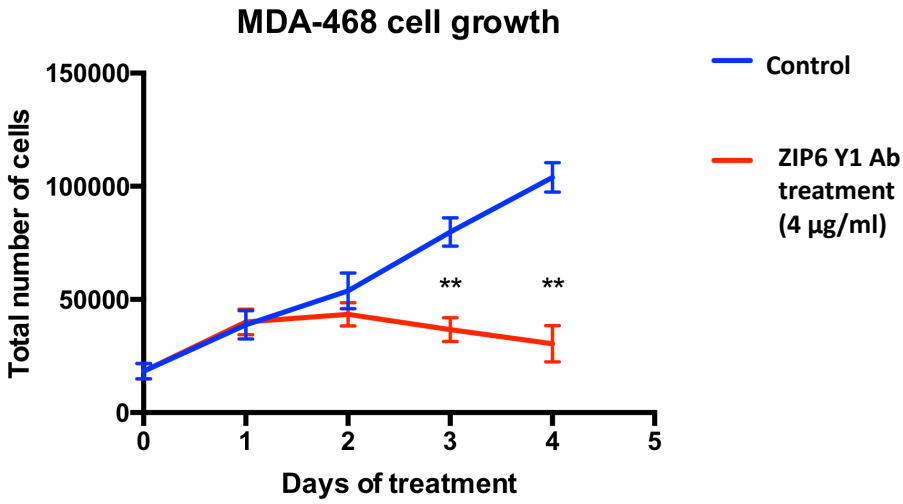

Figure 4.10 ***Effect of ZIP6 antibody treatment on cell growth of breast cancer cells.***
*Cells of MCF-7 (A), and MDA-468 (B) were seeded in a 24 wells plate and treated at 24 hours (day 0) with our ZIP6 Y1 antibody at 4 µg/ml. Cells were counted every 24 hours for 4 days. The number of cells counted for each day were platted in a line graph. The experiment was performed on three biological replicates (n=3 +SEM) and the statistical significance of treated cells compared to the non-treated ones (control) is shown by ** ($p<0.01$).*

4.3.4 Investigation of the fate of ZIP6/ZIP10 antibody inhibited cells

A cytotoxicity assay was carried out in order to assess whether the antibody treatment was cytotoxic. This was achieved by performing an MTT assay. The assay compared the control to cells treated with nocodazole plus or minus 4 μg/ml of ZIP6 or 10.5 μg/ml of ZIP10 antibody for 20 hours. The assay revealed that the antibody treatment was not cytotoxic, at least in the short term (20 hours), as no significant difference to the control was found (Figure 4.11). Interestingly, samples treated with nocodazole revealed a cell viability higher than 100% (CON) (Figure 4.11). Cell viability is normally lower than the control when a treatment is toxic to cells. While these results highlighted that the antibody treatment with nocodazole was not toxic to cells, it was surprising that the cell viability of cells treated with nocodazole was so different to the control (Figure 4.11). This could stem from nocodazole inducing the cells to undertake an enzymatic reaction which interfered with the product of the MTT assay or could have been offset by cell death. It is known that reducing compounds such as chemotherapy agents can interfere with the reduction of tetrazolium and increase the absorbance values of the samples in the wells (Ulukaya, Colakogullari & Wood, 2004). Nocodazole is an anti-neoplastic agent, so the results observed may be explained by this evidence.

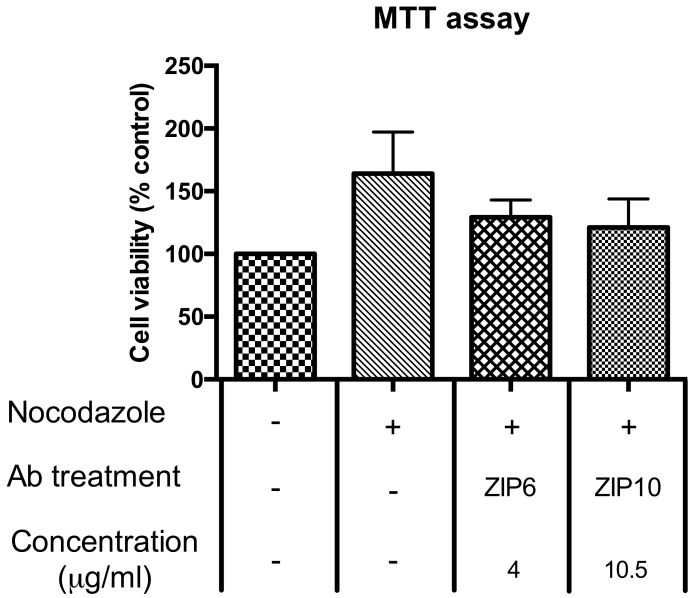

Figure 4.11 ***Effect of ZIP6 or ZIP10 antibody treatment****.*
MCF-7 cells were seeded in 35 mm dishes until 70% confluence before being treated with 150 nM nocodazole ± ZIP6 (4 μg/ml)or ZIP10 (10.5 μg/ml) antibody for 20 hours. After the treatment cells were washed with PBS and added 800 μl of MTT (0.5 mg/ml) at 37 °C for 4 hours. The MTT was then removed and cells were lysated with Triton X-100. The lysates were transferred into a 96 well plate before the colorimetric assay was assessed at 540 nm using a scanning spectrophotometer. Statistical significance was measured on n=3, but was not observed.

After confirming that the treatment with our ZIP6 or ZIP10 antibodies did not cause cell toxicity, cells treated with the antibodies at 4 μg/ml for ZIP6 and 10.5 μg/ml for ZIP10 were tested for signs of apoptosis such as cleavage of caspase 3 and PARP. This was achieved by using an apoptosis cocktail kit for western blot which allowed the simultaneous detection of cleaved PARP, procaspase 3 and cleaved caspase, all markers of apoptosis, along with β-actin for normalisation. Surprisingly, analysis of apoptosis with this kit did not reveal any signal for both procaspase 3 and cleaved caspase. This was explained by the evidence that MCF-7 cells were discovered in a previous study to be caspase 3 deficient cells (Sprengart, Wati & Porter, 1998), thus they use other pathways to undergo apoptosis. Therefore, only cleaved PARP was assessed.

The positive control used for this experiment was camptothecin 5 μM, a potent inhibitor of topoisomerase I, which is often used *in vitro* to induce apoptosis (Wall & Wani, 1996). Cells were treated with 5 μM camptothecin for 20 hours, in order to maintain the same condition used for the treatment with nocodazole ± ZIP6 or ZIP10 antibodies (20 hours treatment). Results showed that cells treated with 5 μM camptothecin had a significant increase of cleaved PARP ($p<0.01$, $p<0.05$) when compared to untreated cells (CON) (Figure 4.12 A-B), confirming that this treatment induced apoptosis. In particular, Figure 4.12-A shows that the samples treated with camptothecin had a significant increase of cleaved PARP when compared to either the control, nocodazole or the sample treated with both nocodazole and the ZIP6 antibody ($p<0.01$). On the contrary, cells treated with the ZIP6 antibody did not show any sign of apoptosis when compared to the nocodazole or control sample (Figure 4.12-A). Similarly, the ZIP10-directed antibody treatment showed no significant cleaved PARP in comparison to the control or nocodazole-treated samples, suggesting that this treatment was not causing apoptosis in the short term (Figure 4.12-B).

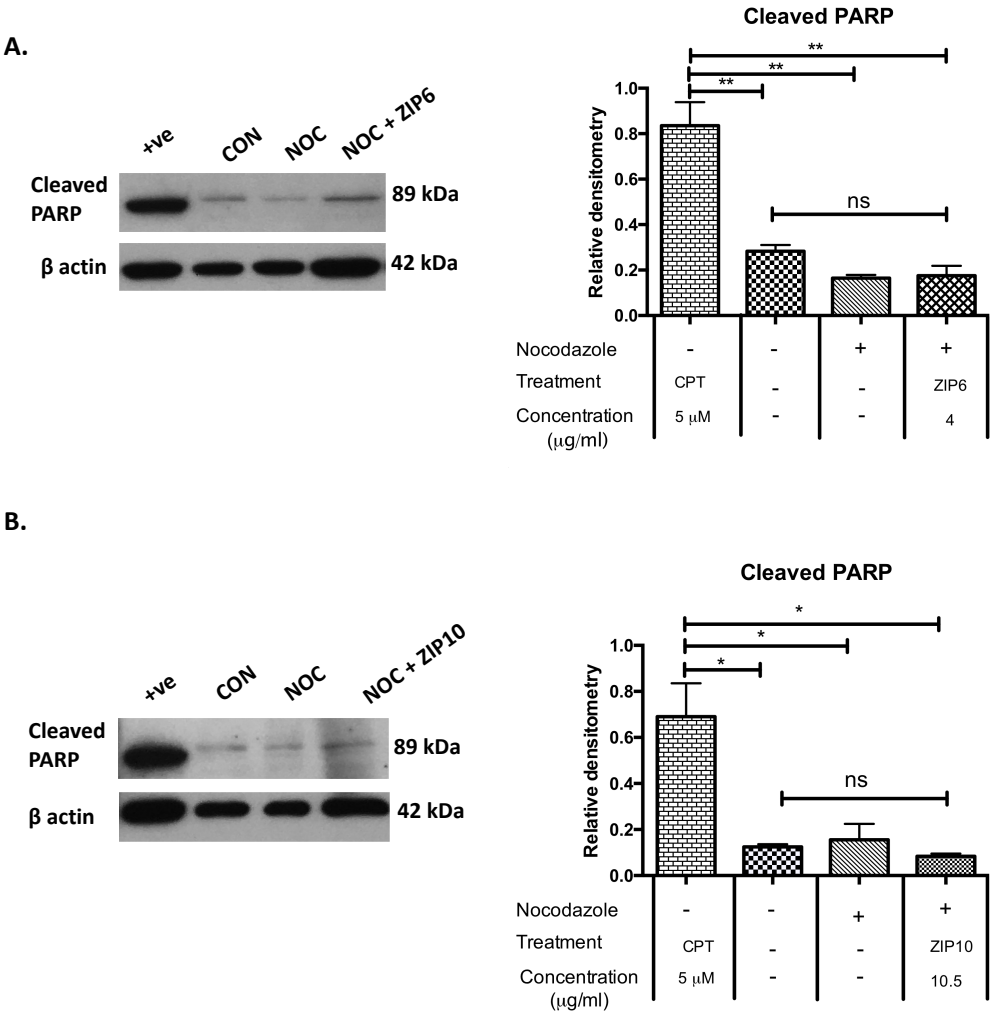

Figure 4.12 ***ZIP6/ZIP10 antibody treatment do not cause apoptosis in the short term.***
*MCF-7 cells were treated at 70% confluence with 150 nM nocodazole (NOC) ± ZIP6 Y1 or ZIP10 R antibody at 4mg/ml or 10.5 mg/ml respectively or with 5 mM camptothecin (CPT) for 20 hours as positive control (+ve). After 20 hours treatment, cells were harvested and samples were prepared. The immunoblotting was carried out using an apoptosis kit for Western Blot (Abcam) which detects cleaved PARP along with β-actin for normalisation (Figure A-B). The graphs show the levels of cleaved PARP for the treated cells when compared to the positive control (+ve) (Figure A-B). The graphs show the mean of n=3 ± SEM (standard error of the mean). Statistical significance comparing the +ve to the different cell treatment and the non-treated samples (CON) is shown as * ($p<0.05$) or ** ($p<0.01$). No statistical significance was found between the samples treated with nocodazole ±ZIP6 or ZIP10 antibody and the non-treated samples (CON).*

4.3.4.1 Cell cycle analysis of ZIP6 or ZIP10 antibody-treated cells

After having ruled out that the treatment with either ZIP6 or ZIP10 antibody was cytotoxic or induced apoptosis, the next investigation analysed whether cells undergoing this treatment were arrested at a different stage of the cell cycle prior to mitosis. In fact, zinc was discovered to be necessary for cells to progress from the G2 phase of the cell cycle to the cell division stage (Chesters & Petrie, 1999). Since our group have demonstrated that progression of cells from G2 to M phase relies on the action of ZIP6 and ZIP10 (*Taylor et al, unpublished*), it was likely that by blocking the zinc influx mediated by these two zinc transporters, cells could be arrested in G2.

A previous study in our group that analysed cells treated with nocodazole and our ZIP6 or ZIP10 antibody by cell cycle FACS-analysis, revealed a significant decrease in the G2/M population of cells treated with the antibody (Nimmanon, 2016). Cells treated with ZIP6 Y antibody at 1:20 dilution (2 μg/ml) showed 29% of cells in the G2/M phase of the cell cycle, lower than the cells treated with nocodazole (41%), but higher than the control (22%) (Figure 4.13). On the other hand, 69% of control cells were found in G0/G1 in comparison to the 50% of the ZIP6 antibody-treated cells and to 37% of the nocodazole-treated only (Figure 4.13). Analysis of the S phase revealed that 9% of control cells were S phase, compared to 22% for the nocodazole sample and the 20% of ZIP6-treated cells (Figure 4.13). Similarly, cell cycle analysis of ZIP10-antibody treated cells at the dilution 1:20 (5.25 μg/ml) showed a decrease in the percentage of cells in the G2/M phase (28%) when compared to the nocodazole treatment (41%), but higher than the control (22%) (Figure 4.13). ZIP10 antibody-treated cells showed 58% of cells in G0/G1 and 14% of cells in S phase (Figure 4.13). It was important to notice that the previous experiments had confirmed that cell treatment with either ZIP6 or ZIP10 antibody and nocodazole significantly reduced the number of cells in mitosis. Therefore, the increased percentage of treated cells in the G2/M phase of the cell cycle compared to the control non-treated cells could be due to a higher proportion of cells in G2.

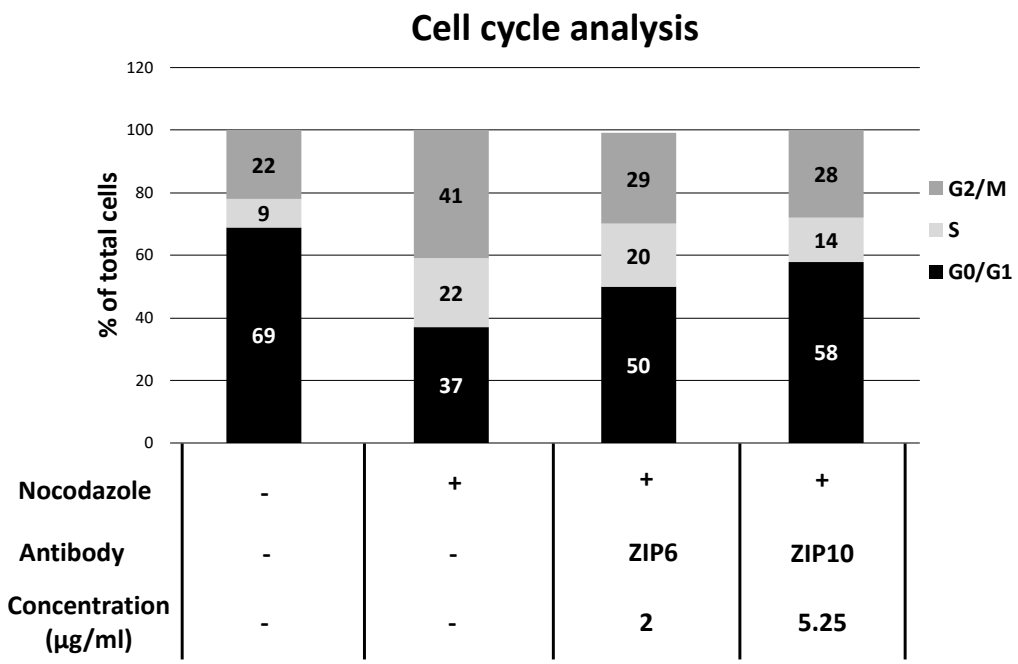

Figure 4.13 ***Decreased G2/M population by ZIP6 Y or ZIP10 R antibody.***
MCF-7 cells were treated with 150 nM nocodazole ± ZIP6 or ZIP10 antibody at 2 µg/ml or 5.25 µg/ml, respectively, for 20 hours. Cells were then stained with propidium iodide. DNA content was measured using FACS analysis. The percentage of the cells in the G0/G1, S and G2/M phases of the cell cycle was determined using FlowJo Software and are shown as 100% stacked column chart. Courtesy of Thirayost Nimmanon (Nimmanon, 2016)*.*

4.3.4.2 Investigation of cyclin levels in the ZIP6 or ZIP10 antibody-treated cells

Since FACS cell cycle analysis does not distinguish between the G2 and M phases, analysis of the cyclin levels in the antibody-treated cells was performed in an effort to clarify the likelihood of cells arrested in G2 when treated with the ZIP6 or ZIP10 antibody. In fact, if the treatment with the ZIP6 or ZIP10-directed antibodies blocked the zinc influx necessary to trigger mitosis, the following hypothesis would be that the cells undergoing this treatment could be arrested at a phase of the cell cycle which is prior to mitosis, thus the G2 phase.

Zinc is also known to be required during the S phase of the cell cycle (Prasad & Oberleas, 1974; Chesters, Petrie & Vint, 1989; Chesters, Petrie & Travis, 1990; Watanabe *et al.*, 1993), when DNA duplication occurs. During S phase, zinc was predicted to come from the inside of the cell rather than the extracellular space (Li & Maret, 2009). It is likely that the zinc required during S phase would require a ZIP transporter located inside the cell, such as ZIP7. Therefore, mobilisation of zinc during S phase should not require the involvement of either ZIP6 or ZIP10. This evidence would support the hypothesis that the ZIP6 or ZIP10 antibody-treated cells may be arrested in G2, which is the phase of the cell cycle which follows S phase. In order to confirm this hypothesis, an in-depth investigation of the different cyclins was carried out. Cyclins are proteins whose expression fluctuates throughout the cell cycle and, as their name suggests, they are synthesised and degraded at the end of each stage of the cell cycle (Evans *et al.*, 1983). As their expression is typical of each stage of the cell cycle, they are good indicators of each phase (Figure 4.15-A).

MCF-7 cells treated with or without nocodazole (150 nM) and our ZIP6 or ZIP10 antibody at 4 μg/ml and 10.5 μg/ml, respectively, were analysed by western blotting and probed for cyclin D1, E, A and B1. It was noticeable that cells treated with our ZIP6 antibody had a significant decrease of the cyclin D1 ($p<0.01$) and cyclin B1 ($p<0.05$) when compared to the cells synchronised with nocodazole (Figure 4.14-B). However, results for cyclin E and A showed no significant change (Figure 4.14-B). The same investigation performed with the cells treated with the ZIP10 R antibody showed similar results to the ZIP6-treated cells. In particular, results showed a significant decrease of cyclin D1 ($p<0.05$) and cyclin B1 ($p<0.05$) compared to nocodazole samples, but again no

significant decrease of cyclin E or A (Figure 4.14-C). While these results confirmed once again that cells treated with either ZIP6 or ZIP10 antibody were not in mitosis as they showed a significant decrease of cyclin B1, a marker of mitosis, it suggested that cells could be arrested between the S and G2 phase of the cell cycle. In fact, while cyclin E is specific for S phase, cyclin A has an important role both during the S phase and G2 phase (Pagano *et al.*, 1992).

The analysis of the cyclins A (G2 phase) and B1 (G2/M phase) was also performed with immunofluorescence, probing for pS^{10}Histone H3 as a marker of mitosis (Figure 4.15-4.16). Results showed that cells which were positive for pS^{10}Histone H3 were only positive for cyclin B1 (Figure 4.15) but not cyclin A (Figure 4.16), confirming the role played by cyclin A prior to mitosis in the G2 phase. Immunofluorescence results of cyclin B1 showed that the nocodazole sample had a clear increase in the number of cells positive for both pS^{10}Histone H3 and cyclin B1 in comparison to both the control and the antibody-treated samples (both ZIP6 and ZIP10) (Figure 4.15), similar to the results discovered for cyclin B1 with western blotting (Figure 4.14). Moreover, this result further corroborated the previous experiments that cells treated with the ZIP6 or ZIP10 antibody and nocodazole had a significant decrease of mitotic cells in comparison to the nocodazole-only treated samples (Figure 4.5-8). Results for cyclin A staining, even though not as clear as the ones obtained for cyclin B1 (Figure 4.15), did not reveal a visible difference across the different samples (Figure 4.16). It is worth noticing that most of the cells which were positive for the cyclin A were not positive for pS^{10}Histone H3 (Figure 4.16), confirming that this cyclin has a role prior to mitosis.

These results taken all together suggested the possibility that the antibody treatment stopped cells at a stage of the cell cycle between the S and G2 phases, most likely in G2.

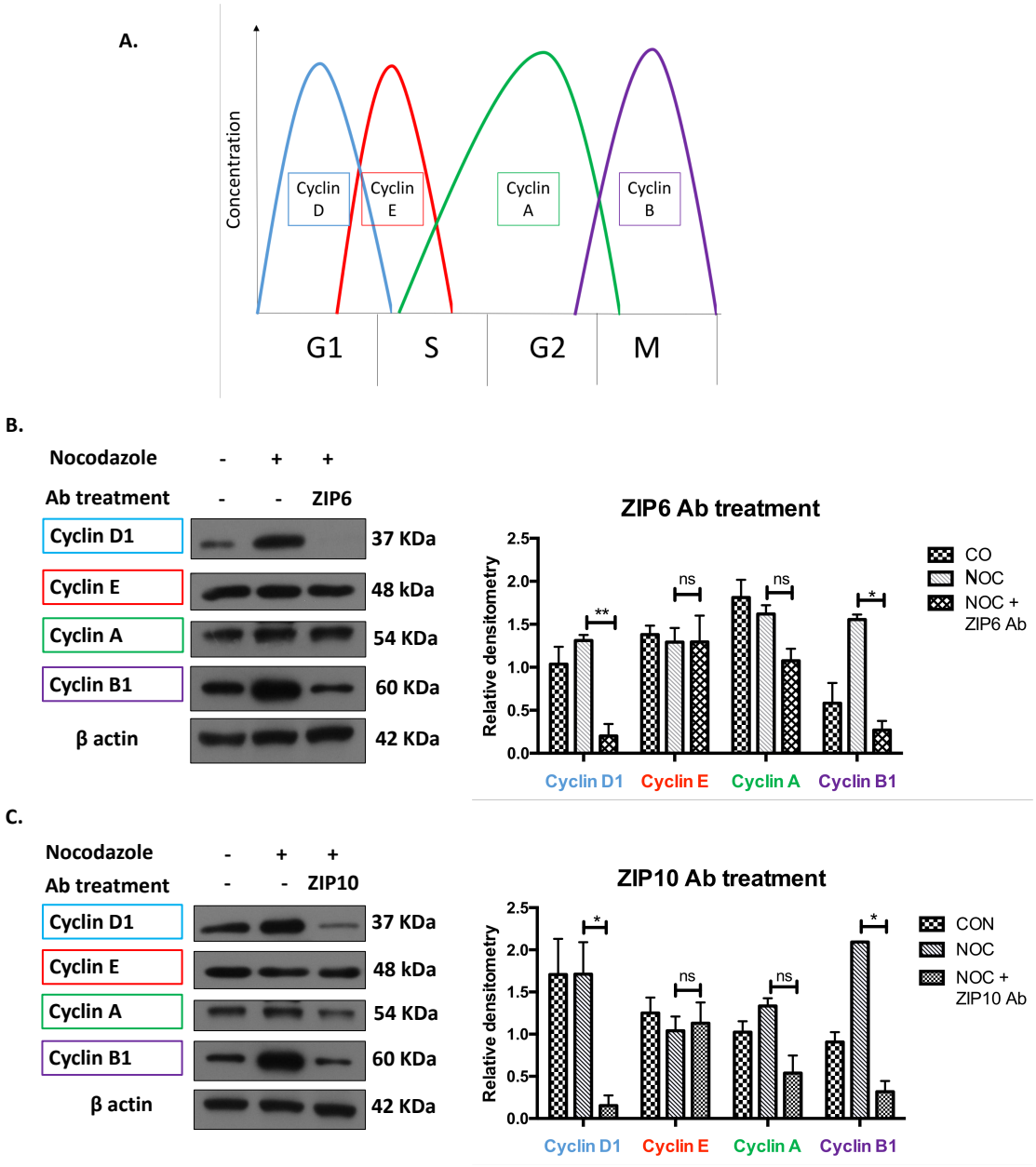

Figure 4.14 ***ZIP6 or ZIP10-directed antibody treatment induced reduction of cyclin B1 and cyclin D1.***
MCF-7 cells were treated at 70% confluence with 150 nM nocodazole ± ZIP6 Y1 or ZIP10 R antibody at 4 μg/ml or 10.5 μg /ml respectively. After 20 hours treatment cells were harvested and samples for western blot were prepared.
*B-C. Western blotting was performed probing samples for cyclin B1, cyclin A, cyclin E and cyclin D1. The experiment was performed using three biological replicates and the densitometric data was normalised to the results of β-actin. The graphs show the mean values of n=3 ± SEM (standard error of the mean). Statistical analysis was performed and statistical significance is shown as ** (p<0.01) and * (p<0.05).*

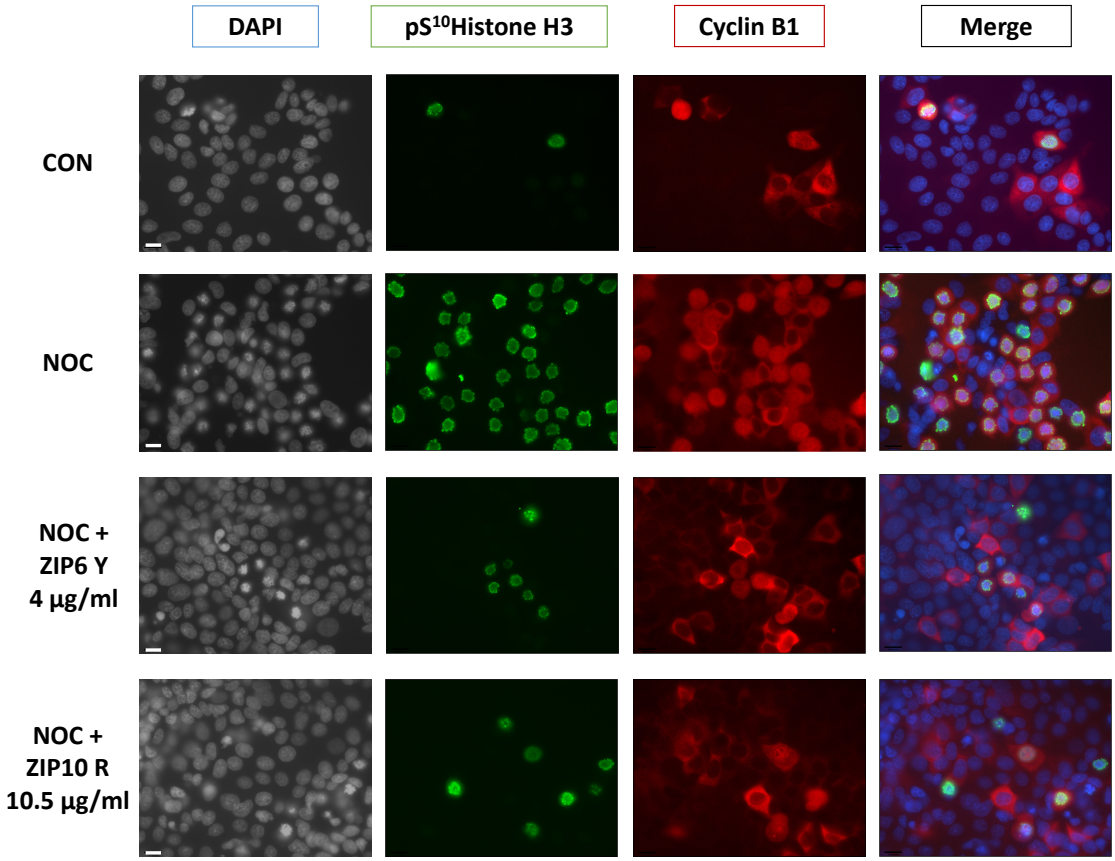

Figure 4.15 ***Investigation of cyclin B1 in cells treated with ZIP6 or ZIP10 antibody and synchronised in mitosis with nocodazole.***

Cells were seeded on coverslips and treated at 70% confluence with nocodazole (150 nM) ± ZIP6 Y1 or ZIP10 R antibody at 4 µg/ml or 10.5 µg/ml, respectively. After 20 hours treatment, cells were fixed and stained with pS[10]Histone H3 (green), cyclin B1 (red) and nuclei counterstained with DAPI (blue fluorescence). Pictures are representative of each different treatment compared to control (no treatment) and were taken with a 63x oil immersion lens microscope (Leica DMIRE2). Scale bar: 10 µm.

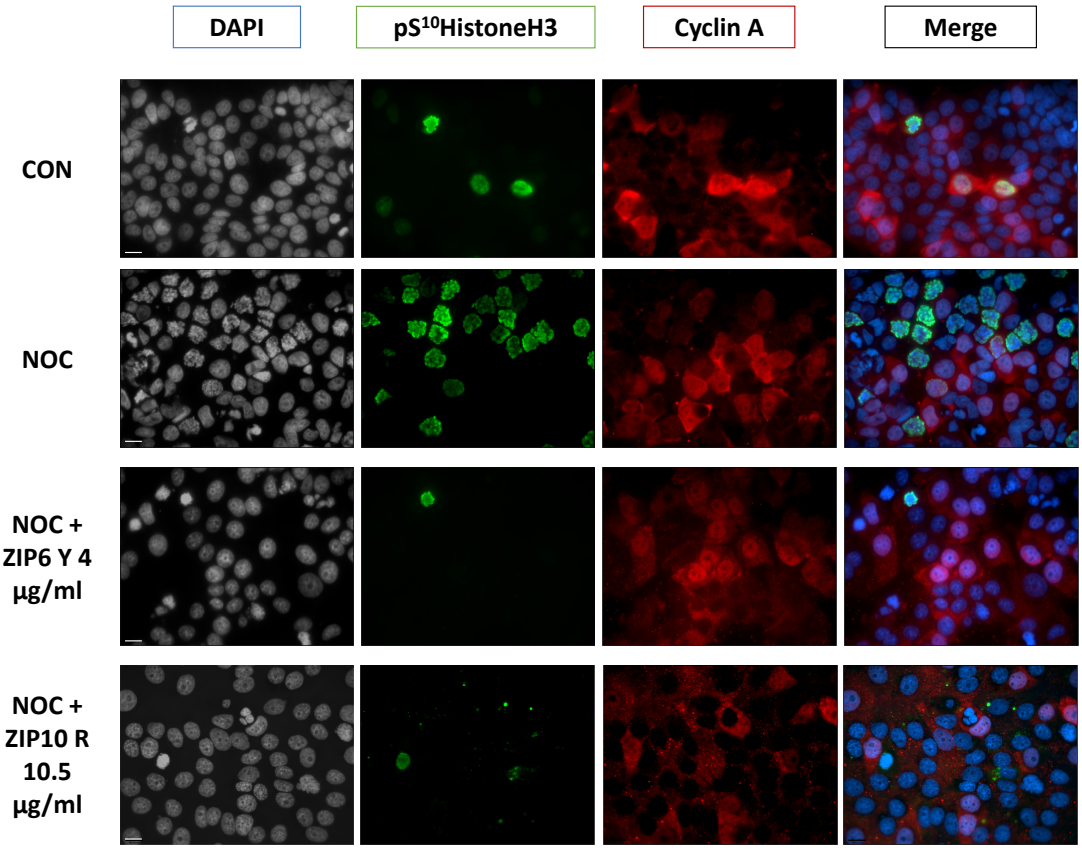

Figure 4.16 ***Investigation of cyclin A in cells treated with ZIP6 or ZIP10 antibody and synchronised in mitosis.***

Cells were seeded on coverslips and treated at 70% confluence with nocodazole (150 nM) ± ZIP6 Y1 or ZIP10 R antibody at 4 µg/ml or 10.5 µg/ml, respectively. After 20 hours treatment, cells were fixed and stained with pS[10]Histone H3 (green), cyclin A (red) along with DAPI (blue fluorescence). Pictures are representative of each different treatment along with control (no treatment) and were taken with a 63x oil immersion lens microscope (Leica DMIRE2). Scale bar: 10 µm.

4.3.4.3 Investigation of PLK1 in ZIP6 or ZIP10 antibody-treated cells

Another protein which is essential for the progression of cells from G2 to M phase is PLK1, a kinase which is involved in the activation of the complex between CDK1 (or cdc-2) and cyclin B1 (Gavet & Pines, 2010a). Without the activation of this complex, mitosis would not start (Gheghiani *et al.*, 2017). Therefore, the protein level of PLK1 was analysed, revealing that ZIP6 or ZIP10-antibody treated cells had no increase of PLK1. PLK1 expression normally peaks during mitosis (Petronczki, Lénárt & Peters, 2008). In fact, Figure 4.17-A shows that the level of PLK1 was significantly increased in the nocodazole sample not only in comparison to the control ($p<0.05$) but also to the cells treated with both nocodazole and the ZIP6 antibody at 4 μg/ml ($p<0.01$). The increased level of PLK1 in the nocodazole sample confirmed the essential role of PLK1 in the regulation of mitosis (Gavet & Pines, 2010a; Gheghiani *et al.*, 2017). Similar to the ZIP6 treatment, Figure 4.17-B showed that the cells treated with nocodazole had a significant increase of PLK1 in comparison to both the control and the sample treated with nocodazole and 10.5 μg/ml of ZIP10-directed antibody ($p<0.05$). In both Figure 4.7-A and Figure 4.7-B there was no significant difference between the control and the antibody-treated cells, confirming that these cells were not capable of entering mitosis as they lacked the zinc necessary to trigger mitosis.

4.3.4.4 Investigation of quiescence in cells treated with the ZIP6 or ZIP10 antibody

The last part of this chapter investigated the fate of the antibody-treated cells. In fact, one question that has not been answered yet is whether the cells entered a stage of quiescence since cell division was prevented by the antibody treatment. When cells stop dividing they normally enter either quiescence or senescence. While these two states are often confused, quiescence is reversible, while senescence is not (Blagosklonny, 2011). In particular, it is known that quiescence happens when cells lack nutrition and/or mitogen and growth factors which are necessary for cells to grow and divide (Terzi, Izmirli & Gogebakan, 2016). For this reason, the next analysis investigated the possibility of cells entering a quiescent state following the treatment with the antibody, potentially due to a lack of the zinc necessary to trigger mitosis resulting in a block of the ZIP6-ZIP10 heteromer.

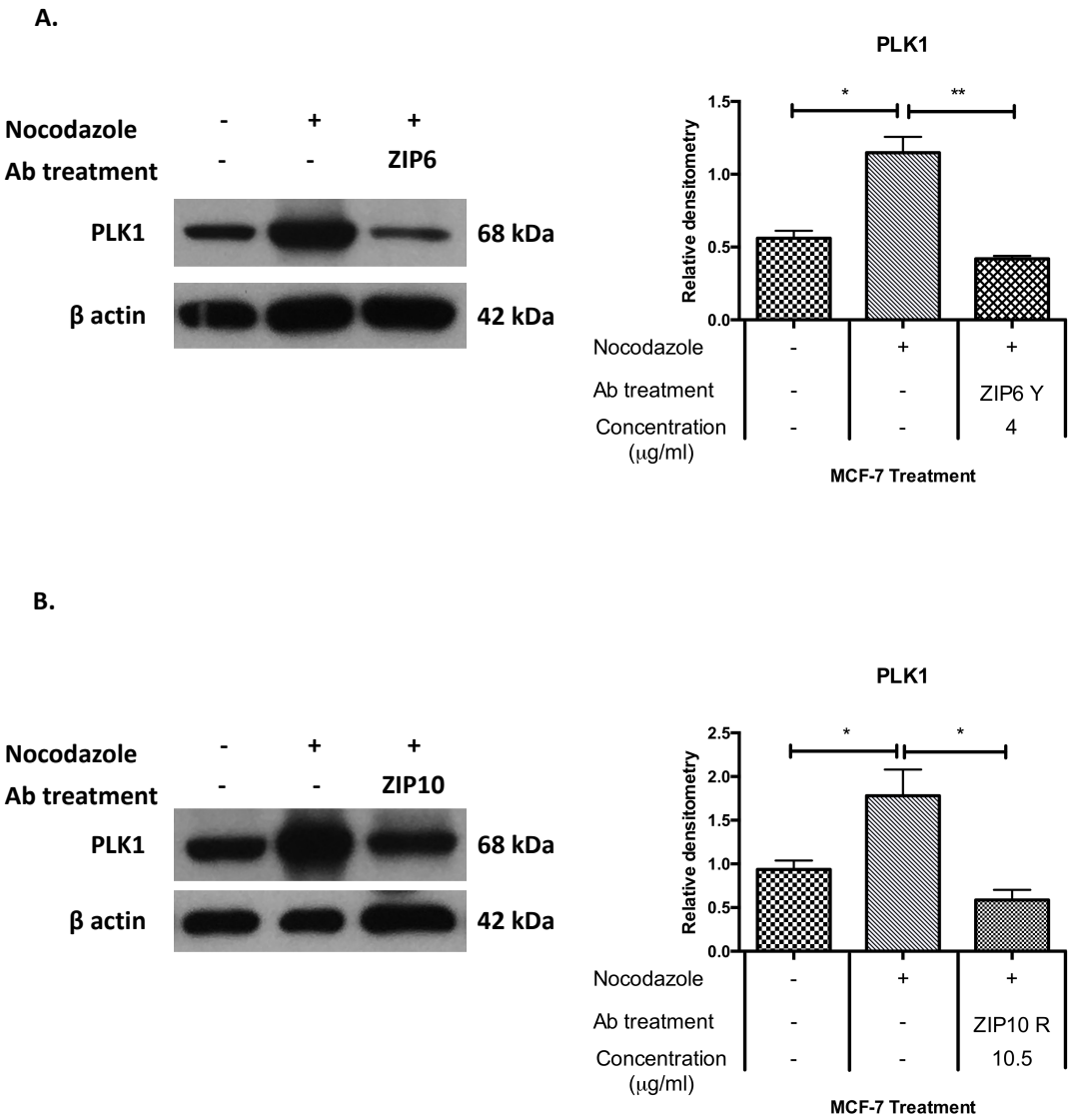

Figure 4.17 ***ZIP6 or ZIP10-treated cells have significant decrease of protein PLK1****.*
*MCF-7 cells were treated at 70% confluence with 150 nM nocodazole ±4 μg/ml ZIP6 or 10.5 μg/ml ZIP10 antibody. After 20 hours treatment cells were harvested and samples for western blot were prepared. Western blot was performed probing samples for PLK1. The experiment was performed using three biological replicates and the densitometric data was normalised to the results of β-actin. The graphs show the mean values of n=3 ±SEM (standard error of the mean). Statistical significance is shown as ** (p<0.01) and * (p<0.05).*

Analysis of quiescence was performed by assessing the protein level of $p27^{kip1}$, a marker of quiescence. This protein is used as a marker of quiescence as it is normally overexpressed in quiescent cells. $p27^{kip1}$ is an inhibitor of the complex between cyclin E and CDK2, which is necessary for the progression of cells from G1 to S phase (Sheaff *et al.*, 1997). Similar to the analysis of the cyclins and PLK1, $p27^{kip1}$ was analysed in cells treated with our ZIP6 or ZIP10-directed antibody in comparison to cells treated with nocodazole and non-treated cells. As shown in Figure 4.18-A cells treated with nocodazole and the ZIP6 Y antibody at 4 μg/ml had a significant decrease of $p27^{kip1}$ in comparison to the nocodazole sample ($p<0.05$), whereas no significance was observed when comparing this sample to the control. On the contrary, the level of $p27^{kip1}$ in the control sample was very similar to the nocodazole sample (Figure 4.18-A). Similarly, cells treated with the ZIP10 antibody at 10.5 μg/ml showed a significant decrease of $p27^{kip1}$ in comparison to the control ($p<0.05$), but no significance to the nocodazole sample (Figure 4.18-B). Therefore, these results contradicted the previous hypothesis, but instead suggested that cells treated with the ZIP6 or ZIP10 antibody were not quiescent. However, this reinforced the hypothesis that cells treated with the antibodies were arrested at a different stage of the cell cycle prior to mitosis, as suggested by the previous results.

Taken all together these results confirmed that when cells were treated with the ZIP6 or ZIP10 antibody, it was possible to block cells from entering mitosis. This data now needs to be expanded by testing the antibodies in animal models to confirm their use as novel immunotherapy agents that could be used to reduce the cell growth of proliferative diseases such as cancer.

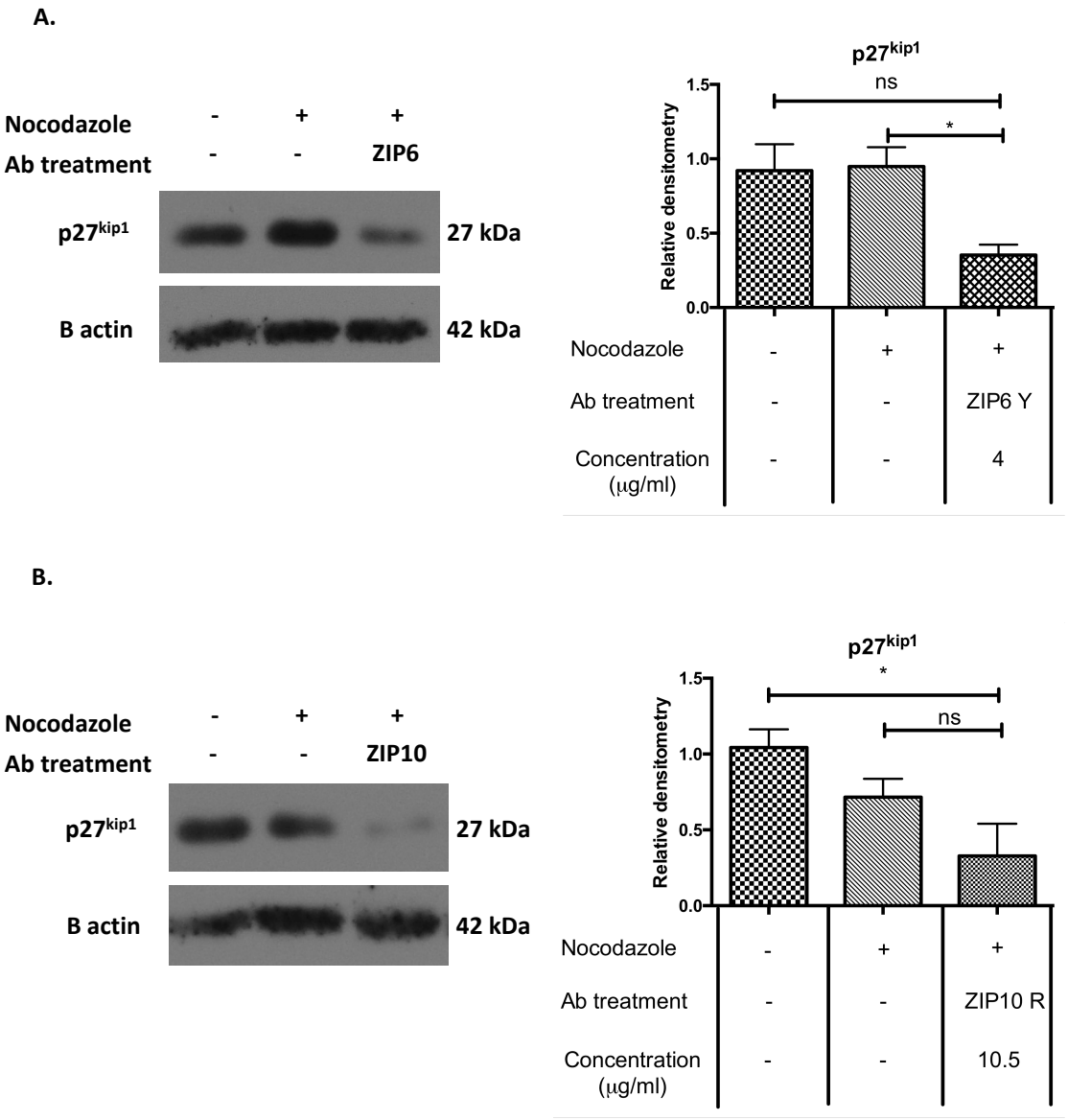

Figure 4.18 ***Cells treated with either the ZIP6 or ZIP10 antibody are not quiescent.***
*MCF-7 cells were treated at 70% confluence with 150 nM nocodazole ±4 μg/ml ZIP6 or 10.5 μg/ml ZIP10 antibody. After 20 hours treatment cells were harvested and samples for western blot were prepared. Western blot was performed probing samples for $p27^{kip1}$. The experiment was performed using three biological replicates and the densitometric data was normalised to the results of β-actin. The graphs show the mean values of n=3 ±SEM (standard error of the mean). Statistical significance is shown as * ($p<0.05$).*

4.4 Discussion

4.4.1 Zinc is necessary for cell division

The involvement of zinc in the regulation of the cell cycle has been known since the mid-sixties (Fujioka & Lieberman, 1964), however its actual role in mitosis is only now starting to be understood. Zinc is known to be essential at different stages of the cell cycle, in particular during the G1 and G2 phases (Chesters & Petrie, 1999). Many studies have identified zinc as essential for DNA synthesis (Prasad & Oberleas, 1974; Chesters, Petrie & Vint, 1989; Chesters, Petrie & Travis, 1990; Watanabe *et al.*, 1993), as insufficient zinc led to inadequate entry of cells into S phase, the stage of the cell cycle where DNA synthesis occurs. Zinc is also required for the transcription of cyclins, proteins involved in the regulation of the cell cycle (Chesters & Petrie, 1999). A study of the cell cycle of undifferentiated PC12 (adrenal gland) cells revealed two peaks of zinc during the cell cycle, one during early G1 phase and the second one during the G1/S transition (Li & Maret, 2009). In fact, the role of zinc during G1/S phase transition relies on the requirement of zinc for the synthesis of cyclin D and cyclin E (Li & Maret, 2009), proteins that are essential for the progression of cells from G1 to S phase. Moreover, zinc was discovered to be essential for cell differentiation, as myoblast differentiation was demonstrated to be dependent on zinc (Petrie, Chesters & Franklin, 1991). In fact, it was observed that inhibition of myoblast differentiation in C2C12 (mouse myoblast) cells by the use of a metal chelator was reverted by addition of zinc instead of copper (Petrie, Buskin & Chesters, 1996).

Beyond its role in G1 phase, zinc was identified as also being essential during the G2 phase (Chesters & Petrie, 1999). A study of human bronchial epithelial cells supplemented with zinc showed that cells were arrested at the G2/M transition by increased expression of p53, followed by an increase of the cell cycle inhibitor p21 (Wong *et al.*, 2008). On the contrary, cells of Xenopus oocytes treated with metal chelator were blocked at the G2/M transition by inhibition of the phosphatase Cdc25C, which is involved in the activation of the complex between cyclin B1 and CDK1 at the onset of mitosis (Sun *et al.*, 2007). Therefore, a proper zinc balance is essential for the progression of cells from the G2 to M phase of the cell cycle. Nevertheless, all these studies did not provide any information regarding the mechanism by which zinc is transported or made accessible at this stage. Zinc concentration is tightly controlled by

zinc transporters and proteins, such as metallothionein. Experiments using zinc supplementation or zinc chelation highlighted the importance of zinc in cell proliferation (Li & Maret, 2009), as well as confirming that its supply comes from the extracellular environment (Rudolf & Červinka, 2008). More recently, it was seen that zinc influx is necessary for oocyte to egg-transition, being essential for the progress of the oocyte through meiosis (Kim *et al.*, 2010). Tests *in vitro* of oocytes maturation have shown that a high concentration of TPEN (a zinc metal chelator) had a dramatic effect at preventing meiosis progression. Although, TPEN binds preferentially copper over zinc, this effect was seen to be dependent on zinc chelation and no other metals (Kim *et al.*, 2010). Lately, zinc transporters ZIP6 and ZIP10 were identified as being essential for the progression of meiosis by providing the zinc necessary for meiotic maturation (Kong *et al.*, 2014). Disruption of these two zinc transporters during meiotic maturation was associated with cell cycle arrest due to the perturbation of zinc levels (Kong *et al.*, 2014). This was the first study addressing these two zinc transporters in the regulation of meiosis. The fact that zinc deficiency was responsible for the arrest of cell division was seen in a previous study where growth of *Euglena gracilis* (a species of alga) was arrested when grown in zinc-deficient medium (Falchuk, Fawcett & Vallee, 1975), but the actual mechanism was still unknown. In this respect, our group have identified that ZIP6 and ZIP10 zinc transporters are required not only for meiosis but also for the regulation of mitosis, the last step of the cell cycle (*Taylor et al, unpublished*). Furthermore, it has recently been demonstrated how ZIP6 and ZIP10 bind to each other, forming a heteromer which acts as a unique complex (Taylor *et al.*, 2016). The way these two molecules bind to each other has yet to be defined as there is no crystal structure available for these zinc transporters. However, a recent study has reported the first crystal structure for another ZIP transporter, ZIP4, highlighting the importance of its dimeric structure as a feature that is also common for the other members of the LIV-1 subfamily (Zhang, Sui & Hu, 2016). The investigation of the function and regulation of this ZIP6-ZIP10 heteromer should help us clarify the exact role played by zinc in mitosis.

4.4.2 ZIP6 or ZIP10-directed antibody treatment prevents cell division

This chapter expanded the recent discovery that ZIP6 and ZIP10 together trigger mitosis by influxing zinc (*Taylor et al, unpublished*). Here that preliminary discovery was corroborated by demonstrating that cell treatment with either ZIP6 or ZIP10 N-terminal

domain specific antibodies prevented mitosis in the presence of nocodazole, an anti-neoplastic agent that synchronises cells into mitosis (Blajeski *et al.*, 2002). This finding suggested that dimerization is a characteristic which may be essential for the proper function of ZIP transporters and implied that the presence of this dimer on the plasma membrane is required to drive cell proliferation. This study showed that when cells were synchronised in mitosis by using nocodazole and were treated with our ZIP6 or ZIP10 antibodies at 4 μg/ml or 10.5 μg/ml respectively, the number of mitotic cells was significantly decreased even though cells were treated with nocodazole (Figure 4.6-8). This effect was due to the action of these ZIP6 or ZIP10-directed antibodies as confirmed by the negative control of IgG (Figure 4.6-7). In fact, while there is evidence that human IgG could bind zinc (Yamanaka *et al.*, 2016), the mitosis inhibition effect was not seen when using a normal IgG as a negative control, but it was only due to the ability of our antibodies to block the ZIP6-ZIP10 heteromer. Moreover, cell growth experiments with breast cancer cells treated with the ZIP6 antibody for 4 days in the absence of nocodazole verified the significant reduction of cell growth induced by the treatment with the antibody (Figure 4.9).

This evidence confirmed the hypothesis that by blocking this heteromer, it was possible to block the zinc influx mediated by this complex and therefore block mitosis. Having confirmed the most effective antibody concentrations *in vitro* (4 μg/ml for ZIP6 and 10.5 μg/ml for ZIP10), these concentrations were used for the rest of the investigation. The efficacy of this treatment was demonstrated not only in breast cancer cell lines but also in a colorectal cancer cell line (Figure 4.8), suggesting that this could be a general mechanism for triggering mitosis in cells. The investigation began in MCF-7 cells because ZIP6 was first discovered as an oestrogen-related gene (Manning *et al.*, 1995). In fact, ZIP6 is highly expressed in oestrogen receptor positive breast cancer and glands such as prostate, whereas its expression in colon is not as high as those tissues (Fagerberg *et al.*, 2014). Most interestingly the ZIP6 antibody-mediated mitosis inhibition was confirmed in different breast cancer cell lines, including those representing triple negative disease (Figure 4.10). The next step of this investigation would be to assess the effect of the ZIP6 antibody-treatment for a longer period of time, but unfortunately for the purpose of this project this was not possible as this experiment

required a lot of antibody to be used. At the time of this investigation, our group did not have enough stock left of the antibodies. In fact, the 4-days treatment with the ZIP10 R antibody was not carried out for this reason. As soon as this was confirmed, it would further corroborate the ability of ZIP6 or ZIP10-directed antibody to reduce the cell growth in hyperproliferative diseases such as cancer, which are characterised by uncontrolled cell growth as one of the main hallmarks that distinguish cancer cells from normal cells.

4.4.3 ZIP6 or ZIP10-directed antibody treatment arrests cells prior to mitosis

Cytotoxicity assay confirmed that the short-term treatment with ZIP6 or ZIP10 antibody did not decrease cell viability and was not toxic to cells (Figure 4.11). This is an important aspect that needs to be assessed in future experiments with these antibodies, as the overall goal of cancer treatment is to induce tumour shrinkage and to kill cancer cells. However, it was interesting to notice that the MTT cytotoxic assay results suggested that the treatment with the ZIP6 and ZIP10 antibodies may be offset by cell death in the long term, as this was not confirmed in the short term by apoptosis analysis. According to the literature, there is controversial evidence as to whether zinc excess or zinc deficiency is pro (Kim *et al.*, 1999; Shumilina *et al.*, 2010) or anti-apoptotic (Nodera, Yanagisawa & Wada, 2001; Ho, Courtemanche & Ames, 2003; Verstraeten *et al.*, 2004; Fraker, 2005).

Some studies have correlated the PI3K/AKT pathway with the prevention of apoptosis (Chang *et al.*, 2003). This is not surprising as the PI3K/AKT pathway is known to be involved with a variety of cancers and human malignancies (Krasilnikov *et al.*, 1999; Fry, 2001; Vivanco & Sawyers, 2002). Moreover, it is also known that zinc can activate AKT directly (Lee *et al.*, 2009) and more recently our group have discovered that the activation of these pathways is mediated by the ZIP7-mediated zinc release (Nimmanon *et al.*, 2017). In our recent paper, it was also demonstrated that activated ZIP7 was able to activate the MAPK pathway. Interestingly, another study has demonstrated that Hep-2 cells (human epithelial cells) displaying higher zinc uptake had increased activation of the MAP kinase signalling, followed by increased activation of the p53-mediated apoptosis pathway (Rudolf, 2008). This data confirmed the role played by zinc as a second messenger (Yamasaki *et al.*, 2007), whose release from the stores induces the

activation of downstream pathways which results in zinc being a promoter of apoptosis. However, in dendritic cells zinc was found to induce apoptosis by stimulation of ceramide production (Shumilina *et al.*, 2010) and similarly in mouse cortical cells exposure to high concentration of zinc resulted in neuronal death (Kim *et al.*, 1999). Analysis of apoptosis in the current study revealed that antibody-treated cells were not apoptotic in the short term when compared to a positive control of apoptosis such as camptothecin (Figure 4.12). This result confirmed that the decrease in mitotic cells due to the antibody treatment did not stem from cell death, but potentially from the lack of zinc induced by blocking the ZIP6-ZIP10 heteromer.

This discovery led to the formulation of the hypothesis that by blocking the zinc influx necessary to trigger mitosis, cells may be arrested at a stage of the cell cycle prior to mitosis, in particular the G2 phase. Since zinc plays an essential role in the regulation of the cyclins (Chesters & Petrie, 1999), blocking the zinc influx at that stage of the cell cycle may have an effect on their expression. The current investigation showed that cells treated with both nocodazole and the ZIP6 or ZIP10 antibody had a significant decrease of cyclin D1 and B1, but not a significant decrease of cyclin E or A (Figure 4.14B-D). This evidence was further confirmed with immunofluorescence (Figure 4.15-4.16), showing that cells-treated with our ZIP6 or ZIP10-directed antibody (Figure 4.15) had less cyclin B1 than cells synchronised in mitosis with nocodazole. These results suggested that when cells were treated with our ZIP6 or ZIP10 antibody they may be arrested between the S and G2 phase of the cell cycle, as suggested also by the cell cycle analysis which showed that cells treated with the antibody and nocodazole had more cells in G2/M phase and S phase in comparison to control non-treated cells.

Further evidence that cells treated with the ZIP6 or ZIP10 antibodies could not enter mitosis came from the analysis of the protein level of PLK1. PLK1 has a crucial role in the activation of the complex between cyclin B and CDK1, which is required at the onset of mitosis (Gavet & Pines, 2010a; Gheghiani *et al.*, 2017). The analysis revealed a significant decrease of PLK1 in the antibody-treated samples in comparison to nocodazole treated samples, but a similar level to the control (Figure 4.17). This further confirmed that cells treated with these antibodies were not able to proceed through

mitosis. Although the current study did not measure zinc, this had already been done in a previous investigation in our group. In fact, previous studies confirmed that when cells were treated with these antibodies, a significant decrease of cytoplasmic zinc was observed (Nimmanon, 2016). This project expanded this preliminary evidence and demonstrated that treatment with the ZIP6 or ZIP10-directed antibody stops cells prior to mitosis, more likely in G2, and confirmed the requirement of both ZIP6 and ZIP10 at the onset of mitosis. This evidence is also supported by the fact that, in normal zinc conditions, zinc binds the phosphatase Cdc25C which is essential for the G2/M phase transition of the cell cycle. In fact, Cdc25C is involved in the dephosphorylation of CDK1 and activation of its complex with cyclin B1 (Sun *et al.*, 2007), a requirement of G2/M transition.

4.4.4 Treatment of cells with ZIP6 or ZIP10-directed antibody does not lead to quiescence

The confirmation that cancer cell growth was arrested by treatment with a ZIP6 or ZIP10 antibody raised another important question regarding the fate of these cells. One possible fate of cells that stop dividing is to enter a state called quiescence (Pardee, 1974). This state of inactivity is typical of cells which lack nutrients essential for cell growth and replication (Terzi, Izmirli & Gogebakan, 2016). As antibody-treated cells have decreased cytoplasmic zinc (Nimmanon, 2016), the lack of this nutrient could induce cells to exit the cell cycle and become quiescent. Quiescence is promoted by the action of a CDK inhibitor called $p27^{kip1}$ whose activity is regulated by the cyclin-CDK complex (Sheaff *et al.*, 1997). It was found that when cells were treated with our specific antibodies they showed a significant decrease in $p27^{kip1}$ (Figure 4.18), suggesting that cells were not quiescent, as an increase would be expected in quiescence (Sherr & Roberts, 1999). Normally, an increase of $p27^{kip1}$ is associated with the arrest of cells at the G1/S transition (Polyak *et al.*, 1994), therefore suggesting that cells treated with the ZIP6 or ZIP10 antibody may have overcome this stage and were arrested at a later stage, most likely the G2 phase. Decrease of $p27^{kip1}$ is associated with aggressive behaviour in cancer and increased proliferation, since $p27^{kip1}$ is a tumour suppressor (Lloyd *et al.*, 1999). Despite this evidence, all of the above results showed the opposite, since the cells treated with the antibodies had reduced cell growth (Figure 4.9-4.10). Moreover, the analysis of the cyclins did not reveal any significant increase of cyclin E, which is often

increased along with decreased p27 in tumour development (Gladden & Diehl, 2003; Lloyd *et al.*, 1999). This data further corroborated the hypothesis of cells arrested between the S and G2 phase of the cell cycle.

All this data demonstrated that treatment with ZIP6 and ZIP10 antibody arrested cells prior to mitosis (Figure 4.19). The ultimate fate of these cells still needs to be elucidated by future work, which must include the use of this treatment for a longer period of time. It would be interesting to see what the effect of the long-term use of these antibodies is and whether cells can adapt to this condition by using other zinc transporters to mediate zinc influx. So far, this possibility was ruled out, as recent investigations in our groups have shown that when cells, treated with either ZIP6 or ZIP10, were released from the treatment, they started to grow again. However, as soon as the treatment was added back, the cell growth was reduced (Taylor et al, unpublished). This evidence would confirm that ZIP6 and ZIP10 are the two essential zinc transporters for driving cell division. As soon as the efficacy of the long-term treatment with the antibodies is confirmed, it could provide potential new agents to be used in therapy to block aggressiveness in cancer, which relies on increased proliferation and increased cell growth. This study was fundamental to precede future work in animal models now that the effective concentration at preventing cell division *in vitro* was established. This data is promising for future work, as there is already evidence in the literature of a ZIP6 humanized monoclonal antibody conjugated to a potent microtubule disrupting agent which was demonstrated to reduce tumour cell growth in breast cancer xenograft models (Sussman *et al.*, 2014). The benefit of targeting ZIP6 and ZIP10 is that they both reside on the plasma membrane during mitosis, making them accessible targets for the inhibition of mitosis. Furthermore, expression of ZIP6 is a downstream target of STAT3, a transcription factor known to be overexpressed and to drive cell proliferation in many cancers (Buettner, Mora & Jove, 2002). ZIP6 and STAT3 together have been shown to regulate EMT in zebrafish gastrula organizer cells (Yamashita *et al.*, 2004), and the same mechanism has also been seen in breast cancer cells (Hogstrand *et al.*, 2013). Furthermore, ZIP10 expression is also regulated by STAT3 (Miyai *et al.*, 2014), suggesting that both ZIP6 and ZIP10 have a role in cell proliferation and metastasis, making them more feasible targets for proliferative and invasive diseases. Although

many antimitotic drugs such as taxanes and vinca alkaloids are currently used in chemotherapy, their cytotoxic effect on non-tumorigenic cells is a serious issue in therapy (Van Vuuren *et al.*, 2015). Knowing that ZIP6 and ZIP10 are overexpressed in many tumours (Manning *et al.*, 1995; Mcclelland *et al.*, 1998; Kagara *et al.*, 2007; Taylor, 2008; Sussman *et al.*, 2014; Pal *et al.*, 2014) and are both involved in metastatic events (Hogstrand *et al.*, 2013; Taylor *et al.*, 2016), provide an additional benefit to their use as cancer targets.

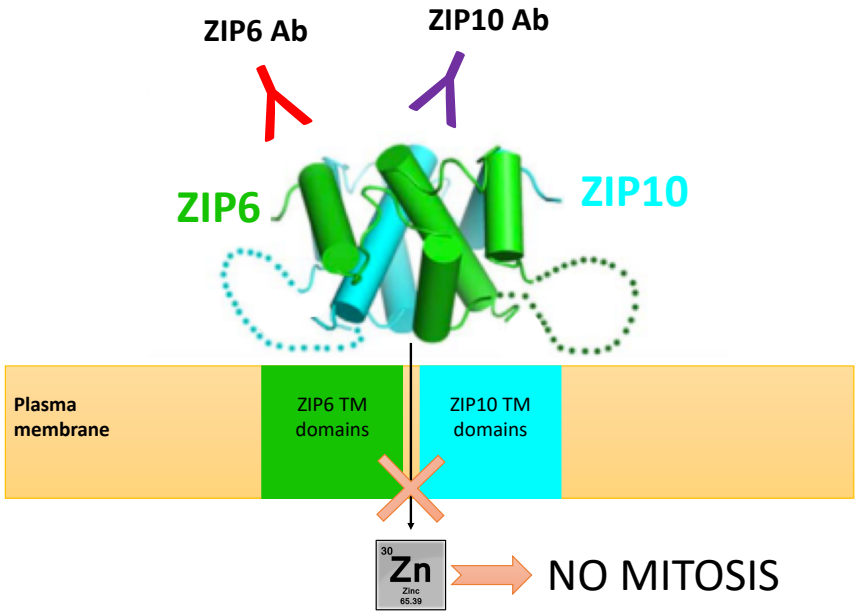

Figure 4.19 ***ZIP6 or ZIP10-directed antibody prevents the zinc influx necessary to trigger mitosis.*** *ZIP6 and ZIP10 form a heteromer on the plasma membrane* (Taylor *et al.*, 2016) *which is necessary to provide the zinc influx to trigger mitosis (Taylor et al, unpublished). As their N-terminal domain is predicted to be intertwined with each other* (Zhang, Sui & Hu, 2016)*, targeting one or the other is effective at blocking the heteromer.*

4.5 Chapter summary

This chapter expanded our recent discovery that two zinc transporters belonging to the LIV-1 subfamily of the SLC39A family act as a heteromer on the plasma membrane and are involved in providing the zinc influx necessary to trigger mitosis (*Taylor et al, unpublished*), a mechanism that has never been investigated previously. In light of this, this investigation analysed whether by using specific ZIP6 and ZIP10 antibodies directed to the N-terminal domain of these two zinc transporters, it was possible to block this zinc influx and therefore stop mitosis. It was discovered that cells belonging to different cancer cell lines treated with either ZIP6 or ZIP10 antibody were not able to enter mitosis (Figure 4.19) and arrested at a stage of the cell cycle prior to mitosis. This treatment was

revealed not to be toxic to cells in the short term, and needs now to be expanded to longer term. However, when this treatment was prolonged to 4 days, the growth of different cancer cell lines was significantly reduced, providing new promising targets for therapy of aggressive diseases such as cancer, which are characterised by increased and uncontrolled cell growth.

5 INVESTIGATING THE ROLE OF ZIP6 AND ZIP10 IN MITOSIS BY USING A MODEL OF ZIP6 KNOCKOUT CELLS

5.1 Introduction

In Chapter 4 it was demonstrated how both ZIP6 and ZIP10 are involved in the regulation of mitosis and that it was possible to downregulate cell division by using specific ZIP6 or ZIP10 antibodies. For this reason, the next investigation aimed at discovering the mechanism by which these two zinc transporters regulate cell division and cell growth. In order to better understand this, in this chapter a mouse mammary cell line with ZIP6 knocked out was used (NMuMg ZIP6 ko). This cell line was kindly gifted to us by one of our collaborators in Canada and it was developed using the CRISPR-Cas9 technique (Brethour *et al.*, 2017). This ZIP6 knockout cell line was compared to the corresponding wild type throughout the project to investigate how the downregulation of ZIP6 affected cells. This research group in Canada had used this knocked-out cell line to investigate the role of ZIP6 in EMT (epithelial to mesenchymal transition), as ZIP6 was previously discovered to have an important role in EMT and cancer development (Yamashita *et al.*, 2004; Hogstrand *et al.*, 2013). EMT is a mechanism by which epithelial cells acquire mesenchymal properties during embryonic development and it is a process often used by cancer cells to acquire invasive properties (Kalluri, 2009). Brethour *et al* showed that ZIP6 expression was significantly increased during EMT induced by transforming growth factor beta 1 (TGFB1) treatment in NMuMg wild type cells (Brethour *et al.*, 2017). Moreover, this investigation confirmed the previous discovery of ZIP6 forming a heteromer with ZIP10 and, in particular, demonstrated that this dimer primarily interacted with NCAM1, a protein involved in forming focal adhesions. Most interestingly, it was also shown that ZIP6 and ZIP10 displayed interdependency during their expression, as the expression of one influenced the expression of the other (Brethour *et al.*, 2017). However, the interdependency of ZIP6 and ZIP10 has not yet been studied for its role in cell division and for investigating the consequence that downregulation of one member of this dimer could have on cell cycle progression and cell growth, the aim of the current chapter.

5.1.1 Aims and objectives

The aim of this chapter was to investigate the role of ZIP6 in cell growth and mitosis by using a cell line of NMuMg ZIP6 knockout cells. This was achieved by comparing these ZIP6 knockout cells to the corresponding wild type. Consequently, the objectives of this chapter were:

1. To compare the cell growth of ZIP6 knockout cells in comparison to the corresponding wild type and to look for other proteins that have an important role in the regulation of cell growth and the cell cycle;
2. To downregulate ZIP10 in the ZIP6 knockout cells and to assess the effect that the downregulation of both ZIP6 and ZIP10 has on cell growth or cell viability.

5.2 Materials and methods

The comparison of the cell growth rate of the NMuMg wild type and NMuMg ZIP6 knockout cells was carried out by performing a cell growth assay where cells were counted every day for 4 days. Protein levels of ZIP10, cyclins and STAT3 were assessed by western blotting in order to investigate how the knockout model coped with the lack of ZIP6. Moreover, since ZIP6 and ZIP10 were discovered to be important zinc transporters on the plasma membrane and to be required for the zinc influx to trigger mitosis, the content of zinc was measured in the two different cell models by using a flow cytometry Fluozin-3 zinc assay. The ZIP6 knockout model was also used to investigate the effect of ZIP10 downregulation on the cell viability and cell growth of this cell line by performing a ZIP10 siRNA transfection. For more details about the methods, refer to Chapter 2.

5.3 Results

5.3.1 The effect of ZIP6 knockout on cell growth

Having demonstrated in the previous chapter how treatment with specific ZIP6 or ZIP10 antibodies was able to inhibit the growth of different cancer cell lines, the first aim of this chapter was to evaluate the effect of ZIP6 downregulation on cell growth. The NMuMg wild type cell line expresses both ZIP6 and ZIP10. In fact, since both ZIP6 and ZIP10 are necessary for cell division, it was interesting to look at how the ZIP6 knockout cells coped with the downregulation of ZIP6. NMuMg wild type and ZIP6 knockout cells were seeded at the same density in a 24 well plate and monitored every day by counting cells with a Coulter counter (Figure 5.1). The analysis revealed that the ZIP6 knockout model had a slower growth rate when compared to the corresponding wild type at day 2, 3 and 4 ($p<0.05$) (Figure 5.1). No significant difference was detected at day 1 probably because when cells were seeded for the experiment they took a while to start growing. This result confirmed that the lack of ZIP6 was affecting the growth of cells and indicated that the presence of a dimer on the plasma membrane may be essential for the progression of cells through G2 and M phase.

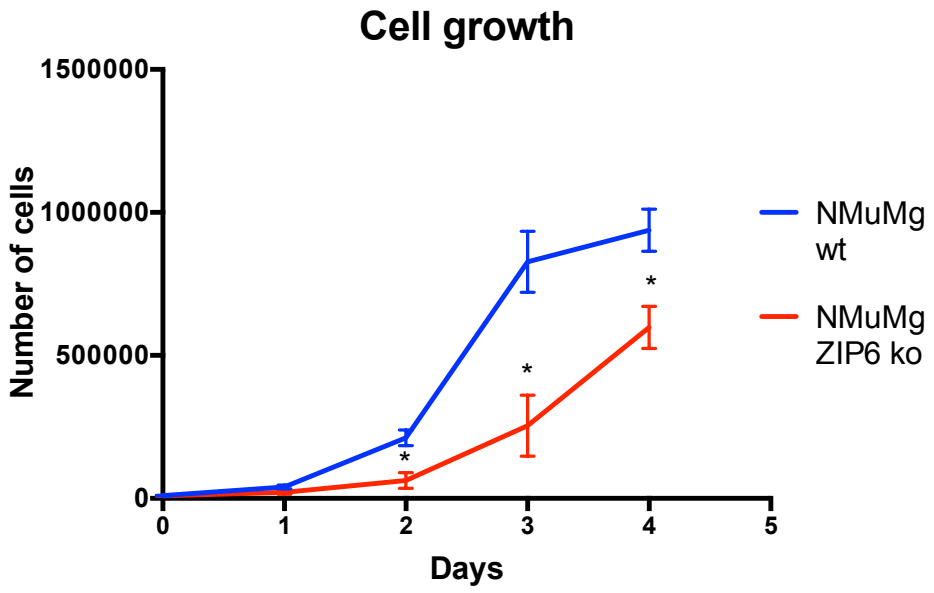

Figure 5.1 ***NMuMg ZIP6 knockout cells have a reduced cell growth rate compared to wild type cells.*** *NMuMg wild type (wt) and ZIP6 knockout (ko) cells were seeded on a 24 well plate and counted every 24 hours for 4 days using a cell Coulter counter. The number of cells counted was plotted in a line graph. The experiment was performed on three biological replicate and the graph shows n=3 ± SEM (standard error of mean). Statistical analysis was performed and is shown as * (p<0.05).*

5.3.1.1 Cell cycle analysis of ZIP6 knockout cells

It was surprising to notice that despite the fact that the knockout cell line were deprived of ZIP6, these cells were still able to grow. In order to better decipher how this cell line coped with the downregulation of ZIP6, the previous data was compared to the FACS cell cycle analysis previously obtained in our group which compared the ZIP6 knockout cells to the corresponding wild type (Nimmanon, 2016). Interestingly, this data showed only a slight decrease in the percentage of cells in the G2/M phase of the cell cycle from 27% of the wild type to 25% of the ZIP6 knockout cells (Figure 5.2). This evidence confirmed that these cells were still able to grow and divide even without ZIP6. Conversely, a dramatic decrease in the population of cells in S phase was observed from 23% in the wild type to 7% in the knockout model (Figure 5.2). This analysis also revealed that the knockout cells had a larger population of cells in the G0/G1 phase (73%) compared to the wild type (45%) (Figure 5.2). This data suggested that ZIP6 may also play a role in the S phase of the cell cycle.

It is well established that zinc is required for S phase, acting as an important cofactor for many enzymes required for DNA synthesis (Prasad & Oberleas, 1974; Chesters, Petrie & Vint, 1989; Chesters, Petrie & Travis, 1990). However, it was speculated that the zinc necessary for the S phase was provided by zinc release from inside intracellular stores (Li & Maret, 2009), most likely zinc transported by ZIP7, another member of the SLC39A family which was discovered to reside on the endoplasmic reticulum (Taylor *et al.*, 2004). This evidence was also supported by the highly positive prediction score from PHOSIDA (score 3.03) (Gnad, Gunawardena & Mann, 2011) that predicted phosphorylation of residues S275 and S276 of ZIP7 by the kinase CK2 at late G1/S phase. Therefore, whether ZIP6 may have a role in S phase is not yet known and needs to be investigated further.

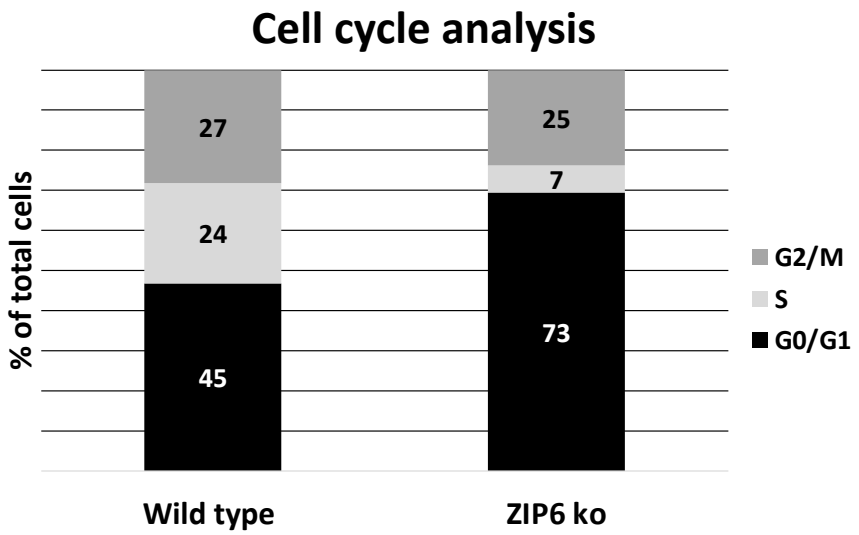

Figure 5.2 ***Comparison of cell cycle analysis in NMuMg wild type and ZIP6 knockout cells.***
NMuMg wt and ZIP6 ko cells were stained with propidium iodide and DNA content was measured using FACS analysis. Percentage of cells in G0/G1, S or G2/M phase was analysed using FlowJo software and are represented as a 100% stacked column chart. Courtesy of Thirayost Nimmanon.

5.3.2 Effect of ZIP6 downregulation on ZIP10 level

Figure 5.1 showed that the cell growth of the ZIP6 knockout cells was affected by the lack of ZIP6 but that the cells were still able to grow. This implied that the cells lacking ZIP6 may find a compensatory mechanism by which they were still able to grow. This was also confirmed in Figure 5.2 as the knockout cells did not show a drastic reduction of cells in the G2/M phase population compared to the wild type. In order to investigate this further, the protein level of ZIP10 was assessed. In fact, it was seen in a previous study that knockdown of ZIP10 in zebrafish embryos resulted in upregulation of mRNA for both ZIP6 and STAT3 (Taylor *et al.*, 2016). Furthermore, the expression of ZIP6 has been found to be interdependent with the expression of ZIP10 (Brethour *et al.*, 2017). Analysis of ZIP10 level was investigated by western blotting probing for ZIP10 in wild type and ZIP6 knockout cell samples. The analysis revealed that the ZIP6 knockout cells had a three-fold significant increase of ZIP10 protein levels ($p<0.05$) (Figure 5.3). This suggested that upregulation of ZIP10 could be used as a compensatory mechanism to counteract the lack of ZIP6.

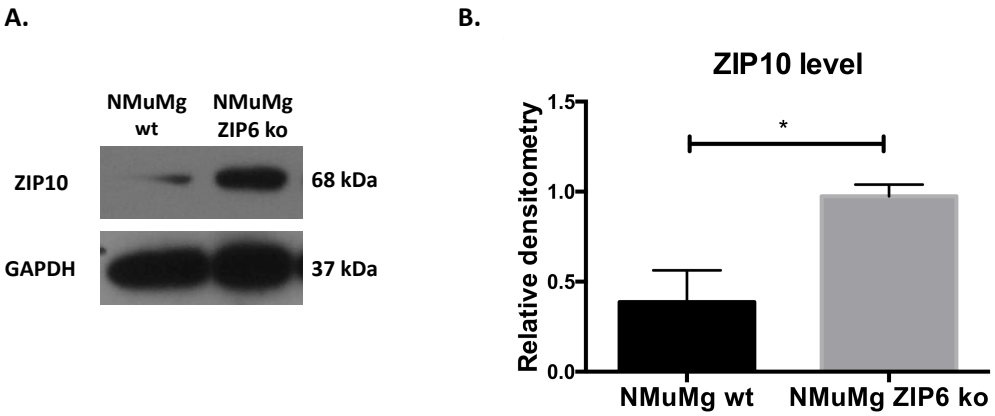

Figure 5.3 ***ZIP10 is three-fold increased in NMuMg ZIP6 knockout cells.***
A. NMuMg wild type (wt) and ZIP6 knockout (ko) cells were probed for ZIP10 by western blotting.
*B. The experiment was performed on three biological replicates and the mean of n=3 ± SEM (standard error of mean) is indicated as a bar graph. Statistical significance is shown as * (p<0.05).*

5.3.3 Analysis of STAT3 on ZIP6 knockout cells

In a previous study it was shown that downregulation of ZIP10 resulted in upregulation of both ZIP6 and STAT3 (Taylor *et al.*, 2016). For this reason, it was interesting to analyse the effect of ZIP6 downregulation on STAT3. Figure 5.4-A-B shows that western blotting analysis of total STAT3 revealed no significant difference between the wild type and ZIP6 knockout cells. The investigation also analysed the level of activated STAT3. STAT3 is an important transcription factor whose tyrosine phosphorylation on 705 is involved in the regulation of a variety of processes including cell cycle regulation, apoptosis and the immune response (Levy & Lee, 2002). In addition, the role of STAT3 in cancer is well established (Bromberg, 2002) and phosphorylation of STAT3 is the key to these mechanisms. STAT3 can also be phosphorylated on serine residue 727 (Decker & Kovarik, 2000). The two phosphorylation sites are regulated by different kinases and play different roles in biology, in particular in oncogenesis (Bromberg, 2002; Decker & Kovarik, 2000). In a recent study in our group it was seen that the zinc influx mediated by the ZIP6-ZIP10 heteromer during mitosis was involved in zinc-dependant switch of the STAT3 phosphorylation from Y705 to S727 (*Taylor et al, unpublished*). This has been previously confirmed by others where nocodazole-induced cells had increased $pSer^{727}$STAT3 and decreased $pTyr^{705}$STAT3 (Shi *et al.*, 2006). For this reason phosphorylation of STAT3 on serine residue 727 could be used as another marker of mitosis status. Other studies have also shown that serine phosphorylation of STAT3 was constitutively active in cells with a higher cell proliferation rate (Decker & Kovarik, 2000). Therefore, in this experiment the level of STAT3 phosphorylation was assessed in basal conditions.

Results showed no significant difference in the total amount of STAT3 in the two cell lines (Figure 5.4-B). The two different phosphorylation sites of STAT3 were investigated in the ZIP6 knockout cells and results revealed a significant increase in phosphoserine STAT3 compared to the wild type cells ($p<0.05$) (Figure 5.4-C). Conversely, the phosphotyrosine STAT3 analysis, despite revealing a slight increase in the ZIP6 knockout model, was not significant (Figure 5.4-D).

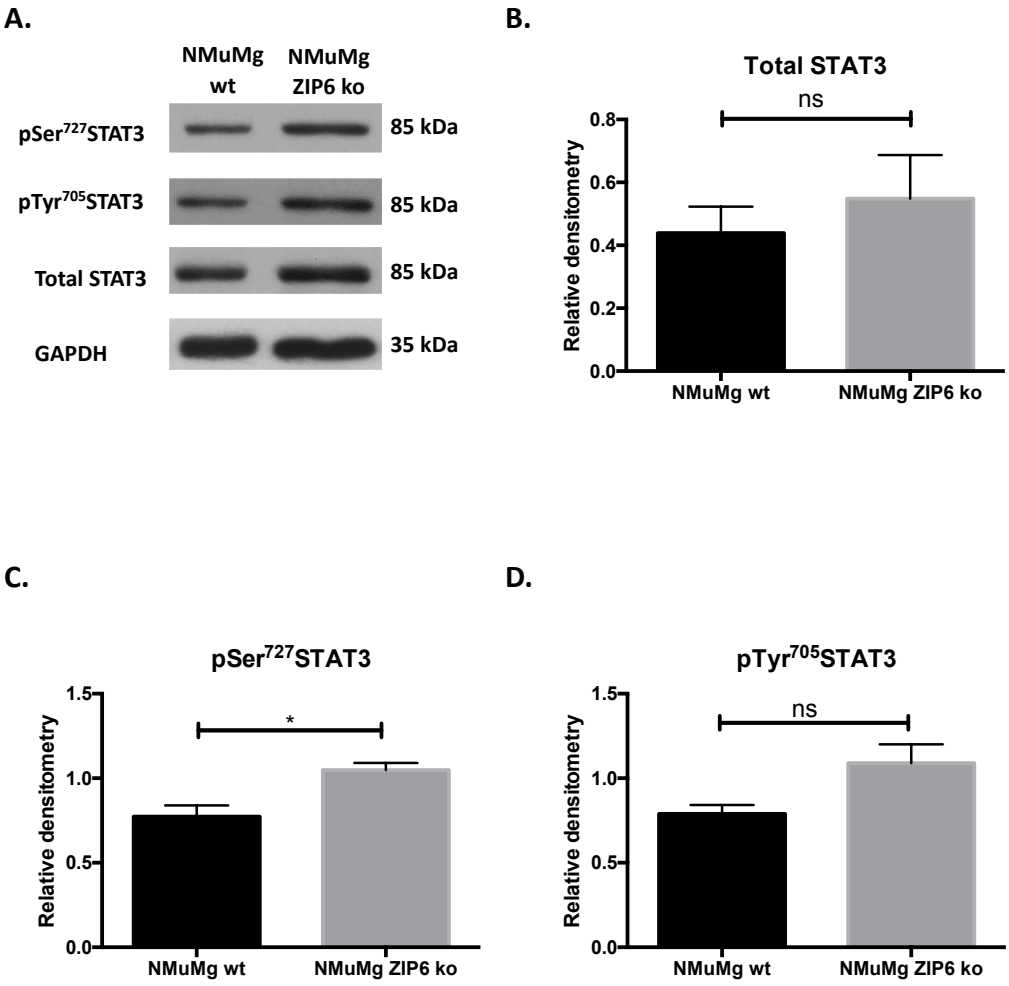

Figure 5.4 ***ZIP6 ko cells have increased pSer^{727}STAT3 in comparison to the wild type in basal conditions.*** *A. NMuMg wild type and ZIP6 ko cells were probed for total STAT3, pSer^{727}STAT3 and pTyr^{705}STAT3. B-C-D. The experiment was performed on three biological replicates and the mean of n=3 ±SEM (standard error of mean) is indicated as a bar graph. The densitometric data of total STAT3 was normalised to the level of GAPDH, whereas the densitometric data of activated STAT3 was normalised to the total level of STAT3. Statistical significance comparing the wild type to the ko cells is shown as * (p<0.05).*

5.3.4 Analysis of cytoplasmic zinc in the ZIP6 knockout cells

Our group have demonstrated that ZIP6 and ZIP10 are required to provide the zinc influx to trigger mitosis (*Taylor et al, unpublished*), therefore downregulation of ZIP6 may have an effect on the level of intracellular zinc. For this reason, the level of zinc in the NMuMg wild type and ZIP6 knockout cells was analysed. This analysis was carried out by using Fluozin-3 zinc specific dye indicator and performed using FACS analysis. Results of this experiment revealed that the NMuMg ZIP6 knockout cells had a significant decrease of cytoplasmic zinc when compared to the corresponding wild type (Figure 5.5). The total amount of fluorescence was measured and the analysis showed a significant decrease of total cell fluorescence of over 50% between the wild type NMuMg cells and the ZIP6 knockout cell model ($p<0.05$) (Figure 5.5). This result confirmed what was demonstrated previously in our group, where immunofluorescence analysis of Fluozin-3 in the ZIP6 knockout cells showed less cytoplasmic zinc when compared to the wild type cells (Figure 5.6) (Nimmanon, 2016).

Decreased cytoplasmic zinc in the knockout cell line could be due to the lack of ZIP6, since it is one of the main zinc importers on the plasma membrane (Taylor *et al.*, 2003) and ZIP6 is required to influx zinc at the beginning of mitosis (*Taylor et al, unpublished*). The decrease of zinc in the ZIP6 knockout cell model could also explain why these cells had a reduced cell growth rate in comparison to the corresponding wild type (Figure 5.1).

A.

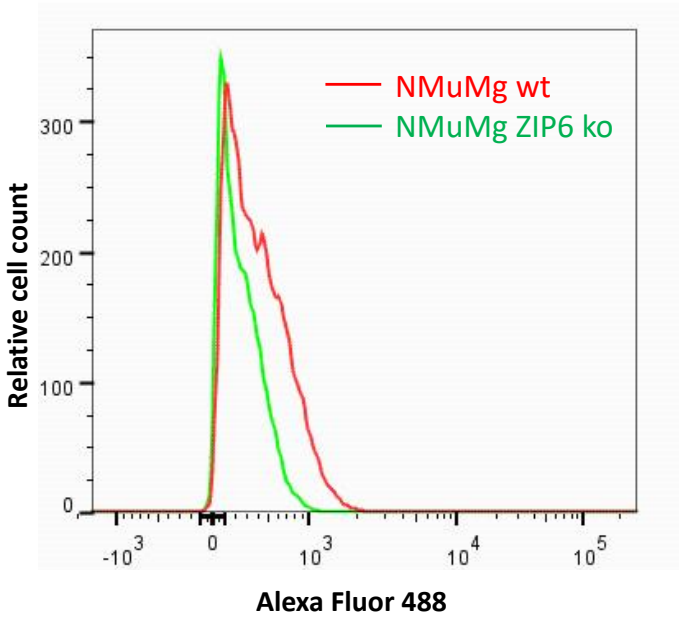

B.

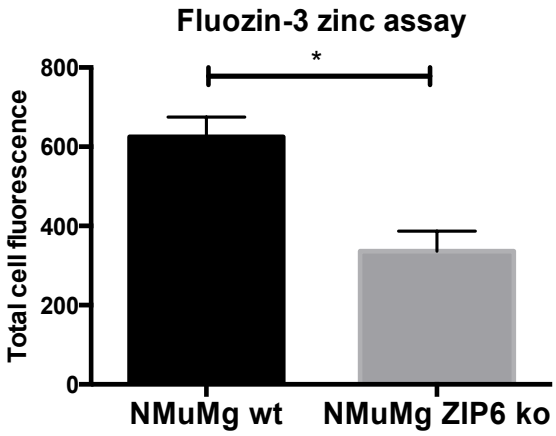

Figure 5.5 ***NMuMg ZIP6 ko cells have a reduced level of cytoplasmic zinc.***
A. NMuMg wild type and ZIP6 ko cells were stained with Fluozin-3. FACS analysis was performed and the data are shown in an overlay histogram.
*B. Total cell fluorescence is expressed as geometric mean fluorescence and it is shown in a bar graph as mean values of n=3 ±SEM (standard error of mean). Statistical significance is shown as * ($p<0.05$).*

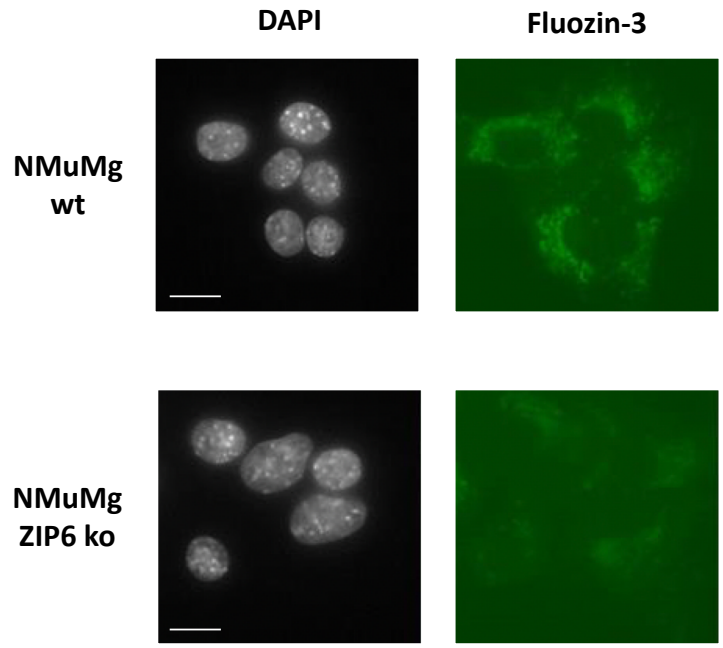

Figure 5.6 ***Fluozin-3 zinc dye indicates lower cytoplasmic zinc levels in the NMuMg ZIP6 ko cells.*** *NMuMg wild type and ZIP6 knockout cells were stained with Fluozin-3 and fixed in 3.7% formaldehyde. The nuclei were stained with DAPI and mounted onto slides. Pictures were acquired using a 63x oil lens Leica DMIRE2 microscope. Scale bar: 10 μm. Courtesy of Thirayost Nimmanon.*

5.3.4.1 Investigation of cyclin protein levels in ZIP6 ko cells

The results gained so far in this chapter demonstrate that the lack of ZIP6 in the ZIP6 knockout cell model leads to reduced cell growth rate, upregulation of ZIP10 and reduced levels of cytoplasmic zinc. A previous paper showed that cyclins expression is significantly decreased in zinc deficient cells (Chesters & Petrie, 1999). Since zinc was discovered to be involved in the expression of cyclins, it was intriguing to see whether the decreased level of cytoplasmic zinc discovered in the ZIP6 knockout cell line had an impact on the protein levels of cyclins.

The analysis of the cyclins in the NMuMg cells was performed on both wild type and knockout cells by western blotting. Moreover, considering the important role played by ZIP6 and ZIP10 in the regulation of mitosis (*Taylor et al, unpublished*), this experiment was carried out with or without nocodazole to detect any difference in the cyclin levels when cells were synchronised in mitosis. In these cell lines it was not possible to obtain any band on western blotting for the cyclin A and B1, but only cyclin D1 and E were detected. The lack of signal for cyclin A and B1 is yet to be understood, but it may suggest that the levels of these cyclins were too low in these cell lines to be identified on western blotting. Analysis of cyclin D1, despite being slightly decreased in the ZIP6 knockout cells, revealed no significant difference between the two cell lines (Figure 5.7). However, analysis of cyclin E revealed a significant difference between the wt and wt + NOC ($p<0.01$), the wt and ZIP6 knockout model ($p<0.001$) and between the wt and the ZIP6 knockout treated with nocodazole ($p<0.01$) (Figure 5.7). Since no result was found for the cyclin B1, which is the mitotic cyclin, it was not possible to draw any conclusion regarding the effect of ZIP6 downregulation on the level of cyclin B1 during mitosis. However, the results obtained for cyclin E may suggest that the zinc decrease observed in the ZIP6 knockout model may affect the regulation of the S phase of the cell cycle, as cyclin E is involved in the progress of cells from G1 to S phase (Lew, Dulić & Reed, 1991) (see Figure 1.11). This result would also fit with Figure 5.2, which showed a significant decrease in the population of cells in S phase in the ZIP6 knockout model, implying a role for ZIP6 in the S phase of the cell cycle.

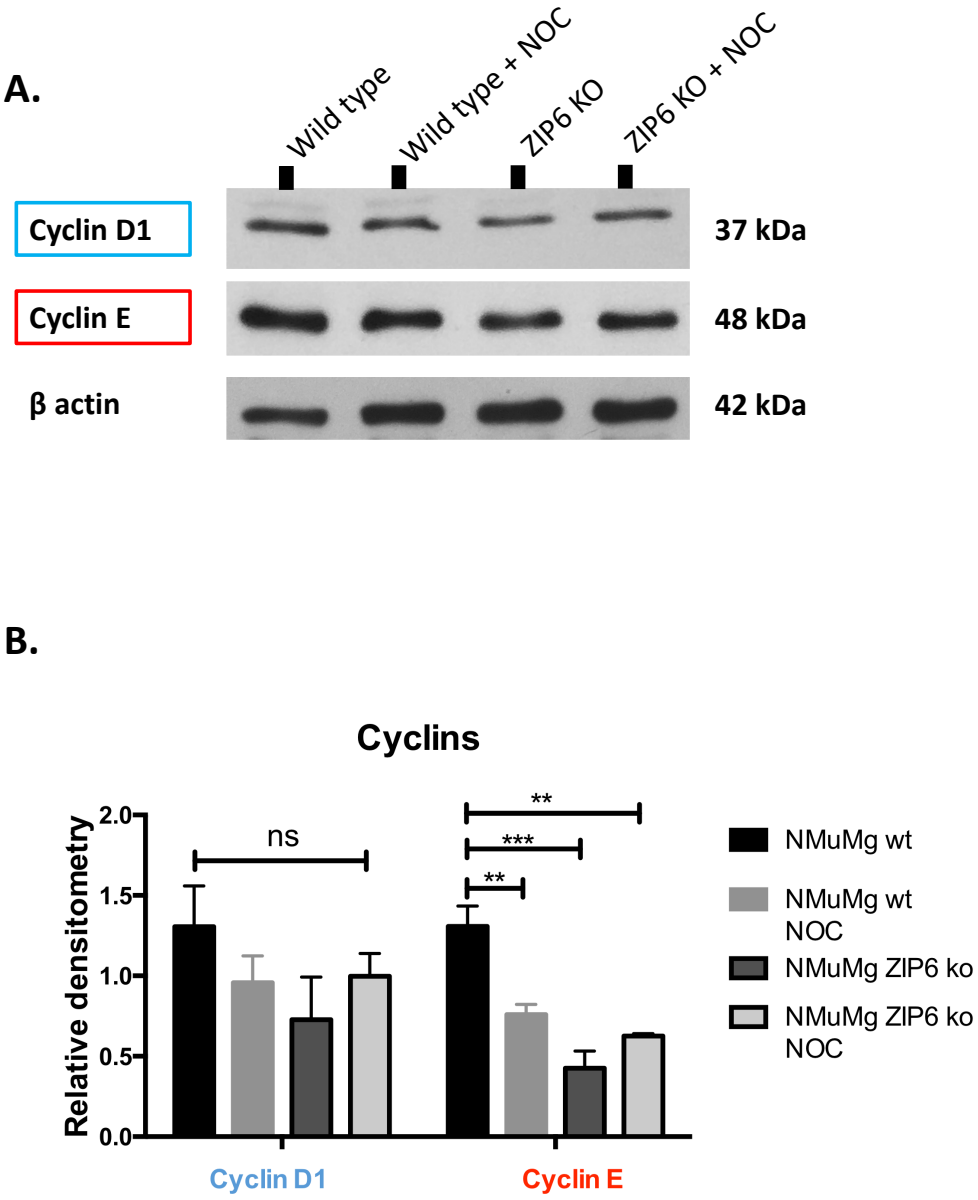

Figure 5.7 ***NMuMg ZIP6 knockout cells have decreased levels of cyclin E.***
A. NMuMg wild type or ZIP6 knockout cells were treated at 70% confluence with or without 150 nM nocodazole for 20 hours. Western blot analysis probed samples for cyclin D1 and cyclin E.
*B. The experiment was performed on three biological replicates and the densitometric data was normalised to the results of the β actin. Densitometric analysis was performed showing the mean values of n=3 ± SEM (standard error of the mean) as a bar graph. Statistical significance is shown as ** (p<0.01) and *** (p<0.001).*

5.3.5 Effect of ZIP10 downregulation on ZIP6 knockout cells

Following the discovery of the upregulation of ZIP10 in the ZIP6 knockout cells, the investigation moved to analyse what happened to cells when ZIP10 was also downregulated. Knockdown of ZIP10 was achieved with ZIP10 siRNA transfection. Differently from the CRISPR model, the siRNA experiment provided a transient downregulation which was measured after 3 days of transfection. The siRNA experiment was carried out by using a pool of 4 siRNAs directed against the mouse sequence of ZIP10 (Dharmacon, USA) and with an siRNA control (see Table 2.9). The first analysis post-siRNA was performed to check whether the downregulation had been successful by probing for the presence of ZIP10. Western blotting analysis revealed that the protein level of ZIP10 was reduced by over 50% following ZIP10 siRNA transfection for 72 hours (*p<0.01*) (Figure 5.8-A-B).

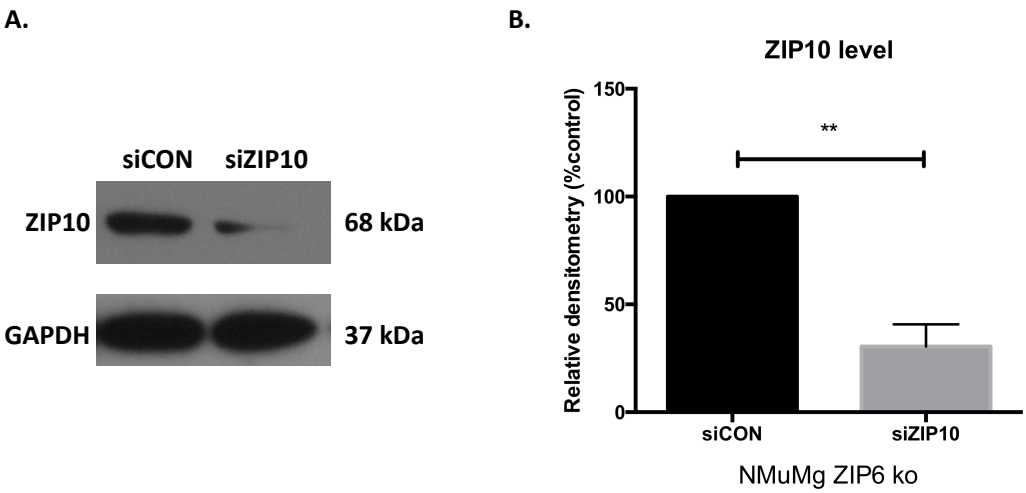

Figure 5.8 ***ZIP10 downregulation in ZIP6 ko cells.***
A. The siRNA experiment was performed for 72 hours using a pool of 4 siRNAs directed against the mouse sequence of ZIP10 along with an siRNA control (Dharmacon, see details on Table 2.9). The efficacy of siRNA was tested by performing a western blot where cells were probed for ZIP10.
*B. The experiment was performed on three biological replicates and the mean of n=3 ± SEM (standard error of mean) is indicated as a bar graph. Statistical significance comparing the wild type to the knockout cells is shown as ** (p<0.01).*

Cells which had been downregulated for ZIP10 were then assessed for their cell viability. Since ZIP6 and ZIP10 have an important role in the regulation of mitosis and cell growth, downregulation of ZIP10 could have an impact on the overall cell viability and cell proliferation of this ZIP6 knockout model. The cell viability assay showed that knockdown of ZIP10 using siRNA in ZIP6 knockout cells produced a 25% reduction in cell viability compared to control siRNA ($p<0.01$) (Figure 5.9-A). Reduction in cell viability consists of reduction of overall cell metabolism and is indicative of decreased cell proliferation. Therefore, this result confirmed the importance of ZIP10 for the cell viability of the NMuMg ZIP6 knockout cells, highlighting that ZIP10 was essential for the growth and correct metabolism of this cell line, especially considering the lack of ZIP6.

Having discovered that the cell viability of the knockout cells was significantly reduced following a transient ZIP10 downregulation, it was interesting to investigate whether this downregulation had any impact on the ZIP6 knockout cell growth. In Figure 5.8 it was demonstrated that 72 hours of ZIP10 siRNA transfection reduced the level of ZIP10 by over 50%. For this reason, ZIP6 knockout cells were counted for 3 days following the ZIP10 siRNA with the aim of assessing whether the downregulation of ZIP10 had any further impact on their cell growth. Figure 5.9-B showed that the cell growth of NMuMg ZIP6 ko cells following the ZIP10 downregulation was not significantly reduced in comparison to the cells which had been transfected with siCON, despite showing a decreased growth rate. As it was discovered that the ZIP6 knockout cells upregulated ZIP10 to counteract the lack of ZIP6, this data showed that cells could recover the ZIP10 protein level post-siRNA. In fact, western blotting analysis revealed a slight increase of ZIP10 protein level after the release from the treatment, albeit not at a significant level (Figure 5.10). This result implied that ZIP10 was important for the growth of this cell line and that these cells counteracted the transient ZIP10 downregulation by starting to restore ZIP10 protein level post-siRNA (Figure 5.10). It could also imply that other proteins may be involved in the regulation of the cell growth of this knockout cell line.

A.

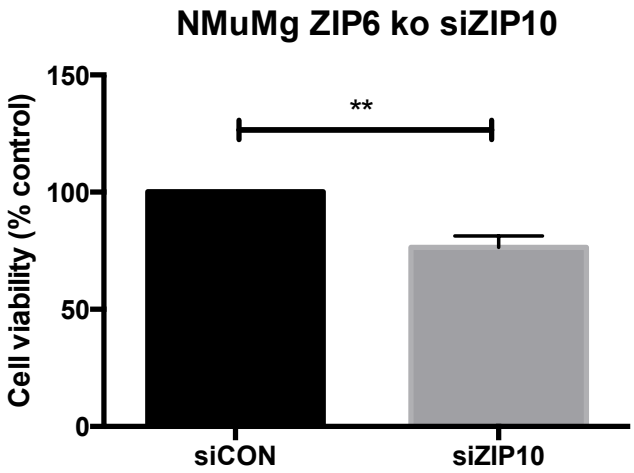

B.

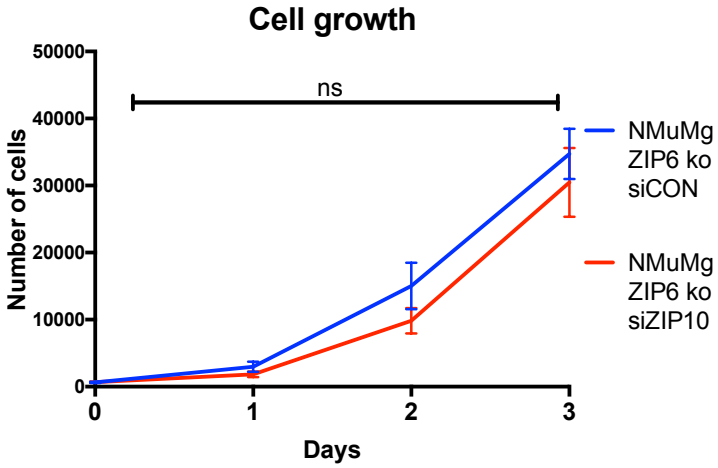

Figure 5.9 ***Effect of ZIP10 downregulation in NMuMg ZIP6 ko cells on cell viability and cell growth.***
The experiment was performed for 72 hours using a pool of 4 ZIP10 siRNAs directed against the mouse sequence of ZIP10 along with an siRNA control (Dharmacon, see details on Table 2.9).
*A. MTT experiment was performed on NMuMg ZIP6 ko cells ± ZIP10 siRNA and the cell viability was measured as OD (540 nm). Cell viability is expressed as percentage of control. The experiment was performed on three biological replicates and the mean of n=3 ± SEM (standard error of mean) is indicated as a bar graph. Statistical significance comparing the siCON to siZIP10 is shown as ** ($p<0.01$).*
B. NMuMg ZIP6 ko cells transfected for 72 hours with ZIP10 siRNA or with siCON were transferred and seeded into a 24 well-plate and counted for 3 days after 24 hours (day 0). The number of cells counted were plotted in a line graph. The experiment was performed on three biological replicates (n=3), but no statistical significance was revealed.

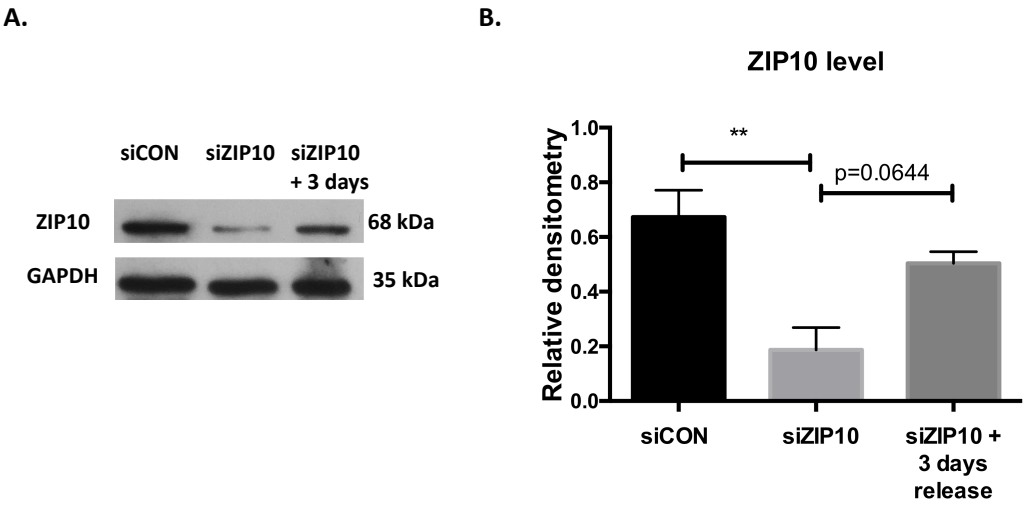

Figure 5.10 ***ZIP10 protein level starts recovering post-siRNA.***
A. The siRNA transfection was performed for 72 hours using a pool of 4 ZIP10 siRNAs directed against the mouse sequence of ZIP10 or with an siRNA control (Dharmacon, see details on Table 2.9). ZIP10 protein level was measured after 3 days post-siRNA. This was compared to the level of ZIP10 in the siCON and siZIP10 samples after 72 hours siRNA downregulation.
*B. The experiment was performed on three biological replicates and the mean of n=3 ± SEM (standard error of mean) is indicated as a bar graph. Statistical significant is shown as ** (p<0.01).*

5.4 Discussion

In the previous chapter it was shown how ZIP6 and ZIP10 play an important role in the regulation of mitosis. Most importantly, it was shown how it was possible to reduce the cell growth of three cancer cell lines by treating cells with specific N-terminal ZIP6 or ZIP10-directed antibodies. This is the first step in trying to understand the regulation of mitosis, but also to provide new potential targets for the treatment of proliferative diseases such as cancer. However, how the ZIP6-ZIP10 heteromer works is not fully understood yet. Thanks to our collaboration with a research group in Canada, this investigation was expanded by using a mouse cell line (mouse breast glandular cells) that has ZIP6 removed by the CRISPR/Cas9 technique (Brethour *et al.*, 2017).

5.4.1 NMuMg ZIP6 knockout cells display increased ZIP10 protein level

It was intriguing to discover that the ZIP6 knockout cell line grew at a slower growth rate in comparison to the corresponding wild type form, but surprisingly these cells were still able to grow despite the lack of ZIP6 (Figure 5.1). This result fits with previous cell cycle analysis from our group, showing that the knockout cell line had a decreased population of cells in the G2/M phase of the cell cycle but an even smaller population of cells in the S phase (Figure 5.2) (Nimmanon, 2016). Therefore, this cell line must rely on a different mechanism to carry out mitosis and to adapt to the lack of ZIP6. Our group have recently demonstrated that the ZIP6 and ZIP10 zinc transporters act as a heteromer (Taylor *et al.*, 2016), but a crystal structure of this heteromer is not yet available. However, a recent investigation has discovered that the zinc transporter ZIP4 acts as a homodimer and this study provided the first crystal structure of the N-terminal domain of a ZIP transporter (Zhang, Sui & Hu, 2016). ZIP4 is another member of the LIV-1 subfamily, and this recent discovery may imply that all the members of the LIV-1 subfamily share this dimeric structure. This evidence led to the hypothesis that since the ZIP6 knockout cells express ZIP10, this transporter could be upregulated in order to counteract the lack of ZIP6, by forming a homodimer. This hypothesis was supported by data in this current chapter which unveiled that the knockout cells had a significantly increased protein level of ZIP10 (Figure 5.3), which could partially compensate for the lack of ZIP6. This was an important result as it might suggest that ZIP10 upregulation and the potential formation of ZIP10 homodimers in these cells is a mechanism adapted in order to influx zinc at the beginning of mitosis. In fact, the presence of a dimeric

structure seems to be an important prerequisite for zinc transporters in order to transport zinc (reviewed by Kambe et al. 2015). This result was exciting as it suggested that the lack of one of the two zinc transporters had an impact on zinc signalling implying that the presence of a dimeric structure is a requirement for proper zinc transporters function. However, since a crystal structure is not yet available, this cannot be confirmed. Alternatively, this finding could suggest that ZIP10 may form a heteromer with another ZIP transporter to counteract the lack of ZIP6. In fact, the zinc transporter ZIP5 is the closest paralog to ZIP6 and ZIP10 as seen in the phylogenetic tree in Figure 1.3. Furthermore, ZIP5 shares many similarities with ZIP6 and ZIP10 (Taylor *et al.*, 2007), and despite a recent investigation of the ZIP6 interactome revealing that ZIP6 interacts with ZIP10 but not ZIP5 (Brethour *et al.*, 2017), the lack of ZIP6 in the ZIP6 knockout model could induce the cells to adapt to this condition by utilising ZIP5 to form a dimeric structure. This is an important aspect to consider for future investigations. As results within this chapter have suggested that the lack of ZIP6 affected the heteromer, the hypothesis that another zinc transporter may replace ZIP6 in the formation of a dimeric structure on the plasma membrane for proper zinc signalling is not to be excluded. Unfortunately, a preliminary assessment of the potential upregulation of ZIP5 on the ZIP6 knockout cell line did not provide any clear results and the upregulation of other zinc transporters is a feature that needs to be assessed in future work.

5.4.2 A potential role for ZIP6 in the S phase of the cell cycle

It was intriguing to discover that the ZIP6 model had a significant decrease in the population of cells in S phase in comparison to the corresponding wild type cells (Figure 5.2). Interestingly, cyclin analysis revealed that the knockout cells also had a decreased protein level of cyclin E (Figure 5.7), a cyclin which is necessary for the regulation of cells from the G1 to S phase of the cell cycle, when DNA synthesis occurs (Lew, Dulić & Reed, 1991). The first study showing the essential role of zinc in the regulation of the cell cycle dates back to the sixties, where it was found that DNA synthesis was arrested when cells were treated with metal chelators, and was only restored when zinc, but no other metals, was added back (Fujioka & Lieberman, 1964). Since then, zinc has been known for its involvement in DNA synthesis as it is required for enzymes such as thymidine kinase (Prasad & Oberleas, 1974; Chesters, Petrie & Vint, 1989; Chesters, Petrie & Travis, 1990). Furthermore, it was demonstrated that during the cell cycle two peaks of zinc

were observed: one during early G1 and one during the G1/S phase transition (Li & Maret, 2009). ZIP6 is one of the main zinc importers residing on the plasma membrane and plays an important role in zinc homeostasis by influxing zinc from the extracellular space (Taylor *et al.*, 2003). The results of the current chapter implied a potential role for ZIP6 also during the S phase of the cell cycle, as ZIP6 may have a role in transporting the zinc necessary for DNA synthesis, something that has not yet been investigated.

5.4.3 ZIP10 is regulated by STAT3

This investigation discovered that ZIP6 knockout cells had increased protein level of pSer^{727}STAT3 in basal conditions (Figure 5.4-C). STAT3 is a transcription factor widely known for its role in cell survival and cell migration (Haura, Turkson & Jove, 2005). A recent investigation has demonstrated that, similar to that previously discovered for ZIP6 (Hogstrand *et al.*, 2013), ZIP10 expression was also regulated by STAT3 (Miyai *et al.*, 2014). The role of pSer^{727}STAT3 is still controversial in the literature, but it appears to play a crucial role in the regulation of cellular growth (Decker & Kovarik, 2000) and cell differentiation (Huang *et al.*, 2014). This data may indicate a role for pSer^{727}STAT3 in the regulation of the cell growth of this knockout model by regulating ZIP10 expression. ZIP6 and ZIP10 expression was demonstrated to be interdependent (Brethour *et al.*, 2017), but it may be that the key regulator of their role is STAT3. A previous study has demonstrated that ZIP10 is involved in B-cell survival (Hojyo *et al.*, 2014) and that ZIP10 expression is regulated by activation of STAT3, having identified the potential binding site of STAT3 to ZIP10 in the proximal region of the human ZIP10 promoter (Miyai *et al.*, 2014). In fact, although the protein level of pTyr^{705}STAT3 was not significantly increased in the current investigation, it showed a similar increase as pSer^{727}STAT3, which could suggest that the upregulation of ZIP10 in the ZIP6 knockout cells was regulated by activated STAT3.

5.4.4 NMuMg ZIP6 knockout cells have decreased cytoplasmic zinc

Another important finding of this chapter was the fact that the NMuMg ZIP6 knockout cells had a significantly decreased amount of intracellular zinc compared to the corresponding wild type (Figure 5.5-6). This data was consistent with all the previous results, confirming that the slower growth of the ZIP6 knockout model could be explained by the decrease of intracellular zinc which is essential for the regulation of the

cell cycle and in particular of mitosis (Beyersmann & Haase, 2001). A decrease in intracellular zinc has also demonstrated that the NMuMg ZIP6 knockout cells required upregulation of ZIP10 in order to cope with the lack of the ZIP6-ZIP10 heteromer. However, despite upregulation of ZIP10, this cell line was not able to return its zinc level to normal conditions, highlighting the important role of ZIP6 as one of the main zinc importers on the plasma membrane (Taylor *et al.*, 2003). Upregulation of ZIP10 raised the question of whether ZIP10 could act as a homodimer in the ZIP6 knockout cell model or utilise another ZIP transporter such as ZIP5 to form a heteromer to transport zinc inside the cells. Furthermore, the discovery of decreased intracellular zinc in the ZIP6 knockout model and the consequent ZIP10 upregulation supported that found previously in the literature. In fact, it was previously demonstrated in both brain and liver of zinc-deficient mice that the expression of ZIP10 was significantly increased compared to normal mice (Lichten *et al.*, 2011). In addition, ZIP10 expression was significantly decreased in conditions of zinc repletion (Lichten *et al.*, 2011), confirming that the upregulation of this zinc transporter was a mechanism adopted by cells to replenish zinc homeostasis.

5.4.5 Downregulation of ZIP10 in ZIP6 knockout cells decreases cell viability

Having discovered that the ZIP6 knockout model upregulated ZIP10 in order to counteract the lack of ZIP6, it was interesting to investigate what happened to this knockout cell line when the expression of ZIP10 was transiently silenced using ZIP10 siRNA. Analysis of the cell viability of the NMuMg ZIP6 knockout model, where ZIP10 was transiently downregulated, showed a significant decrease in cell viability (Figure 5.9-A). This was an exciting result, especially in light of both ZIP6 and ZIP10 having an essential role in the regulation of mitosis (*Taylor et al, unpublished*) and therefore, being essential for cell proliferation. This evidence would make them suitable targets for treatment of proliferative diseases. This result also supported the data shown in Chapter 4, as cell treatment with ZIP6 or ZIP10-directed antibodies was able to reduce the growth of different cancer cell lines. Cancer cells are characterised by increased cell proliferation, which according to our data is sustained by the action of these two zinc transporters. In fact, both ZIP6 and ZIP10 were previously described to be overexpressed in a variety of different cancer types (Ziliotto, Ogle & Taylor, 2018), such as invasive breast cancer or renal cell carcinoma (Mcclelland *et al.*, 1998; Perou *et al.*, 2000; Pal *et*

al., 2014). In addition to their role in cell proliferation, ZIP6 and ZIP10 have also an important role in epithelial to mesenchymal transition (Yamashita *et al.*, 2004; Hogstrand *et al.*, 2013; Taylor *et al.*, 2016; Brethour *et al.*, 2017), making them suitable target for diseases not only characterised by increased cell proliferation but also for those which acquire more invasive properties. Nevertheless, the siRNA knockdown of ZIP10 performed in this investigation was only a transient downregulation and it was shown that the ZIP6 knockout cells started to restore ZIP10 protein level shortly after the siRNA was removed (Figure 5.10). This result could also be explained by the evidence that the knockout cell line had increased pSer^{727}STAT3 which may regulate the expression of ZIP10. However, as previously discussed this result also hinted the possibility that another zinc transporter may be upregulated in this cell line in order to cope with the downregulation of ZIP6 and ZIP10 and ensure proper cell growth. Taken together this data highlighted the importance of ZIP10 in the cell growth of this ZIP6 knockout model. It would be intriguing to see how a robust downregulation of both ZIP6 and ZIP10 would affect cells. Unfortunately, this has not yet been possible as it appears that the ZIP10 knockdown is lethal. This evidence is exciting as it suggests that ZIP10 may be the main driver of cell proliferation, as it is essential for cell survival. This hypothesis would fit with the data shown in this chapter which has demonstrated that a transient ZIP10 downregulation was accompanied by a sudden increase of ZIP10 protein level, suggesting that ZIP10 expression is immediately restored as essential for the cell viability of this cell line. The discovery of ZIP10 being essential in cell survival highlights once again how targeting this molecule could be beneficial in the management of diseases characterised by increased cell proliferation.

The investigations in this chapter also revealed that ZIP6 and ZIP10 are interdependent, as downregulation of ZIP6 leads to upregulation of ZIP10. This confirmed what was shown in a recent paper wherein analysis of the ZIP6 interactome revealed ZIP10 being the main interactor of ZIP6 (Brethour *et al.*, 2017). Moreover, the decrease of intracellular zinc discovered in the ZIP6 knockout model suggested that the heteromer may be a prerequisite for zinc transport. More information on the crystal structures of ZIP6 and ZIP10 would help us decipher this mechanism and understand the importance of this dimeric structure in the regulation of their function. The discovery of

the first crystal structure of a member of the ZIP family (Zhang, Sui & Hu, 2016) has brought an exciting insight to an area of zinc biology that now needs to be expanded.

The discovery of the importance of ZIP6 in the regulation of mitosis and potentially the S phase of the cell cycle has provided a fruitful area for future research in this field. Knowing that downregulation of ZIP6 affected cell growth makes both ZIP6 and ZIP10 important targets for therapy in the treatment of proliferative diseases such as cancer. These results taken together with those demonstrated in Chapter 4 can be used to expand the use of a targeted ZIP6 antibody in immunotherapy, that now needs to move towards animal work before it can be tested in the clinic.

5.5 Chapter summary

This chapter expanded the previous finding that ZIP6 and ZIP10 are important in regulating cell division, as they are required to provide the zinc influx to trigger mitosis (*Taylor et al, unpublished*). The examination of a ZIP6 knockout cell model revealed that when ZIP6 was downregulated in cells, cells adapted to this condition by upregulating ZIP10, confirming the interdependency of these two zinc transporters. The downregulation of ZIP6 affected not only the growth of these cells, but also dramatically reduced the level of intracellular zinc. It was argued that the presence of the ZIP6-ZIP10 heteromer on the plasma membrane was an essential requirement for zinc transport and raised the question of whether ZIP10 forms a homodimer in order to counteract the lack of ZIP6 or form a heteromer with another ZIP transporter. Zinc is essential in the regulation of the cell cycle and these findings highlight the particular importance of ZIP6 in controlling this mechanism. Taken together this chapter confirmed once again the potential role of ZIP6 and ZIP10 as novel targets for the treatment of cancer and other proliferative diseases.

6 INVESTIGATION OF POST-TRANSLATIONAL MODIFICATION OF ZIP6

6.1 Introduction

It is only recently that information regarding the ZIP family of zinc transporters has emerged. Each ZIP transporter plays a different role in zinc homeostasis in the human body and they are all assumed to be regulated by different mechanisms (reviewed by Kambe et al. 2015). However, it seems that a common feature combines them all: phosphorylation. Phosphorylation is a common regulatory mechanism of a variety of signalling pathways in the human body and it is also essential in driving the cell cycle through the action of cyclin-dependant kinases (CDKs) (Dephoure *et al.*, 2008). Moreover, our group have discovered that the activation of ZIP7 requires phosphorylation by CK2 on two serine residues on the cytoplasmic loop between TM III and TM IV (Taylor *et al.*, 2012). This phosphorylation was revealed to be an essential requirement for its activation and consequently in driving the several downstream pathways activated by the ZIP7-mediated zinc release into the cytoplasm (Nimmanon *et al.*, 2017). As seen in the alignment of the ZIP family (Figure 1.4), the LIV-1 subfamily represents the biggest subgroup and the close correlation between its members indicated by the phylogenetic tree (Figure 1.3) suggests the possibility that they all may require phosphorylation in order to be activated. Whether ZIP6 and ZIP10 are regulated by the same mechanism is yet to be discovered, but in light of the crucial role of phosphorylation in mitosis (Dephoure *et al.*, 2008) and ZIP6/ZIP10 in the regulation of the cell cycle (*Taylor et al, unpublished*), this is an area of study that may help us decipher how ZIP6 and ZIP10 are regulated and trigger mitosis.

ZIP6 protein is also regulated by proteolytic cleavage. ZIP6 was discovered to be expressed as a pro-protein in the endoplasmic reticulum where it was seen to undergo a proteolytic cleavage before its relocation to the plasma membrane for its role as a zinc importer (Hogstrand *et al.*, 2013). It was also discovered that ZIP6 was cleaved on its N-terminal domain also at an early stage of mitosis, highlighting the importance of cleavage as a potential on/off switch for the regulation of mitosis (Nimmanon, 2016). Moreover, it was shown by protease array that several proteases may be involved in the ZIP6 cleavage. In particular, it was demonstrated that the best candidate protease in the cleavage of ZIP6 during mitosis was presenilin (Nimmanon, 2016), a protease which has a widely known role in neurodegenerative diseases, such as Alzheimer's disease (Micchelli *et al.*, 2002). While ZIP10 was previously shown to undergo a proteolytic

cleavage in zinc starvation conditions (Ehsani *et al.*, 2012), a potential cleavage of ZIP10 after mitosis has not been investigated yet. However, since ZIP6 and ZIP10 were found to be interdependent of each other (Brethour *et al.*, 2017), it may suggest that they both require a similar regulation which now needs to be studied.

The investigation of potential phosphorylation and the effect of using protease inhibitors in the study of ZIP6 proteolytic cleavage would be beneficial in helping us dissect how these zinc transporters are activated and regulated, but also to decipher the mechanism by which ZIP6 and ZIP10 trigger mitosis.

6.1.1 Aims and objectives

Considering the importance of phosphorylation and proteolytic cleavage in the regulation of the members of the LIV-1 subfamily of ZIP transporter, the aim of this chapter was to investigate potential phosphorylation sites and proteolytic cleavages of ZIP6. Therefore, the objectives of the following chapter were:

1. To use several online database to investigate potential phosphorylation sites and potential cleavage of ZIP6;
2. To use specific ZIP6 mutants to study potential phosphorylation sites of ZIP6 by combining different techniques;
3. To investigate the potential of presenilin being involved with the cleavage of ZIP6 by assessing the effect of a presenilin inhibitor on ZIP6 cleavage.

6.2 Materials and methods

The prediction of potential phosphorylation sites and proteolytic cleavages of ZIP6 and ZIP10 used several website tools as shown in Table 6.1.

Potential phosphorylation sites were investigated in ZIP6 using specific ZIP6 mutants that had a serine or tyrosine residue modified to an alanine in order to obtain a phospho-null mutant. Site-directed mutagenesis was performed by Mutagenex (USA) and the mutations were checked by DNA sequencing (Figure 6.1).

These mutants were transfected into NMuMg ZIP6 knockout cells to investigate potential phosphorylation sites of ZIP6. Furthermore, to better characterise the likelihood of ZIP6 phosphorylation, different kinase inhibitors were used. These consisted of a CK2 inhibitor called CX-4945 (10 μM) and a Src inhibitor called AZD0530

(1 μM) that were used to treat transfected cells for 1 hour prior to harvesting. Several molecular biology techniques were used to analyse these ZIP6 mutants such as western blot, immunofluorescence and immunoprecipitation (see details in Chapter 2). The potential of a specific kinase to phosphorylate ZIP6 was analysed by proximity ligation assay (see section 2.12).

The study of the potential of presenilin to be involved with the cleavage of ZIP6 was performed by treating cells with a presenilin inhibitor called DAPT at 10 μM for 20 hours and this was investigated only by western blot. For more details about the methods refer to Chapter 2.

Phosphorylation data	**Reference**
PHOSIDA (Max Planck Institute of Biochemistry)	(Gnad, Gunawardena & Mann, 2011)
PhosphoNET (Kinexus Bioinformatics Corporation)	-
NetPhorest 2.1 (University of Copenhagen)	(Horn *et al.*, 2014)
PhosphoSitePlus® (PSP)	(Hornbeck *et al.*, 2015)
NetPhos 3.1	(Blom *et al.*, 2004)
ELM	(Dinkel *et al.*, 2016)
Proteolytic cleavage	**Reference**
epestfind (EMBOSS explorer)	(Rogers, Wells & Rechsteiner, 1986)
ELM	(Dinkel *et al.*, 2016)

Table 6.1 ***Online databases used for the phosphorylation and proteolytic cleavage investigation.***
These databases were available from:
-PHOSIDA: http://141.61.102.18/phosida/index.aspx
-PhosphoNET: http://www.phosphonet.ca/
-NetPhorest 2.1: http://www.netphorest.info/
-PhosphoSitePlus®: https://www.phosphosite.org/homeAction.action
-NetPhos 3.1: http://www.cbs.dtu.dk/services/NetPhos/
-epestfind: http://emboss.bioinformatics.nl/cgi-bin/emboss/epestfind
-ELM: http://elm.eu.org/

A.

Construct	Wild-type DNA sequence	Mutant DNA sequence
ZIP6 S471A	CAGTTGTCCAAGTAT	CAGTTGgCCAAGTAT
ZIP6 S478A	CAACTTTCAACAAAT	CAACTTgCAACAAAT
ZIP6 Y528A	GAAGTCTACAATGAA	GAAGTCgcCAATGAA
ZIP6 Y531A	AATGAATATGTACCC	AATGAAgcTGTACCC
ZIP6 Y528A/Y531A	GTCTACAATGAATAT	GTCgcCAATGAAgcT

B.

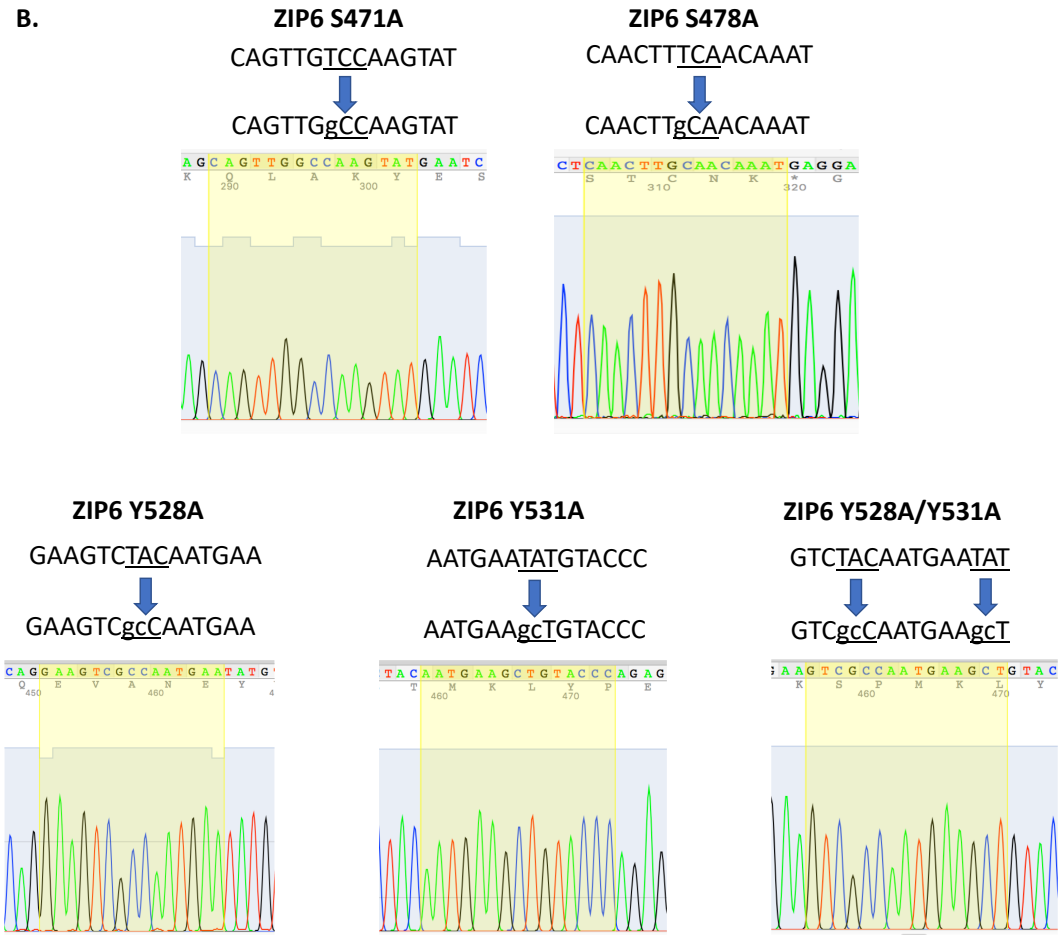

Figure 6.1 ***DNA sequencing of ZIP6 mutants.***
A. The table shows the DNA sequences of the ZIP6 mutants that were used in the following investigations and that were created by site-directed mutagenesis.
B. The schematic shows that the individual serine (codon TCC, TCA) or tyrosine (codon TAT, TAC) at the potential phosphorylation site were correctly substituted for an alanine (codon GCC, GCT, GCA).

6.3 Results

6.3.1 Investigation of ZIP6 phosphorylation

6.3.1.1 Prediction of potential phosphorylation sites

The analysis of predicted phosphorylation sites for ZIP6 revealed that the region with the highest probability of phosphorylation was the long cytoplasmic loop between TM III and TM IV (Figure 6.2) as seen for ZIP7. In order to narrow the number of predicted sites down to a realistic number, only sites with more than one prediction from mass spectrometry data were included (Figure 6.2). This investigation was focused on serine and tyrosine phosphorylation. While phosphorylation on serine residues accounts for over 80% of proteins (Nishi, Hashimoto & Panchenko, 2011) and it was demonstrated essential for the activation of ZIP7 (Taylor *et al.*, 2012), tyrosine phosphorylation was studied in light of the role of zinc in the inhibition of tyrosine phosphatases (Haase & Maret, 2003).

This approach led to the selection of four sites on the long cytoplasmic loop for ZIP6 having a high prediction score from data from whole genome phosphoscreen mass spectrometry and highest number of reference according to PhosphoSitePlus® (Hornbeck *et al.*, 2015). These sites corresponded to serine S471 and S478 and tyrosine Y528 and Y531 (Figure 6.2, highlighted in bold). In order to study these four potential phosphorylation sites of ZIP6, ZIP6 mutants of these residues were used for investigations and transfected into cells in order to overexpress ZIP6 and compare them to wild type (Figure 6.1). Interestingly, the analysis of the potential kinases involved in the phosphorylation of these residues revealed that the serine residue 478 was predicted to be phosphorylated by CK2, the same kinase responsible for the activation of ZIP7 (Figure 6.2) (Taylor *et al.*, 2012). The serine residue 471 was predicted to be phosphorylated by either the PAK or GSK3β kinases (Figure 6.2). Conversely, both the two tyrosine residues Y528 and Y531 were predicted to be phosphorylated by the Src group of kinases (Figure 6.2). This was an exciting result, as tyrosine phosphorylation has never been demonstrated in the ZIP family of zinc transporters before. Interestingly, all these kinases share a similar role in the regulation of the cell cycle, and in particular are involved in mitosis, which will be discussed in more detail later in this chapter. The most striking result discovered from the phosphorylation prediction analysis was the

possibility of kinase CK2 phosphorylating ZIP6 at residue S478. Therefore, the following analysis started from the investigation of this kinase.

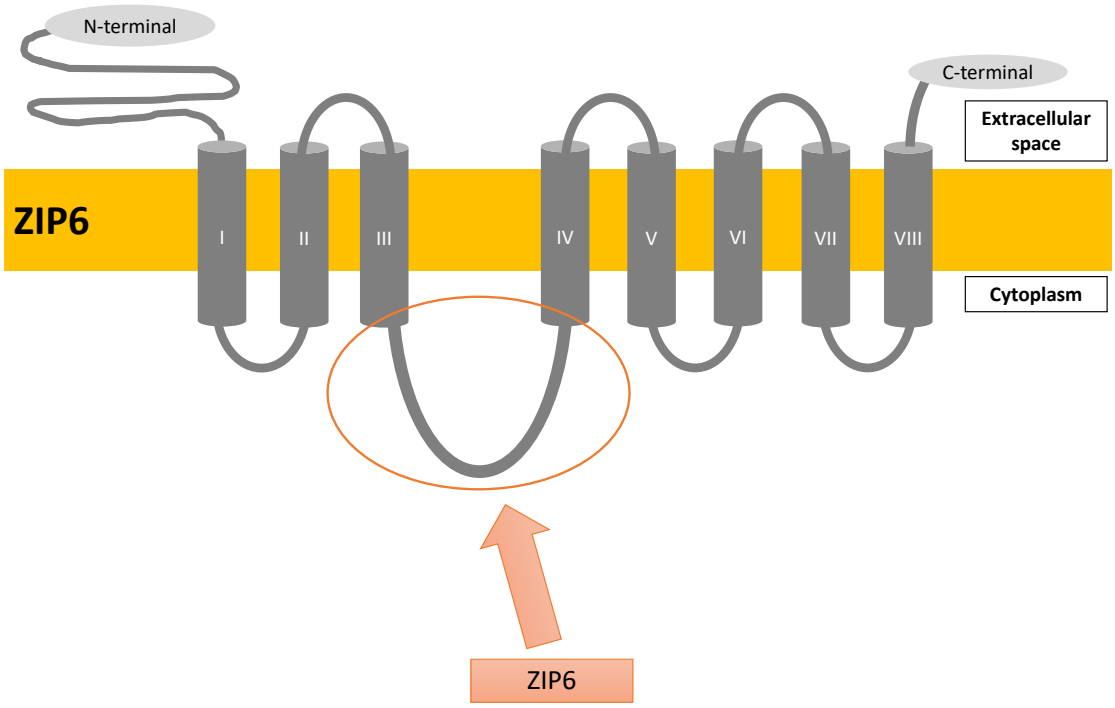

Residue	Predicted kinase
ZIP6 S471	**PAK or GSK3β group**
ZIP6 S475	ATM/ATR group
ZIP6 S478	**CK2**
ZIP6 Y493	MAP2K
ZIP6 Y528	**Src group**
ZIP6 Y531	**Src group**
ZIP6 S583	PKA

Figure 6.2 ***Predicted phosphorylation sites for ZIP6 in the cytoplasmic loop between TM III and TM IV.*** *The sequence of ZIP6 was retrieved on the NCBI database in FASTA format. The analysis was performed using several phosphorylation site databases such as Phosphonet (Kinexus Bioinformatics Corporation), NetPhorest 2.1 (University of Copenhagen) and PhosphoSitePlus® (PSP) (see methods section for reference). ZIP6 was predicted to have several potential phosphorylation sites, but in particular the ones highlighted in bold were the ones which had the highest scores of predictions according to mass spectrometry data, hence more likely to be real. The kinase predicted to be responsible for the phosphorylation on each site is indicated on the table.*

6.3.1.2 Investigating the potential of CK2 binding to ZIP6

The best method to assess whether CK2 was bound to ZIP6 was assessed to be proximity ligation assay. This technique allows detection of binding of two proteins up to 40 nm apart from one other and could therefore give us information about proteins which may be bound to each other. Moreover, as ZIP6 was discovered to be involved in the regulation of mitosis (*Taylor et al, unpublished*), it was interesting to analyse whether the two proteins bound to each other during mitosis.

Figure 6.3 confirmed that CK2 was binding ZIP6 as hypothesised, showing an average of 6 signals per cell ($p<0.05$), which was double the number of the negative control of CK2 or ZIP6 alone which only gave an average of 3 signals per cell (Figure 6.3-B). A more in-depth analysis revealed that CK2 bound ZIP6, particularly in mitotic cells (Figure 6.3-C). In fact, while non-mitotic cells showed an average of 2 signals per cell, the binding of CK2 to ZIP6 in mitotic cells revealed an average of 6 signals per cell ($p<0.01$). This result was also confirmed by another student working in our lab under my supervision. This was an exciting result, especially in light of the important role of ZIP6 during mitosis, which also corroborated the possibility of CK2 being responsible for the phosphorylation of ZIP6. As seen for ZIP7 in the past where CK2 phosphorylation was found to be essential for the activation of this zinc transporter (Taylor *et al.*, 2012), this result could suggest that CK2 was involved in the on/off switch mechanism of ZIP6 during mitosis which is not known yet.

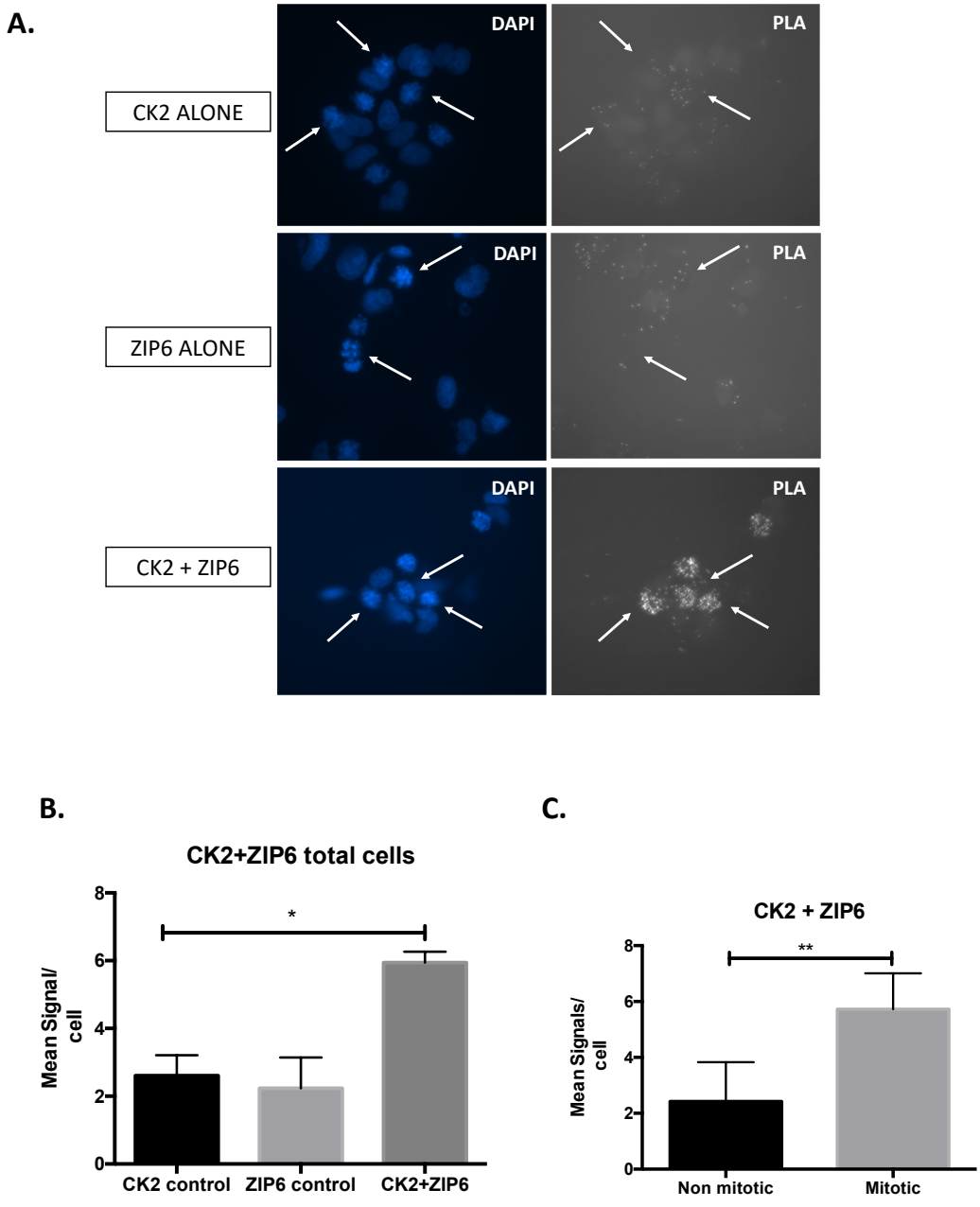

Figure 6.3 ***CK2 binds ZIP6 during mitosis.***
A. MCF-7 cells were seeded in an 8-well chamber slide and treated at 70% confluence with 150 nM nocodazole for 20 hours. Cells were then fixed and probed for proximity ligation assay using anti-CK2 antibody ± anti-ZIP6 antibody, comparing to controls using either of the antibodies alone. Mitotic cells are indicated by white arrows.
*B-C. Quantitative measurements were performed on at least 6 pictures of 25 stacks taken 0.3 μm apart. The graph shows the count of dots for both control and the antibodies together and a more in depth analysis of cells during mitosis. The experiment was performed on three biological replicates (n=3) and statistical significance is shown as * ($p<0.05$), or ** ($p<0.01$).*

6.3.1.3 Analysis of ZIP6 phosphorylation by transfection of ZIP6 mutant in ko cells model

In order to investigate phosphorylation of ZIP6, the ZIP6 knockout cell line was used with ZIP6 wild type or ZIP6 mutants transfected back. The ZIP6 mutants were all potentially phospho-null mutants, having had the relevant residue mutated to an alanine (Figure 6.1). This strategy would allow a more accurate investigation of potential ZIP6 phosphorylation sites, as previous transfection of these mutants in MCF-7 gave results of the endogenous ZIP6 as well as recombinant ZIP6. On the contrary, transfection of ZIP6 mutants in the ZIP6 knockout cell line only provided results of recombinant ZIP6, since no endogenous ZIP6 was present.

As the ZIP6 mutant sequences available in our group corresponded to the ZIP6 human sequence, the first analysis aimed to assess whether a transfection of human ZIP6 into mouse cells was possible. There was already precedence for human ZIPs having the ability to replace mouse sequences (Liuzzi & Cousins, 2004). Moreover, as shown in the alignment in Figure 6.4, the mouse sequence of ZIP6 was confirmed to be very similar to the human sequence, with the sites chosen for the phosphorylation analysis being conserved also in the mouse species. Conservation of residues suggests an importance to ZIP6 function.

Results shown in Figure 6.5 confirmed that the transfection of human recombinant ZIP6 into ZIP6 knockout cells was successful. This was detected by presence of V5 staining both in immunofluorescence and western blotting (Figure 6.5-B-C). The V5 tag was inserted in the recombinant DNA sequence to allow distinction from the endogenous protein (Figure 6.5-A). Western blotting analysis showed that the non-targeting sample (lipid only) compared to ZIP6 wild type transfected in NMuMg ZIP6 knockout cells showed no V5 band as no recombinant ZIP6 was present in that sample in comparison to those transfected with the ZIP6 wild type (Figure 6.5-B). This result confirmed the suitability of the use of our ZIP6 recombinant mutants in the ZIP6 knockout cells and allowed the perpetuation of the next investigation. Similarly, immunofluorescence analysis showed the presence of recombinant ZIP6 wild type in NMuMg ZIP6 knockout cells as indicated by the presence of V5 staining (Figure 6.5-C).

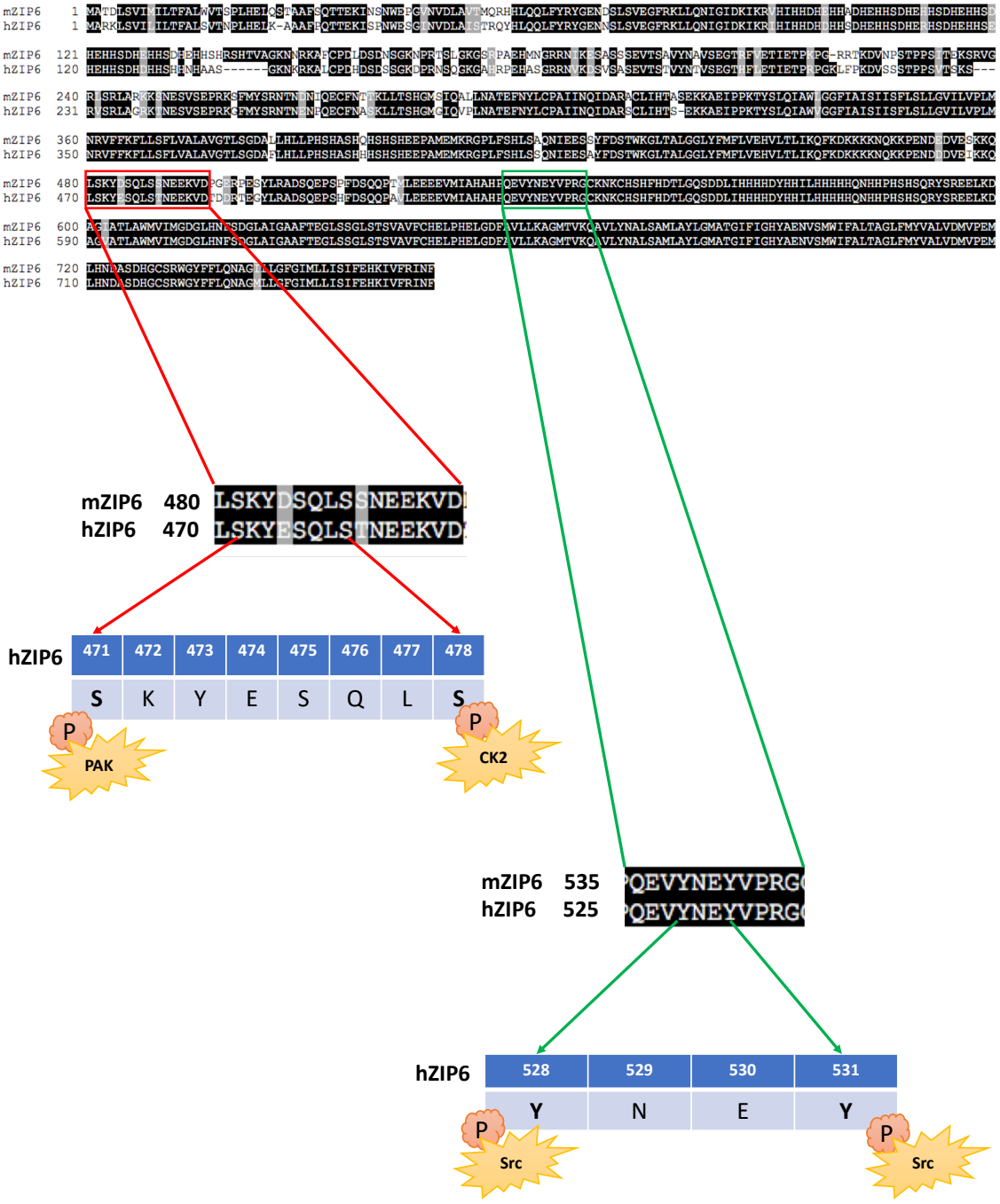

Figure 6.4 ***Mouse ZIP6 vs human ZIP6 alignment.***
The mouse (mZIP6) and human (hZIP6) sequence of ZIP6 were retrieved on NCBI database with FASTA format and aligned using the ClustalW alignment tool (Larkin *et al.*, 2007). *The aligned sequences were shaded using the Boxshade program (Swiss Institute of Bioinformatics). The black and grey colours represent at least 70% identical or complementary residues, respectively. The ZIP6 human residues S471, S478, Y528 and Y531 were highlighted to show they are conserved between the human and mouse species. These were chosen as they had the highest number of references from mass spectrometry data. The kinase predicted to be involved in their phosphorylation is also shown.*

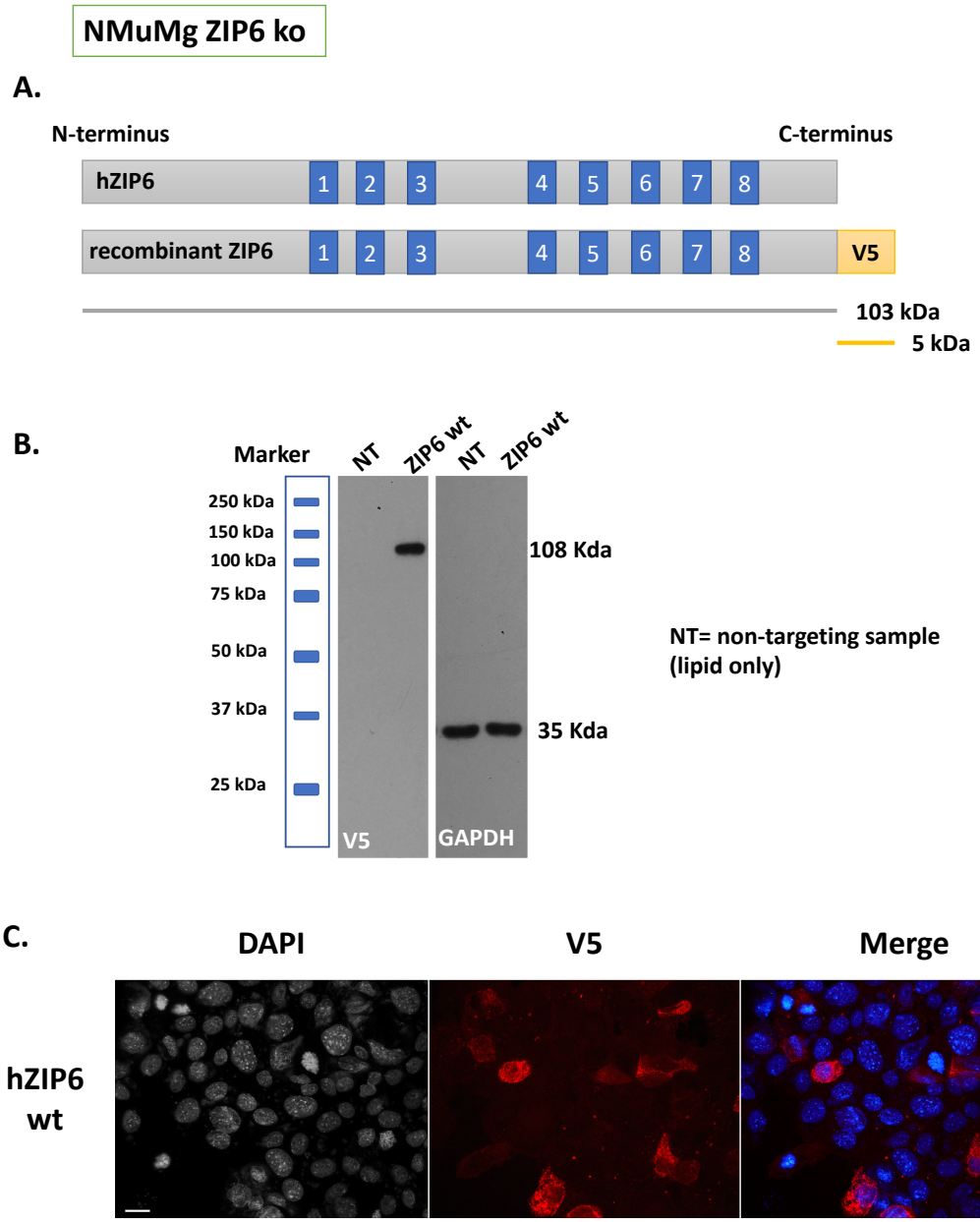

Figure 6.5 ***Recombinant human ZIP6 can be successfully transfected in NMuMg ZIP6 ko cells.***
A. Schematic showing that the V5 tag is inserted at the C-terminus of the recombinant ZIP6 DNA sequence. The V5 tag corresponds to a molecular weight of 5 kDa. Full length ZIP6 corresponds to 103 kDa.
B. NMuMg ZIP6 ko cells were transfected at 70% confluence with recombinant hZIP6 wild type together with non-targeting control (lipid only). Samples for western blotting were prepared and analysed by probing for V5 and GAPDH. The V5 band is only present in the recombinant sample but not in the non-targeting control.
C. NMuMg ZIP6 ko cells were transfected at 70% confluence with recombinant hZIP6 wild type. Cells were probed for V5 (red) and the nuclei counterstained with DAPI (blue). The pictures were taken on a Leica 63x oil immersion Leica DMIRE2 microscope and each picture is representative of one field of view of n=6. Scale bar: 10 μm.

6.3.1.4 Investigating the phosphorylation of ZIP6 on serine residue 478

Having confirmed the suitability of transfecting human recombinant ZIP6 into the mouse ZIP6 knockout cells, the investigation of potential phosphorylation sites was carried out by confirming whether the ZIP6 serine residue 478 was phosphorylated. In order to do so, a preliminary experiment was performed by immunoprecipitation. The ZIP6 S478A mutant (Figure 6.1) was used in comparison to ZIP6 wild type in order to assess the serine phosphorylation on that residue. These mutants were transfected into NMuMg ZIP6 knockout cells in the presence of nocodazole and then the lysates harvested and immunoprecipated with V5. The cells were treated with nocodazole as the previous result revealed that CK2 bound ZIP6 in particular in mitosis (Figure 6.3) and previous investigations confirmed that nocodazole did not affect the transfection. Moreover, ZIP6 was known to be overexpressed in mitosis (*Taylor et al, unpublished*). Similarly to ZIP6 wild type, the S478A mutant also had a V5 tag inserted at the C-terminus of the recombinant DNA sequence (Figure 6.6-A). The immunoprecipated samples were probed for phosphoserine, but also for V5 in order to check whether the samples had been successfully immunoprecipitated.

Figure 6.6 shows that the wild type and ZIP6 S478A mutant were successfully transfected in the NMuMg ZIP6 knockout cells, as shown by the several bands found for the membrane probed for V5 (Figure 6.6-B). In particular, the blot probed for V5 showed a band at 108 kDa and one at 73 kDa which corresponded to the usual 103 and 68 kDa bands which are normally found for ZIP6 (Hogstrand *et al.*, 2013) (Figure 6.6-A). The extra 5 kDa is due to the V5 tag which is embedded in the recombinant protein sequence (Elomaa *et al.*, 2001) (Figure 6.6-A). Unfortunately, the 73 kDa band of the membrane probed for V5 could not be seen properly in the blot as it was covered by the strong signal of the heavy chain of the antibody which is typical of immunoprecipitation. This did not allow proper assessment of the protein and therefore densitometric analysis of this band was not possible. Nevertheless, it was worth noticing that the band for phosphoserine at 73 kDa looked decreased in the ZIP6 S478A mutant, suggesting the potential for this residue to be phosphorylated (Figure 6.6-B). Moreover, further bands for V5 at 35 and 42 kDa were found, which have not been investigated before. However, it was previously demonstrated that ZIP6 undergoes a proteolytic cleavage before its relocation to the plasma membrane (Hogstrand *et al.*, 2013), and it was also found that

ZIP6 has other potential predicted proteolytic cleavages which will be discussed later in this chapter. Since V5 is embedded in the DNA sequence after the C-terminal domain (Figure 6.6-A), the presence of these lower V5 bands on the blot might be indicative of a proteolytic cleavage which comprises the last few transmembrane domains of ZIP6, including the C-terminal domain with the V5 tag.

Furthermore, it was important to notice that the V5 band at 35 kDa was at the same size as the band seen for the blot probed with phosphoserine (Figure 6.6-B). Densitometric analysis of this band revealed a slight decrease of phosphoserine level in the ZIP6 mutant when compared to the wild type, albeit not significant (Figure 6.6-C). Since the 35 kDa band may be indicative of a proteolytic cleavage of ZIP6, it was not known whether this cleavage includes the residue S478, which occurs in the long cytoplasmic loop between TM III and TM IV. Therefore, this result did not rule out the possibility of ZIP6 being phosphorylated at residue S478. Moreover, the evidence that a band for phosphoserine was also displayed for the mutant suggested that ZIP6 may be phosphorylated on multiple sites, as predicted in Figure 6.1. For this reason, residue S471 was also tested in the next investigation, even though it was discovered to have a lower number of prediction from mass spectrometry analysis according to data from PhosphoSitePlus® (Hornbeck *et al.*, 2015).

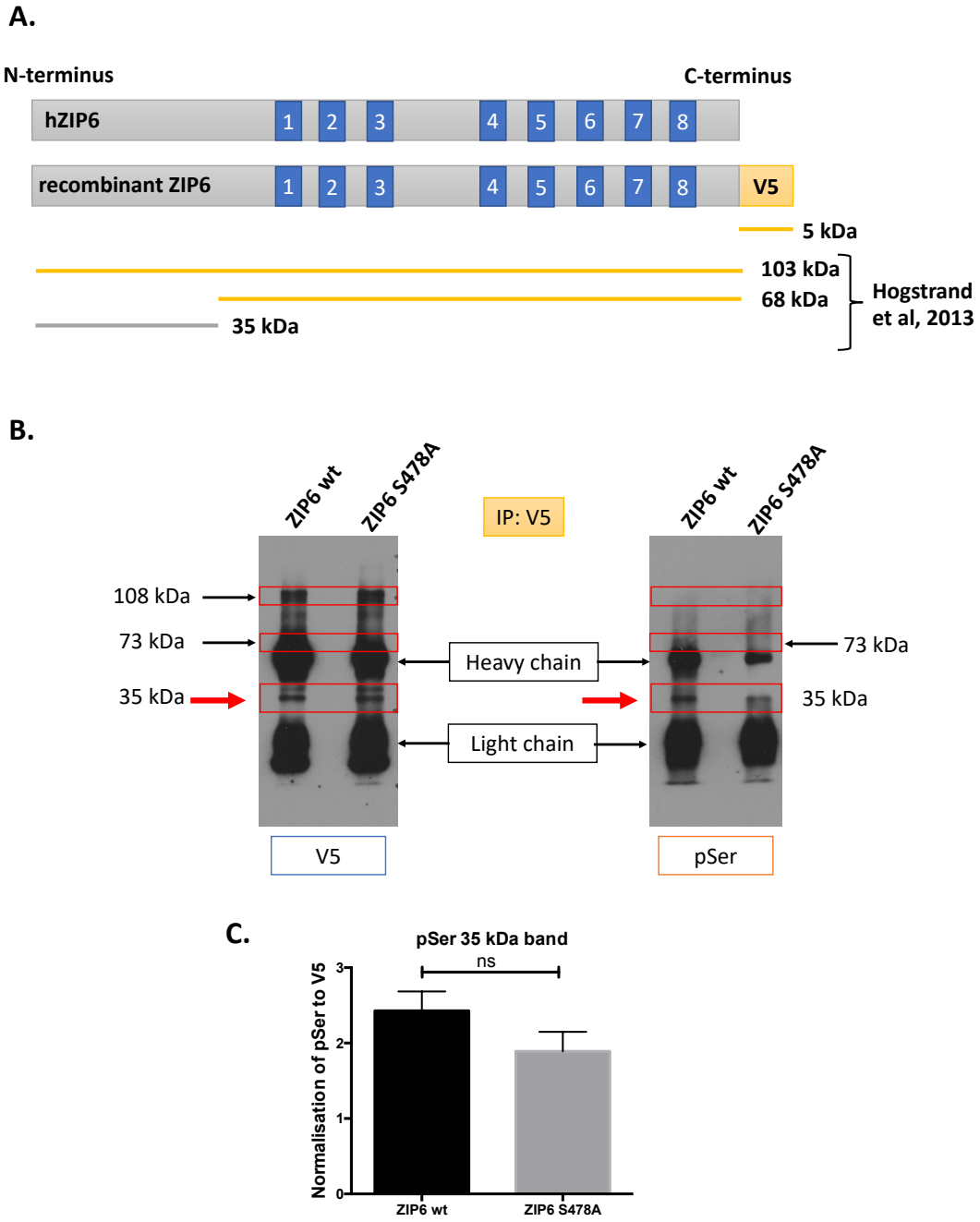

Figure 6.6 ***ZIP6 may undergo several proteolytic cleavages and be phosphorylated on multiple serine residues.***

A. Schematic showing the bands originated by ZIP6 proteolytic cleavage with their correspondent molecular weight (Hogstrand *et al.*, 2013)*. The V5 antibody can only bind to the 103 and 68 kDa bands.*

B. NMuMg ZIP6 ko cells were transfected with recombinant ZIP6 wild type and ZIP6 S478 in the presence of nocodazole for 18 hours. Samples were harvested and immunoprecipated with anti-V5 antibody. Immunoblotting was performed probing for V5 and phosphoserine.

C. Quantitative analysis for the 35 kDa was performed by normalisation of phosphoserine to V5 and it is shown as a bar graph of n=3 ± SEM (standard error of the mean). Statistical analysis was performed but did not reveal any significance.

6.3.1.5 Investigation of serine ZIP6 phosphorylation by using a CK2 kinase inhibitor

Data has so far demonstrated that ZIP6 was bound to CK2, and therefore that CK2 could be involved in the phosphorylation of ZIP6. Another strategy to investigate the potential of residue S478 to be phosphorylated by CK2 was to use a CK2 inhibitor called CX-4945 (Siddiqui-Jain *et al.*, 2010). Cells that were transfected with ZIP6 wild type and ZIP6 mutants were treated with this CK2 inhibitor in order to assess any effect on serine phosphorylation. Since previous results with immunoprecipitation suggested the possibility of ZIP6 being phosphorylated on multiple sites (Figure 6.6), as supported by analysis of potential phosphorylation sites (Figure 6.1), the following investigation also included the residue S471A. Since the ZIP6 S471A mutant bore no mutation at S478, the comparison of these mutants could be useful to assess the potential of ZIP6 to be phosphorylated on S478 or on multiple sites. NMuMg ZIP6 knockout cells were transfected with ZIP6 wild type, the S471A and S478A mutants in the presence of nocodazole, considering that CK2 binds ZIP6 in mitosis (Figure 6.3).

The overall aim of this experiment was to assess the effect of the CK2 inhibitor on the phosphorylation of ZIP6 and to compare this between the different ZIP6 mutants. As shown in Figure 6.7, the blot revealed a unique V5 band at around 108 kDa, which fit with the full size of ZIP6 at 103 kDa (see Figure 6.5-A). The phosphoserine blot showed several bands, which were typical of this antibody. The phosphoserine antibody could recognise all the proteins that were phosphorylated on serine residues, and it was not as specific as the V5 antibody which only recognised the recombinant proteins (Figure 6.7-A). As the aim of this experiment was to look at ZIP6 phosphorylation, only the band which colocalised with V5 was analysed, as this was corresponding to recombinant ZIP6. Analysis of serine phosphorylation on recombinant ZIP6 did not reveal any significance across the different samples (Figure 6.7 A-B). Moreover, the use of the CK2 inhibitor did not affect the serine phosphorylation of neither the wild type form of ZIP6, nor the ZIP6 mutants. This result implied that ZIP6 may be phosphorylated on multiple serine residues. Additionally, while it was possible to confirm the binding of ZIP6 with CK2 with proximity ligation assay (Figure 6.3), this experiment did not rule out the possibility of ZIP6 being phosphorylated by other kinases.

However, it was interesting to notice in Figure 6.7-A a strong phosphoserine band at 68 kDa. Since no V5 band was detected at this molecular size, this could not be corresponding to recombinant ZIP6, but it represented serine phosphorylation of endogenous proteins. As seen in Chapter 5, the ZIP6 knockout cells upregulated ZIP10 and that 68 kDa band could correspond to endogenous ZIP10. Although densitometric analysis of the serine phosphorylation of these endogenous proteins did not reveal any significant difference across the samples (Figure 6.7-C), it did show a slight decrease in the CK2 treated samples. If that 68 kDa band corresponded to endogenous ZIP10, it would imply that the use of the CK2 inhibitor may have had an effect in the overall phosphorylation of ZIP10 (Figure 6.7-C).

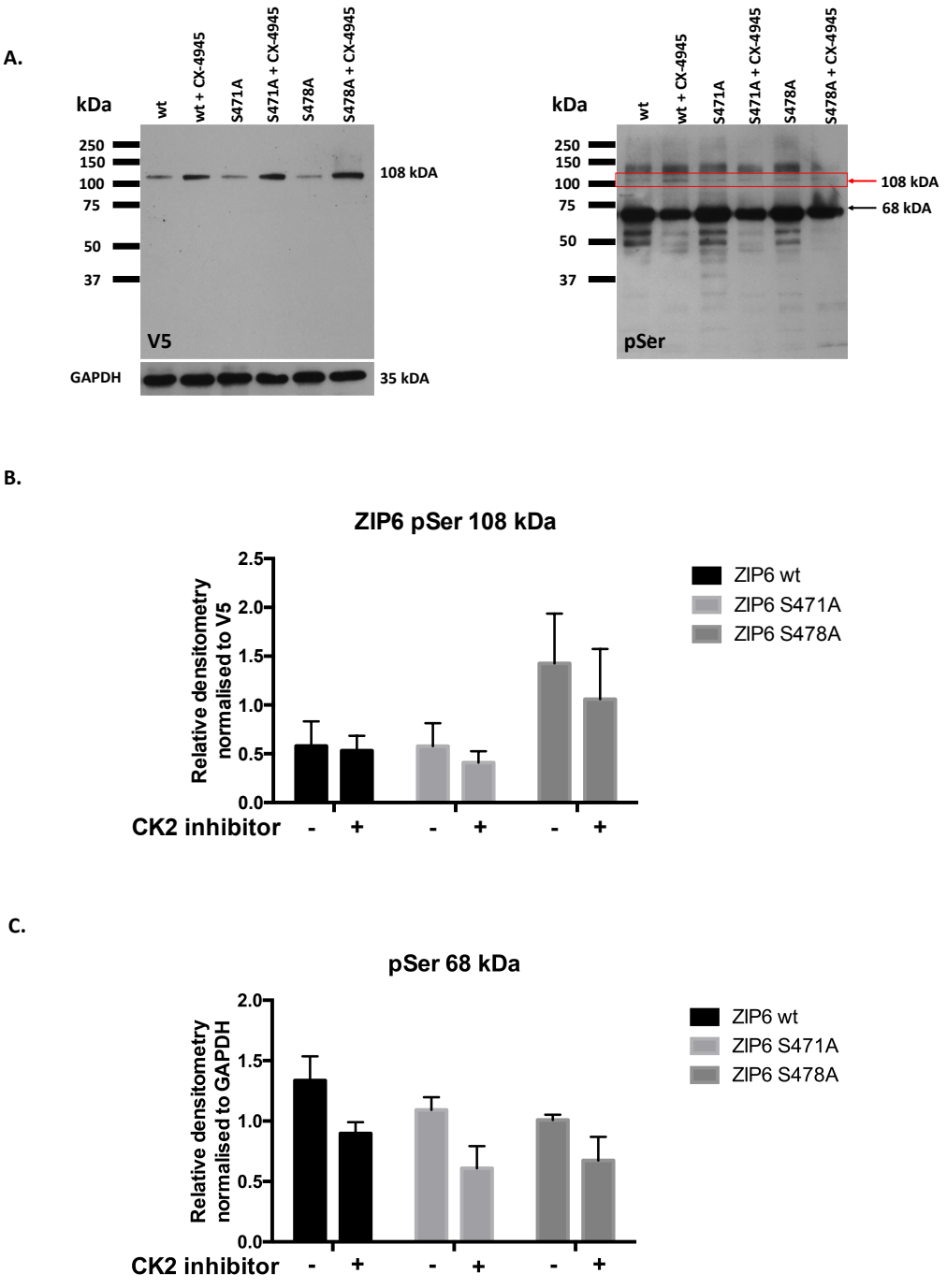

Figure 6.7 ***ZIP6 could be phosphorylated on multiple serine residues.***
A. NMuMg ZIP6 ko cells were transfected with ZIP6 wild type and ZIP6 serine mutants in the presence of 150 nM nocodazole. Samples were treated with 10 μM CK2 inhibitor (CX-4945) an hour before harvesting. B-C. Samples were probed for V5 and phosphoserine. The experiment was performed on three biological replicates. The densitometric analysis was carried out by normalisation of the densitometry of phosphoserine to V5 for the 108 kDa band or GAPDH for the 68 kDa band and is shown as a graph of n=3 ±SEM (standard error of mean). Statistical analysis was performed but did not reveal any significance.

6.3.1.6 Investigation of ZIP6 tyrosine phosphorylation by using a Src kinase inhibitor

The investigation of tyrosine phosphorylation in ZIP transporters was unprecedented, but it was promising in light of the important role of zinc on tyrosine kinase signalling (Fukada *et al.*, 2011). Previous studies demonstrated how zinc is involved in the activation of several tyrosine kinases pathways mediated by the ability of zinc to inhibit tyrosine phosphatases (Haase & Maret, 2003). Whether this has any implication with the activation of ZIP6 is yet to be defined. In a previous paper it was found that the zinc transporter ZIP7 was a crucial hub for the release of zinc to the cytoplasm and its consequent tyrosine phosphatase inhibition (Hogstrand *et al.*, 2009). It would be intriguing to investigate whether this ZIP7-mediated zinc release had any association with the tyrosine phosphorylation of ZIP6. According to data from PhosphoSitePlus® (Hornbeck *et al.*, 2015) the tyrosine residues which displayed the highest number of reference from mass spectrometry data were Y528 and Y531. These two tyrosine residues were predicted to be phosphorylated by the Src family of kinases. Src was identified as a kinase with implications as an oncogene in cell adhesion and cell migration (Parsons & Parsons, 2004). In addition to its role in migration, gene transcription and immune response, this kinase was also discovered to have a role in the regulation of the cell cycle. It is for this reason that the investigation of tyrosine phosphorylation was performed by using a Src inhibitor called AZD0530 (Sarcatinib), which was used on NMuMg ZIP6 knockout cells transfected with ZIP6 wild type and ZIP6 Y528A and Y531A mutants. This time a further mutant was used which bore a double mutation. Since the residue Y528 is in close proximity to the residue Y531, our group had a phospho-null mutant made for both residues (Y528A/Y531A) (Figure 6.1).

Results in Figure 6.8-A revealed a unique band at 108 kDa for V5, corresponding to the full length of ZIP6 (103 kDa) plus the 5 kDa size of the V5 tag. Similar to what was seen in Figure 6.7 for the phosphoserine antibody, the phosphotyrosine antibody could recognise all of the proteins which were phosphorylated on tyrosine residues, and therefore the blot showed many bands at different molecular sizes (Figure 6.8-A). However, only the band at the same size of V5 was considered for this investigation, as corresponding to recombinant ZIP6. The phosphotyrosine investigation did not reveal any significant difference between the ZIP6 wild type and the different mutants (Figure 6.8-B). Nevertheless, it was worth noticing that the sample bearing the double tyrosine

mutation and treated with the Src inhibitor showed a slight decrease of tyrosine phosphorylation in comparison to the wild type ZIP6, hinting a potential role for Src in the phosphorylation of ZIP6 in residues other than Y528 or Y531. However, this decrease was not significant. Although Src kinase was not verified to be involved with the phosphorylation of ZIP6, this result did not rule out the possibility of ZIP6 being phosphorylated by other kinases not only on Y528 and Y531 but also on different tyrosine residues.

These results altogether provided important insights into the study of ZIP6 serine and tyrosine phosphorylation. However, this was only the beginning of an investigation that now needs to be further explored by combining different techniques and kinases inhibitors. Nevertheless, it has suggested the possibility of protein kinase CK2 in the regulation of post-translation modifications of ZIP6 and potentially ZIP10.

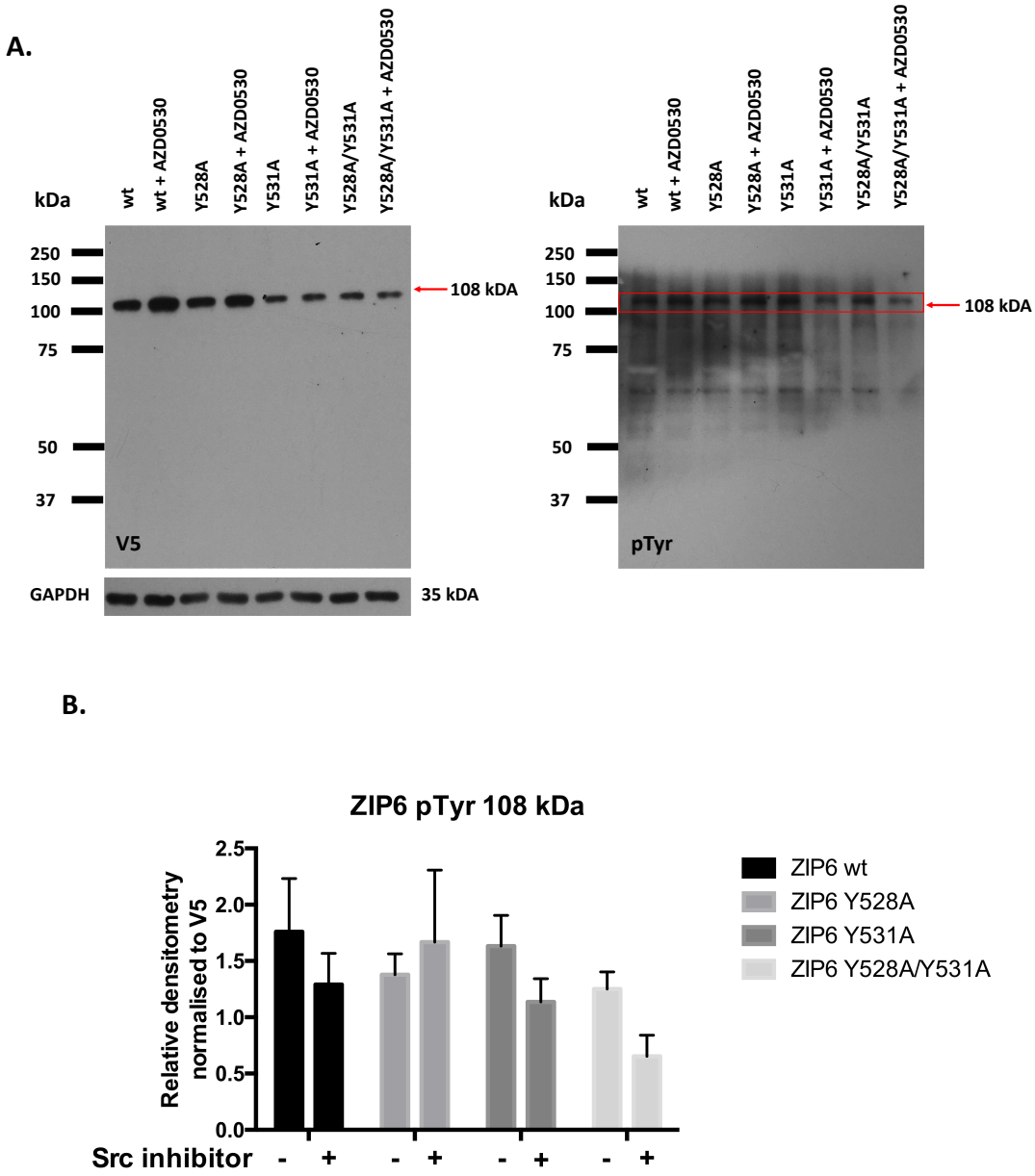

Figure 6.8 ***ZIP6 could be phosphorylated on multiple tyrosine residues.***
A. NMuMg ZIP6 ko cells were transfected with ZIP6 wild type and ZIP6 tyrosine mutants in the presence of 150 nM nocodazole. Samples were treated with 1 μM Src inhibitor (AZD0530) an hour before harvesting and probed with anti-V5 antibody and anti-phosphotyrosine antibody.
B. The experiment was performed on three biological replicates. Densitometric analysis was carried out by normalisation of the densitometry of phosphotyrosine to V5 and is shown as a bar graph of n=3 ± SEM (standard error of mean). Statistical analysis was performed but did not reveal any significance.

6.3.2 ZIP6 proteolytic cleavages and its role in ZIP6 function

6.3.2.1 Pest cleavage sites of ZIP6 and ZIP10

ZIP6 was discovered to be expressed as a pro-protein in the endoplasmic reticulum before undergoing a PEST-site proteolytic cleavage which was followed by its relocation to the plasma membrane (Hogstrand *et al.*, 2013). Once on the plasma membrane, ZIP6 can finally function as a zinc transporter and influx zinc to trigger mitosis (*Taylor et al, unpublished*).

Similar to ZIP6, ZIP10 was also predicted to have a potential PEST cleavage site on its N-terminal domain (Figure 6.9). Moreover, analysis of proteolytic cleavage of ZIP10 revealed the potential of a second PEST cleavage site on the long intracellular loop between transmembrane III and IV, which was unprecedented amongst zinc transporters (Figure 6.9). Whether this was indicative of a degradation cleavage to stop the protein function is yet to be proved. As shown in Figure 6.9, ZIP6 was also predicted to have a second proteolytic cleavage similar to ZIP10, but it did not reach the threshold for a reliable prediction and was therefore unlikely to be important. Nevertheless, it was interesting to take this into consideration, especially in light of the close correlation and similarity between ZIP6 and ZIP10. Moreover, this proteolytic intracellular loop cleavage may explain the 35 kDa band seen in Figure 6.6. A 35 kDa band for ZIP6 was normally seen as a result of the PEST cleavage site of the N-terminal domain (Hogstrand *et al.*, 2013). However, the 35 kDa band seen in Figure 6.6 could not correspond to the N-terminal cleavage, as the V5 antibody would have not been able to recognise the N-terminal cleavage since the V5 tag was inserted on the C-terminal domain of the recombinant DNA sequence. Interestingly, the analysis of post translational modifications of the ZIP6 protein structure revealed that the PEST cleavage site at the N-terminus of ZIP6 was highly conserved across different species (Figure 6.10), suggesting it was essential for ZIP6 function. Similarly, the predicted PEST cleavage site of ZIP6 on the cytoplasmic loop was also found to be conserved across different species, despite the fact that it was a poorly predicted site (Figure 6.10).

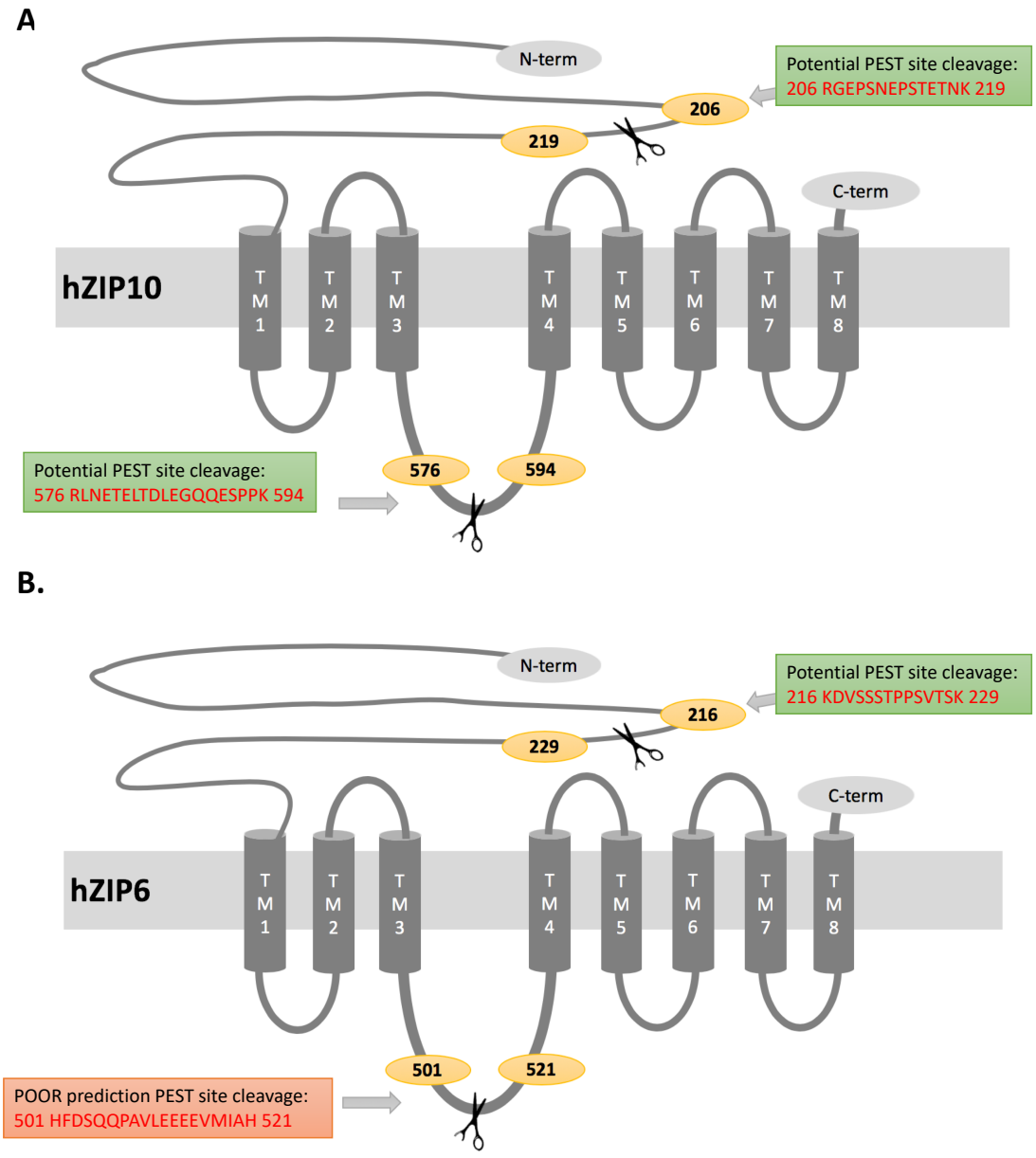

Figure 6.9 ***ZIP6 and ZIP10 are predicted to have similar PEST cleavages site****.*
The sequences of ZIP6 and ZIP10 were retrieved using the NCBI database and the potential PEST cleavage sites were predicted by using epestfind database (EMBOSS Bioinformatics) (Rogers, Wells & Rechsteiner, 1986)*. The schematics show the predicted PEST cleavage site found for ZIP6 and ZIP10 in order to compare them.*

N-terminal PEST site

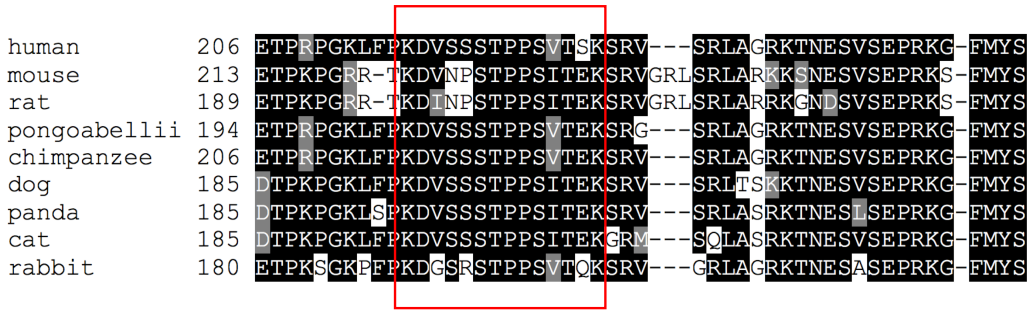

Cytoplasmic PEST site

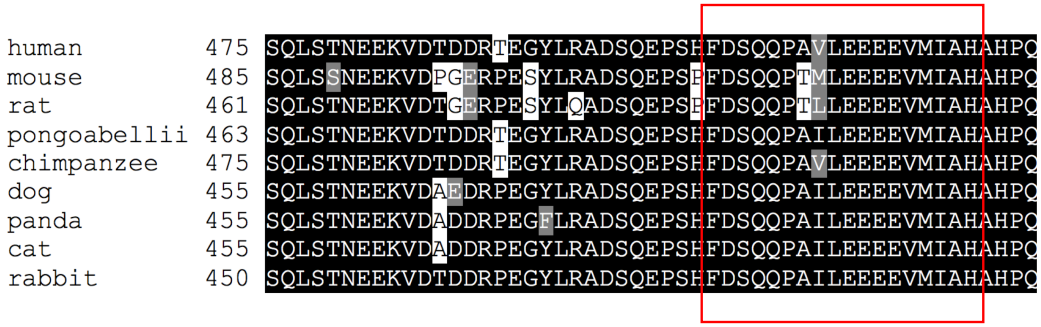

Figure 6.10. ***The PEST cleavage sites for ZIP6 transporter are conserved across different species.*** *The sequences of ZIP6 from different species were retrieved using the NCBI database and aligned using the ClustalW5 alignment tool* (Larkin *et al.*, 2007)*. The aligned sequences were then analysed and shaded using the BoxShade program (Swiss Institute of Bioinformatics). The black and grey colours show the correspondence of at least 70% identical or complementary residues, respectively.*

6.3.2.2 Investigating ZIP6 cleavage by using a presenilin inhibitor

A recent investigation in our group investigated potential proteases activated during mitosis by using protease arrays. This investigation demonstrated that the protease with the highest potential of being involved in ZIP6 cleavage was presenilin, as this protease was the one with the highest increase in samples treated with nocodazole in comparison to control (Nimmanon, 2016). For this reason, the following investigation carried on this preliminary finding by analysing the effect of a presenilin inhibitor on ZIP6 cleavage during mitosis.

The presenilin inhibitor used for this investigation is called DAPT, which is a γ-secretase inhibitor (Morohashi *et al.*, 2006). The analysis revealed two bands with western blotting for ZIP6: one at 103 kDa and one at 68 kDa (Figure 6.12-B). The 103 kDa band represented the full length of ZIP6 and agreed with the evidence that ZIP6 is expressed as a pro-protein which is cleaved before its relocation to the plasma membrane where it becomes active (Hogstrand *et al.*, 2013). The N-terminal cleavage of ZIP6 generated a smaller protein which was revealed at 68 kDa band and was indicative of active ZIP6. Figure 6.11-C showed that when cells were synchronised in mitosis with nocodazole there was a significant increase of the 68 kDa band of ZIP6 between the control and the nocodazole sample ($p<0.05$), representing the active form of ZIP6. The cleaved band of ZIP6 at 68 kDa was significantly decreased in the sample treated with the presenilin inhibitor when compared to the control ($p<0.01$) or the nocodazole sample ($p<0.01$) (Figure 6.11-C). Conversely, Figure 6.11-D showed that the 103 kDa band was significantly decreased in the nocodazole sample when compared to the control ($p<0.01$). Surprisingly, the 103 kDa band of ZIP6 was also significantly decreased in the sample treated with the presenilin inhibitor in comparison to the control ($p<0.01$). While samples treated with both nocodazole and DAPT did not show any significant difference in the 103 kDa band (Figure 6.11-D), this double treatment affected the 68 kDa band of cleaved ZIP6 which was significantly decreased in comparison to the nocodazole sample ($p<0.05$) (Figure 6.11-C), showing that less active ZIP6 was present when cells were treated with the presenilin inhibitor.

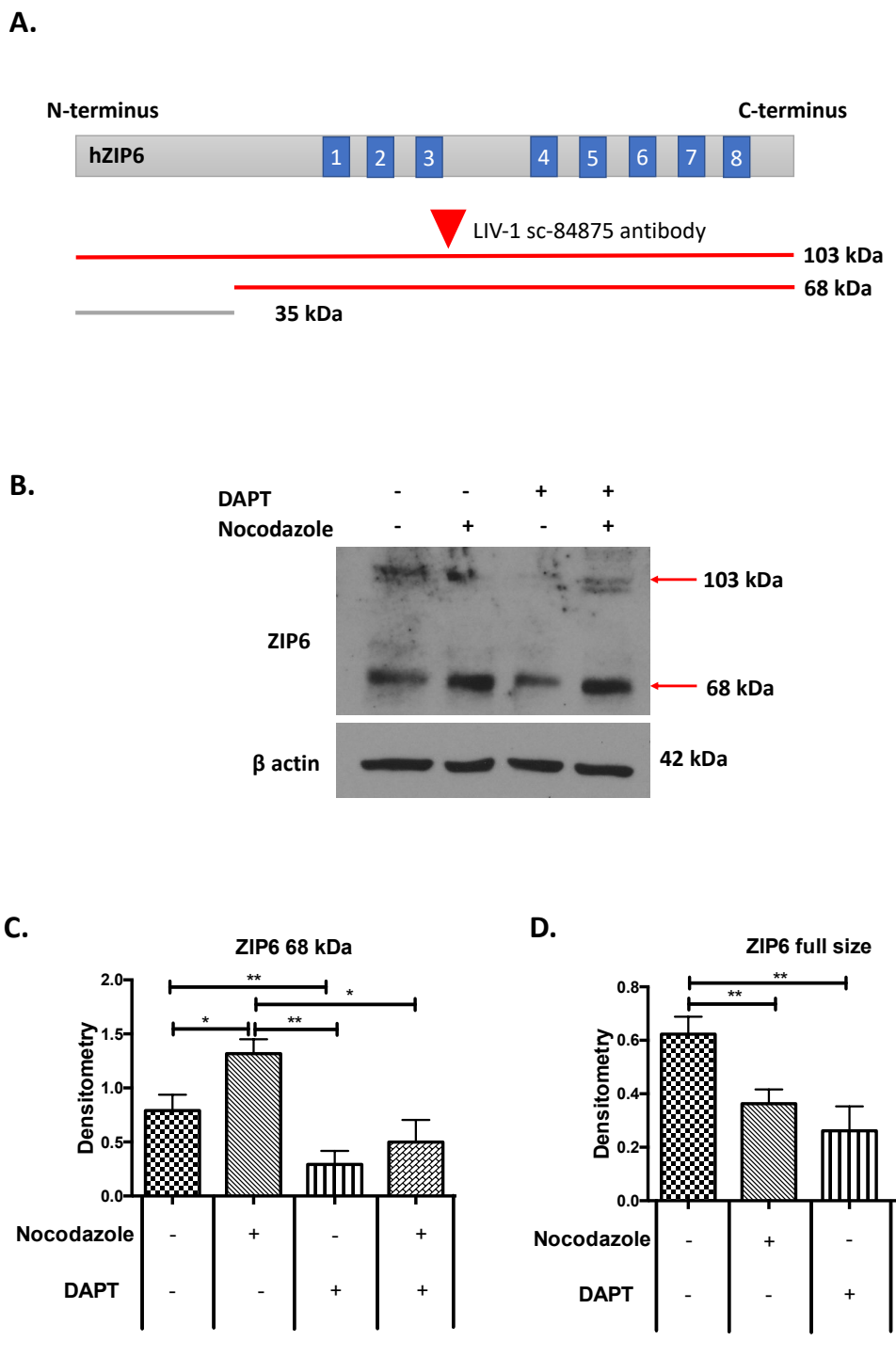

Figure 6.11 ***A presenilin inhibitor affects the cleavage of ZIP6.***
A. Schematic showing the two confirmed ZIP6 cleavages with the corresponding molecular weight. The bands coloured in red represent the ones that can be recognised by the LIV-1 antibody used for this experiment.
B. MCF-7 cells were treated with or without 150 nM nocodazole for 20 hours and in the presence or absence of DAPT (10 μM). Samples were harvested and probed for ZIP6 using the LIV-1 sc antibody.
*C-D. The experiment was performed on three biological replicates and densitometric data of ZIP6 were normalised to the results of β-actin and are shown as a graph of n=3 ± SEM (standard error of mean). Statistical analysis is shown as * (p<0.05) and **(p<0.01).*

6.4 Discussion

It is only recently that we have started to understand how zinc transporters can be regulated by phosphorylation. ZIP7, one of the members of the LIV-1 subfamily was discovered to be phosphorylated by CK2 on two serine residues on the long cytoplasmic loop between TM III and IV. This CK2 phosphorylation was demonstrated to be essential for ZIP7 to transport zinc (Taylor *et al.*, 2012). The close correlation between all the members of the LIV-1 subfamily shown by the alignment of their sequences (Taylor & Nicholson, 2003) suggested that the other members of the subfamily may also undergo the same regulation in order to be activated. Furthermore, phosphorylation was revealed to be an essential requirement during the cell cycle, as phosphorylation mediated by the cyclin-dependant kinases drives the entire cell cycle (Nigg, 2001). Therefore, this chapter has provided new insights into the mechanism by which ZIP6 is regulated by showing that CK2 binds ZIP6 in mitosis and that the protease presenilin plays a role in regulating the proteolytic cleavage of ZIP6.

6.4.1 CK2 binds ZIP6 during mitosis

6.4.1.1 ZIP6 is predicted to be phosphorylated by kinases which are involved in the regulation of the cell cycle

The analysis of potential phosphorylation sites for ZIP6 identified several potential serine and tyrosine sites on the long cytoplasmic loop between TM III and TM IV (Figure 6.2). Surprisingly, the analysis predicted several potential tyrosine phosphorylation sites that have never been studied before in zinc transporters. In fact, not only does tyrosine phosphorylation play a crucial role in cell proliferation, it also plays an essential role in oncogenesis (Paul & Mukhopadhyay, 2004) and could be crucial for the function of ZIP6. Most importantly, zinc was discovered to inhibit tyrosine phosphatases, which led to a failure to deactivate several tyrosine kinase signalling (Haase & Maret, 2003). Most of the predicted kinases involved in the phosphorylation of these residues were discovered to be kinases associated with cell cycle regulation and mitosis, suggesting that phosphorylation on these residues may be necessary for the activation and regulation of ZIP6 in mitosis. In particular, the analysis of potential phosphorylation sites of ZIP6 led to the selection of four residues for ZIP6 having the highest number of prediction and reference according to PhosphoSitePlus® (Hornbeck *et al.*, 2015). One of these residues was serine 471. This residue was predicted to be phosphorylated by either the PAK or GSK3β kinase. The family of PAK kinases was shown

to be essential for the progression of cells through the G2/M phase of the cell cycle through regulation of PLK1 kinase activity (Maroto *et al.*, 2008), a molecule involved with the activation of the complex between cyclin B1 and CDK1 at the onset of mitosis (Gavet & Pines, 2010b; Gheghiani *et al.*, 2017). A similar role is played by GSK3β, since it was previously shown how GSK3β controls the chromosomal alignment and mitosis progression (Wakefield, Stephens & Tavaré, 2003).

Residues Y528 and Y531 in ZIP6 were predicted to be phosphorylated by the Src family of kinases, a group of kinases associated with cell cycle progression, apoptosis, transformation and migration (Parsons & Parsons, 2004). Overall, these four residues appeared to have great potential for phosphorylation in a manner that may be important for the known role of ZIP6 in driving cell division (*Taylor et al, unpublished*) and have been subject of investigation.

The serine residue with the highest number of reference from mass spectrometry data and highest prediction score for ZIP6 was the S478, which was predicted to be phosphorylated by CK2, the same kinase involved in the activation of ZIP7 (Taylor *et al.*, 2012). Interestingly, there was evidence of the involvement of CK2 in the regulation of the cell cycle, in particular at the onset of mitosis, as it was shown that downregulation of the β subunit of CK2 in somatic cells resulted in delayed entry of cells into mitosis (Yde *et al.*, 2008). Interestingly, this current study confirmed the binding of ZIP6 to CK2 during mitosis (Figure 6.3), highlighting the important role played by CK2 in the regulation of mitosis. Most importantly, this finding revealed the potential role for CK2 to phosphorylate ZIP6 during mitosis.

6.4.1.2 The potential of ZIP6 being phosphorylated on multiple sites

In an attempt to demonstrate that CK2 phosphorylated ZIP6 during mitosis on the residue S478, the ZIP6 knockout cell model was used for the phosphorylation analysis, since it was a valuable and useful tool to investigate potential phosphorylation sites by using recombinant ZIP6 while excluding any contribution of endogenous ZIP6 which may alter the results. In fact, the human and mouse sequence of ZIP6 were shown to retain a high similarity as seen in the alignment in Figure 6.4. Most interestingly, the

sites predicted to be phosphorylated in ZIP6 were revealed to be conserved in the mouse sequence as well (Figure 6.4), implying that these phosphorylation sites could play in important role in the regulation of ZIP6 across the two different species. Here, it was confirmed that transfection of human ZIP6 recombinant protein was successful in mouse cells (Figure 6.5) and therefore allowed us to carry on this investigation by using this model of ZIP6 knockout cells. Preliminary immunoprecipitation data for ZIP6 serine phosphorylation was not able to confirm whether ZIP6 was phosphorylated on residue S478 (Figure 6.6), which was analysed in an attempt to confirm whether binding of CK2 to ZIP6 resulted in phosphorylation of this residue. However, this result did not rule out the possibility that the residue S478 could be phosphorylated in ZIP6, as it gave some evidence that the phosphoserine band was decreased in comparison to wild type ZIP6. Unfortunately, this could not be quantified as the corresponding V5 band was covered by the heavy chain of the antibody used for the immunoprecipitation.

For this reason, further analysis to study the role of CK2 in the phosphorylation of ZIP6 was performed by using a CK2 inhibitor called CX-4945 (Siddiqui-Jain *et al.*, 2010) which is now in clinical trials for its use in the treatment of a variety of cancer types (ClinicalTrials.Gov Identifier: NCT02128282). Since ZIP6 is known to be overexpressed in many different type of cancers (Manning *et al.*, 1995; Mcclelland *et al.*, 1998; Zhao *et al.*, 2007; Taylor, 2008; Lue *et al.*, 2011) and because of its important role in driving cell division (*Taylor et al, unpublished*), the discovery of CK2 phosphorylation involvement in the activation of ZIP6 would provide an additional target to tackle ZIP6 activation and its subsequent ZIP6-mediated zinc release. Transfection of different ZIP6 mutants including the CK2 site S478 with or without treatment with the CK2 inhibitor CX-4945 did not confirm that ZIP6 was phosphorylated on this residue. Although cells were synchronised in mitosis by using nocodazole, the analysis of the recombinant ZIP6 only revealed a band at 108 kDa for V5, which corresponded to the full length of ZIP6. The full length of ZIP6 corresponded to the pro-protein of ZIP6 which is also pre-mitotic, as when ZIP6 is on the plasma membrane the N-terminal is cleaved off, as also confirmed in Figure 6.11-C. However, these results raised the question whether this was due to the fact that the recombinant ZIP6 transfected into the mouse cells was not active at this stage of mitosis and maybe phosphorylated at a later stage, or whether ZIP6 was

phosphorylated on multiple sites. The former hypothesis may be due to the fact that, despite CK2 was discovered to have an important role at the onset mitosis, it was also revealed to be maximally phosphorylated and active during prophase and metaphase (Yde *et al.*, 2008; St-denis, Derksen & Litchfield, 2009). The full size of ZIP6 identified in the current analysis corresponded to a pre-mitotic ZIP6 and the CK2 inhibitor may not have had any effect on ZIP6 phosphorylation at this stage. The latter hypothesis could be explained by the fact that CK2 was discovered to be involved in hierarchical phosphorylation, a mechanism by which a kinase that phosphorylates one substrate induces the phosphorylation of another substrate by the action of another kinase (St-denis *et al.*, 2014). Interestingly, CK2 was demonstrated to be necessary as a priming kinase for the subsequent ability of GSK3β to phosphorylate other residues during glucose metabolism (Fiol *et al.*, 1987). The synergetic mechanism of phosphorylation of CK2 and GSK3β is exciting since residue S471 of ZIP6, which is in close proximity to residue S478, was predicted to be phosphorylated by either PAK or GSK3β kinase. This could suggest that as CK2 is a kinase which is constitutively active (Pinna, 2002), it may act as a priming kinase for the following activation of different kinases which could lead to the phosphorylation of ZIP6 on multiple sites. The synergy between CK2 and GSK3β was also corroborated by a preliminary investigation in our group that has confirmed the binding of GSK3β to ZIP6 (data not shown). Furthermore, there are now more and more phosphorylation databases available online which have revealed many more potential phosphorylation sites of ZIP6. Examination of potential phosphorylation sites in ZIP6 including all residues at sites other than the cytoplasmic loop between TM III and TM IV revealed that there are multiple sites of ZIP6 that have the potential to be phosphorylated by CK2 (highlighted in yellow) (Table 6.2). This table include not only serine, but also threonine residues. Most interestingly, the threonine T479 was predicted to be phosphorylated by CK2 and this residue is adjacent to S478, implying that CK2 could phosphorylate both.

Similar to the results gained for the serine phosphorylation, the analysis of the tyrosine phosphorylation of ZIP6 did not provide a clear answer regarding whether the Src kinase was involved in the phosphorylation of the tyrosine residues 528 and 531. This analysis was promising in light of the involvement of zinc in the activation of several

tyrosine kinase pathways through inhibition of tyrosine phosphatases (Haase & Maret, 2003), and since it is an emerging new area of zinc biology. Unfortunately, similar to that seen for the analysis of serine phosphorylation, investigation of tyrosine phosphorylation showed a unique band for V5 at 108 kDa, corresponding to the full size of ZIP6, which was corresponding to pre-mitotic ZIP6. This data did not necessarily rule out the possibility of Src kinase to phosphorylate ZIP6, but as no significant difference was seen between the different ZIP6 mutants, it did suggest that ZIP6 may be phosphorylated on multiple tyrosine residues as predicted in Table 6.2. Tyrosine phosphorylation of ZIP6 could involve also other kinases. Nevertheless, it is important to highlight that the catalytic subunit of CK2 was shown to be tyrosine phosphorylated by members of the Src family of kinases, and this phosphorylation results in increased catalytic activity of CK2 (Donella-Deana *et al.*, 2003). This evidence may suggest that these two kinases could act synergistically and phosphorylate ZIP6 at different serine and tyrosine residues, something that still remains elusive and requires future investigations. Moreover, analysis of potential kinases responsible of the phosphorylation of ZIP6 on Y528 and Y531 with NetPhos 3.1 (Blom *et al.*, 2004) has now predicted the possibility that also the EGFR kinase could be involved with the phosphorylation of these sites, which needs to be tested in future work.

Nevertheless, the serine phosphorylation investigation provided an interesting result. The presence of a 68 kDa band in Figure 6.7 was indicative of serine phosphorylation of endogenous proteins other than the ZIP6 recombinant proteins. Since it was demonstrated in Chapter 5 that the ZIP6 knockout cells upregulated ZIP10, this band at 68 kDa could be due to the phosphorylation of endogenous ZIP10. It was worth noticing that, despite not being significant, the samples which were treated with the CK2 inhibitor showed reduced serine phosphorylation in comparison to the non-treated ones, suggesting that the use of the CK2 inhibitor could have had a role in reducing the serine phosphorylation of ZIP10. In fact, prediction of potential phosphorylation sites for ZIP10 showed that ZIP10 have few serine and threonine residues which are predicted to be phosphorylated by the protein kinase CK2 (Table 6.3) that could explain the result observed. As mentioned previously, CK2 is involved in hierarchical phosphorylation (St-denis *et al.*, 2014), which may suggest that treatment

with a CK2 inhibitor reduced the phosphorylation of those predicted serine residues and the consequent phosphorylation of other serine residues by other kinases. This now fosters a new area for future investigation.

ZIP6 residue	Sequence	NetPhorest prediction	Kinexus prediction	NetPhos prediction
T32	AAFPQTTEKIS	DAPK, MAPK2	CDK3	PKC
T33	AFPQTTEKISP	PKC, GSK3β	GSK3β	CK1
S37	TTEKISPNWES	MAPK	JNK1	GSK3β
Y55	ISTRQYHLQQL	Eph	MERTK	INSR
S69	YGENNSLSVEG	GRK	PIM1	DNAPK
S71	ENNSLSVEGFR	DMPK	SgK307	Cdc2
S106	DHEHHSDHERH	CK2	CK2a2	CK2
S112	DHERHSDHEHH	CK2	CK2a2	CK2
S124	EHEHHSDHDHH	CK2		CK2
T188	STVYNTVSEGT	PDHK	MEK1	
S189	ASEVTSTVYNT	GRK		
Y192	VTSTVYNTVSE	Src		EGFR
S219	SSTPPSVTSKS	ACT2/2B TGFbR2	ERK1	unsp
S384	HHHSHSHEEPA	PKC, GSK3β	ATR, PLK3	PKC
S409	FSHLSSQNIEE	ATM/ATR	PLK3, CK1a1	ATM, CK2
S471	IKKQLSKYESQ	PAK, GSK3		PKA
Y473	KQLSKYESQLS	Eph		INSR
S475	LSKYESQLSTN	ATM/ATR		DNAP
S478	YESQLSTNEEK	CK2		CK2
T479	ESQLSTNEEKV	CK2		CK2
T486	EEKVDTDDRTE	CK2		CK2
T490	DTDDRTEGYLR	ACT2/2B TGFbR2		GSK3β
Y493	DRTEGYLRADS	MAP2K		unsp
Y528	HPQEVYNEYVP	Src		Src, EGFR
Y531	EVYNEYVPRGC	Src		Src, EGFR
S577	NHHPHSHSQRY	PKC	PKG1	unsp
S583	HSQRYSREELK	PKA		CK2
S609	GLHNFSDGLAI	CK2		CK2
T619	IGAAFTEGLSS	GRK, DAPK		CK1
S629	SGLSTSVAVFC	PKC		Cdc2
T653	LKAGMTVKQAV	PKC		PKC
T693	WIFALTAGLFM	DAPK		PKC

Table 6.2 ***ZIP6 has the potential to be phosphorylated on multiple sites.***
The sequence of ZIP6 was retrieved on the NCBI database in FASTA format. The analysis was performed using several phosphorylation site databases such as Phosphonet (Kinexus Bioinformatics Corporation), NetPhorest 2.1 (University of Copenhagen) and NetPhos 3.1 (see methods section for reference). The kinase predicted to be responsible for the phosphorylation on each site is indicated on the table. The residues highlighted in yellow are the residues which are predicted to be phosphorylated by protein kinase CK2.

ZIP10 residue	NetPhorest prediction	Kinexus prediction	NetPhos prediction
S556	CK2	CK2	CK2
T567	MAP2K	CK2	CK2
S573	CK2	CK2	CK2
T580	CK2	CK2	
T583	CK2	CK2	CK2
S610	CK2	CK2	
T615	CK2	CK2	

Table 6.3 ***ZIP10 phosphorylation sites that are predicted to be phosphorylated by CK2.***
The sequence of ZIP10 was retrieved on the NCBI database in FASTA format. The analysis was performed using several phosphorylation site databases such as Phosphonet (Kinexus Bioinformatics Corporation), NetPhorest 2.1 (University of Copenhagen) and NetPhos 3.1 (see methods section for reference).

The investigation of potential serine or tyrosine phosphorylation sites of ZIP6 is quite a complex area of study. Although this analysis did not unveil any major breakthrough, it has suggested the potential involvement of CK2 in the regulation of ZIP6 and has provided interesting suggestions and a base for future work in this area.

6.4.2 The importance of ZIP6 proteolytic cleavage

The proteolytic cleavage of ZIP6 is essential for the correct function of this zinc transporter which involves its relocation from the endoplasmic reticulum to the plasma membrane (Hogstrand *et al.*, 2013). This cleavage was excepted to occur at a PEST cleavage site on its N-terminal domain which was confirmed to be highly conserved in different species (Figure 6.10), suggesting a significant role for this proteolytic cleavage in the correct function of the protein. The PEST cleavage site is a sequence of amino acids which is associated with proteins having a short half-life (Rogers, Wells & Rechsteiner, 1986). Moreover, ZIP10 is the only other member of the LIV-1 subfamily to contain a PEST cleavage site in the N-terminus (Taylor *et al.*, 2016) which was shown to generate several ZIP10 cleavage products (Ehsani *et al.*, 2012) Interestingly, the prion protein, a protein involved in neurodegenerative diseases of humans and animals was shown to have descended from the LIV-1 subfamily of ZIP transporters and has a close similarity to ZIP6 and ZIP10 (Schmitt-Ulms *et al.*, 2009). The prion protein was shown to undergo an N-terminus proteolytic cleavage in zinc-depleted condition, similar to that observed for ZIP10 (Ehsani *et al.*, 2012). This highlighted how the modification and proteolytic cleavage of these proteins must be a prerequisite of their functional control.

Proteolytic cleavage is an essential regulatory mechanism used by proteins to regulate physiological events such as cell cycle and not only for their degradation (Rogers & Overall, 2013).

The study within this current chapter has shown the prediction of a second PEST cleavage site for ZIP10 in the middle of its long intracellular loop between transmembrane III and IV, which has never been investigated before and was unprecedented in ZIP transporters. The immunoprecipitation data within this chapter showed the presence of a lower band for ZIP6 at 35 kDa which was indicative of a potential cytoplasmic loop proteolytic cleavage. Analysis of potential PEST cleavage site for ZIP6 in Figure 6.9 showed the presence of a PEST cleavage site in the middle of the long cytoplasmic loop between TM III and TM IV similar to that found for ZIP10. Although the ZIP6 cytoplasmic cleavage was not strongly predicted, the site was seen to be conserved in other species, suggesting the potential for an important role in this protein. If this cleavage was real, it would generate a ZIP6 cleavage from the middle of the cytoplasmic loop to the C-terminal domain corresponding to a molecular weight of 28 kDa according to the online tool Compute pi/Mw (Gasteiger *et al.*, 2005). Considering also the 5 kDa band of the V5-His tag (Elomaa *et al.*, 2001) and the potential glycosylation site of ZIP6 on residue N684 (Taylor *et al.*, 2003), this could correspond to a 35 kDa band generated by the cytoplasmic cleavage. This cleavage may suggest the potential of ZIP6 protein breakdown for degradation which could be used as a regulatory mechanism to let cells progress in G1 at the end of mitosis. However, this mechanism is yet to be fully understood and provides a new area of study for zinc transporters.

6.4.2.1 Assessing involvement of presenilin in the proteolytic cleavage of ZIP6

The analysis of ZIP6 proteolytic cleavage was focused on the investigation of the presenilin protease, as a previous study in our group revealed that presenilin is the protease with the highest probability of being involved with ZIP6 cleavage during mitosis (Nimmanon, 2016). In fact, protease arrays of cells synchronised in mitosis with nocodazole have revealed that presenilin was the protease which showed the highest increase in mitosis in comparison to control samples. Most interestingly, presenilin was known to have a role in the transcription and cleavage of the prion protein (Vincent *et al.*, 2009), a protein which shares many similarities with both ZIP6 and ZIP10 (Schmitt-

Ulms *et al.*, 2009). The data within this current study has shown that the active form of ZIP6 during mitosis was significantly decreased in the sample treated with the presenilin inhibitor DAPT. These results suggested that presenilin could have been involved with the cleavage of ZIP6, explaining why less active ZIP6 was seen when this protease was inhibited. However, the full size of ZIP6 was also reduced in the sample treated with the presenilin inhibitor in comparison to the control. Thus, this result contradicted the previous hypothesis and suggested that while presenilin may have a role in the regulation of ZIP6 proteolytic cleavage, other proteases may be involved in this process. Taken together these findings did not unveil whether presenilin was involved in the cleavage of ZIP6 during mitosis but corroborated that the use of a presenilin inhibitor affected the overall ZIP6 protein level and its regulation in mitosis.

The study of post-translational modifications of ZIP6 was only the beginning of a more extended area that has provided exciting new work to be undertaken. As soon as the mechanism lying behind the activation and regulation of ZIP6 and ZIP10 is fully understood, it will be possible to investigate new potential targets that can be used for the treatment and management of highly proliferative diseases such as cancer.

6.5 Chapter summary

The study of post-translational modification of ZIP6 and ZIP10 identified many potential phosphorylation sites that were predicted to be phosphorylated by kinases which have an important role in the regulation of mitosis. In particular, it was found that ZIP6 bound the protein kinase CK2 during mitosis, a kinase involved in several malignancies including cancer and that has an established role in the regulation of mitosis. It was found that ZIP6 had the potential of being phosphorylated on multiple serine and tyrosine residues, and that CK2 may have a role in driving hierarchical phosphorylation. Combining different techniques with the use of different kinases inhibitors could be helpful in the follow-through of this area of study. This chapter also highlighted the important role for proteolytic cleavage as a prerequisite of the correct function of ZIP6, which was discovered to be conserved across different species.

7 GENERAL DISCUSSION

The importance of zinc for normal human health has been known for the last 55 years (Prasad *et al.*, 1963). This was confirmed by the fact that zinc dysregulation was discovered to be involved in several pathologies and illnesses such as neurodegenerative diseases, immunodeficiency, growth retardation, diabetes and cancer (Rink & Gabriel, 2000; Chimienti, Favier & Seve, 2005; Wenzlau *et al.*, 2007; Mocchegiani, Giacconi & Malavolta, 2008; Taylor, Gee & Kille, 2011; Fukada *et al.*, 2011; Ziliotto, Ogle & Taylor, 2018). Therefore, it is essential to maintain correct zinc homeostasis for human health. For this reason, zinc biology is a new emerging area of investigation that has been gaining much interest in recent years. While more is known about the members of the ZnT family due in part to the availability of a 3D structure (Lu & Fu, 2007; Coudray *et al.*, 2013), the mechanism by which the ZIP transporters work still remains elusive. In order to shed light on the ZIP family functional mechanism, this project has focused on three zinc transporters of the ZIP family: ZIP7, ZIP6 and ZIP10. The project expanded a few recent discoveries in our group and has provided a deeper insight into the role of these zinc transporters in breast cancer and in the regulation of the cell cycle. Firstly, the discovery that ZIP7 has a role in driving anti-hormone resistance in breast cancer (Taylor *et al.*, 2008) and is reliant on CK2 phosphorylation to function (Taylor *et al.*, 2012) was expanded, and it has unveiled for the first time the correlation between ZIP7 and ZIP6 in driving the aggressiveness of tamoxifen resistant breast cancer. Secondly, a more recent study in our group has discovered the involvement of both ZIP6 and ZIP10 in the regulation of mitosis (*Taylor et al, unpublished*). In-depth analysis starting from this evidence has investigated the possibility of targeting ZIP6 and ZIP10 in cancer and has provided a new understanding of how these zinc transporters are regulated, that will now be discussed in detail.

The most striking breakthrough of this current project was the ability to stop cell division by targeting zinc signalling, a mechanism that can potentially be used to prevent the spread and worsening of hyperproliferative diseases such as cancer, which rely on increased cell growth to sustain their development. The follow-up of this new finding could benefit a significant number of people that are affected by cancer, which remains one of the main burdens of our society (Bray *et al.*, 2018).

7.1 Phosphorylated ZIP7 is a biomarker of tamoxifen resistant breast cancer

ZIP7 is a member of the LIV-1 subfamily which, unlike other members, does not reside on the plasma membrane. Intracellular zinc signalling is regulated by different zinc transporters, such as ZnT2 or ZnT4 which sequester zinc inside lysosomes or ZIP8 which works in the opposite direction by increasing the level of cytoplasmic zinc by releasing zinc from lysosomes (reviewed by Kambe *et al.*, 2015). Other important mediators of cytoplasmic zinc include ZIP9, which is localised on the apical membrane of the Golgi apparatus (Matsuura *et al.*, 2009) or ZIP13 which, similarly to ZIP9, is localised to the Golgi membrane and on cytoplasmic vesicles, transporting zinc from this compartments to the cytosol (reviewed by Kambe *et al.*, 2015). Among these, ZIP7 is one of the main regulators of intracellular zinc homeostasis, as it controls transport of zinc from the endoplasmic reticulum to the cytoplasm (Taylor *et al.*, 2004; Woodruff *et al.*, 2018). ZIP7 controls zinc homeostasis by increasing the level of cytoplasmic zinc following its phosphorylation mediated by the protein kinase CK2 on two serine residues located on the cytoplasmic loop between TM III and TM IV (Taylor *et al.*, 2012). This activation happens in response to an extracellular stimulus, such as zinc or EGF, coupled with an intracellular calcium release (Yamasaki *et al.*, 2007). It was recently shown that ZIP7 activation occurs within two minutes of an extracellular stimulus which, in that study, was mediated by zinc (Nimmanon *et al.*, 2017). This confirms the role played by zinc as a second messenger (Yamasaki *et al.*, 2007), being released from stores within minutes of an extracellular stimulus and being involved in the activation of other signalling pathways.

7.1.1 ZIP7 drives the aggressiveness of tamoxifen-resistant breast cancer

Breast cancer is the most common cancer amongst women (Bray *et al.*, 2018) and development of endocrine resistance is one of the main issues in the management of breast cancer therapy (Larionov & Miller, 2009). In particular, resistance to tamoxifen is one of the main concerns, as tamoxifen is still one of the preferential drugs used in pre-menopausal women affected by ER-positive breast cancer (Clarke, Tyson & Dixon, 2015). Many research groups have been studying the mechanism by which cells acquire resistance to tamoxifen by using model of TamR cells, and a common feature of these cells is the expression of a more aggressive phenotype in comparison to the parental MCF-7 (Hiscox *et al.*, 2004, 2006a, 2006c; Taylor *et al.*, 2008; Kim *et al.*, 2009; Bui *et al.*,

2017). Aggressive phenotype of breast cancer is a term used to describe breast cancer with a poor prognosis which have a higher chance to metastasise (Arpino, Milano & De Placido, 2015). Our group have previously demonstrated that the TamR resistant cell line is characterised by an increased motility and invasive phenotype (Hiscox *et al.*, 2004), having adopted the EGFR signalling pathway (Knowlden *et al.*, 2003) as well as activated Src kinase (Hiscox *et al.*, 2006c), a protein with a well-established role as an oncogene (Parsons & Parsons, 2004). The increased motility of TamR cells is induced by loss of cellular adhesion proteins with acquisition of mesenchymal properties (Hiscox *et al.*, 2006a), typical of cells undergoing epithelial to mesenchymal transitions (Kalluri, 2009). In particular, it was discovered that the reduction of cell-cell adhesion interactions in TamR cells was mediated by increased expression of β-catenin, both mRNA and protein (Hiscox *et al.*, 2006a). β-catenin together with E-cadherin is involved in the cell-adhesion machinery and epithelial integrity, and overexpression of β-catenin is related to many invasive cancers, displaying an EMT-transition phenotype (Tian *et al.*, 2011). It is interesting to notice that TamR cells were associated with increased inactivation of GSK3β (Hiscox *et al.*, 2006a) and increased activation of AKT (Jordan *et al.*, 2004; Hiscox *et al.*, 2006a), which was further confirmed also in the current project. In this respect, it is important to highlight that zinc was discovered to be involved with both activation of AKT (Lee *et al.*, 2009) and inhibition of GSK3β (Ilouz *et al.*, 2002). Increased activation of the PI3K/AKT/mTOR pathway in TamR cells has also been confirmed in more recent papers not only in TamR cells (Phuong *et al.*, 2014) but also in a model of TamR xenografts (Cottu *et al.*, 2014). The current thesis project has also shown that the increased activation of AKT in comparison to the parental MCF-7 cells is not only present in TamR cells, but also in our long-term resistant model of TamR, called TamRL, which better mimics the clinical situation. For this reason, recent investigations have focused on the use of AKT or mTOR inhibitors to test their efficacy at decreasing the cell proliferation of this aggressive phenotype of breast cancer resistance. Our group have tested an mTOR inhibitor called RAD001 (everolimus/Afinitor®) and a dual mTORC1/2 mTOR kinase inhibitor called AZD8055 on our model of TamR-MCF-7 resistance showing that the latter was successful at reducing the cell growth of TamR, and that this effect was enhanced by the combination of this drug with the pure anti-oestrogen fulvestrant (Jordan *et al.*, 2014). Another research group tested the AKT

inhibitor AZD5363 on TamR cells and confirmed that their cell growth was reduced and that the use of this drug was effective at resensitising the cells to the antiproliferative effect of tamoxifen (Ribas *et al.*, 2015).

Another pathway which was discovered to be increased in TamR cells was Src (Hiscox *et al.*, 2006c). The increased activation of the Src kinase signalling discovered in TamR cells activates tyrosine kinase pathways that contribute to the aggressiveness of this cell line and to its increased cell growth rate (Hiscox *et al.*, 2006c). Not surprisingly, zinc is known to inhibit tyrosine phosphatases (Haase & Maret, 2003) and considering that TamR cells were discovered to have a significant increase of intracellular zinc (Taylor *et al.*, 2008), which was further confirmed in the current project, it suggests a pivotal role for zinc in the activation of downstream pathways which regulate the aggressive behaviour of this resistant cell line. Moreover, an upstream molecule of Src kinase is the focal-adhesion kinase FAK (Brunton *et al.*, 2005). Analysis of TamR cells identified that increased Src was related to increase FAK phosphorylation and cell treatment with a Src inhibitor, called AZD0530, was able to reduce FAK activity (Hiscox *et al.*, 2007). A follow-up study on FAK has also shown that the use of a FAK inhibitor was associated with reduction of invasive proprieties of TamR cells (Hiscox *et al.*, 2011). Interestingly, FAK is phosphorylated on several tyrosine residues, and the fact that the active form of FAK is increased in TamR cells (Hiscox *et al.*, 2011) is exciting since this cell line has increased zinc (Taylor *et al.*, 2008). As zinc is responsible for inhibition of tyrosine phosphatases (Haase & Maret, 2003), it suggests a role for zinc in the increased activation of FAK observed in TamR by maintaining this pathway constitutively active. This evidence is corroborated by a recent paper which has demonstrated that treatment of human lung cancer cells with zinc induced EMT, and consequently these cells displayed a metastatic behaviour that was associated with increased activation of FAK (Ninsontia, Phiboonchaiyanan & Chanvorachote, 2016).

It is important to notice that all of the above signalling pathways, such as PI3K, AKT, GSK3β or mTOR have been recently discovered by our group to be directly downstream of ZIP7 activation (Nimmanon *et al.*, 2017), which fit with the current discovery of this thesis revealing how TamR cells displayed a significant ZIP7

hyperactivation. The current thesis project speculated that the aggressive phenotype displayed by TamR cells was a direct consequence of the ZIP7-mediated zinc release following its increased activation. The first correlation between ZIP7 and breast cancer was found in our models of anti-hormone resistant breast cancer which revealed increased expression of the ZIP7 gene in comparison to the parental MCF-7 cells (Taylor *et al.*, 2007). Moreover, TamR cells not only had increased expression of the SLC39A7 gene (ZIP7) but also increased zinc (Taylor *et al.*, 2008). This zinc increase was a direct consequence of elevated ZIP7 expression, as downregulation of the ZIP7 gene resulted in reduced activation of EGFR, IGF-1R or Src signalling which was accompanied by cytosolic zinc decrease (Taylor *et al.*, 2008). Furthermore, the increased use of EGFR signalling discovered in TamR cells resulted in elevated levels of activated ERK1/2 MAPK signalling (Knowlden *et al.*, 2003), another pathway whose activation was previously associated with reduced cancer survival rate in clinical breast cancer (Gee *et al.*, 2001). A recent paper has investigated and identified the complex genomic landscape of endocrine-resistant advanced breast cancer, identifying lesions and mutation on the MAPK pathway as one of the mainstays of endocrine resistance, together with the already known ESR1 (oestrogen receptor alpha gene) mutations (Razavi *et al.*, 2018). Interestingly, MAPK is another main downstream pathway of activated ZIP7 (Nimmanon *et al.*, 2017), confirming once again the important role played by ZIP7-mediated zinc release in the development of endocrine resistance.

Interestingly, after a new immunohistochemistry assay for pZIP7 was developed, this was applied to a small series of clinical breast cancer samples available in our group with analysis of corresponding clinical parameters to pZIP7 Hscore revealing a significant direct association to pMAPK, the active form of the ERK1/2 pathway. This result further supported our discovery of activated ZIP7 involved in the development of the aggressive phenotype in endocrine-resistant breast cancer, and confirmed what was previously discovered in TamR cells regarding the increased activation of the ERK pathway (Knowlden *et al.*, 2003). Furthermore, investigation of clinical parameters discovered a significant association of pZIP7 to the proto-oncogene Fos and the transferrin receptor CD71. Both these two molecules have been previously studied for their involvement in tamoxifen-resistant breast cancer.

One study has identified the transferrin receptor as a marker of a poor prognosis breast cancer cohort with associated tamoxifen resistance (Habashy *et al.*, 2010). The discovery of the correlation of pZIP7 to CD71 was exciting since the transferrin receptor, which normally transports iron (Ponka & Lok, 1999), has also been demonstrated to transport zinc into cells (Charlwood, 1979). Investigations of the transferrin receptor in the TamR cell line revealed a 5-fold increased expression of CD71 in comparison to MCF-7 cells, and analysis of a cohort of ER-positive breast cancer treated with only tamoxifen showed that CD71 was significantly related to a decrease in breast cancer survival and disease-free interval (Habashy *et al.*, 2010). The direct association of CD71 to TamR cells and the evidence that this cell line was characterised by increased cytoplasmic zinc suggested that the transferrin receptor may contribute along with pZIP7 to the increased level of cytoplasmic zinc seen in this cell line, which resulted in activation of multiple downstream pathways that are involved with aggressive cancer.

Another result which contributed to verify the hypothesis of pZIP7 being a major player in the development of tamoxifen-resistance was the association with the proto-oncogene Fos. In this respect, a study of human bronchial epithelial cells supplemented with zinc showed increased expression of c-Fos in comparison to cells with normal zinc levels (Fanzo *et al.*, 2001). As TamR cells was discovered to have more zinc than their parental MCF-7 cells (Taylor *et al.*, 2008), it could imply that the significant correlation of the proto-oncogene Fos to pZIP7 was due to the direct correlation between zinc status and Fos expression. Moreover, the protein c-Fos was also previously correlated to endocrine resistance, as an investigation on breast cancer samples at different treatment stages showed that patients responding to tamoxifen had decreased cell proliferation and expression of Fos, while patients with a poor response had more Fos expression (Gee *et al.*, 1999). In fact, more recently it was seen that the expression of Fos was significantly raised in ductal carcinoma biopsies in comparison to normal tissue, highlighting the role of this oncogene in driving cancer aggressiveness (Motrich, Castro & Caputto, 2013).

All this evidence corroborates our finding that activated ZIP7 and its consequent zinc-mediated signalling is a major player in the development of tamoxifen resistance.

Now that a new immunohistochemical assay has been developed this could be tested in other clinical samples, including samples at relapse, and it could be used as a novel biomarker of tamoxifen resistance in breast cancer.

7.1.2 A mechanism for ZIP6 and ZIP7 in the regulation of epithelial to mesenchymal transition of TamR cells

A recent investigation has demonstrated that the epithelial to mesenchymal transition behaviour of MCF-7 cells was induced by a ZIP6-mediated zinc mechanism (Hogstrand *et al.*, 2013). ZIP6-mediated intracellular zinc release resulted in inhibition of GSK3β, via a direct mechanism (Ilouz *et al.*, 2002) or via phosphorylation mediated by AKT, which can also be activated by zinc (Lee *et al.*, 2009). These events resulted in downregulation of E-cadherin induced by retention of active Snail in the nucleus (Hogstrand *et al.*, 2013). A similar mechanism involving GSK3β and AKT in the regulation of EMT in TamR cells was also confirmed in a previous paper (Kim *et al.*, 2009). Considering the current study has discovered that TamR cells have increased activation of ZIP7, and knowing that zinc acts as a second messenger (Yamasaki *et al.*, 2007) which can be involved in the activation of ZIP7 itself (Taylor *et al.*, 2012), it may suggest that the ZIP6-mediated zinc release stimulates the activation of ZIP7, which results in increased activation of AKT, as a direct downstream pathway of ZIP7 (Nimmanon *et al.*, 2017). Additional evidence of zinc contributing to the activation of ZIP7 comes from a recent paper which has identified the zinc-sensing G-protein coupled receptor ZnR/GPR39 in the aggressive phenotype of TamR cells (Ventura-Bixenshpaner *et al.*, 2018). This paper has demonstrated that changes in zinc homeostasis activated the ZnR/GPR39 receptor which was overexpressed in this cell line and that its activation resulted in calcium release followed by activation of downstream pathways such as AKT and MAPK. Therefore, this data led us to postulate that changes of zinc homeostasis could be accompanied by ZIP6-mediated zinc release. Mobilisation of zinc could induce both activation of ZnR/GPR39 and of ZIP7, as it was previously demonstrated that zinc induced zinc release (Taylor *et al.*, 2012). The IP3R-mediated calcium release could contribute to further activate ZIP7, as calcium was previously identified as essential for zinc mobilisation from stores (Yamasaki *et al.*, 2007). The link between calcium and zinc is well established, as studies in Hela cells have shown that changes in intracellular zinc mediated calcium release from the endoplasmic reticulum and vice versa (Qin *et al.*,

2011). All these data corroborate our findings of increased zinc driving the aggressiveness of TamR cells by utilising ZIP7-mediated zinc signalling. The increased activation of ZIP7 was demonstrated to be responsible of the activation of PI3K/AKT/mTOR and MAPK pathways (Nimmanon *et al.*, 2017) which drive the invasive and aggressive behaviour of this endocrine resistant cell line. This, together with the well-established role of ZIP6 in driving EMT, highlighted the importance of zinc signalling in driving the aggressiveness of this model of tamoxifen resistant cells. It is postulated that activation of AKT mediated by ZIP7 inhibits GSK3β, which retains Snail in the nucleus where it acts as a E-cadherin repressor, inducing epithelial to mesenchymal transition (Figure 7.1).

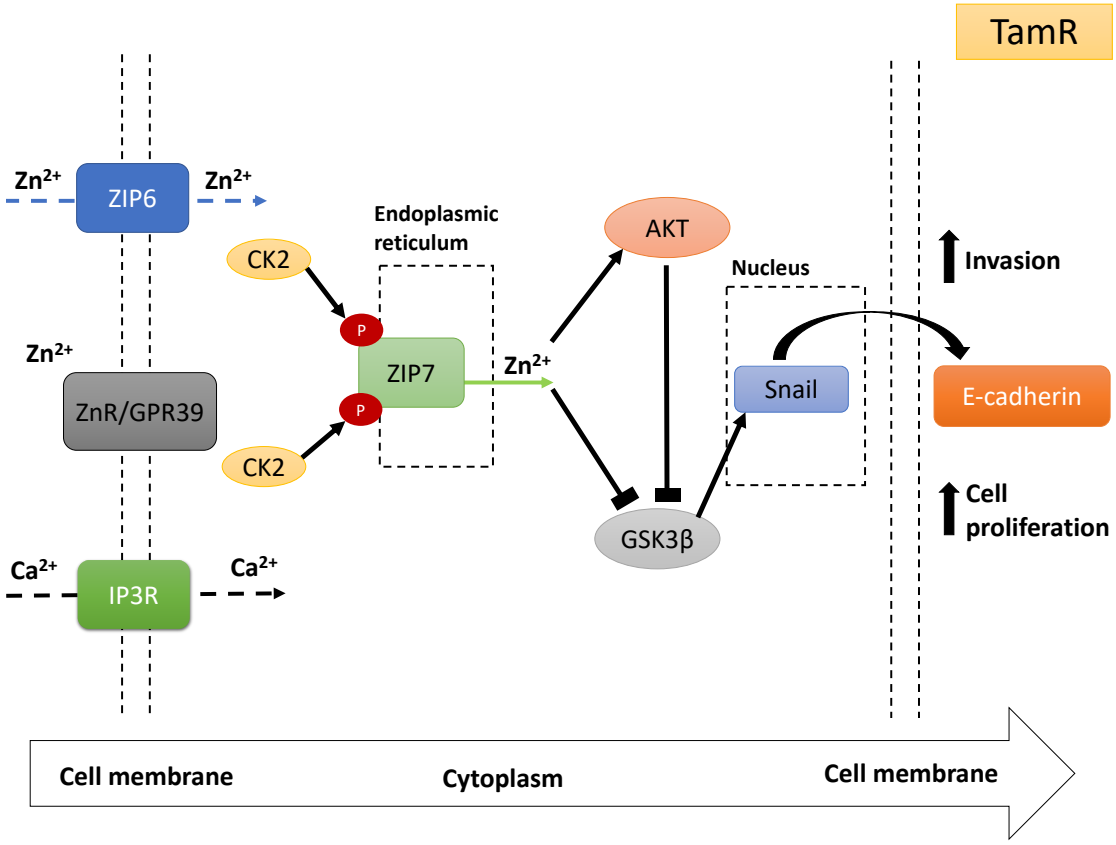

Figure 7.1 ***Proposed mechanism for ZIP6 and ZIP7 driving EMT in TamR cells.***
ZIP6 imports zinc from the extracellular space. Mobilisation of zinc and activation of the zinc-sensing receptor ZnR/GPRR39 induces the IP3R-mediated calcium release which further stimulates the activation of ZIP7 mediated by CK2 phosphorylation. Activated ZIP7 induces release of zinc from the endoplasmic reticulum which results in increased activation of AKT. AKT is responsible of the inactivation of GSK3β which retains Snail in the nucleus where it acts as a E-cadherin repressor. This results in increased cell proliferation and invasive properties of TamR cells.

Another important link between TamR-induced EMT and ZIP6 comes from the evidence that TamR cells were discovered to have constitutively activated STAT3 (Bui *et al.*, 2017). In this recent paper it was shown that TamR cells had also increased expression of Notch4, a member of the Notch signalling family which is normally involved in the regulation of the destiny of cells during development, including promoting cell growth in cancer (Bray, 2016). That study demonstrated that inhibition of Notch4 in TamR cells resulted in a significant decrease of STAT3 tyrosine phosphorylation (Bui *et al.*, 2017). Interestingly, ZIP6 expression was discovered to be a downstream target of STAT3 (Yamashita *et al.*, 2004), and these two molecules were both identified in the regulation of epithelial to mesenchymal transition (Yamashita *et al.*, 2004; Hogstrand *et al.*, 2013). Moreover, the discovery that ZIP7 was significantly associated with STAT3 in breast cancer samples (Taylor *et al.*, 2007) further links STAT3, ZIP6 and ZIP7-mediated zinc signalling to the aggressive phenotype of tamoxifen-resistant cells. Furthermore, the current project revealed a significant direct association of activated ZIP7 with higher tumour grade. Tumour grade is an indicator of tumour progression as high tumour grade is typical of poor differentiated tumour cells which exhibit more mitotic figures and more disorganised nuclei, markers of tumour progression (Edge *et al.*, 2010). Despite the fact that phospho-ZIP7 was not significantly correlated to tumour stage, which is an indicator of tumour spread and lymph node involvement, this was still an important result to corroborate the use of ZIP7-mediated zinc signalling in a poor prognosis cohort of breast cancer, which could be related to endocrine resistance. The critical role of ZIP7 in the regulation of cell proliferation was also confirmed in a recent paper where knockdown of ZIP7 was associated with ER stress and aberrant cell proliferation (Woodruff *et al.*, 2018). Most interestingly, this recent paper has also confirmed the important role of ZIP7 as one of the major regulators of cytosolic zinc, as a model of ZIP7 CRISPR/Cas9 cells was discovered to have upregulation of ZIP8, ZIP14, ZnT1 and ZnT5, showing that cytosolic zinc level was significantly reduced when ZIP7 was ablated. Furthermore, it was shown that the upregulation of other zinc transporters involved in the regulation of intracellular zinc was not sufficient to compensate for the lack of ZIP7 (Woodruff *et al.*, 2018). All this data corroborate the findings of this project, confirming the important role played by ZIP7 and ZIP6 as

essential drivers of cell proliferation. To date, this is the first study relating the mechanism of ZIP6 in EMT to ZIP7-mediated zinc signalling (Figure 7.1).

7.1.3 A mechanism to tackle tamoxifen-resistance in breast cancer by targeting CK2

When ZIP7 was first shown to be involved in the development of anti-hormone resistant breast cancer (Taylor *et al.*, 2008), it was not known that ZIP7 activation was mediated by CK2 phosphorylation (Taylor *et al.*, 2012). This was an important discovery, as it helped clarify how the ZIP7-mediated zinc release mechanism was regulated. Knowing that CK2 phosphorylation is a requirement for ZIP7 activation, it provides a potential new mechanism to target ZIP7 indirectly. CK2 is a ubiquitous protein involved in a variety of physiological pathways which also include cell-cell adhesion maintenance control (Bek & Kemler, 2002; Ji *et al.*, 2009). CK2 exists as a tetrameric structure composed of two α catalytic subunits and two β regulatory subunits (Litchfield, 2003) which contains a zinc finger domain that mediates dimerization of CK2β (Chantalat *et al.*, 1999). Although CK2 is not directly an oncogene, it was discovered to be highly abundant in tumour cells, suggesting its important role in tumorigenesis (Trembley *et al.*, 2009). Imbalance of the two CK2 subunits was seen to be involved in epithelial to mesenchymal behaviour via induction of EMT-regulated genes (Deshiere *et al.*, 2013). In particular, it was seen that overexpression of the CK2α subunit in mammary glands was associated with increased risk of metastasis in breast cancer, being a marker of poor prognosis (Giusiano *et al.*, 2011), and more recently the same was identified in epithelial ovarian cancer (Ma *et al.*, 2017). In this respect, it is interesting to notice that overexpression of CK2α was associated with invasiveness of colorectal cancer tissues and cell lines via regulation of EMT genes, such as upregulation of Snail (Zou *et al.*, 2011). In that study it was shown that downregulation of CK2α resulted in increased expression of E-cadherin and consequent reduction of EMT. Considering our finding of a link between ZIP6 and ZIP7 in the regulation of the EMT-like behaviour of TamR (Figure 7.1) and what has been found in previous papers regarding the role of CK2 in EMT, all this data highlights once again how the increased activation of ZIP7 mediated by CK2 in TamR cells drives the invasive and aggressive phenotype of these cells. In this respect, it is also interesting to notice that data within this current project has discovered that CK2 bound also ZIP6, which further corroborate the discovery of the link between ZIP6 and ZIP7 in

driving EMT in TamR cells. Whether CK2 is essential for the activation of ZIP6 is not clear yet, but further work could help us dissect this mechanism.

Because of the involvement of CK2 in tumorigenesis (Trembley *et al.*, 2009), the use of CK2 inhibitors has become established in the treatment of cancer in the last few years, and the CK2 inhibitor CX-4945 was shown to exert anti-proliferative effects on haematological tumours and other cancer cell lines *in vitro* (Siddiqui-Jain *et al.*, 2010; Zanin *et al.*, 2012; Chon *et al.*, 2015), but also in xenograft models of prostate cancer (Pierre *et al.*, 2011). Another study on adenocarcinoma epithelial cells stimulated with TGFβ1 and treated with CX-4945 has induced reduction of the invasive properties of the cells via downregulation of EMT genes and matrix metalloproteinases 2 and 9 (Kim & Hwan Kim, 2013), members of a family of zinc binding proteins (Nagase & Woessner, 1998). Interestingly, there is evidence that stimulation of a cell line of mouse mammary gland with TGFβ1 induced a 5-fold increase of ZIP6 transcript level (Brethour *et al.*, 2017). Moreover, TGFβ1 was shown to be a downstream target of STAT3 (Liu *et al.*, 2014), and since ZIP6 expression was demonstrated to be driven by STAT3 (Yamashita *et al.*, 2004), this evidence further supported our discovery of the ZIP6-ZIP7-mediated EMT mechanism. The CK2 inhibitor CX-4945 was also demonstrated to be internalised in drug-resistant cells and to induce cell death (Zanin *et al.*, 2012). Lastly, CX-4945 is currently in clinical trials in combination with other chemotherapy drugs to treat cholangiocarcinoma, a form of bile ductal cancer (ClinicalTrials.Gov Identifier: NCT02128282). The use of CK2 inhibitors to prevent the activation of ZIP7 could have a significant impact on stopping the activation of several downstream pathways that drive tamoxifen-resistance, and therefore reducing the aggressiveness of this breast cancer phenotype. A preliminary investigation in our group using the CK2 inhibitor CX-4945 (Siddiqui-Jain *et al.*, 2010) has given promising results at reducing the growth rate of TamR cells (data not shown). This now needs to be investigated in more depth, as it could provide a new therapy in the treatment of aggressive and metastatic breast cancer which no longer responds to tamoxifen due to the acquirement of resistance mediated by the increase activation of ZIP7.

7.1.4 The role of ZIP7 in a model of Faslodex®-resistant breast cancer

Patients who relapse from tamoxifen or aromatase inhibitor treatment are normally treated with a pure anti-oestrogen called fulvestrant (Faslodex®) (Robertson *et al.*, 2014). Nevertheless, development of resistance to this treatment represents an issue in therapy, similar to that seen for tamoxifen (Huang *et al.*, 2017). For this reason, another model of anti-hormone resistant breast cancer has been developed in our group. This was represented by Faslodex®-resistant MCF-7 cells, named FasR (McClelland *et al.*, 2001). Similar to that discovered for TamR cells, it was seen that this cell line exhibited a more aggressive phenotype in comparison to the parental MCF-7 cells. FasR cells displayed increased expression of the EGFR receptor, together with deletion of the ER receptor as a downstream effect induced by the action of the pure anti-oestrogen fulvestrant (McClelland *et al.*, 2001). Furthermore, these cells had increased migration and invasion which relied on the overexpression of the tyrosine kinase c-Met receptor (Hiscox *et al.*, 2006b). Overexpression of c-Met is associated with higher tumour stage, which involves increased lymph nodes involvement, a marker of tumour aggressiveness (Lengyel *et al.*, 2005). Increased expression of c-Met in FasR cells was accompanied by increased activation of Src, AKT and ERK1/2, similar to that seen in the TamR cells (Hiscox *et al.*, 2006b). Increased activation of these pathways could be a result of increased cytoplasmic zinc in this model of Faslodex® resistance, as pathways such as AKT and ERK1/2 are downstream of ZIP7-mediated zinc release (Nimmanon *et al.*, 2017).

Evidence from both preclinical and clinical studies have now recognised the activation of these pathways as the mechanism underlying the development of resistance to fulvestrant (Huang *et al.*, 2017). For this reason, treatment of ER-positive HER2-negative and ER-positive HER2-positive breast cancer has been expanded to include both anti-hormone agents together with agents targeting these downstream pathways (Nathan & Schmid, 2017). This combined therapy seems promising to enhance the anti-tumour response of anti-hormone drugs, as well as delaying the acquirement of endocrine resistance (Boér, 2017). However, this combined treatment still has a lot of limitations due to the great heterogeneity of endocrine resistance *in vivo* (Miller & Larionov, 2010; Razavi *et al.*, 2018). This issue has already been reported in studies *in vitro*. For example, a study in our group has shown that a model of long-term resistance

of FasR cells called FasRL, which better reflected the clinical spectrum, lost a significant proportion of EGFR expression (Nicholson *et al.*, 2007) and all of the HER2 receptors (Gee *et al.*, 2011). This event led to the development of a different phenotype in comparison to its parental model of short resistance (FasR). Conversely, FasR cells were discovered to exhibit an increased expression of HER2 (also known as ErbB2) receptors in comparison to MCF-7 cells (McClelland *et al.*, 2001), confirming that a long exposure to the anti-hormonal drug resulted in changes to the cell phenotype. Nevertheless, clinical data showed that patients with anti-hormone relapse did not have an obvious increase of ErbB2 receptor, suggesting that the duration of the treatment can influence the activation and response to growth factor signalling and modulate the outcome of endocrine therapy efficacy (Gee *et al.*, 2011). The lack of specific biomarkers that could predict fulvestrant response outcome remains a limitation in therapy.

For this reason, the present study has expanded the previous discovery of the involvement of zinc transporter ZIP7 in driving the aggressiveness of the tamoxifen-resistant breast cancer model (Taylor *et al.*, 2008) to the model of Falsodex® resistance. Although a previous study had already shown that ZIP7 expression was significantly increased in the MCF-7 model of Faslodex® resistant (Taylor *et al.*, 2007), no one had investigated the zinc status of this cell line. In this thesis it was shown that, as previously discovered for TamR cells, FasR cells also had a significant increase of intracellular zinc in comparison to the parental MCF-7 cells. Despite the increase of intracellular zinc, it was interesting to notice that in comparison to the TamR model, this cell line did not show increased activation of ZIP7. This was accompanied by no significant increase in the activation of downstream pathways such as AKT and MAPK, and in particular showed a significant decrease of MAPK activation in comparison to MCF-7 cells. This project proposed the possibility that the difference seen in the activation of AKT between TamR and FasR cells was due to the high expression in the FasR cells of the zinc transporter ZnT1, the only zinc transporter on the plasma membrane which exports zinc from the cell (Palmiter & Findley, 1995).

Increased expression of the zinc transporter ZnT1 was only seen previously in lymphoma-gallium resistant cells in order to counteract the cytotoxicity of gallium

nitrate on cells (Yang, Kroft & Chitambar, 2007), which is normally used as a treatment for non-Hodgkin's lymphoma (Chitambar, 2004). However, in that study the level of cytoplasmic zinc was not measured (Yang, Kroft & Chitambar, 2007). Conversely, decreased expression of ZnT1 was seen in prostate cancer (Hasumi *et al.*, 2003) which showed a decrease of cytoplasmic zinc in comparison to normal prostate tissue which had a significantly high level of zinc (Costello & Franklin, 1998). Nevertheless, it was shown that zinc treatment in human prostate cancer cells resulted in increased ZnT1 protein level (Hasumi *et al.*, 2003). These data may indicate that the overexpression of ZnT1 in FasR cells may be induced by the higher level of cytoplasmic zinc discovered in the present study and that this event was adopted by these resistant cells to prevent the cytotoxicity of increased cytoplasmic zinc. ZnT1 may function by transporting zinc out of the cells as soon as it is released in the cytoplasm, reducing the level of activation of AKT. In a recent paper in our group, it was shown that the activation of AKT in MCF-7 cells transfected with recombinant ZIP7 reached its peak between 5 to 15 minutes of zinc stimulation (Nimmanon *et al.*, 2017). In this respect, the expression of ZnT1 in the long-term resistant model of Faslodex®-breast cancer resistance (FasRL) was not as significantly increased as in FasR cells, and this could explain why FasRL cells showed a slight increase in both AKT and MAPK activation in comparison to FasR cells, although not significant.

The clinical assessment of the "Cell Signalling Series" showed direct association between pZIP7 HScore and active MAPK signalling. As it was revealed that FasR cells had no significant increased activation of pZIP7 in comparison to the parental MCF-7 cells, this would corroborate this finding, as MAPK was demonstrated to be downstream of ZIP7 activation (Nimmanon *et al.*, 2017). Nevertheless, the decrease of activated MAPK *in vitro* discovered in this study did not match with that seen in the literature, where increase of EGFR, HER2 and MAPK activity was discovered to be a common characteristic that contributed to fulvestrant resistance (Massarweh *et al.*, 2006; Frogne *et al.*, 2009). However, there was also evidence of models of fulvestrant resistance that did not belong to this category, as they showed that fulvestrant resistance was not associated to increase of HER2 expression (Larsen *et al.*, 1999), and as suggested by our model of long-term resistant of FasR which lost a large proportion of EGFR (Nicholson *et al.*, 2007)

and all of the HER2 receptors (Gee *et al.*, 2011). In this respect, it was interesting to notice that clinical assessment of pZIP7 showed a significant direct association with ErbB2 receptor, which could help us explain the results obtained in this study for pMAPK, as FasR cells were discovered not to have increased pZIP7, and ErbB2 is upstream of MAPK signalling (Ben-Levy *et al.*, 1994). Moreover, the decreased activation of MAPK discovered *in vitro* in the current project was supported by a recent study that has investigated for the first time ER-positive breast cancer clinical samples after 6 weeks, 6 months and beyond, of treatment with 250 mg/month of fulvestrant. In this paper it was discovered that biopsies of ER-positive breast cancer patients had a significant decrease of MAPK phosphorylation by 6 months of fulvestrant treatment (Agrawal *et al.*, 2016). Decrease of activated MAPK signalling could contribute to the anti-proliferative effect of fulvestrant, considering the cross-talk between the ER and MAPK signalling (Gee *et al.*, 2003; Massarweh *et al.*, 2006).

Additionally, the oestrogen receptor is phosphorylated at Ser118 by MAPK (Britton *et al.*, 2006). Therefore the fall seen in pMAPK could be responsible for the decrease of ER phosphorylation seen in some patients treated with fulvestrant (Agrawal *et al.*, 2016). The decrease of MAPK signalling would be potentially a benefit in therapy; but *in vitro* analyses of the FasR models have shown that, with additional exposure to Faslodex®, cells begin to restore MAPK activation (McClelland *et al.*, 2001; Massarweh *et al.*, 2006). This was also confirmed by evidence that biopsies of ER-positive breast cancer patients at relapse had a moderate pMAPK recovery (Agrawal *et al.*, 2016). Whether this is due to zinc needs to be investigated further, however our data suggested that the decrease in ZnT1 expression and the slight increase of pZIP7 signalling in the long-term model of Faslodex®-resistance (FasRL) may be used by these cells to contrast the anti-proliferative effect of fulvestrant and contribute to the fulvestrant resistance in therapy.

Despite highlighting the huge complexity of endocrine resistance, this study has revealed that activation of ZIP7 plays a pivotal role in the mechanism of endocrine resistance to tamoxifen, while suggesting that Faslodex®-resistance relies on other mechanisms in addition to zinc, which need to be expanded. However, the current study

has demonstrated that a higher increase in intracellular zinc and ZIP7 expression is a characteristic which is common of anti-hormone resistance models *in vitro*. Moreover, evaluation of pZIP7 in a clinical series of breast cancer samples revealed that activation of ZIP7 was evenly expressed in tumours compared to normal tissue and it hinted that pZIP7 is enriched in tumours which are HER2-positive and have active MAPK signalling, implying that pZIP7 is a good indicator of poor outcome in relation to endocrine resistance. Having developed a phospho-ZIP7 immunoassay, this now needs to be tested and supported by further clinical data, due to the high heterogeneity of breast cancer samples both *in vivo* and *in vitro*, which is one of the main limitations of this area of study. It is really important to extend the investigation at different relapse stages, considering the significant variability discovered *in vitro* between models of early and late resistance. While endocrine resistance is still a current unmet need in clinics, this study has brought new insight into this matter, which can help researchers to finally pinpoint its intricate framework.

7.2 ZIP6 or ZIP10 antibody treatment on cancer cell lines inhibits cell growth and mitosis in vitro

One of the mainstays of cancer cells is their uncontrolled cell growth which relies above all on deregulation of cell cycle controls. It is for this reason that a number of drugs targeting the cell cycle have been developed, most of which are currently being investigated by clinical trials (Asghar *et al.*, 2015; Velic *et al.*, 2015; O'Connor, 2015; Sherr, Beach & Shapiro, 2016). Despite the proven efficacy of these drugs, one of the most common problems related to their use is the lack of specificity to cancer cells which results in harm to normal cells. Therefore, the main goal of researchers nowadays is to develop targeted therapies which exploit the molecular differences of cancer cells in order to reduce side effects on healthy cells (Sherr & Bartek, 2017). The overall aim of targeted therapies is to diminish cytotoxicity on normal cells. Finding specific traits of cancer cells is crucial in the management of cancer treatment.

7.2.1 Current drugs targeting the cell cycle and their limitations

Many of the current drugs targeting the cell cycle are cyclin dependant kinase (CDK) inhibitors, as CDKs are molecules essential for the progression of the cell cycle. Among these, we find the CDK4 and CDK6 inhibitors, such as ademaciclib, palbociclib, or

ribociclib (Fry, Harvey & Keller, 2004; Kim *et al.*, 2013; Gelbert *et al.*, 2014; Sherr, Beach & Shapiro, 2016), which induce G1 phase arrest in tumour expressing the protein retinoblastoma, a tumour suppressor gene which has important implications in different cancers and which is phosphorylated by these two kinases (Meyerson & Harlow, 1994; Matsushime *et al.*, 1994). One of these inhibitors, palbociclib was recently approved by the USA Food and Drug Administration for its use in the treatment of ER-positive HER2-negative breast cancer in combination with an aromatase inhibitor, having shown the ability to extend relapse-free survival in women with advanced disease, without showing excessive toxicity (Finn *et al.*, 2015). Nevertheless, this agent alone was found to have limited activity, in comparison to its administration with an aromatase inhibitor and therefore, the co-administration of the two drugs was reported to be more effective at arresting breast cancer progression (Finn *et al.*, 2015). The limited activity of some of these agents alone represents one limitation of these drugs, together with their inability to act on tumours which lack functional retinoblastoma as they become resistant to them (Knudsen & Witkiewicz, 2017).

Another strategy is to target the S phase of the cell cycle. One of the hallmarks of cancer development is the large amounts of mutations that occur during the malfunction of DNA repair mechanisms. This event forces cells to undertake suboptimal mechanisms to preserve their genome integrity (Jackson & Bartek, 2009). One of the main causes of the failure of this mechanism is that during tumorigenesis cancer cells exhibit oncogenes overexpression and tumour suppressors downregulation, leading to replicative stress (Hills & Diffley, 2014). Under normal conditions, replicative stress is tightly controlled by the ATM/ATR kinases which activate the repair machinery and prevent proliferation of tumour cells (Shiloh, 2003; Cimprich & Cortez, 2008). Mutations of these kinases are well tolerated in cancer, as resistance to genotoxic treatment is often associated with increased DNA damage repair (Weber & Ryan, 2015). For this reason, drugs which inhibit these kinases have now been clinically tested for cancer treatment, in combination with chemotherapy or radiotherapy (Velic *et al.*, 2015). However, one of the main shortcomings of this strategy is that mutations of the DNA damage repair mechanism leads to further mutations, making their use less viable (Sherr

& Bartek, 2017). Specific biomarkers which could predict the likelihood of benefit from this treatment are therefore needed.

7.2.2 The benefit of ZIP6 and ZIP10-directed antibodies as antimitotic drugs

Drugs interfering with the G2/M phase checkpoint commonly target the Aurora A and PLK1 kinases, which are essential for the activation of the complex between CDK1 and cyclin B1 (Nigg, 2001; Keen & Taylor, 2004). These developed drugs are yet to show therapeutic clinical efficacy in solid tumours, primarily due to their inability to discern between normal and cancer cells (Huang *et al.*, 2009; Dominguez-Brauer *et al.*, 2015). Similarly, the well-known vinca alkaloids and microtubule disrupting agents which have been used for a long time in cancer treatment also present some shortcomings, including the high sensitivity of normal cells to these agents (Van Vuuren *et al.*, 2015). Moreover, these agents are limited by their failure to induce apoptosis shortly after their induced mitotic arrest (Huang *et al.*, 2009). This mechanism seems to rely on the ability of cancer cells to escape death by mitotic slippage, a mechanism that makes cells bypass apoptosis and exit mitosis without undergoing cytokinesis and then enter G1 again in a tetraploid state (Rieder & Maiato, 2004; Gascoigne & Taylor, 2008; Orth *et al.*, 2008). Although cells which undergo mitotic slippage eventually die through alternative pathways, there is still a great percentage of cells which re-enter the cell cycle (Balachandran & Kipreos, 2017). In a recent review, it was argued that there are currently no antimitotic agents which prevent the occurrence of mitotic slippage (Sherr & Bartek, 2017). For this reason, it was speculated that targeting the exit of mitosis, by targeting molecules such as cyclin B1 and CDC20, would be a better target than spindle assembly (Huang *et al.*, 2009). However, none of the current literature have addressed the implication of zinc in the regulation of cell division. As discussed in Chapter 1, zinc is essential for the progression of the cell cycle. Zinc is required for DNA synthesis (Prasad & Oberleas, 1974; Chesters, Petrie & Vint, 1989; Chesters, Petrie & Travis, 1990; Watanabe *et al.*, 1993), for the transition of cell through the G2/M phase (Chesters & Petrie, 1999; Li & Maret, 2009) and for mitosis (Beyersmann & Haase, 2001). However, it was not until our group's recent discovery of the mechanism by which ZIP6 and ZIP10 regulates the G2/M transition that the role of zinc in the regulation of the cell cycle is finally starting to be understood. The discovery of the ZIP6-ZIP10 heteromer on the plasma membrane as an essential trigger for the zinc influx necessary for mitosis (*Taylor*

et al, unpublished) has provided new exciting targets for the treatment of hyperproliferative diseases such as cancer, which could overcome some of the limitations of the current antimitotic drugs available, by reducing the chance of cells escaping cell death by mitotic slippage.

The most important finding of this present study was that the use of N-terminal specific ZIP6 and ZIP10 antibodies enabled the prevention of cell division in different cancer cell lines by blocking the zinc influx necessary to trigger mitosis. The benefit of targeting ZIP6 and ZIP10 is that these zinc transporters are expressed as pro-proteins in the endoplasmic reticulum and only available on the plasma membrane just before mitosis (Hogstrand *et al.*, 2013, *Taylor et al, unpublished*). Therefore, targeting the ZIP6-ZIP10 heteromer would limit the side effects of these agents and this treatment would potentially target specifically cells with an increased proliferation rate, such as cancer cells. Moreover, both ZIP6 and ZIP10 have been associated with epithelial to mesenchymal transition (EMT) (Yamashita *et al.*, 2004; Kagara *et al.*, 2007; Unno *et al.*, 2009; Hogstrand *et al.*, 2013; Taylor *et al.*, 2016; Brethour *et al.*, 2017), a mechanism by which epithelial cells acquire invasive and migratory properties to become mesenchymal cells, a typical hallmark of cancer (Kalluri, 2009). Both of these zinc transporters were discovered to be overexpressed in metastasis and targeting them would therefore have the additional benefit of preventing cancer spread from its initial surroundings. Since it was established that one of the main weaknesses of the current antimitotic drugs is the high chance of cells escaping cell death by mitotic slippage (Balachandran & Kipreos, 2017), it was suggested to target the exit of mitosis rather than the spindle assembly (Huang *et al.*, 2009). Evading mitotic slippage would be possible by targeting ZIP6 and ZIP10 as cells would be targeted before their entry into mitosis. There is a high chance that if blocked at the G2/M phase, cells would undergo apoptosis, and eventually die. This was supported by the evidence discovered in this study that cells showed a drastic decrease in cell growth after being treated with the ZIP6 or ZIP10 antibodies for a few days, therefore ruling out the possibility of cells re-entering the cell cycle.

Although data within this current project did not show any sign of apoptosis following a short-term cancer cell treatment with either ZIP6 or ZIP10 antibody, preliminary results in our group have demonstrated that cancer cell lines treated with the ZIP6 or ZIP10 antibody over a period of four weeks resulted in the complete cessation of cell growth followed by cell death (*Taylor et al, unpublished*). Furthermore, this investigation confirmed that when treated with one of these antibodies, cells were arrested prior to mitosis, most likely in G2, and were no longer able to progress through mitosis. A previous study demonstrated that zinc is required by the phosphatase Cdc25C to activate CDK1 and consequently meiotic entry (Sun *et al.*, 2007). This last study showed by mass spectrometry analysis that the Cdc25C is a metalloprotein binding zinc, and treatment with TPEN, a zinc metal chelator, was demonstrated to strip zinc away from the phosphatase, which compromised the ability of Cdc25C to dephosphorylate and activate the complex of cyclin B1/CDK1. Moreover, investigation within this current project of the protein kinase PLK1, which acts upstream of Cdc25C (Roshak *et al.*, 2000), has revealed a significant decrease of protein level of PLK1 in the antibody-treated samples in comparison to samples synchronised in mitosis with nocodazole. The peak level of PLK1 expression culminates during mitosis (Petronczki, Lénárt & Peters, 2008) and not surprisingly increased expression of PLK1 is found in several human tumours (Eckerdt, Yuan & Strebhardt, 2005). While there are no investigations of the direct involvement of zinc in the expression of PLK1, one study has demonstrated that cells deprived of serum resulted in a significant decrease of PLK1 mRNA expression (Holtrich *et al.*, 1994). This was argued to be due to the lack of growth factor. However, cells deprived of serum are also zinc-deficient and no effort was made to replenish the zinc. This evidence, together with the requirement of zinc for the ability of Cdc25C to regulate the entry of cells into mitosis, suggested that blocking the ZIP6/ZIP10-mediated zinc influx induced by treatment with specific ZIP6 or ZIP10 antibodies prevents the downstream activation of CDK1. Consequently, this treatment prevents the activity of the complex between cyclin B1 and CDK1 which results in failure of mitotic entry (Figure 7.2).

Other evidence that the use of the ZIP6 and ZIP10 antibodies stops cells prior to mitosis was demonstrated in this thesis by the significant decrease of cyclin B1 found in

antibody-treated cells. Not only did the expression of cyclin B1 increase normally during the G2/M transition, but cancer cells treated with antimitotic drugs such as taxol also showed normal accumulation of cyclin B1 (Ling *et al.*, 1998) due to the failure of the APC^{CDC20} ubiquitin ligase to degrade cyclin B1 during anaphase (Sherr & Bartek, 2017). Conversely, this current investigation showed that cyclin B1 is significantly reduced as a consequence of cell cycle arrest prior to mitosis when cells are treated with ZIP6 or ZIP10 antibody.

Therefore, this thesis has speculated that the mechanisms by which ZIP6 and ZIP10 prevents the cell entry into mitosis is by blocking the zinc necessary to trigger the activation of the axis of PLK1/Cdc25C responsible for the activation of the complex between cyclin B1 and CDK1, which is essential for the progression of cells through the G2 to M phase of the cell cycle (Figure 7.2).

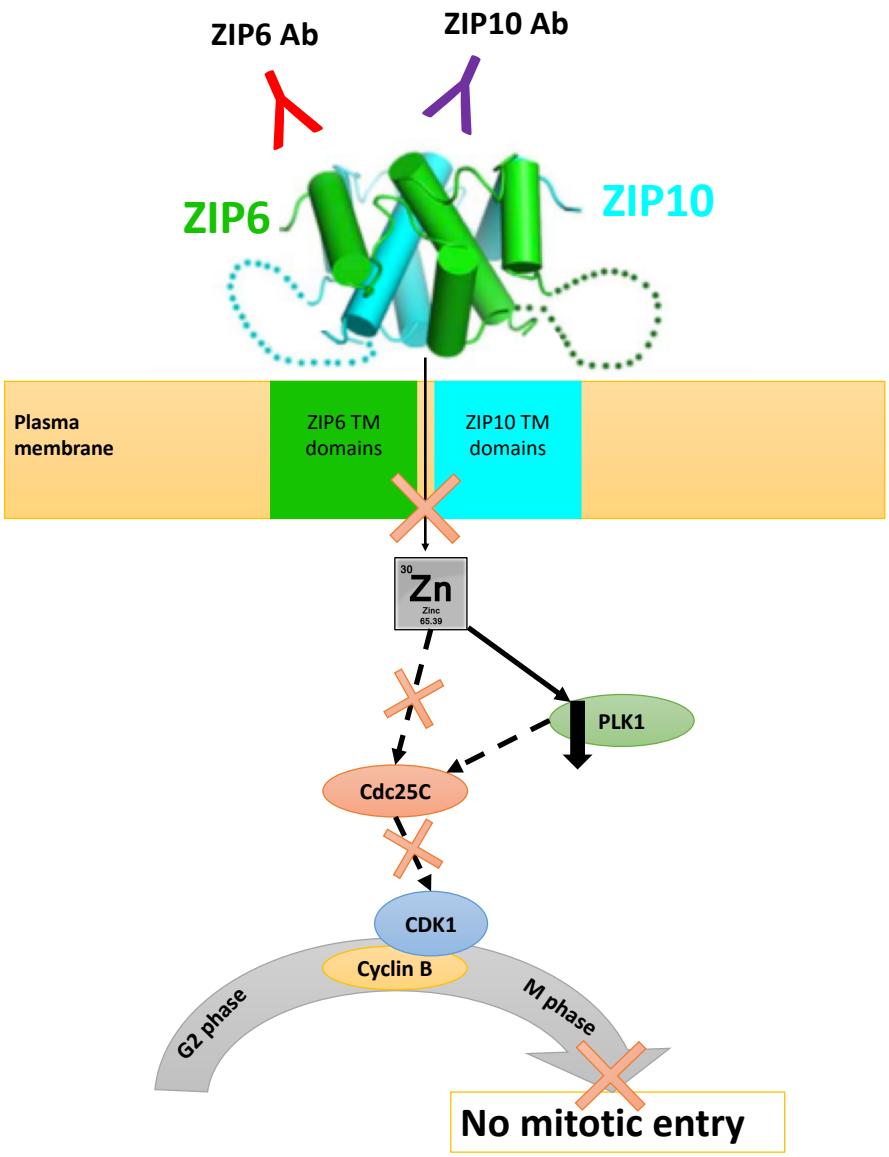

Figure 7.2 ***Mechanism of mitosis inhibition induced by ZIP6 or ZIP10 antibody treatment.***
The use of N-terminal ZIP6 or ZIP10-directed antibodies is able to block the zinc influx to trigger mitosis mediated by the ZIP6-ZIP10 heteromer. Blocking this zinc influx results in the decreased protein level of PLK1 and in failure of Cdc25C to activate the complex of cyclin B1 with CDK1, which prevents mitotic entry.

7.2.3 The potential for ZIP6 and ZIP10 antibodies as a novel immunotherapy

Dated at 2017 there were 15 monoclonal antibodies approved by the Food and Drug Administration (FDA) for treatment of solid tumours, and many others are under clinical trials, emphasising the efficacy and potential success of this type of treatment (Chiavenna, Jaworski & Vendrell, 2017). The new findings of this project are extremely promising as ZIP6 and ZIP10-directed antibodies could offer a better alternative to current anti-mitotic drugs and other drugs targeting the cell cycle which still have several limitations in the clinic (Sherr & Bartek, 2017). Whether this treatment also has some limitations will not be ascertained before animal tests are available. However, there is some promising evidence that their use *in vivo* could be successful. In fact, a novel LIV-1 antibody conjugated with a cytotoxic agent has already been developed to target ZIP6 on the plasma membrane of ER-positive breast cancer cells (Sussman *et al.*, 2014). SGN-LIV1A is a LIV-1 humanised monoclonal antibody conjugated with monomethyl auristatin E, a microtubule disrupting agent. This novel antibody was confirmed to be internalised and to give cytotoxicity *in vitro* and antitumor activity *in vivo* (Sussman *et al.*, 2014). SGN-LIV1A is currently in phase I and II clinical trials for its use in the treatment of metastatic breast cancer, including patients with triple negative breast cancer, having shown good tolerability in patients (Tray, Adams & Esteva, 2018). SGN-LIV1A is an example of an antibody-drug conjugate (ADC), an effective therapy treatment that takes advantage of the specificity of a monoclonal antibody to deliver a cytotoxic agent (Beck *et al.*, 2017). For this reason, ADCs are often considered to be more effective than delivering a naked antibody (Sassoon & Blanc, 2013). For example, it was shown that the antitumor efficacy of SGN-LIV1A was higher in xenograft models of tissue expressing a higher level of LIV-1, showing significant tumour regression (Sussman *et al.*, 2014). Most interestingly, SGN-LIV1A activity was found to be well-tolerated without any serious side effects. Furthermore, Sussman *et al* showed that LIV-1 (ZIP6) is highly expressed not only in breast cancer but also in melanoma, prostate, ovarian and uterine cancer, having a limited frequency in normal tissues (Sussman *et al.*, 2014). This finding suggests the possibility of ZIP6 as a target for the treatment of a variety of cancers. However, this paper did not show any efficacy when using the naked antibody *in vitro* to high LIV-1 expressing cell lines, such as MCF-7. This finding conflicts with that in the current thesis, therefore it is speculated that this could be due to the different epitope recognised by that antibody in comparison to ours. While the epitope

of the antibody used for the SGN-LIV1A antibody-drug conjugates comprises all of the ZIP6 N-terminal domain from residue 1 to 329 (Sussman *et al.*, 2014), our ZIP6 Y antibody recognises a smaller epitope after the PEST cleavage site of the N-terminus (residues 238-254). Our group demonstrated that ZIP6 undergoes a proteolytic cleavage at the N-terminal domain before it relocates on the plasma membrane (Hogstrand *et al.*, 2013). Therefore, that part of the N-terminus would have been cleaved off by the time ZIP6 is located on the plasma membrane prior to mitosis. This is corroborated by previous investigation in our group using a different antibody whose epitope resides at the beginning of the ZIP6 N-terminus (ZIP6 M, epitope 93-107, see Figure 2.2), which was not able to recognise mitotic ZIP6 but only pre-mitotic ZIP6. Furthermore, when tested for mitosis inhibition, the ZIP6 M was discovered to not be effective at preventing nocodazole-induced cell division (Nimmanon, 2016). For this reason, we speculate that our ZIP6 Y antibody may be more specific than the one used for the SGN-LIV1 conjugate. If this is the case, our naked antibody could be effective *in vivo* as well, as it has only been tested *in vitro* to date. However, this can only be confirmed by data from animal work, which is currently in the planning stage. If our naked ZIP6 antibody is found to be effective *in vivo*, it could have the additional benefit of reducing the side effects of cytotoxic agents which target the microtubules, the limitations of these agents having already been discussed in this chapter. Overall, it is important to highlight that this study, together with what was discovered by Sussman *et al* has confirmed the suitability of ZIP6 as a novel target for cancer therapy and has confirmed the likelihood of tolerability *in vivo*.

7.3 Downregulation of ZIP6 results in upregulation of ZIP10

The discovery that ZIP6 and ZIP10 form a heteromer has brought new insight into the understanding of how the members of the ZIP family work (Taylor *et al.*, 2016). Our group have shown that this heteromer is essential in providing the zinc necessary for cell division (*Taylor et al, unpublished*), but previous studies have also demonstrated how these zinc transporters are both involved in epithelial to mesenchymal transition, an essential step in metastasis (Yamashita *et al.*, 2004; Unno *et al.*, 2009; Lue *et al.*, 2011; Hogstrand *et al.*, 2013; Taylor *et al.*, 2016; Brethour *et al.*, 2017). Moreover, it was shown that ZIP6 forms a heteromer with ZIP10 and that this heteromer interacts with the protein NCAM1, a focal-adhesion protein, revealing that the expression of ZIP6 is

dramatically increased during EMT (Brethour *et al.*, 2017). This data emphasises the important role played by this heteromer in cell adhesion and migration, and Ulms *et al* therefore expanded this study to investigate the role played by ZIP6 in EMT and its interaction with NCAM1 by using a model of ZIP6 knockout cells. NMuMg cells were selected as host of the CRISPR-Cas9, and this cell line has been a precious tool for our group to study the effect of ZIP6 downregulation in mitosis regulation, which has not been investigated before.

In this thesis it was demonstrated how downregulation of ZIP6 had a significant impact on the growth of the ZIP6 knockout cell line in comparison to the corresponding wild type, which expresses both transporters. This result confirmed the important role played by ZIP6 in regulating cell growth, in particular of mitosis. Additionally, the ZIP6 knockout cell line was discovered to have a significant decrease of cytoplasmic zinc when compared to the parental wild type. These cells had also an increased ZIP10 protein level allowing speculation that increased ZIP10 levels had somehow been able to compensate for loss of ZIP6. Together, this data corroborated the synergy of ZIP6 and ZIP10 zinc transporters and confirmed their essential role in controlling zinc homeostasis and cell growth by acting as a heteromer. Because many studies have already suggested the similarities of these two zinc transporters, both in their structure and function (Taylor & Nicholson, 2003; Kambe *et al.*, 2006; Taylor *et al.*, 2007; Kong *et al.*, 2014; Taylor *et al.*, 2016), the ZIP6 interactome was studied in a recent study, confirming once again that ZIP6 interacts with ZIP10 and no other ZIP transporters (Brethour *et al.*, 2017). Furthermore, in this paper it was also demonstrated that ZIP6 and ZIP10 are co-regulated, meaning that the expression of one influences the expression of the other, which is typical of proteins which are part of a subunit complex. Previously, it was seen that ZIP10 downregulation in zebrafish embryos results in upregulation of ZIP6 mRNA (Taylor *et al.*, 2016). The interdependency of these two zinc transporters was further confirmed in this thesis by the evidence that the opposite was also true. In fact, ZIP6 downregulation in the knockout cell model resulted in a three-fold upregulation of ZIP10 (see Chapter 5).

The evidence that ZIP10 was upregulated in the ZIP6 knockout cells raised the question of whether ZIP10 acted as a homodimer or interacted with another member of the ZIP family in order to cope with the lack of ZIP6. Despite the crystal structure of the ZIP6-ZIP10 heteromer not being currently available, it is interesting to speculate that ZIP10 may form a homodimer to counteract the lack of ZIP6. This would not be unprecedented in the ZIP family, as a recent investigation which discovered the first crystal structure of the ectodomain of a ZIP member, has shown that the ectodomain of ZIP4 forms a dimer at the PAL structure, which is predicted to have a role in optimal zinc mobilisation (Zhang, Sui & Hu, 2016). This investigation also unveiled that this dimeric structure is a common feature of the members of the LIV-1 subfamily for proper zinc transport. This characteristic is shared also by the zinc exporters ZnT, which are known to form homodimers (reviewed by Kambe *et al.*, 2015), with the exception of ZnT5 which forms a heterodimer with ZnT6 (Fukunaka *et al.*, 2009). It was exciting to discover that these ZIP6 knockout cells had also a significant decrease of cytoplasmic zinc which explained the decreased growth rate observed when comparing their cell growth to the corresponding wild type. Since ZIP6 is required for zinc mobilisation from the plasma membrane (Taylor *et al.*, 2003), ZIP10 may form a homodimer to counteract the lack of ZIP6 and restore proper zinc homeostasis. Nevertheless, transient downregulation of ZIP10 in the ZIP6 knockout model revealed that these cells were still able to grow, although exhibiting a slower growth rate compared to the control. Another hypothesis explaining why the ZIP6 knockout cells can still grow would be that another ZIP transporter may be involved in the mobilisation of zinc from the plasma membrane together with ZIP10. As shown in the phylogenetic tree in Figure 1.3, the closest homologues to ZIP6 and ZIP10 is the zinc transporter ZIP5, which is on the same branch as these two. Interestingly, ZIP6, ZIP10 and ZIP5 share a common ancestor with the prion protein, a protein involved in neurogenerative diseases which undergoes several proteolytic cleavages similar to these zinc transporters (Schmitt-Ulms *et al.*, 2009; Ehsani *et al.*, 2011). While the study of the ZIP6 interactome did not show any direct interaction between ZIP5 and ZIP6 (Brethour *et al.*, 2017), a more recent paper has now revealed the potential for ZIP10 to interact with ZIP5 (Huttlin *et al.*, 2017). To date, there is no evidence that ZIP5 can form a heteromer like ZIP6 and ZIP10, as it was confirmed that the ectodomain of ZIP5 forms an α-helical dimeric structure similar to that of the

prion protein (Pocanschi *et al.*, 2013). Moreover, while the cell-surface-localisation of most ZIP transporters such as ZIP4 and ZIP10 increases in zinc depletion condition (Dufner-Beattie *et al.*, 2003; Lichten *et al.*, 2011), this does not happen for ZIP5 (Wang *et al.*, 2004). However, the discovery of the crystal structure of the member of the ZIP family would help us answer this query.

Furthermore, this present study has further confirmed the link between ZIP10 expression and STAT3. ZIP6 expression was already known to be transcriptionally regulated by STAT3 (Yamashita *et al.*, 2004; Taylor *et al.*, 2003), and more recently, it was discovered that ZIP10 is also transcriptionally regulated by this molecule (Miyai *et al.*, 2014). Knockdown of ZIP10 in zebrafish embryos resulted in upregulation of not only ZIP6, but also of STAT3 mRNA (Taylor *et al.*, 2016). Moreover, downregulation of either ZIP6 or ZIP10 resulted in EMT inhibition, explaining their non-redundant requirement for this event. Therefore, it was argued that the increased expression of ZIP6 and STAT3 mRNA was used as a compensatory mechanism to counteract the loss of ZIP10 (Taylor *et al.*, 2016). This is similar to what is speculated in the current study. Nevertheless, although this study did not show a significant increase of total STAT3 in the ZIP6 knockout model, it did show a significant increase of the serine S727 phosphorylation of STAT3 and an increase in tyrosine Y705 phosphorylation, albeit not significant. A previous study has shown that nocodazole induced cells displayed a decrease in pTyr^{705}STAT3 and increase of pSer^{727}STAT3, suggesting a role for the serine phosphorylation of STAT3 in the regulation of mitosis, as inhibition of serine phosphorylation of STAT3 by using an alanine-substituted mutant resulted in inhibition of the mitotic arrest induced by nocodazole (Shi *et al.*, 2006). Also our group have demonstrated that the zinc influx induced by the ZIP6-ZIP10 heteromer is responsible of the switch of pTyr^{705}STAT3 to pSer^{727}STAT3 in mitosis (*Taylor et al, unpublished*). The discovery that the ZIP6 knockout cells had an increased level of pSer^{727}STAT3 in basal conditions, which was not accompanied by a decrease of pTyr^{705}-STAT3, would corroborate the hypothesis that the overall increased protein level of activated STAT3 in the knockout model was a mechanism used by these cells to regulate ZIP10 expression in order to cope with the lack of ZIP6. Tyrosine phosphorylated STAT3 was discovered to be important for the dimerization of STAT3 and its binding to DNA (Levy & Lee, 2002)

and it was also considered as the transcriptionally active form of STAT3. In contrast, serine phosphorylated STAT3 was revealed to have a certain role in cellular growth control (Decker & Kovarik, 2000). Constitutive active pSer^{727}STAT3 but not constitutive active pTyr^{705}STAT3 was also seen in B-cells of chronic lymphocytic leukaemia (Frank, Mahajan & Ritz, 1997). This event was speculated to be a mechanism acquired by cells in order to develop a malignant phenotype, as constitutive active pSer^{727}STAT3 was not found in normal B cells. This data highlighted the importance of the serine phosphorylation of STAT3 in controlling cell proliferation and therefore corroborates its role as an oncogene (Bromberg *et al.*, 1999). Moreover, a recent paper studying the antiapoptotic effect of ZIP10 in early B-cell development has shown that activation of STAT3 regulates ZIP10 expression (Miyai *et al.*, 2014). Most importantly, this paper has also shown the potential binding sites of STAT3 in ZIP10 promoters. Taken together, it was speculated that the increased protein level of activated STAT3 discovered in the ZIP6 knockout model was a mechanism adopted by these cells in order to counteract the lack of ZIP6 and to maintain cell proliferation by regulating ZIP10 expression. This current investigation corroborated previous data that ZIP6 and ZIP10 are STAT3-regulated genes and confirmed the interdependency of these two zinc transporters by playing an essential role in cell proliferation and the regulation of the cell cycle.

7.4 Post-translational modification of ZIP6

Our understanding of the mechanism of regulation of the ZIP transporters is not clear yet, and a lot of current research on zinc transporters is focused on deciphering this. The discovery that ZIP6 and ZIP10 regulate the cell cycle has brought to our attention that the involvement of ZIP6 and ZIP10 in mitosis might be triggered by phosphorylation. This hypothesis came from the established evidence that ZIP7, another member of the LIV-1 subfamily, is activated by CK2 phosphorylation on the long intracellular loop between TM III and TM IV (Taylor *et al.*, 2012). Moreover, phosphorylation is known to be important in the regulation of the cell cycle as proteins like CDKs regulate the progression from one phase of the cell cycle to another by phosphorylating appropriate substrates (Lim & Kaldis, 2013).

7.4.1 The potential for ZIP6 to be phosphorylated by CK2

The entire eukaryotic cell cycle, but in particular mitosis, is regulated by phosphorylation, as events such as formation of mitotic spindles, cessation of transcription/translation and condensation of chromosomes all require tight control by mitotic kinases (Nigg, 2001). The most compelling result of the phosphorylation chapter was the fact that ZIP6 binds CK2 and therefore, has hinted the possibility that CK2 is phosphorylating ZIP6 in mitosis. A previous study using mass spectrometry on HeLa cells that were synchronised at different stages of the cell cycle including mitosis by double thymidine block and nocodazole had identified 3181 proteins phosphorylated during mitosis, one of which was ZIP6, which was demonstrated to be phosphorylated in mitosis on residue S478 (Dephoure *et al.*, 2008). Analysis of potential kinases responsible for the phosphorylation of ZIP6 revealed that residue S478 was predicted to be phosphorylated by the protein kinase CK2. The protein kinase CK2 is a ubiquitous kinase which is known to phosphorylate many substrates involved in gene regulation and cell growth, and the fact this its expression is significantly upregulated in cancer is further evidence of its implication in driving cell growth and proliferation (Guerra & Issinger, 1999; Pinna, 2002; Litchfield, 2003). During normal cell proliferation, CK2 protein levels increase before returning to basal conditions, while a high level is maintained in cancer cells (Trembley *et al.*, 2009). Furthermore, it was seen that depletion of CK2 blocked cell cycle progression in *Saccharomyces cerevisiae* and that CK2 was essential for the G1/S and G2/M phase transition (Glover, 1998). Therefore, the fact that the data from this thesis showed ZIP6 binding CK2 especially in mitosis, fits with previous studies which showed increased CK2 in cancer and cell proliferation (Trembley *et al.*, 2009). While it is well established that proteins such as Aurora B, PLK1 or CDK1 are only active during the G2/M phase, CK2 is constitutively active (Pinna, 2002) and its role in mitosis is therefore yet to be fully understood (Rusin, Adamo & Kettenbach, 2017). The role of CK2 in mitosis can be defined by its role as a chromosome condensation regulator (Takemoto *et al.*, 2006) and for its function in phosphorylating proteins such as Cdc25B and topoisomerase IIα/β (Daum & Gorbsky, 1998; Escargueil *et al.*, 2000; Theis-Febvre *et al.*, 2003).

Another investigation of HeLa cells that were arrested in mitosis by using the microtubule disrupting agent taxol and treated with the CK2 inhibitor CX-4945 revealed

more than 330 phosphorylation sites in 202 proteins that are significantly decreased upon inhibition of CK2 (Rusin, Adamo & Kettenbach, 2017). The phosphoproteomics data of CX-4945-treated cells from this study did not identify either ZIP6 or ZIP10 as being substrates of CK2 phosphorylation in mitosis. However, this does not necessarily rule out the possibility of ZIP6 and ZIP10 being phosphorylated by CK2. In fact, in that study cells were arrested in mitosis by using taxol (Rusin, Adamo & Kettenbach, 2017), an agent that blocks cells at the metaphase/anaphase transition (Jordan *et al.*, 1993). Therefore, it is speculated that ZIP6 could be phosphorylated by CK2, in residues other than S478, at a later stage of mitosis as a "switch off" mechanism to regulate the end of mitosis. This mechanism could regulate the degradation of ZIP6 for the progression of cells in G1. The phosphoproteomics investigation by Dephoure *et al* identified residue S478 to be phosphorylated in mitosis when cells were synchronised with nocodazole (Dephoure *et al.*, 2008). Differently from taxol which blocks cells at the metaphase/anaphase transition (Jordan *et al.*, 1993), nocodazole blocks cells in prometaphase (Blajeski *et al.*, 2002), one of the first few stages of mitosis (see Figure 1.11). Taken all together, this evidence suggested that phosphorylation of ZIP6 on residue S478 may be a prerequisite for following hierarchical phosphorylation induced by CK2 (St-denis *et al.*, 2014), which could result in ZIP6 phosphorylation on multiple sites, as the data of this thesis have suggested. In fact, while the data within this current project could not ascertain whether CK2 phosphorylated ZIP6 on residue S478, it was interesting to notice that ZIP6 has several sites that are predicted to be phosphorylated by this kinase (see Table 6.1).

7.4.2 ZIP6 is phosphorylated on multiple sites

The investigation in this thesis has unveiled that ZIP6 could be phosphorylated on multiple serine and tyrosine residues. Since CK2 is known to be involved in hierarchical phosphorylation (St-denis *et al.*, 2014), the initial phosphorylation of one residue by CK2 may be the trigger for the phosphorylation of others. Alternatively, other kinases may need to phosphorylate ZIP6 first before CK2 can exhibit its activity. In fact, the inclusion of all the residues of human ZIP6 beyond the TM III-IV cytoplasmic loop identified many serine, tyrosine and also threonine residues that could be phosphorylated not only by CK2 (see Table 6.1), but also many other kinases, confirming the potential of ZIP6 to be phosphorylated on multiple sites. To date there is no

precedence for any member of the ZIP family to be phosphorylated either on tyrosine or threonine residues, but this is an important feature to consider for future work on this area, especially in light of zinc being involved in the inhibition of tyrosine phosphatases (Haase & Maret, 2003). In this respect, tyrosine phosphorylation of ZIP6 could be sustained by the ability of zinc to inhibit tyrosine phosphatases (Haase & Maret, 2005a) and could be used as a mechanism to keep the ZIP6-ZIP10 heteromer active at the onset of mitosis. Although results within this current thesis were not able to clarify the potential of Src to phosphorylate ZIP6, the prediction of ZIP6 being phosphorylated by this kinase was exciting. In fact, the activity of Src kinase was demonstrated to increase at the G2/M phase transition and this explains why it is considered as a potential target in mitosis (Chackalaparampil & Shalloway, 1988; Fumagalli *et al.*, 1994). Furthermore, the potential involvement of Src kinase in the phosphorylation of ZIP6 was interesting in light of the role of Src family of kinases in regulating EMT (Patel *et al.*, 2016) and coupled with the evidence found in our model of endocrine resistant breast cancer which exhibits increased cell motility and invasiveness accompanied by increased Src kinase activity (Hiscox *et al.*, 2006c, 2006b). In this chapter it was speculated that the EMT-like behaviour and aggressive phenotype of the TamR cells could be due to the ZIP6 and ZIP7-mediated zinc signalling. Considering the discovery that CK2 bound ZIP6, particularly in mitosis, it may suggest that tyrosine phosphorylation of ZIP6 could be used as a "switch on" mechanism at the onset of mitosis, whereas CK2 phosphorylation could be used as a "switch off" mechanism towards the end of mitosis which could lead to the degradation of the ZIP6-ZIP10 heteromer. This speculation is corroborated by the evidence that the Src family of kinases are involved in the tyrosine phosphorylation of CK2, which results in increased catalytic activity of CK2 (Donella-Deana *et al.*, 2003). This evidence would support the hypothesis of the synergistic activity of these two kinases in controlling the role of ZIP6 during mitosis. However, the possibility that ZIP6 could be phosphorylated on multiple sites have made this investigation more complicated than expected, and for this reason this hypothesis now needs to be confirmed by future investigations.

Whilst this study did not confirm a specific site for the phosphorylation of ZIP6, it has provided important information in helping us to decipher how ZIP6 is regulated in

mitosis. The discovery of the specific CK2-mediated phosphorylation sites of ZIP6 could lead us to develop a new monoclonal antibody directed against the phosphorylated form-only of ZIP6, as our group have already generated for ZIP7 (Nimmanon *et al.*, 2017). This would be an extremely valuable tool for future analyses of ZIP6 phosphorylation and to investigate its role in mitosis.

7.4.3 Proteolytic cleavage of ZIP6 is essential for its function

Proteolytic cleavage is an important event undertaken by proteins in response to an extracellular stimulus which induces proteins to have a different conformation and, most importantly, a different function (Rogers & Overall, 2013). Protein cleavage is essential in cell biology for several functions, not merely for protein degradation. For example, protein cleavage is important in the activation of proteins that are initially expressed as inactive precursors, also referred to as pro-proteins (Shinde & Inouye, 1993). Thus, proteolytic cleavage of pro-proteins is essential for the relocation of these molecules to subcellular compartments where they exhibit their action (Shinde & Inouye, 2000). Proteolytic cleavage is also important for the regulation of the cell cycle, as for example, degradation of cyclins is regulated by ubiquitin-induced proteolysis (Glotzer, Murray & Kirschner, 1991; Hershko, 1997). Another important proteolytic event in mitosis occurs by the action of the anaphase-promoting complex (APC), a ubiquitin-ligase which is responsible for chromosomes segregation and controlling the transition from metaphase to anaphase (King *et al.*, 1996).

ZIP6 is expressed as a pro-protein in the endoplasmic reticulum and it is only after it gets cleaved on the N-terminal domain, that it relocates to the plasma membrane (Hogstrand *et al.*, 2013). The investigation within this current project has confirmed that the full-length of ZIP6 is typical of ZIP6 as a pro-protein, as the active form of ZIP6 during mitosis requires the N-terminus proteolytic cleavage, as previously confirmed by Hogstrand *et al*, 2013. Furthermore, a recent investigation in our group has also discovered that ZIP6 is cleaved a second time on its ectodomain at the onset of mitosis, suggesting that these cleavages have an important role in the ZIP6-mediated mitosis regulation (Nimmanon, 2016). Cleavage of the ZIP10 ectodomain during mitosis was also confirmed by recent data in our group which identified the presence of a cleaved ectodomain band which is increased in nocodazole-induced mitotic samples (data not

shown). Additionally, it was discovered that both ZIP6 and ZIP10 have a potential PEST cleavage site on the long intracellular loop between TM III and TM IV. PEST cleavage sites are typical of proteins with a very short half-life, often less than two hours (Rogers, Wells & Rechsteiner, 1986). Proteins containing PEST cleavage sites are regulated by proteolysis and not surprisingly many of these proteins are involved in the regulation of the cell cycle, such as p53 or cyclins (Rechsteiner & Rogers, 1996). This feature highlights the importance of the rapid turnover of proteins which regulates the cell cycle, as the cell cycle needs to be tightly controlled in order to prevent any aberrations occurring and it is also time-regulated in each different type of cells (Weber *et al.*, 2014). Interestingly, since ZIP6 and ZIP10 are involved in the regulation of mitosis, which is the shortest stage of the cell cycle, the presence of a few PEST cleavage sites in these molecules highlights that they may be degraded immediately after mitosis. The presence of a potential intracellular cleavage site for the members of the ZIP family has never been investigated before. This current investigation has suggested the possibility of a cytoplasmic cleavage since the presence of a lower 35 kDa ZIP6 band on western blotting. Although the function of this cleavage has not been explored yet, it was speculated that this cleavage could be of a "switch off" mechanism at the end of mitosis to allow degradation of the protein following its increase on the plasma membrane at the onset of mitosis. The potential for ZIP6 and ZIP10 to undergo cytoplasmic cleavage may be important for their roles in mitosis and progression of cells into G1.

Moreover, ZIP6, ZIP10 and ZIP5 are the three members of the LIV-1 subfamily that share similarities with the N-terminus sequence of the cellular prion protein (PrP^{c}) (Schmitt-Ulms *et al.*, 2009). The prion protein plays a major role in neurodegenerative diseases, as this protein is highly expressed in the nervous system (Prusiner, 1991). In the disease, the cellular prion protein (PrP^{c}) undergoes structural modifications that leads to transition into its disease-causing form (PrP^{Sc}) which involves the refolding of its structure into β-sheets and makes it protease-resistant (Prusiner, 1998). One of the common features that the ZIP transporters share with the prion protein is the remodelling of their ectodomain caused by proteolytic cleavages. The prion protein undergoes three main proteolytic cleavages: an α-cleavage (Vincent *et al.*, 2000), β-cleavage (McMahon *et al.*, 2001) and ectodomain shedding (Borchelt *et al.*, 1993;

Altmeppen *et al.*, 2012). Similar to that seen for ZIP6 (Hogstrand *et al.*, 2013), also ZIP10 undergoes a proteolytic cleavage at its ectodomain, akin to the one of the prion protein (Ehsani *et al.*, 2012). In this study it was shown that ZIP10 is N-glycosylated and that its ectodomain is cleaved off showing a 45 kDa band on a western blot, as a result of this cleavage when cells were starved of transition metals. In particular, during zinc starvation the expression of the full-length of ZIP10 was increased (Ehsani *et al.*, 2012), suggesting the importance of ZIP10 as a zinc importer located on the plasma membrane. This is not unprecedented, as previous studies have seen that expression of zinc transporters such as ZIP2 (Inoue *et al.*, 2014), ZIP4 (Andrews, 2008) or ZIP10 (Ryu *et al.*, 2008) were increased in conditions of zinc starvation, highlighting the importance of these zinc transporters in maintaining appropriate zinc homeostasis.

Investigation of the potential of presenilin to cleave ZIP6 did not confirm whether this protease is responsible for the cleavage of ZIP6 during mitosis. Nevertheless, considering the similarities between ZIP6 and ZIP10 to the prion protein (Schmitt-Ulms *et al.*, 2009), it was interesting to observe that the use of a presenilin inhibitor perturbated ZIP6 cleavage. A previous study has discovered that presenilin is involved in the transcription of cellular prion protein and that the use of the presenilin inhibitor DAPT significantly decreased its expression (Vincent *et al.*, 2009). Similarly, here it was found that the overall ZIP6 protein level of both the full length and mitosis-activated form was affected by the use of the same presenilin inhibitor, suggesting a potential role for presenilin in the regulation of ZIP6 transcription, similar to that revealed for the prion protein (Vincent *et al.*, 2009). Altogether these data have confirmed the importance of proteolytic cleavage in the regulation of ZIP6 in mitosis, and has provided the first evidence that presenilin may be involved in the regulation of ZIP6.

7.5 General study limitations and future considerations

The data presented in the current thesis has examined the role played by ZIP7, ZIP6 and ZIP10 in regulating different aspects of aggressive cancer behaviour, as well as discussed the benefit of using them as targets for proliferative diseases such as cancer. However, it is worth mentioning that the follow-up of these new findings needs to take into consideration several aspects:

- A new immunohistochemistry assay was developed for phospho-ZIP7; however, this was tested in one small series of clinical materials at breast cancer diagnosis. Considering the widespread heterogeneity of breast cancer patients (Razavi *et al.*, 2018), this assay can now be used in different series of clinical materials by using samples from breast cancer tissue banks which include also patients at relapse. This investigation would confirm the feasibility of phospho-ZIP7 as a biomarker of anti-hormone resistant breast cancer *in vivo* and could be the first step for future investigations aimed at targeting ZIP7 activation by using CK2 inhibitors.

- The data showed in this study for the mitotic inhibition was explored in 2D *in vitro* cell models, and whilst this is highly beneficial and essential for understanding cancer biology and discovering new molecular targets, these findings now need to be confirmed also *in vivo.* This could be attained by confirming whether this treatment is well tolerated in cancer animal models, and whether the treatment is effective at reducing the cancer growth of existing tumours as was achieved *in vitro.* The potential for a collaboration with a research group which has breast cancer animal models available for testing has already been discussed. The initial plan would be to administer the treatment via tail vein injection with the aim of assessing also the potential of this treatment to be tolerated by animals and whether it would be able to stop and reduce tumour growth. Further analyses would also investigate the likelihood of this treatment to stop metastasis.

- The phosphorylation analysis has provided some interesting results that could be further investigated with the combination of other techniques such as affinity chromatography and mass spectrometry, due to the likely complexity of results suggesting involvement of multiple sites. However, this thesis project has unveiled the feasibility of ZIP6 knockout cells as a good setting for investigating ZIP6 phosphorylation by using recombinant ZIP6 proteins which now needs the use of multiple mutants. Collaborations with other research groups could be considered. In particular, our group have previously discussed the potential of a

collaboration with Tine Thingholm and her research group in Denmark which is specialised in mass spectrometry and they are interested in studying the role of protein phosphorylation in zinc transporters.

7.6 General conclusion

The data discussed in this thesis has confirmed the involvement of zinc signalling in different aspects of cancer development, in particular the establishment of a more aggressive phenotype. The investigation of ZIP7, ZIP6 and ZIP10 have revealed that these zinc transporters can be novel targets for cancer treatment. This study has linked for the first time the role of ZIP7 in driving the aggressive behaviour of tamoxifen-resistant breast cancer cells together with ZIP6 by inducing epithelial to mesenchymal transition. Moreover, it has provided the first immunoassay for activated ZIP7 that can now be further investigated as a biomarker of breast cancer, considering the enrichment of pZIP7 in breast cancer samples in comparison to tumour associated normal breast tissue. Additionally, this study has highlighted the potential for ZIP7 to be targeted in therapy in order to prevent the progression of breast cancer, in particular the development of endocrine resistance, which is one of the main burdens in therapy.

The discovery that N-terminal ZIP6 and ZIP10-directed antibodies were effective at preventing mitotic entry has unveiled new therapeutic agents for the treatment of proliferative diseases, such as cancer. This investigation also discovered that these two zinc transporters act synergically, reason why a combined therapy could be tested further. It is crucial to carry on the investigation on these antibodies to determine whether their use can be beneficial in therapy and whether they can represent better antimitotic agents than the ones that are currently available.

8 REFERENCES

Agrawal, A., Robertson, J.F.R., Cheung, K.L., Gutteridge, E., et al. (2016) Biological effects of fulvestrant on estrogen receptor positive human breast cancer: Short, medium and long-term effects based on sequential biopsies. *International Journal of Cancer*. **138** (1), 146–159.

Alessi, D.R., Andjelkovic, M., Caudwell, B., Cron, P., et al. (1996) Mechanism of activation of protein kinase B by insulin and IGF-1. *The EMBO journal*. **15** (23), 6541–6551.

Altmeppen, H.C., Puig, B., Dohler, F., Thurm, D.K., et al. (2012) Proteolytic processing of the prion protein in health and disease. *American Journal of Neurodegenerative Disease*. **1** (1), 15–31.

Andreini, C., Banci, L., Bertini, I. & Rosato, A. (2006) Counting the zinc-proteins encoded in the human genome. *Journal of proteome research*. **5** (1), 196–201.

Andrews, G.K. (2008) Regulation and function of Zip4, the acrodermatitis enteropathica gene. *Biochemical Society transactions*. **36** (6), 1242–1246.

Ardito, F., Giuliani, M., Perrone, D., Troiano, G., et al. (2017) The crucial role of protein phosphorylation in cell signaling and its use as targeted therapy (Review). *International Journal of Molecular Medicine*. **40**, 271–280.

Arpino, G., Milano, M. & De Placido, S. (2015) Features of aggressive breast cancer. *Breast*. **24** (5), 594–600.

Asghar, U., Witkiewicz, A.K., Turner, N.C. & Knudsen, E.S. (2015) The history and future of targeting cyclin-dependent kinases in cancer therapy. *Nature Reviews Drug Discovery*. **14** (2), 130–146.

Baer, M.T. & King, J.C. (1984) Tissue zinc levels and zinc excretion during experimental zinc depletion in young men. *American Journal of Clinical Nutrition*. **39** (4), 556–570.

Bafaro, E., Liu, Y., Xu, Y. & Dempski, R.E. (2017) The emerging role of zinc transporters in cellular homeostasis and cancer. *Signal Transduction and Targeted Therapy*. **2** (April), 17029.

Balachandran, R.S. & Kipreos, E.T. (2017) Addressing a weakness of anticancer therapy with mitosis inhibitors: Mitotic slippage. *Molecular and Cellular Oncology*. **4** (2), 1–3.

Barret, A.J., Rawlings, N.D. & Woessner, J.F. (1998) *Handbook of proteolytic enzymes*. Academic P. London.

Bartlett, J.M.S., Brookes, C.L., Robson, T., Velde, C.J.H. Van De, et al. (2011) Estrogen Receptor and Progesterone Receptor As Predictive Biomarkers of Response to Endocrine Therapy : A Prospectively Powered Pathology Study in the Tamoxifen and Exemestane Adjuvant Multinational Trial. *Journal of Clinical Oncology*. **29** (12), 1531–1538.

Batlle, E., Sancho, E., Francí, C., Domínguez, D., et al. (2000) The transcription factor Snail is a repressor of E-cadherin gene expression in epithelial tumour cells. *Nature Cell Biology*. **2** (2), 84–89.

Beck, A., Goetsch, L., Dumontet, C. & Corvaïa, N. (2017) Strategies and challenges for the next generation of antibody–drug conjugates. *Nature Reviews Drug Discovery*. **16** (5), 315–337.

Bek, S. & Kemler, R. (2002) Protein kinase CKII regulates the interaction of beta-catenin with alpha-catenin and its protein stability. *Journal of Cell Science*. **115** (24), 4743–4753.

Bellomo, E., Massarotti, A., Hogstrand, C. & Maret, W. (2014) Zinc ions modulate protein tyrosine phosphatase 1B activity. *Metallomics*. **6** (7), 1229–1239.

Ben-Levy, R., Paterson, H.F., Marshall, C.J. & Yarden, Y. (1994) A single autophosphorylation site confers oncogenicity to the Neu/ErbB-2 receptor and enables coupling to the MAP kinase pathway. *The EMBO journal*. **13** (14), 3302–3311.

Bernhardt, M.L., Kim, A.M., O'Halloran, T. V & Woodruff, T.K. (2011) Zinc requirement during meiosis I-meiosis II transition in mouse oocytes is independent of the MOS-MAPK pathway. *Biology of Reproduction*. **84** (3), 526–536.

Bernhardt, M.L., Kong, B.Y., Kim, A.M., O'Halloran, T. V., et al. (2012) A Zinc-Dependent Mechanism Regulates Meiotic Progression in Mammalian Oocytes1. *Biology of Reproduction*. **86** (4), 1–10.

Beyersmann, D. & Haase, H. (2001) Functions of zinc in signaling, proliferation and differentiation of mammalian cells. *BioMetals*. **14** (3–4), 331–341.

Bikle, D.D. (2011) Vitamin D Metabolism and Function in the Skin. Molecular and cellular endocrinology. *Molecular and cellular endocrinology.* **347** (1–2), 80–89.

Bin, B.-H., Bhin, J., Takaishi, M., Toyoshima, K.-E., et al. (2017) Requirement of zinc transporter ZIP10 for epidermal development: Implication of the ZIP10-p63 axis in

epithelial homeostasis. *Proceedings of the National Academy of Sciences*. **114** (46), 12243–12248.

Bjornsti, M.A. & Houghton, P.J. (2004) The TOR pathway: A target for cancer therapy. *Nature Reviews Cancer*. **4** (5), 335–348.

Blagosklonny, M. V. (2011) Cell cycle arrest is not senescence. *Aging*. **3** (2), 94–101.

Blajeski, A.L., Phan, V. a, Kottke, T.J. & Kaufmann, S.H. (2002) G1 and G2 cell-cycle arrest following microtubule depolymerization in human breast cancer cells. *The Journal of Clinical Investigation*. **110** (1), 91–99.

Blom, N., Sicheritz-Pontén, T., Gupta, R., Gammeltoft, S., et al. (2004) Prediction of post-translational glycosylation and phosphorylation of proteins from the amino acid sequence. *Proteomics*. **4** (6), 1633–1649.

Boér, K. (2017) Fulvestrant in advanced breast cancer: evidence to date and place in therapy. *Therapeutic Advances in Medical Oncology*. **9** (7), 465–479.

Bohnsack, B.L. & Hirschi, K.K. (2004) Nutrient Regulation of Cell Cycle Progression. *Annual Review of Nutrition*. **24**, 433–453.

Borchelt, D.R., Rogers, M., Stahp, N. & Prusiner, S.B. (1993) Release of the cellular prion protein from cultured cells after loss of its glycoinositol phospholipid anchor. *Glycobiology*. **3** (4), 319–329.

Bray, F., Ferlay, J., Soerjomataram, I., Siegel, R., et al. (2018) Global Cancer Statistics 2018 : GLOBOCAN Estimates of Incidence and Mortality Worldwide for 36 Cancers in 185 Countries. *CA: A Cancer Journal for Clinicians*. **68**, 394–424.

Bray, S.J. (2016) Notch signalling in context. *Nature Reviews Molecular Cell Biology*. **17** (11), 722–735.

Brethour, D., Mehrabian, M., Williams, D., Wang, X., et al. (2017) A ZIP6-ZIP10 heteromer controls NCAM1 phosphorylation and integration into focal adhesion complexes during epithelial-to-mesenchymal transition. *Scientific Reports*. **7** (January), 40313.

Britton, D.J., Hutcheson, I.R., Knowlden, J.M., Barrow, D., et al. (2006) Bidirectional cross talk between ERα and EGFR signalling pathways regulates tamoxifen-resistant growth. *Breast Cancer Research and Treatment*. **96** (2), 131–146.

Bromberg, J. (2002) Stat proteins and oncogenesis. *Journal of Clinical Investigation*. **109** (9), 1139–1142.

Bromberg, J., Wrzeszczynska, M., Devgan, G., Zhao, Y., et al. (1999) Stat3 as an oncogene. *Cell*. **98** (6), 295–303.

Brown, M., Thom, J., Orth, G., Cova, P., et al. (1964) Food poisoning involving zinc contamination. *Archives of Environmental Health*. **8** (May), 657–660.

Brunton, V.G., Avizienyte, E., Fincham, V.J., Serrels, B., et al. (2005) Identification of Src-specific phosphorylation site on focal adhesion kinase: Dissection of the role of Src SH2 and catalytic functions and their consequences for tumor cell behavior. *Cancer Research*. **65** (4), 1335–1342.

Buettner, R., Mora, L.B. & Jove, R. (2002) Activated STAT Signaling in Human Tumors Provides Novel Molecular Targets for Therapeutic Intervention Activated STAT Signaling in Human Tumors Provides Novel Molecular Targets for Therapeutic Intervention 1. *Clinical Cancer Research*. **8** (April), 945–954.

Bui, Q.T., Im, J.H., Jeong, S.B., Kim, Y.M., et al. (2017) Essential role of Notch4/STAT3 signaling in epithelial–mesenchymal transition of tamoxifen-resistant human breast cancer. *Cancer Letters*. **390**, 115–125.

Bush, A.I., Pettingell, W.H., Paradis, M.D. & Tanzi, R.E. (1994) Modulation of Aβ adhesiveness and secretase site cleavage by zinc. *Journal of Biological Chemistry*. **269** (16), 12152–12158.

Van Campen, D.R. (1969) Copper Interference with the Intestinal Absorption of Zinc-65 by Rats. *The Journal of Nutrition*. **97** (1), 104–108.

Cano, A., Pérez-moreno, M.A., Rodrigo, I., Locascio, A., et al. (2000) The transcription factor Snail controls epithelial – mesenchymal transitions by repressing E-cadherin expression. *Nature Cell Biology*. **2** (February), 76–83.

Carioli, G., Malvezzi, M., Rodriguez, T., Bertuccio, P., et al. (2018) Trends and predictions to 2020 in breast cancer mortality: Americas and Australasia. *Breast*. **37**, 163–169.

Chackalaparampil, I. & Shalloway, D. (1988) Altered Phosphotylation and Activation of pp60 c-src during Fibroblast Mitosis. *Cell*. **52** (March), 801–810.

Chang, F., Lee, J.T., Navolanic, P.M., Steelman, L.S., et al. (2003) Involvement of PI3K/Akt pathway in cell cycle progression, apoptosis, and neoplastic transformation: a target for cancer chemotherapy. *Leukemia*. **17** (3), 590–603.

Chantalat, L., Leroy, D., Filhol, O., Nueda, A., et al. (1999) Crystal structure of the human protein kinase CK2 regulatory subunit reveals its zinc finger-mediated dimerization.

EMBO Journal. **18** (11), 2930–2940.

Charlwood, P.A. (1979) The relative affinity of transferrin and albumin for zinc. *Biochimica et Biophysica Acta*. **581** (2), 260–265.

Chen, Z., Gibson, T.B., Robinson, F., Silvestro, L., et al. (2001) MAP kinases. *Chemical Reviews*. **101** (8), 2449–2476.

Chesters, J.K. (1972) The Role of Zinc Ions in the Transformation of Lymphocytes by Phytohaemagglutinin. *Biochemical Journal*. (130), 133–139.

Chesters, J.K. & Petrie, L. (1999) A possible role for cyclins in the zinc requirements during G1 and G2 phases of the cell cycle. *Journal of Nutritional Biochemistry*. **10** (99), 279–290.

Chesters, J.K., Petrie, L. & Travis, A.J. (1990) A requirement for Zn2+ for the induction of thymidine kinase but not ornithine decarboxylase in 3T3 cells stimulated from quiescence. *The Biochemical journal*. **272** (2), 525–527.

Chesters, J.K., Petrie, L. & Vint, H. (1989) Specificity and timing of the Zn2+ requirement for DNA synthesis by 3T3 cells. *Experimental cell research.* **184** (2), 499–508.

Chiavenna, S.M., Jaworski, J.P. & Vendrell, A. (2017) State of the art in anti-cancer mAbs. *Journal of Biomedical Science*. **24** (15), 1–12.

Chimienti, F., Favier, A. & Seve, M. (2005) ZnT-8, a pancreatic beta-cell-specific zinc transporter. *BioMetals*. **18** (4), 313–317.

Chitambar, C. (2004) Gallium nitrate for the treatment of non-Hodgkin's lymphoma. *Expert opinion on investigational drugs*. **13** (5), 531–541.

Chon, H.J., Bae, K.J., Lee, Y. & Kim, J. (2015) The casein kinase 2 inhibitor , CX-4945 , as an anti-cancer drug in treatment of human hematological malignancies. *Frontiers in Pharmacology*. **6** (March), 1–5.

Cimprich, K.A. & Cortez, D. (2008) ATR: An essential regulator of genome integrity. *Nature Reviews Molecular Cell Biology*. **9** (8), 616–627.

Clarke, R., Tyson, J.J. & Dixon, J.M. (2015) *Endocrine resistance in breast cancer - An overview and update*.

Cleveland, D.W., Mao, Y. & Sullivan, K.F. (2003) Centromeres and Kinetochores: from Epigentics to Mitotic Checkpoint Signaling. *Cell*. **112**, 407–421.

Colvin, R.A., Bush, A.I., Volitakis, I., Fontaine, C.P., et al. (2008) *Insights into Zn 2 ε homeostasis in neurons from experimental and modeling studies*. **45701**, 726–742.

Colvin, R.A., Holmes, W.R., Fontaine, C.P. & Maret, W. (2010) Cytosolic zinc buffering and muffling: their role in intracellular zinc homeostasis. *Metallomics*. **2** (5), 306–317.

Costello, L.C. & Franklin, R.B. (1998) Novel Role of Zinc in the Regulation of Prostate Citrate Metabolism and Its Implications in Prostate Cancer. *The prostate*. **35**, 285–296.

Cottu, P., Bièche, I., Assayag, F., El Botty, R., et al. (2014) Acquired resistance to endocrine treatments is associated with tumor-specific molecular changes in patient-derived luminal breast cancer xenografts. *Clinical Cancer Research*. **20** (16), 4314–4325.

Coudray, N., Valvo, S., Hu, M., Lasala, R., et al. (2013) Inward-facing conformation of the zinc transporter YiiP revealed by cryoelectron microscopy. *Proceedings of the National Academy of Sciences*. **110** (6), 2140–2145.

Dai, X., Li, T., Bai, Z., Yang, Y., et al. (2015) Breast cancer intrinsic subtype classification, clinical use and future trends. *American journal of cancer research*. **5** (10), 2929–2943.

Daum, J.R. & Gorbsky, G.J. (1998) Casein Kinase II Catalyzes a Mitotic Phosphorylation on Threonine 1342 of Human DNA Topoisomerase IIα, Which Is Recognized by the 3F3/2 Phosphoepitope Antibody. *The Journal of Biological Chemistry*. **273** (46), 30622–30629.

Decker, T. & Kovarik, P. (2000) Serine phosphorylation of STATs. *Oncogene*. **19** (21), 2628–2637.

Dephoure, N., Zhou, C., Villén, J., Beausoleil, S.A., et al. (2008) A quantitative atlas of mitotic phosphorylation. *Proceedings of the National Academy of Sciences*. **105** (31), 10762–10767.

Dereeper, A., Guignon, V., Blanc, G., Audic, S., et al. (2008) Phylogeny.fr: robust phylogenetic analysis for the non-specialist. *Nucleic acids research*. **36** (Web Server issue), 465–469.

Deshiere, A., Duchemin-Pelletier, E., Spreux, E., Ciais, D., et al. (2013) Unbalanced expression of CK2 kinase subunits is sufficient to drive epithelial-to-mesenchymal transition by Snail1 induction. *Oncogene*. **32** (11), 1373–1383.

Dinkel, H., Roey, K., Michael, S., Kumar, M., et al. (2016) ELM 2016 - Data update and

new functionality of the eukaryotic linear motif resource. *Nucleic Acids Research*. **44** (D1), D294–D300.

Dixon, J.M. (2014) Endocrine Resistance in Breast Cancer. *New Journal of Science*. **2014** (10), 1–27.

Dominguez-Brauer, C., Thu, K.L., Mason, J.M., Blaser, H., et al. (2015) Targeting Mitosis in Cancer: Emerging Strategies. *Molecular Cell*. **60** (4), 524–536.

Donella-Deana, A., Cesaro, L., Sarno, S., Ruzzene, M., et al. (2003) Tyrosine phosphorylation of protein kinase CK2 by Src-related tyrosine kinases correlates with increased catalytic activity. *The Biochemical journal*. **372**, 841–849.

Duckert, P., Brunak, S. & Blom, N. (2004) Prediction of proprotein convertase cleavage sites. *Protein Engineering, Design & Selection*. **17** (1), 107–112.

Dufner-Beattie, J., Wang, F., Kuo, Y., Gitschier, J., et al. (2003) The Acrodermatitis Enteropathica Gene ZIP4 Encodes a Tissue-specific , Zinc-regulated Zinc Transporter in Mice. *The Journal of Biological Chemistry*. **278** (35), 33474–33481.

Dufner-Beattie, J., Weaver, B.P., Geiser, J., Bilgen, M., et al. (2007) The mouse acrodermatitis enteropathica gene Slc39a4 (Zip4) is essential for early development and heterozygosity causes hypersensitivity to zinc deficiency. *Human molecular genetics*. **16** (12), 1391–1399.

Dunnwald, L.K., Rossing, M.A. & Li, C.I. (2007) Hormone receptor status, tumor characteristics, and prognosis: A prospective cohort of breast cancer patients. *Breast Cancer Research*. **9** (1), 1–10.

Dutertre, M. & Smith, C.L. (2000) Molecular mechanisms of selective estrogen receptor modulator (SERM) action. *The Journal of pharmacology and experimental therapeutics*. **295** (2), 431–437.

Eckerdt, F., Yuan, J. & Strebhardt, K. (2005) Polo-like kinases and oncogenesis. *Oncogene*. **24** (2), 267–276.

Edge, S., Byrd, D., Compton, C., Fritz, A., et al. (2010) *AJCC cancer staging manual (7th ed).* New York, Springer.

Ehsani, S., Huo, H., Salehzadeh, A., Pocanschi, C.L., et al. (2011) Family reunion – The ZIP / prion gene family. *Progress in Neurobiology*. **93** (3), 405–420.

Ehsani, S., Salehzadeh, A., Huo, H., Reginold, W., et al. (2012) LIV-1 ZIP ectodomain shedding in prion-infected mice resembles cellular response to transition metal

starvation. *Journal of molecular biology*. **422** (4), 556–574.

Elomaa, O., Pulkkinen, K., Hannelius, U., Mikkola, M., et al. (2001) Ectodysplasin is released by proteolytic shedding and binds to the EDAR protein. *Human Molecular Genetics*. **10** (9), 953–962.

Ertefai, B. (2016) *Resistance mechanisms during endocrine treatment in breast cancer.* Cardiff University.

Escargueil, A.E., Plisov, S.Y., Filhol, O., Cochet, C., et al. (2000) Mitotic Phosphorylation of DNA Topoisomerase IIα by Protein Kinase CK2 Creates the MPM-2 Phosphoepitope on Ser-1469. *The Journal of Biological Chemistry*. **275** (44), 34710–34718.

Evans, T., Rosenthal, E.T., Youngblom, J., Dan, D., et al. (1983) Cyclin: A protein Specified by Maternal mRNA in Sea Urchin Eggs That is Destroyed at Each Cleavage Division. *Cell*. **33** (June), 389–396.

Fagerberg, L., Hallström, B.M., Oksvold, P., Kampf, C., et al. (2014) Analysis of the Human Tissue-specific Expression by Genome-wide Integration of Transcriptomics and Antibody-based Proteomics. *Molecular & Cellular Proteomics*. **13** (2), 397–406.

Falchuk, K.H., Fawcett, D.W. & Vallee, B.L. (1975) Role of zinc in cell division of Euglena gracilis. *Journal of Cell Science*. **17**, 57–78.

Fanzo, J.C., Reaves, S.K., Cui, L., Zhu, L., et al. (2001) Zinc status affects p53, gadd45, and c-fos expression and caspase-3 activity in human bronchial epithelial cells. *Am J Physiol Cell Physiol*. **281** (2), 751–757.

Fededa, J.P. & Gerlich, D.W. (2012) Molecular control of animal cell cytokinesis. *Nature Cell Biology*. **14** (5), 440–447.

Figlewicz, D.P., Forhan, S.E., Hodgson, A.T. & Grodsky, G.M. (1984) 65Zinc and endogenous zinc content and distribution in islets in relationship to insulin content. *Endocrinology*. **115** (3), 877–881.

Finn, R.S., Crown, J.P., Lang, I., Boer, K., et al. (2015) The cyclin-dependent kinase 4/6 inhibitor palbociclib in combination with letrozole versus letrozole alone as first-line treatment of oestrogen receptor-positive, HER2-negative, advanced breast cancer (PALOMA-1/TRIO-18): A randomised phase 2 study. *The Lancet Oncology*. **16** (1), 25–35.

Fiol, C.J., Mahrenholz, A.M., Wang, Y., Roeske, R.W., et al. (1987) Formation of protein

kinase recognition sites by covalent modification of the substrate. Molecular mechanism for the synergistic action of casein kinase II and glycogen synthase kinase 3. *Journal of Biological Chemistry*. **262** (29), 14042–14048.

Fisher, D., Krasinska, L., Coudreuse, D. & Novak, B. (2012) Phosphorylation network dynamics in the control of cell cycle transitions. *Journal of Cell Science*. **125** (20), 4703–4711.

Fraker, P.J. (2005) Recent Advances in Nutritional Sciences Roles for Cell Death in Zinc. *The Journal of Nutrition*. **135** (3), 359–362.

Frank, D.A., Mahajan, S. & Ritz, J. (1997) B lymphocytes from patients with chronic lymphocytic leukemia contain signal transducer and activator of transcription (STAT) 1 and STAT3 constitutively phosphorylated on serine residues. *Journal of Clinical Investigation*. **100** (12), 3140–3148.

Franklin, R.B., Feng, P., Milon, B., Desouki, M.M., et al. (2005) hZIP1 zinc uptake transporter down regulation and zinc depletion in prostate cancer. *Molecular cancer*. **4**, 32.

Franklin, R.B., Levy, B.A., Zou, J., Hanna, N., et al. (2012) ZIP14 Zinc Transporter Downregulation and Zinc Depletion in the Development and Progression of Hepatocellular Cancer. *Journal of gastrointestinal cancer*. **43** (2), 249–257.

Frederickson, C.J. & Bush, a I. (2001) Synaptically released zinc: physiological functions and pathological effects. *Biometals : an international journal on the role of metal ions in biology, biochemistry, and medicine*. **14** (3–4), 353–366.

Frogne, T., Benjaminsen, R. V., Sonne-Hansen, K., Sorensen, B.S., et al. (2009) Activation of ErbB3, EGFR and Erk is essential for growth of human breast cancer cell lines with acquired resistance to fulvestrant. *Breast Cancer Research and Treatment*. **114** (2), 263–275.

Fry, D., Harvey, P. & Keller, P. (2004) Specific inhibition of cyclin-dependent kinase 4/6 by PD 0332991 and associated antitumor activity in human tumor xenografts. *Molecular Cancer Therapeutics*. **3** (November), 1427–1438.

Fry, M.J. (2001) Phosphoinositide 3-kinase signalling in breast cancer: How big a role might it play? *Breast Cancer Research*. **3** (5), 304–312.

Fujioka, M. & Lieberman, I. (1964) A Zn ++ Requirement for Synthesis of Deoxyribonucleic Acid by Rat Liver. *The Journal of Biological Chemistry*. **239** (4).

Fujishiro, H., Yano, Y., Takada, Y., Tanihara, M., et al. (2012) Roles of ZIP8, ZIP14, and DMT1 in transport of cadmium and manganese in mouse kidney proximal tubule cells. *Metallomics*. **4** (7), 700–708.

Fukada, T., Yamasaki, S., Nishida, K., Murakami, M., et al. (2011) Zinc homeostasis and signaling in health and diseases. *Journal of Biological Inorganic Chemistry*. **16** (7), 1123–1134.

Fukunaka, A., Suzuki, T., Kurokawa, Y., Yamazaki, T., et al. (2009) Demonstration and Characterization of the Heterodimerization of ZnT5 and ZnT6 in the Early Secretory Pathway. *The Journal of Biological Chemistry*. **284** (45), 30798–30806.

Fumagalli, S., Totty, N.F., Hsuan, J.J. & Courtneidge, S.A. (1994) A target for Src in mitosis. *Nature*. **368** (April), 871–874.

Gaither, L.A. & Eide, D.J. (2001) Eukaryotic zinc transporters and their regulation. *BioMetals*. **14** (3–4), 251–270.

Gao, J., Zhao, N., Knutson, M.D. & Enns, C.A. (2008) The hereditary hemochromatosis protein, HFE, inhibits iron uptake via down-regulation of Zip14 in HepG2 Cells. *Journal of Biological Chemistry*. **283** (31), 21462–21468.

Garai, K., Sengupta, P., Sahoo, B. & Maiti, S. (2006) Selective destabilization of soluble amyloid β oligomers by divalent metal ions. *Biochemical and Biophysical Research Communications*. **345** (1), 210–215.

Gascoigne, K.E. & Taylor, S.S. (2008) Cancer Cells Display Profound Intra- and Interline Variation following Prolonged Exposure to Antimitotic Drugs. *Cancer Cell*. **14** (2), 111–122.

Gasteiger, E., Hoogland, C., Gattiker, A., Duvaud, S., et al. (2005) Protein Identification and Analysis Tools on the ExPASy Server. In: *The Proteomics Protocols Handbook, Humana Press*. p.

Gavet, O. & Pines, J. (2010a) Activation of cyclin B1-Cdk1 synchronizes events in the nucleus and the cytoplasm at mitosis. *Journal of Cell Biology*. **189** (2), 247–259.

Gavet, O. & Pines, J. (2010b) Progressive Activation of CyclinB1-Cdk1 Coordinates Entry to Mitosis. *Developmental Cell*. **18** (4), 533–543.

Gee, J.M., Meng, M.Y., McClelland, Richard A. Mottram, H.J., Kyme, S.R., et al. (2015) A new cell panel to study oestrogen receptor loss in acquired endocrine resistant breast cancer. *Cancer Research*. **75** (9).

Gee, J.M.W., Harper, M.E., Hutcheson, I.R., Madden, T.A., et al. (2003) The Antiepidermal Growth Factor Receptor Agent Gefitinib (ZD1839/Iressa) Improves Antihormone Response and Prevents Development of Resistance in Breast Cancer in Vitro. *Endocrinology*. **144** (11), 5105–5117.

Gee, J.M.W., Nicholson, R.I., Barrow, D., Dutkowski, C.M., et al. (2011) Antihormone induced compensatory signalling in breast cancer: An adverse event in the development of endocrine resistance. *Hormone Molecular Biology and Clinical Investigation*. **5** (2), 67–77.

Gee, J.M.W., Robertson, J.F.R., Ellis, I.O. & Nicholson, R.I. (2001) Phosphorylation of Erk1 / 2 Mitogen-Activated Protein Kinase Is Associated With Poor Response To Anti-Hormonal Therapy and decreased patient survival in clinical breast cancer. *International Journal of Cancer*. **95**, 247–254.

Gee, J.M.W.G., Willsher, P.C.W., Kenny, F.S.K., Robertson, J.F.R.R., et al. (1999) Endocrine response and resistance in breast cancer: a role for the transcription factor Fos. *International Journal of Cancer*. **61** (June 1998), 54–61.

Gelbert, L.M., Cai, S., Lin, X., Sanchez-Martinez, C., et al. (2014) Preclinical characterization of the CDK4/6 inhibitor LY2835219: In-vivo cell cycle-dependent/independent anti-tumor activities alone/in combination with gemcitabine. *Investigational New Drugs*. **32** (5), 825–837.

Gheghiani, L., Loew, D., Lombard, B., Mansfeld, J., et al. (2017) PLK1 Activation in Late G2 Sets Up Commitment to Mitosis. *Cell Reports*. **19** (10), 2060–2073.

Giusiano, S., Cochet, C., Filhol, O., Duchemin-Pelletier, E., et al. (2011) Protein kinase CK2α subunit over-expression correlates with metastatic risk in breast carcinomas: Quantitative immunohistochemistry in tissue microarrays. *European Journal of Cancer*. **47** (5), 792–801.

Gladden, A.B. & Diehl, J.A. (2003) Cell cycle progression without cyclin E/CDK2. *Cancer Cell*. **4** (3), 160–162.

Glotzer, M., Murray, A.W. & Kirschner, M.W. (1991) Cyclin is degraded by the ubiquitin pathway. *Nature*. **349**, 132–138.

Glover, C. (1998) On the physiological role of casein kinase II in Saccharomyces cerevisiae. *Prog Nucleic Acid Res Mol Biol*. **59**, 95–133.

Gnad, F., Gunawardena, J. & Mann, M. (2011) PHOSIDA 2011: The posttranslational

modification database. *Nucleic Acids Research*. **39** (SUPPL. 1), 253–260.

Goel, S., Decristo, M.J., Watt, A.C., Brinjones, H., et al. (2017) CDK4/6 inhibition triggers anti-tumour immunity. *Nature*. **548** (7668), 471–475.

Guerinot, M. Lou (2000) The ZIP family of metal transporters. *Biochimica et Biophysica Acta*. **1465** (1–2), 190–198.

Guerra, B. & Issinger, O.-G. (1999) Protein kinase CK2 and its role in cellular proliferation , development and pathology. *Electrophoresis*. **20**, 391–408.

Gurley, L.R., Anna, J.A.D., Barham, S.S., Deaven, L.L., et al. (1978) Histone Phosphorylation and Chromatin Structure during Mitosis in Chinese Hamster Cells. *European Journal of Biochemistry*. **15**, 1–15.

Haase, H. & Maret, W. (2005a) Fluctuations of cellular, available zinc modulate insulin signaling via inhibition of protein tyrosine phosphatases. *Journal of Trace Elements in Medicine and Biology*. **19** (1 SPEC. ISS.), 37–42.

Haase, H. & Maret, W. (2003) Intracellular zinc fluctuations modulate protein tyrosine phosphatase activity in insulin/insulin-like growth factor-1 signaling. *Experimental Cell Research*. **291** (2), 289–298.

Haase, H. & Maret, W. (2005b) Protein tyrosine phosphatases as targets of the combined insulinomimetic effects of zinc and oxidants. *BioMetals*. **18** (4), 333–338.

Habashy, H.O., Powe, D.G., Staka, C.M., Rakha, E.A., et al. (2010) Transferrin receptor (CD71) is a marker of poor prognosis in breast cancer and can predict response to tamoxifen. *Breast Cancer Research and Treatment*. **119**, 283–293.

Han, Y., Gol, J.M., Lippard, S.J. & Palmer, A.E. (2018) Superiority of SpiroZin2 Versus FluoZin-3 for monitoring vesicular Zn 2 + allows tracking of lysosomal Zn 2 + pools. *Scientific Reports*. **8** (September), 1–15.

Hanstein, B., Djahansouzi, S., Dall, P., Beckmann, M.W., et al. (2004) Insights into the molecular biology of the estrogen receptor define novel therapeutic targets for breast cancer. *European Journal of Endocrinology*. **150** (3), 243–255.

Harsha, H.C. & Pandey, A. (2010) Phosphoproteomics in cancer. *Molecular Oncology*. **4** (6), 482–495.

Hasumi, M., Suzuki, K., Matsui, H., Koike, H., et al. (2003) Regulation of metallothionein and zinc transporter expression in human prostate cancer cells and tissues. *Cancer Letters*. **200** (2), 187–195.

Haura, E.B., Turkson, J. & Jove, R. (2005) Mechanisms of disease: Insights into the emerging role of signal transducers and activators of transcription in cancer. *Nature Clinical Practice Oncology*. **2** (6), 325–324.

Hayes, T.K. & Der, C.J. (2007) Targeting the Raf-MEK-ERK mitogen-activated protein kinase cascade for the treatment of cancer. *Oncogene*. **26**, 3291–3310.

Henshall, S.M., Afar, D.E.H., Rasiah, K.K., Horvath, L.G., et al. (2003) Expression of the zinc transporter ZnT4 is decreased in the progression from early prostate disease to invasive prostate cancer. *Oncogene*. **22** (38), 6005–6012.

Hershko, A. (1997) Roles of ubiquitin-mediated proteolysis in cell cycle control. *Current Opinion in Cell Biology*. **9** (6), 788–799.

Hills, S.A. & Diffley, J.F.X. (2014) DNA replication and oncogene-induced replicative stress. *Current Biology*. **24** (10), R435–R444.

Hiscox, S., Barnfather, P., Hayes, E., Bramble, P., et al. (2011) Inhibition of focal adhesion kinase suppresses the adverse phenotype of endocrine-resistant breast cancer cells and improves endocrine response in endocrine-sensitive cells. *Breast Cancer Research and Treatment*. **125**, 659–669.

Hiscox, S., Jiang, W.G., Obermeier, K., Taylor, K., et al. (2006a) Tamoxifen resistance in MCF7 cells promotes EMT-like behaviour and involves modulation of β-catenin phosphorylation. *International Journal of Cancer*. **118** (2), 290–301.

Hiscox, S., Jordan, N.J., Jiang, W., Harper, M., et al. (2006b) Chronic exposure to fulvestrant promotes overexpression of the c-Met receptor in breast cancer cells: Implications for tumour-stroma interactions. *Endocrine-Related Cancer*. **13** (4), 1085–1099.

Hiscox, S., Jordan, N.J., Morgan, L., Green, T.P., et al. (2007) Src kinase promotes adhesion-independent activation of FAK and enhances cellular migration in tamoxifen-resistant breast cancer cells. *Clinical and Experimental Metastasis*. **24** (3), 157–167.

Hiscox, S., Morgan, L., Barrow, D., Dutkowski, C., et al. (2004) Tamoxifen resistance in breast cancer cells is accompanied by an enhanced motile and invasive phenotype: Inhibition by gefitinib ('Iressa', ZD1839). *Clinical and Experimental Metastasis*. **21**, 201–212.

Hiscox, S., Morgan, L., Green, T.P., Barrow, D., et al. (2006c) Elevated Src activity

promotes cellular invasion and motility in tamoxifen resistant breast cancer cells. *Breast Cancer Research and Treatment*. **97** (3), 263–274.

Ho, E., Courtemanche, C. & Ames, B.N. (2003) Zinc deficiency induces oxidative DNA damage and increases p53 expression in human lung fibroblasts. *American Society for Nutritional Sciences*. **133** (8), 2543–2548.

Hogstrand, C., Kille, P., Ackland, M.L., Hiscox, S., et al. (2013) A mechanism for epithelial-mesenchymal transition and anoikis resistance in breast cancer triggered by zinc channel ZIP6 and STAT3 (signal transducer and activator of transcription 3). *The Biochemical journal*. **455** (2), 229–237.

Hogstrand, C., Kille, P., Nicholson, R.I. & Taylor, K.M. (2009) Zinc transporters and cancer: a potential role for ZIP7 as a hub for tyrosine kinase activation. *Trends in Molecular Medicine*. **15** (February), 101–111.

Hojyo, S., Miyai, T., Fujishiro, H., Kawamura, M., et al. (2014) Zinc transporter SLC39A10/ZIP10 controls humoral immunity by modulating B-cell receptor signal strength. *Proceedings of the National Academy of Sciences of the United States of America*. **111** (32), 11786–11791.

Holtrich, U., Wolf, G., Bräuninger, A., Karn, T., et al. (1994) Induction and down-regulation of PLK, a human serine/threonine kinase expressed in proliferating cells and tumors. *Proceedings of the National Academy of Sciences*. **91**, 1736–1740.

Hooper, N.M. (1994) Families of zinc metalloproteases. *FEBS Letters*. **354**, 1–6.

Horn, H., Schoof, E.M., Kim, J., Robin, X., et al. (2014) KinomeXplorer: An integrated platform for kinome biology studies. *Nature Methods*. **11** (6), 603–604.

Hornbeck, P. V., Zhang, B., Murray, B., Kornhauser, J.M., et al. (2015) PhosphoSitePlus, 2014: Mutations, PTMs and recalibrations. *Nucleic Acids Research*. **43** (D1), D512–D520.

Huang, D., Yang, F., Wang, Y. & Guan, X. (2017) Mechanisms of resistance to selective estrogen receptor down-regulator in metastatic breast cancer. *Biochimica et Biophysica Acta - Reviews on Cancer*. **1868** (1), 148–156.

Huang, G., Yan, H., Ye, S., Tong, C., et al. (2014) STAT3 phosphorylation at tyrosine 705 and serine 727 differentially regulates mouse ES cell fates. *Stem Cells*. **32** (5), 1149–1160.

Huang, H.-C., Shi, J., Orth, J.D. & Mitchison, T.J. (2009) Evidence that mitotic exit is a

better cancer therapeutic target than spindle assembly. *Cancer Cell*. **16** (4), 347–358.

Huang, L., Kirschke, C.P., Zhang, Y. & Yan, Y.Y. (2005) The ZIP7 gene (Slc39a7) encodes a zinc transporter involved in zinc homeostasis of the Golgi apparatus. *Journal of Biological Chemistry*. **280** (15), 15456–15463.

Huttlin, E.L., Bruckner, R.J., Paulo, J.A., Cannon, J.R., et al. (2017) Architecture of the human interactome defines protein communities and disease networks. *Nature*. **545** (7655), 505–509.

Ilouz, R., Kaidanovich, O., Gurwitz, D. & Eldar-Finkelman, H. (2002) Inhibition of glycogen synthase kinase-3beta by bivalent zinc ions: insight into the insulin-mimetic action of zinc. *Biochemical and biophysical research communications*. **295** (1), 102–106.

Inoue, Y., Hasegawa, S., Ban, S., Yamada, T., et al. (2014) ZIP2 protein, a zinc transporter, is associated with keratinocyte differentiation. *Journal of Biological Chemistry*. **289** (31), 21451–21462.

Jackson, S.P. & Bartek, J. (2009) The DNA-damage response in human biology and disease. *Nature*. **461** (7267), 1071–1078.

Jayaraman, A.K. & Jayaraman, S. (2011) Increased level of exogenous zinc induces cytotoxicity and up-regulates the expression of the ZnT-1 zinc transporter gene in pancreatic cancer cells. *The Journal of nutritional biochemistry*. **22** (1), 79–88.

Jenkitkasemwong, S., Wang, C.-Y., Mackenzie, B. & Knutson, M.D. (2012) Physiologic implications of metal-ion transport by ZIP14 and ZIP8. *BioMetals*. **25** (4), 643–655.

Ji, H., Wang, J., Nika, H., Hawke, D., et al. (2009) EGF-induced ERK activation promotes CK2-mediated disassociation of α-catenin from β-catenin and transactivation of β-catenin. *Molecular Cell*. **36** (4), 547–559.

Jiang, L.-J., Maret, W. & Vallee, B.L. (1998) The glutathione redox couple modulates zinc transfer from metallothionein to zinc-depleted sorbitol dehydrogenase. *Proceedings of the National Academy of Sciences*. **95** (7), 3483–3488.

Jin, R., Bay, B., Tan, P. & Tan, B. (1999) Metallothionein expression and zinc levels in invasive ductal breast carcinoma. *Oncology Reports*. **6.4**, 871–876.

John, E., Laskow, T.C., Buchser, W.J., Pitt, B.R., et al. (2010) Zinc in innate and adaptive tumor immunity. *Journal of translational medicine*. **8** (1), 118.

Johnson, L.N. (2009) The regulation of protein phosphorylation. *Biochemical Society*

Transactions. **37** (4), 627–641.

Johnston, S.R.D. (2004) Clinical Pharmacology of SERMs and Pure Anti-estrogens. In: James N. Ingle & Mitchell Dowsett (eds.). *Advances in Endocrine Therapy of Breast Cancer*. Summit Communications. pp. 1–15.

Jong, N.N. & McKeage, M.J. (2014) Emerging roles of metal solute carriers in cancer mechanisms and treatment. *Biopharmaceutics & drug disposition*. **2835**, 450–462.

Jordan, M.A., Toso, R.J., Thrower, D. & Wilson, L. (1993) Mechanism of mitotic block and inhibition of cell proliferation by taxol at low concentrations. *Proceedings of the National Academy of Sciences*. **90** (October), 9552–9556.

Jordan, N.J., Dutkowski, C.M., Barrow, D., Mottram, H.J., et al. (2014) Impact of dual mTORC1/2 mTOR kinase inhibitor AZD8055 on acquired endocrine resistance in breast cancer in vitro. *Breast Cancer ResearchCancer Research*. **16** (12).

Jordan, N.J., Gee, J.M.W., Barrow, D., Wakeling, A.E., et al. (2004) Increased constitutive activity of PKB/Akt in tamoxifen resistant breast cancer MCF-7 cells. *Breast Cancer Research and Treatment*. **87** (2), 167–180.

Julien, S.G., Dubé, N., Read, M., Penney, J., et al. (2007) Protein tyrosine phosphatase 1B deficiency or inhibition delays ErbB2-induced mammary tumorigenesis and protects from lung metastasis. *Nature Genetics*. **39** (3), 338–346.

Kagara, N., Tanaka, N., Noguchi, S. & Hirano, T. (2007) Zinc and its transporter ZIP10 are involved in invasive behavior of breast cancer cells. *Cancer science*. **98** (5), 692–697.

Kalluri, R. (2009) EMT: When epithelial cells decide to become mesenchymal-like cells. *Journal of Clinical Investigation*. **119** (6), 1417–1419.

Kalluri, R. & Weinberg, R. a (2009) The basics of epithelial-mesenchymal transition. *Journal of Clinical Investigation*. **119** (6), 1420–1428.

Kambe, T. & Andrews, G.K. (2009) Novel proteolytic processing of the ectodomain of the zinc transporter ZIP4 (SLC39A4) during zinc deficiency is inhibited by acrodermatitis enteropathica mutations. *Molecular and cellular biology*. **29** (1), 129–139.

Kambe, T., Suzuki, T., Nagao, M. & Yamaguchi-Iwai, Y. (2006) Sequence similarity and functional relationship among eukaryotic ZIP and CDF transporters. *Genomics, Proteomics and Bioinformatics*. **4** (1), 1–9.

Kambe, T., Tsuji, T., Hashimoto, A. & Itsumura, N. (2015) The physiological, biochemical,

and molecular roles of zinc transporters in zinc homeostasis and metabolism. *Physiological Reviews*. (344), 749–784.

Kato, S., Endoh, H., Masuhiro, Y., Masushige, S., et al. (1995) Activation of the Estrogen Receptor Through Phosphorylation by Mitogen-Activated Protein Kinase. *Science*. **270** (5241), 1491–1494.

Kawachi, M., Kobae, Y., Kogawa, S., Mimura, T., et al. (2012) Amino acid screening based on structural modeling identifies critical residues for the function, ion selectivity and structure of Arabidopsis MTP1. *FEBS Journal*. **279** (13), 2339–2356.

Keen, N. & Taylor, S. (2004) Aurora-kinase inhibitors as anticancer agents. *Nature Reviews Cancer*. **4** (12), 927–936.

Kerr, J.F.R. (2002) History of the events leading to the formulation of the apoptosis concept. *Toxicology*. **181**–**182**, 471–474.

Kim, A.M., Vogt, S., Halloran, T.V.O. & Woodruff, T.K. (2010) Zinc Availability Regulates Exit from Meiosis in Maturing Mammalian Oocytes. *Nature Chemical Biology*. **6** (9), 674–681.

Kim, J. & Hwan Kim, S. (2013) CK2 Inhibitor CX-4945 Blocks TGF-β1-Induced Epithelial-to-Mesenchymal Transition in A549 Human Lung Adenocarcinoma Cells. *PLoS ONE*. **8** (9), 1–13.

Kim, M.R., Choi, H.K., Cho, K. Bin, Kim, H.S., et al. (2009) Involvement of Pin1 induction in epithelial-mesenchymal transition of tamoxifen-resistant breast cancer cells. *Cancer Science*. **100** (10), 1834–1841.

Kim, S., Jung, Y., Kim, D., Koh, H., et al. (2000) Extracellular zinc activates p70 S6 kinase through the phosphatidylinositol 3-kinase signaling pathway. *Journal of Biological Chemistry*. **275** (34), 25979–25984.

Kim, S., Loo, A., Chopra, R., Caponigro, G., et al. (2013) Abstract PR02: LEE011: An orally bioavailable, selective small molecule inhibitor of CDK4/6- Reactivating Rb in cancer. *Molecular cancer Therapeutics*. **12** ((11 Suppl):Abstract nr PR02.).

Kim, Y.H., Kim, E.Y., Gwag, B.J., Sohn, S., et al. (1999) Zinc-induced cortical neuronal death with features of apoptosis and necrosis: Mediation by free radicals. *Neuroscience*. **89** (1), 175–182.

Kim, Y.H. & Koh, J.Y. (2002) The role of NADPH oxidase and neuronal nitric oxide synthase in zinc-induced poly(ADP-ribose) polymerase activation and cell death in

cortical culture. *Experimental Neurology*. **177** (2), 407–418.

King, J.C. (2011) Zinc: An essential but elusive nutrient. *American Journal of Clinical Nutrition*. **94** (2), 679–684.

King, R.W., Deshaies, R.J., Peters, J. & Kirschner, M.W. (1996) How Proteolysis Drives the Cell Cycle. *Science*. **3011** (1995).

Kinlaw, W.B., Levine, A.S., Morley, J.E., Silvis, S.E., et al. (1983) Abnormal zinc metabolism in type II diabetes mellitus. *The American Journal of Medicine*. **75** (2), 273–277.

Kitabayashi, C., Fukada, T., Kanamoto, M., Ohashi, W., et al. (2010) Zinc suppresses Th17 development via inhibition of STAT3 activation. *International Immunology*. **22** (5), 375–386.

Klein, T., Eckhard, U., Dufour, A., Solis, N., et al. (2018) Proteolytic Cleavage - Mechanisms, Function, and 'omic' Approaches for a Near-Ubiquitous Posttranslational Modification. *Chemical Reviews*. **118** (3), 1137–1168.

Knowlden, J.M., Hutcheson, I.R., Barrow, D., Gee, J.M.W., et al. (2005) Insulin-like growth factor-I receptor signaling in tamoxifen-resistant breast cancer: A supporting role to the epidermal growth factor receptor. *Endocrinology*. **146** (11), 4609–4618.

Knowlden, J.M., Hutcheson, I.R., Jones, H.E., Madden, T., et al. (2003) Elevated Levels of Epidermal Growth Factor Receptor/c-erbB2 Heterodimers Mediate an Autocrine Growth Regulatory Pathway in Tamoxifen-Resistant MCF-7 Cells. *Endocrinology*. **144** (3), 1032–1044.

Knudsen, E.S. & Witkiewicz, A.K. (2017) The Strange Case of CDK4/6 Inhibitors: Mechanisms, Resistance, and Combination Strategies. *Trends in Cancer*. **3** (1), 39–55.

Koff, A., Cross, F., Fisher, A., Schumacher, J., et al. (1991) Human cyclin E, a new cyclin that interacts with two members of the CDC2 gene family. *Cell*. **66** (6), 1217–1228.

Kong, B., Duncan, F., Que, E., AM, K., et al. (2014) Maternally-derived zinc transporters ZIP6 and ZIP10 drive the mammalian oocyte-to-egg transition. *Molecular human reproduction*. **20** (11), 1077–1089.

Krasilnikov, M., Adler, V., Fuchs, S.Y., Dong, Z., et al. (1999) Contribution of phosphatidylinositol 3-kinase to radiation resistance in human melanoma cells.

Molecular Carcinogenesis. **24** (1), 64–69.

Krężel, A., Hao, Q. & Maret, W. (2007) The zinc / thiolate redox biochemistry of metallothionein and the control of zinc ion X uctuations in cell signaling. *Archives of Biochemistry and Biophysics*. **463**, 188–200.

Kuiper, G.G.J.M., Enmark, E., Pelto-Huikko, M., Nilsson, S., et al. (1996) Cloning of a novel estrogen receptor expressed in rat prostate and ovary. *Proceedings of the National Academy of Sciences*. **93** (June), 5925–5930.

Kyung, H.C., Basma, H., Singh, J. & Cheng, P.W. (2005) Activation of CMV promoter-controlled glycosyltransferase and β-galactosidase glycogenes by butyrate, tricostatin A, and 5-aza-2′-deoxycytidine. *Glycoconjugate Journal*. **22** (1–2), 63–69.

Lansdown, A.B.G., Mirastschijski, U., Stubbs, N., Scanlon, E., et al. (2007) Zinc in wound healing: Theoretical, experimental, and clinical aspects. *Wound Repair and Regeneration*. **15** (1), 2–16.

Larionov, A.A. & Miller, W.R. (2009) Challenges in defining predictive markers for response to endocrine therapy in breast cancer. *Future oncology*. **9** (5), 1415–1428.

Larkin, M.A., Blackshields, G., Brown, N.P., Chenna, R., et al. (2007) Clustal W and Clustal X version 2.0. *Bioinformatics*. **23** (21), 2947–2948.

Larsen, S.S., Egeblad, M., Jäättelä, M. & Lykkesfeldt, A.E. (1999) Acquired antiestrogen resistance in MCF-7 human breast cancer sublines is not accomplished by altered expression of receptors in the ErbB-family. *Breast Cancer Research and Treatment*. **58**, 41–56.

Lee, S., Chanoit, G., McIntosh, R., Zvara, D. a, et al. (2009) Molecular mechanism underlying Akt activation in zinc-induced cardioprotection. *American journal of physiology. Heart and circulatory physiology*. **297** (2), H569-75.

Van Leeuwen, J., Van Driel, M., Van Dem BemD, G. & Pols, H. (2011) Vitamin D control of osteoblast function and bone extracellular matrix mineralization. *Critical Reviews in Eukaryotic Gene Expression*. **11** (1–3), 199–226.

Lengyel, E., Prechtel, D., Resau, J.H., Gauger, K., et al. (2005) c-Met overexpression in node-positive breast cancer identifies patients with poor clinical outcome independent of Her2/neu. *International Journal of Cancer*. **113** (4), 678–682.

Leptin, M. & Grunenwald, B. (1990) Cell shape changes during gastrulation in Drosophila. *Development*. **110**, 73–84.

Levi, F., Lucchini, F., Negri, E. & La Vecchia, C. (2004) Trends in mortality from major cancers in the European Union, including acceding countries, in 2004. *Cancer*. **101** (12), 2843–2850.

Levy, D.E. & Lee, C. (2002) What does Stat3 do? *J. Clin. Invest.* **109** (9), 1143–1148.

Lew, D.J., Dulić, V. & Reed, S.I. (1991) Isolation of three novel human cyclins by rescue of G1 cyclin (Cln) function in yeast. *Cell*. **66** (6), 1197–1206.

Lewis, L.J. (2010) *Deciphering Faslodex resistance in breast cancer*. Cardiff University.

Li, M., Zhang, Y., Bharadwaj, U., Zhai, Q., et al. (2009) Down-regulation of ZIP4 by RNA interference inhibits pancreatic cancer growth and increases the survival of nude mice with pancreatic cancer xenografts. *Clinical Cancer Research*. **15** (19), 5993–6001.

Li, M., Zhang, Y., Liu, Z., Bharadwaj, U., et al. (2007) Aberrant expression of zinc transporter ZIP4 (SLC39A4) significantly contributes to human pancreatic cancer pathogenesis and progression. *Proceedings of the National Academy of Sciences*. **104** (47), 18636–18641.

Li, X., Wilmanns, M., Thornton, J. & Köhn, M. (2013) Elucidating human phosphatase-substrate networks. *Science Signaling*. **6** (275), 1–15.

Li, Y. & Maret, W. (2009) Transient fluctuations of intracellular zinc ions in cell proliferation. *Experimental Cell Research*. **315** (14), 2463–2470.

Lichten, L.A., Ryu, M.S., Guo, L., Embury, J., et al. (2011) MTF-1-mediated repression of the Zinc transporter Zip10 is alleviated by Zinc restriction. *PLoS ONE*. **6** (6), 1–12.

Lim, S. & Kaldis, P. (2013) Cdks, cyclins and CKIs: roles beyond cell cycle regulation. *Development*. **140** (15), 3079–3093.

Ling, Y.H., Consoli, U., Tornos, C., Andreeff, M., et al. (1998) Accumulation of cyclin B1, activation of cyclin B1-dependent kinase and induction of programmed cell death in human epidermoid carcinoma KB cells treated with taxol. *International Journal of Cancer*. **75** (6), 925–932.

Litchfield, D.W. (2003) Protein kinase CK2: structure, regulation and role in cellular decisions of life and death. *Biochemical Journal*. **369**, 1–15.

Liu, R.Y., Zeng, Y., Lei, Z., Wang, L., et al. (2014) JAK/STAT3 signaling is required for TGF-β-induced epithelial- mesenchymal transition in lung cancer cells. *International Journal of Oncology*. **44** (5), 1643–1651.

Liuzzi, J.P. & Cousins, R.J. (2004) Mammalian Zinc Transporters. *Annual review of nutrition*. **24**, 151–172.

Lloyd, R. V, Erickson, L. a, Jin, L., Kulig, E., et al. (1999) p27kip1: A Multifunctional Cyclin-Dependent Kinase Inhibitor with Prognostic Significance in Human Cancers. *American Journal pf Pathology*. **154** (2), 313–323.

Lopez, V., Foolad, F. & Kelleher, S.L. (2011) ZnT2-overexpression represses the cytotoxic effects of zinc hyper-accumulation in malignant metallothionein-null T47D breast tumor cells. *Cancer Letters*. **304** (1), 41–51.

Lu, M. & Fu, D. (2007) Structure of the zinc transporter YiiP. *Science*. **317** (5845), 1746–1748.

Lue, H.W., Yang, X., Wang, R., Qian, W., et al. (2011) LIV-1 promotes prostate cancer epithelial-to-mesenchymal transition and metastasis through HB-EGF shedding and EGFR-mediated ERK signaling. *PLoS ONE*. **6** (11).

Lupien, M., Meyer, C.A., Bailey, S.T., Eeckhoute, J., et al. (2010) Growth factor stimulation induces a distinct ERα cistrome underlying breast cancer endocrine resistance. *Genes and Development*. **24** (19), 2219–2227.

Ma, Z., Wang, X., He, J., Xia, J., et al. (2017) Increased expression of protein kinase CK2 α correlates with poor patient prognosis in epithelial ovarian cancer. *PLoS ONE*. **12** (3), 1–18.

Malumbres, M. (2011) Physiological Relevance of Cell Cycle Kinases. *Physiological Reviews*. **91** (3), 973–1007.

Manning, D.L., McClelland, R.A., Knowlden, J.M., Bryant, S., et al. (1995) Differential Expression of Oestrogen Regulated Genes in Breast Cancer. *Acta Oncologica*. **34** (5), 641–646.

Maret, W. (2011) Metals on the move: zinc ions in cellular regulation and in the coordination dynamics of zinc proteins. *BioMetals*. **24** (3), 411–418.

Maret, W. & Vallee, B.L. (1998) Thiolate ligands in metallothionein confer redox activity on zinc clusters. *Proceedings of the National Academy of Sciences*. **95** (7), 3478–3482.

Margalioth, E.J., Schenker, J.G. & Chevion, M. (1983) Copper and zinc levels in normal and malignant tissues. *Cancer*. **52**, 868–872.

Maroto, B., Ye, M.B., Von Lohneysen, K., Schnelzer, A., et al. (2008) P21-activated kinase

is required for mitotic progression and regulates Plk1. *Oncogene*. **27** (36), 4900–4908.

Massarweh, S., Osborne, C.K., Jiang, S., Wakeling, A.E., et al. (2006) Mechanisms of tumor regression and resistance to estrogen deprivation and fulvestrant in a model of estrogen receptor-positive, HER-2/neu-positive breast cancer. *Cancer Research*. **66** (16), 8266–8273.

Matsushime, H., Quelle, E., Shurtleff, S.A., Shibuya, M., et al. (1994) D-Type Cyclin-dependent Kinase activity in mammalian cells. *Molecular and cellular biology*. **14** (3), 2066–2076.

Matsuura, W., Yamazaki, T., Yamaguchi-Iwai, Y., Masuda, S., et al. (2009) SLC39A9 (ZIP9) Regulates Zinc Homeostasis in the Secretory Pathway: Characterization of the ZIP Subfamily I Protein in Vertebrate Cells. *Bioscience, Biotechnology, and Biochemistry*. **73** (5), 1142–1148.

Mcclelland, R.A., Manning, D.L., Gee, J.M.W., Willsher, P., et al. (1998) Oestrogen-regulated genes in breast cancer : association of pLIVI with response to endocrine therapy. *British Journal of Cancer*. **77**, 1653–1656.

McClelland, R. a., Barrow, D., Madden, T.-A., Dutkowski, C.M., et al. (2001) Enhanced Epidermal Growth Factor Receptor Signaling in MCF7 Breast Cancer Cells after Long-Term Culture in the Presence of the Pure Antiestrogen ICI 182,780 (Faslodex). *Endocrinology*. **142** (7), 2776–2788.

McMahon, H.E.M., Mangé, A., Nishida, N., Créminon, C., et al. (2001) Cleavage of the Amino Terminus of the Prion Protein by Reactive Oxygen Species. *Journal of Biological Chemistry*. **276** (3), 2286–2291.

Meyerson, M. & Harlow, E. (1994) Identification of G1 Kinase Activity for cdk6, a Novel Cyclin D Partner. *Molecular and Cellular Biology*. **14** (3), 2077–2086.

Micchelli, C.A., Esler, W.P., Kimeberly, T.W., Jack, C., et al. (2002) γ-Secretase/presenilin inhibitors for Alzheimer's disease phenocopy Notch mutations in Drosophila. *The FASEB Journal*.

Miller, W.R. (2004) Aromatase Inhibitors: The Third Generation. In: James N. Ingle & Mitchell Dowsett (eds.). *Advances in Endocrine Therapy of Breast Cancer.* Summit Communications. pp. 17–32.

Miller, W.R. & Larionov, A. (2010) Changes in expression of oestrogen regulated and

proliferation genes with neoadjuvant treatment highlight heterogeneity of clinical resistance to the aromatase inhibitor, letrozole. *Breast Cancer Research*. **12** (R52), 1–9.

Miyai, T., Hojyo, S., Ikawa, T., Kawamura, M., et al. (2014) Zinc transporter SLC39A10/ZIP10 facilitates antiapoptotic signaling during early B-cell development. *Proceedings of the National Academy of Sciences*. **111** (32), 11780–11785.

Mocchegiani, E., Giacconi, R. & Malavolta, M. (2008) Zinc signalling and subcellular distribution: emerging targets in type 2 diabetes. *Trends in Molecular Medicine*. **14** (10), 419–428.

Morohashi, Y., Kan, T., Tominari, Y., Fuwa, H., et al. (2006) C-terminal fragment of presenilin is the molecular target of a dipeptidic γ-secretase-specific inhibitor DAPT (N-[N-(3,5-difluorophenacetyl)-L- alanyl]-S-phenylglycine t-butyl ester). *Journal of Biological Chemistry*. **281** (21), 14670–14676.

Mosselman, S., Polman, J. & Dijkema, R. (1996) ERβ: Identification and characterization of a novel human estrogen receptor. *FEBS Letters*. **392** (1), 49–53.

Motrich, R.D., Castro, G.M. & Caputto, B.L. (2013) Old Players with a Newly Defined Function: Fra-1 and c-Fos Support Growth of Human Malignant Breast Tumors by Activating Membrane Biogenesis at the Cytoplasm. *PLoS ONE*. **8** (1).

Mulay, I.L., Roy, R., Knox, B.E., Suhr, N.H., et al. (1971) Trace-metal analysis of cancerous and noncancerous human tissues. *Journal of the National Cancer Institute*. **47** (1), 1–13.

Myung, K. & Kolodner, R.D. (2002) Suppression of genome instability by redudant S-phase checkpoint pathways in Saccharomyces cerevisiae. *Proceedings of the National Academy of Sciences*. **99** (7), 4500–4507.

Nagase, H. & Woessner, J.F.J. (1998) Matrix metalloproteinases. *The Journal of Biological Chemistry*. **274** (31), 21491–21494.

Nasmyth, K. (2002) Segregating Sister Genomes : The Molecular Biology of Chromosome Separation. *Science*. **297**, 559–566.

Nathan, M.R. & Schmid, P. (2017) A Review of Fulvestrant in Breast Cancer. *Oncology and Therapy*. **5** (1), 17–29.

Newcomb, L.L., Diderich, J.A., Slattery, M.G. & Heideman, W. (2003) Glucose Regulation of Saccharomyces cerevisiae Cell Cycle Genes. *Eukaryotic Cell*. **2** (1), 143–149.

Nicholson, R.I., Hutcheson, I.R., Hiscox, S.E., Knowlden, J.M., et al. (2005) Growth factor signalling and resistance to selective oestrogen receptor modulators and pure anti-oestrogens: The use of anti-growth factor therapies to treat or delay endocrine resistance in breast cancer. *Endocrine-Related Cancer*. **12** (SUPPL. 1), 29–36.

Nicholson, R.I., Hutcheson, I.R., Jones, H.E., Hiscox, S.E., et al. (2007) Growth factor signalling in endocrine and anti-growth factor resistant breast cancer. *Reviews in Endocrine and Metabolic Disorders*. **8** (3), 241–253.

Nicholson, R.I., Mcclelland, R.A., Gee, J.M.W., Manning, D.L., et al. (1994) Transforming Growth Factor-α and Endocrine Sensitivity in Breast Cancer. *Cancer Research*. (54), 1684–1689.

Nigg, E.A. (2001) Mitotic kinases as regulators of cell division and its checkpoints. *Nature Reviews Molecular Cell Biology*. **2**, 21–32.

Nilsson, S., Ma, S., Treuter, E., Tujague, M., et al. (2001) Mechanisms of Estrogen Action. *Physiological Reviews*. **81** (4), 1535–1565.

Nimmanon, T. (2016) *Post − translational mechanisms of the ZIP family of zinc channels*. Cardiff University.

Nimmanon, T., Ziliotto, S., Morris, S., Flanagan, L., et al. (2017) Phosphorylation of zinc channel ZIP7 drives MAPK, PI3K and mTOR growth and proliferation signalling. *Metallomics*. **9** (5), 471–481.

Ninsontia, C., Phiboonchaiyanan, P.P. & Chanvorachote, P. (2016) Zinc induces epithelial to mesenchymal transition in human lung cancer H460 cells via superoxide anion-dependent mechanism. *Cancer Cell International*. **16** (1), 1–16.

Nishi, H., Hashimoto, K. & Panchenko, A.R. (2011) Phosphorylation in protein-protein binding: Effect on stability and function. *Structure*. **19** (12), 1807–1815.

Nodera, M., Yanagisawa, H. & Wada, O. (2001) Increased apoptosis in a variety of tissues of zinc-deficient rats. *Life Sciences*. **69** (14), 1639–1649.

O'Connor, M.J. (2015) Targeting the DNA Damage Response in Cancer. *Molecular Cell*. **60** (4), 547–560.

Ogiso, T., Ogawa, N. & Miura, T. (1978) Inhibitory effect of high dietary zinc on copper absorption in rats. *Chemical and Pharmaceutical Bulletin*. **27** (2), 515–521.

Ohana, E., Hoch, E., Keasar, C., Kambe, T., et al. (2009) Identification of the Zn2+ binding site and mode of operation of a mammalian Zn2+ transporter. *Journal of Biological*

Chemistry. **284** (26), 17677–17686.

Olsen, J. V., Blagoev, B., Gnad, F., Macek, B., et al. (2006) Global, In Vivo, and Site-Specific Phosphorylation Dynamics in Signaling Networks. *Cell*. **127** (3), 635–648.

Onder, T.T., Gupta, P.B., Mani, S.A., Yang, J., et al. (2008) Loss of E-cadherin promotes metastasis via multiple downstream transcriptional pathways. *Cancer Research*. **68** (10), 3645–3654.

Orth, J.D., Tang, Y., Shi, J., Loy, C.T., et al. (2008) Quantitative live imaging of cancer and normal cells treated with Kinesin-5 inhibitors indicates significant differences in phenotypic responses and cell fate. *Molecular Cancer Therapeutics*. **7** (11), 3480–3489.

Pagano, M., Pepperkok, R., Verde, F., Ansorge, W., et al. (1992) Cyclin A is required at two points in the human cell cycle. *The EMBO journal*. **11** (3), 961–971.

Pal, D., Sharma, U., Singh, S.K. & Prasad, R. (2014) Association between ZIP10 gene expression and tumor aggressiveness in renal cell carcinoma. *Gene*. **552** (1), 195–198.

Palmiter, R.D. & Findley, S.D. (1995) Cloning and functional characterization of a mammalian zinc transporter that confers resistance to zinc. *The EMBO journal*. **14** (4), 639–649.

Palmiter, R.D. & Huang, L. (2004) Efflux and compartmentalization of zinc by members of the SLC30 family of solute carriers. *Pflügers Archiv: European Journal of Physiology*. **447** (5), 744–751.

Pan, Z., Choi, S., Ouadid-Ahidouch, H., Yang, J.-M., et al. (2017) Zinc transporters and dysregulated channels in cancers. *Frontiers in Bioscience*. **1** (22), 623–643.

Pardee, A.B. (1974) A Restriction Point for Control of Normal Animal Cell Proliferation. *Proceedings of the National Academy of Sciences*. **71** (4), 1286–1290.

Parsons, S.J. & Parsons, J.T. (2004) Src family kinases, key regulators of signal transduction. *Oncogene*. **23** (48), 7906–7909.

Patel, A., Sabbineni, H., Clarke, A. & Somanath, P.R. (2016) Novel roles of Src in cancer cell epithelial-to-mesenchymal transition , vascular permeability , microinvasion and metastasis. *Life Sciences*. **157**, 52–61.

Paternia, I., Granchia, C., Katzenellenbogen, J.A. & Minutoloa, F. (2015) Estrogen Receptors Alpha (ERα) and Beta (ERβ): Subtype Selective Ligands and Clinical

Potential. *Steroids*. **0**, 13–29.

Paul, M.K. & Mukhopadhyay, A.K. (2004) Tyrosine kinase - Role and significance in Cancer. *International journal of medical sciences*. **1** (2), 101–115.

Perou, C.M., Sørlie, T., Eisen, M.B., van de Rijn, M., et al. (2000) Molecular portraits of human breast tumours. *Nature*. **406** (6797), 747–752.

Petrie, J., Buskin, L. & Chesters, J. (1996) Zinc and the initiation of myoblast differentiation. *The Journal of Nutritional Biochemistry*. **7** (12), 670–676.

Petrie, L., Chesters, J.K. & Franklin, M. (1991) Inhibition of myoblast differentiation by lack of zinc. *Biochemical Journal*. **276**, 109–111.

Petronczki, M., Lénárt, P. & Peters, J.M. (2008) Polo on the Rise-from Mitotic Entry to Cytokinesis with Plk1. *Developmental Cell*. **14** (5), 646–659.

Phuong, N.T.T., Lim, S.C., Kim, Y.M. & Kang, K.W. (2014) Aromatase induction in tamoxifen-resistant breast cancer: Role of phosphoinositide 3-kinase-dependent CREB activation. *Cancer Letters*. **351** (1), 91–99.

Pierre, F., Chua, P.C., Brien, S.E.O., Bourbon, P., et al. (2011) Pre-clinical characterization of CX-4945 , a potent and selective small molecule inhibitor of CK2 for the treatment of cancer. *Molecular Cell Biochemistry*. **356** (1–2), 37–43.

Pinna, L. a (2002) Protein kinase CK2: a challenge to canons. *Journal of cell science*. **115** (Pt 20), 3873–3878.

Plum, L.M., Rink, L. & Haase, H. (2010) The Essential Toxin: Impact of Zinc on Human Health. *International Journal of Environmental Research and Public Health*. **7** (4), 1342–1365.

Pocanschi, C.L., Ehsani, S., Mehrabian, M., Wille, H., et al. (2013) The ZIP5 Ectodomain Co-Localizes with PrP and May Acquire a PrP-Like Fold That Assembles into a Dimer. *PloS one*. **8** (9).

Podar, D., Scherer, J., Noordally, Z., Herzyk, P., et al. (2012) Metal selectivity determinants in a family of transition metal transporters. *Journal of Biological Chemistry*. **287** (5), 3185–3196.

Polyak, K., Kato, J.Y., Solomon, M.J., Sherr, C.J., et al. (1994) p27(Kip1), a cyclin-Cdk inhibitor, links transforming growth factor-β and contact inhibition to cell cycle arrest. *Genes and Development*. **8** (1), 9–22.

Ponka, P. & Lok, C.N. (1999) The transferrin receptor: Role in health and disease.

International Journal of Biochemistry and Cell Biology. **31** (10), 1111–1137.

Prasad, A. (1995) Zinc: an overview. *Nutrition*. **11** (1 Suppl), 93–99.

Prasad, A. (1998) Zinc in human health: an update. *J Trace Elements Exp Med*. **11**, 63–87.

Prasad, A., Halsted, J. & Nadimi, M. (1961) Syndrome of iron deficiency anemia, hepatosplenomegaly, hypogonadism, dwarfism and geophagia. *American Journal of Medicine*. **31**, 532–546.

Prasad, A., Miaie, A.J., Farid, Z., Schulert, A., et al. (1963) Zinc metabolism in patients with the syndrome of iron deficiency anemia, hepatosplenomegaly, dwarfism, and hypognadism. *Journal of Laboratory and clinical medicine*. **83**, 537–549.

Prasad, A.S. & Oberleas, D. (1974) Thymidine kinase activity and incorporation of thymidine into DNA in zinc-deficient tissue. *The Journal of Laboratory and Clinical Medicine*. **83** (4), 634–639.

Prusiner, S.B. (1991) Molecular Biology of Prion Diseases. *Science*. **252** (5012), 1515–1522.

Prusiner, S.B. (1998) Prions. *Proceedings of the National Academy of Sciences*. **95** (November), 13363–13383.

Puente, X.S., Sánchez, L.M., Overall, C.M. & López-Otín, C. (2003) Human and mouse proteases: A comparative genomic approach. *Nature Reviews Genetics*. **4** (7), 544–558.

Qin, Y., Dittmer, P.J., Park, J.G., Jansen, K.B., et al. (2011) Measuring steady-state and dynamic endoplasmic reticulum and Golgi Zn2+ with genetically encoded sensors. *Proceedings of the National Academy of Sciences*. **108** (18), 7351–7356.

Raulin, J. (1869) Etudes Chimique sur al vegetation (chemical studies on plants). In: *Annales des Sciences Naturelles Botanique et Biologie Vegetale*. pp. 293–299.

Razavi, P., Chang, M.T., Xu, G., Bandlamudi, C., et al. (2018) The Genomic Landscape of Endocrine-Resistant Advanced Breast Cancers. *Cancer Cell*. 427–438.

Rechsteiner, M. & Rogers, S.W. (1996) PEST sequences and regulation by proteolysis. *Trends in biochemical sciences.* **21** (7), 267–271.

Ribas, R., Pancholi, S., Guest, S.K., Marangoni, E., et al. (2015) AKT Antagonist AZD5363 Influences Estrogen Receptor Function in Endocrine-Resistant Breast Cancer and Synergizes with Fulvestrant (ICI182780) In Vivo. *Molecular Cancer Therapeutics*. **14**

(9), 2035–2048.

Rieder, C.L. & Maiato, H. (2004) Stuck in Division or Passing through: What Happens When Cells Cannot Satisfy the Spindle Assembly Checkpoint. *Developmental Cell*. **7**, 637–651.

Rink, L. & Gabriel, P. (2000) Zinc and the immune system. *Proceedings of the Nutrition Society*. **59**, 541–552.

Robertson, J.F.R., Lindemann, J., Garnett, S., Anderson, E., et al. (2014) A good drug made better: The fulvestrant dose-response story. *Clinical Breast Cancer*. **14** (6), 381–389.

Rogers, L.D. & Overall, C.M. (2013) Proteolytic Post-translational Modification of Proteins: Proteomic Tools and Methodology. *Molecular & Cellular Proteomics*. **12** (12), 3532–3542.

Rogers, S., Wells, R. & Rechsteiner, M. (1986) Amino acid sequences common to rapidly degraded proteins: The PEST hypothesis. *Science*. **234** (4774), 364–368.

Roshak, A.K., Capper, E.A., Imburgia, C., Fornwald, J., et al. (2000) The human polo-like kinase, PLK, regulates cdc2/cyclin B through phosphorylation and activation of the cdc25C phosphatase. *Cellular Signalling*. **12** (6), 405–411.

Rotherham, J., Price, F.M., Otani, T.T. & Evans, V.J. (1971) Some Aspects of the Role of Vitamin B12 and Folic Acid in DNA-Thymidine Synthesis in a Neoplastic C3H Mouse Cell Strain. *Journal of the National Cancer Institute*. **47**, 277–287.

Rudolf, E. (2008) Increased uptake of zinc in malignant cells is associated with enhanced activation of MAPK signaling and P53-dependent cell injury. *Acta Medica*. **51** (1), 43–49.

Rudolf, E. & Červinka, M. (2008) External zinc stimulates proliferation of tumor Hep-2 cells by active modulation of key signaling pathways. *Journal of Trace Elements in Medicine and Biology*. **22** (2), 149–161.

Rusin, S.F., Adamo, M.E. & Kettenbach, A.N. (2017) Identification of Candidate Casein Kinase 2 Substrates in Mitosis by Quantitative Phosphoproteomics. *Frontiers in Cell and Developmental Biology*. **5** (November), 1–16.

Ryu, M.-S., Lichten, L.A., Liuzzi, J.P. & Cousins, R.J. (2008) Zinc Transporters ZnT1 (Slc30a1), Zip8 (Slc39a8), and Zip10 (Slc39a10) in Mouse Red Blood Cells Are Differentially Regulated during Erythroid Development and by Dietary Zinc

Deficiency. *Journal of Nutrition*. **138** (11), 2076–2083.

Samet, J.M., Graves, L.M., Quay, J., Dailey, L.A., et al. (1998) Activation of MAPKs in human bronchial epithelial cells exposed to metals. *American Journal of Physiology Lung Cellular and Molecular Physiology*. **275** (3 Pt 1), L551-8.

Sassoon, I. & Blanc, V. (2013) Antibody–Drug Conjugate (ADC) Clinical Pipeline: A Review. In: *Methods in Molecular Biology*. pp. 1–27.

Schafer, W.-A. (1998) The cell cycle: A review. *Veterinary Pathology*. **35**, 461–478.

Schmitt-Ulms, G., Ehsani, S., Watts, J.C., Westaway, D., et al. (2009) Evolutionary descent of prion genes from the ZIP family of metal ion transporters. *PloS one*. **4** (9), e7208.

Schmucker, S. & Sumara, I. (2014) Molecular dynamics of PLK1 during mitosis. *Molecular and Cellular Oncology*. **1** (2), 1–9.

Scholzen, T. & Gerdes, J. (2000) The ki-67 Protein: From the Known and the Unknown. *Journal of Cellular Physiology*. **322**, 311–322.

Schwartz, M.K. & Schwartz, K. (1975) Role of Trace Elements in Cancer Role of Trace Elements in Cancer. *Cancer Research*. **35** (11 Part 2), 3481–3487.

Scott, B.J. & Bradwell, A.R. (1983) Identification of the Serum Binding Proteins for Iron, Zinc, Cadmium, Nickel, and Calcium. *Clinical Chemistry*. **29** (4), 629–633.

Seki, A., Coppinger, J.A., Jang, C.Y., Yates, J.R., et al. (2008) Bora and the kinase Aurora A cooperatively activate the kinase Plk1 and control mitotic entry. *Science*. **320** (5883), 1655–1658.

Sensi, S.L., Paoletti, P., Bush, A.I. & Sekler, I. (2009) Zinc in the physiology and pathology of the CNS. *Nature Reviews Neuroscience*. **10** (11), 780–791.

Sheaff, R.J., Groudine, M., Gordon, M., Roberts, J.M., et al. (1997) Cyclin E-CDK2 is a regulator of p27Kip1. *Genes & development*. **11** (11), 1464–1478.

Sherr, C.J. (1994) G1 Phase Progression: cycling on cue. *Cell*. **79** (18), 551–555.

Sherr, C.J. & Bartek, J. (2017) Cell Cycle–Targeted Cancer Therapies. *Annual Review of Cancer Biology*. **1** (1), 41–57.

Sherr, C.J., Beach, D. & Shapiro, G.I. (2016) Targeting CDK4 and CDK6: From discovery to therapy. *Cancer Discovery*. **6** (4), 353–367.

Sherr, C.J. & Roberts, J.M. (1999) CDK inhibitors: Positive and negative regulators of G1-phase progression. *Genes and Development*. **13** (12), 1501–1512.

Shi, X., Zhang, H., Paddon, H., Lee, G., et al. (2006) Phosphorylation of STAT3 serine-727

by cyclin-dependent kinase 1 is critical for nocodazole-induced mitotic arrest. *Biochemistry*. **45** (18), 5857–5867.

Shiloh, Y. (2003) ATM and related protein kinases: safeguarding genome integrity. *Nature Reviews Cancer*. **3**, 155–168.

Shinde, U. & Inouye, M. (2000) Intramolecular chaperones : polypeptide extensions that modulate protein folding. *Seminars in cell and developmental biology*. **11** (1), 35–44.

Shinde, U. & Inouye, M. (1993) Intramolecular chaperones and protein folding. *Trends in biochemical sciences*. **18** (11), 442–226.

Shumilina, E., Xuan, N.T., Schmid, E., Bhavsar, S.K., et al. (2010) Zinc induced apoptotic death of mouse dendritic cells. *Apoptosis*. **15** (10), 1177–1186.

Shusterman, E., Beharier, O., Shiri, L., Zarivach, R., et al. (2014) ZnT-1 extrudes zinc from mammalian cells functioning as a Zn2+/H+ exchanger. *Metallomics*. **6**, 1656–1663.

Siddiqui-Jain, A., Drygin, D., Streiner, N., Chua, P., et al. (2010) CX-4945, an orally bioavailable selective inhibitor of protein kinase CK2, inhibits prosurvival and angiogenic signaling and exhibits antitumor efficacy. *Cancer Research*. **70** (24), 10288–10298.

Sisken, J.E. & Morasca, L. (1965) Intrapopulation kineticks of the mitotic cycle. *The Journal of Cell Biology*. **25**, 179–189.

Sprengart, M.L., Wati, M.R. & Porter, A.G. (1998) Caspase-3 Is Required for DNA Fragmentation and Associated with Apoptosis. *The Journal of Biological Chemistry*. **273** (16), 9357–9360.

St-denis, N.A., Derksen, D.R. & Litchfield, D.W. (2009) Evidence for Regulation of Mitotic Progression through Temporal Phosphorylation and Dephosphorylation of CK2alpha. *Molecular and Cellular Biology*. **29** (8), 2068–2081.

St-denis, N., Gabriel, M., Turowec, J.P., Gloor, G.B., et al. (2014) Systematic investigation of hierarchical phosphorylation by protein kinase CK2. *Journal of Proteomics*. **118**, 49–62.

Stewart, A.J., Blindauer, C. a, Berezenko, S., Sleep, D., et al. (2003) Interdomain zinc site on human albumin. *Proceedings of the National Academy of Sciences*. **100** (7), 3701–3706.

Sun, L., Chai, Y., Hannigan, R., Bhogaraju, V.K., et al. (2007) Zinc regulates the ability of

Cdc25C to activate MPF/cdk1. *Journal of Cellular Physiology*. **213** (1), 98–104.

Sun, Y.S., Zhao, Z., Yang, Z.N., Xu, F., et al. (2017) Risk factors and preventions of breast cancer. *International Journal of Biological Sciences*. **13** (11), 1387–1397.

Sussman, D., Smith, L.M., Anderson, M.E., Duniho, S., et al. (2014) SGN-LIV1A: a novel antibody-drug conjugate targeting LIV-1 for the treatment of metastatic breast cancer. *Molecular cancer therapeutics*. **13** (12), 2991–3000.

Taiho, K. (2014) Introduction : 'Zinc Signaling'-The Blossoming Field of Zinc Biology. In: Fukada Toshiyuki & Kambe Taiho (eds.). *Zinc Signals in Cellular Functions and Disorders*. Tokyo, Springer Japan. pp. 1–6.

Takemoto, A., Kimura, K., Yanagisawa, J., Yokoyama, S., et al. (2006) Negative regulation of condensin I by CK2-mediated phosphorylation. *The EMBO journal*. **25** (22), 5339–5348.

Taniguchi, M., Fukunaka, A., Hagihara, M., Watanabe, K., et al. (2013) Essential Role of the Zinc Transporter ZIP9/SLC39A9 in Regulating the Activations of Akt and Erk in B-Cell Receptor Signaling Pathway in DT40 Cells. *PLoS ONE*. **8** (3), 1–10.

Taylor, K.M. (2008) A distinct role in breast cancer for two LIV-1 family zinc transporters. *Biochemical Society transactions*. **36**, 1247–1251.

Taylor, K.M. (2000) LIV-1 breast cancer protein belongs to new family of histidine-rich membrane proteins with potential to control intracellular Zn2+ homeostasis. *IUBMB life*. **49** (4), 249–253.

Taylor, K.M., Gee, J.M.W. & Kille, P. (2011) Zinc and Cancer. *Zinc in Human Health, Biomedical and Health Research, vol. 76.* 283–304.

Taylor, K.M., Hiscox, S. & Nicholson, R.I. (2004) Zinc transporter LIV-1: a link between cellular development and cancer progression. *Trends in Endocrinology and Metabolism*. **15** (10), 461–463.

Taylor, K.M., Hiscox, S., Nicholson, R.I., Hogstrand, C., et al. (2012) Protein Kinase CK2 Triggers Cytosolic Zinc Signaling Pathways by Phosphorylation of Zinc Channel ZIP7. *Science Signaling*. **5** (210), ra11.

Taylor, K.M., Morgan, H.E., Johnson, A., Hadley, L.J., et al. (2003) Structure-function analysis of LIV-1, the breast cancer-associated protein that belongs to a new subfamily of zinc transporters. *The Biochemical journal*. **375** (Pt 1), 51–59.

Taylor, K.M., Morgan, H.E., Johnson, A. & Nicholson, R.I. (2004) Structure-function

analysis of HKE4, a member of the new LIV-1 subfamily of zinc transporters. *The Biochemical journal*. **377** (Pt 1), 131–139.

Taylor, K.M., Morgan, H.E., Smart, K., Zahari, N.M., et al. (2007) The Emerging Role of the LIV-1 Subfamily of Zinc Transporters in Breast Cancer. *Molecular Medicine*. **13** (7–8), 396–406.

Taylor, K.M., Muraina, I., Brethour, D., Schmitt-ulms, G., et al. (2016) Zinc transporter ZIP10 forms a heteromer with ZIP6 which regulates embryonic development and cell migration. *Biochemical Journal*. **10**, 2531–2544.

Taylor, K.M. & Nicholson, R.I. (2003) The LZT proteins; The LIV-1 subfamily of zinc transporters. *Biochimica et Biophysica Acta - Biomembranes*. **1611**, 16–30.

Taylor, K.M., Vichova, P., Jordan, N., Hiscox, S., et al. (2008) ZIP7-mediated intracellular zinc transport contributes to aberrant growth factor signaling in antihormone-resistant breast cancer cells. *Endocrinology*. **149** (10), 4912–4920.

Terzi, M.Y., Izmirli, M. & Gogebakan, B. (2016) The cell fate: senescence or quiescence. *Molecular Biology Reports*. **43** (11), 1213–1220.

Theis-Febvre, N., Filhol, O., Froment, C., Cazales, M., et al. (2003) Protein kinase CK2 regulates CDC25B phosphatase activity. *Oncogene*. **22**, 220–232.

Thorsen, K., Mansilla, F., Schepeler, T., Øster, B., et al. (2011) Alternative splicing of SLC39A14 in colorectal cancer is regulated by the Wnt pathway. *Molecular & Cellular Proteomics*. **10** (1), M110.002998.

Tian, X., Liu, Z., Niu, B., Zhang, J., et al. (2011) E-Cadherin/β-catenin complex and the epithelial barrier. *Journal of Biomedicine and Biotechnology*. **2011**.

Todd, W., Elvehjem, C. & Hart, E. (1933) Zinc in the nutrition of the rat. *American Journal of Physiology*. **107**, 146–156.

Tray, N., Adams, S. & Esteva, F. (2018) Antibody-drug conjugates in triple negative breast cancer. *Future Oncology*. **14** (25), 2651–2661.

Trembley, J.H., Wang, G., Unger, G., Slaton, J., et al. (2009) CK2: A key player in cancer biology. *Cellular Molecular Life Sciences*. **66** (0), 1858–1867.

Trumbo, P., Yates, A.A., Schlicker, S. & Poos, M. (2001) Dietary reference intakes: vitamin A, vitamin K, arsenic, boron, chromium, copper, iodine, iron, manganese, molybdenum, nickel, silicon, vanadium, and zinc. *Journal of the American Dietetic Association*. **101** (3), 294–301.

Turk, B. (2006) Targeting proteases: Successes, failures and future prospects. *Nature Reviews Drug Discovery*. **5** (9), 785–799.

Ulukaya, E., Colakogullari, M. & Wood, E.J. (2004) Interference by anti-cancer chemotherapeutic agents in the MTT-tumor chemosensitivity assay. *Chemotherapy*. **50** (1), 43–50.

Unno, J., Satoh, K., Hirota, M., Kanno, A., et al. (2009) LIV-1 enhances the aggressive phenotype through the induction of epithelial to mesenchymal transition in human pancreatic carcinoma cells. *International Journal of Oncology*. **35**, 813–821.

Vallee, B.L. & Auld, D.S. (1990) Zinc coordination, function, and structure of zinc enzymes and other proteins. *Biochemistry*. **29** (24), 5647–5659.

Vallejos, C.S., Gómez, H.L., Cruz, W.R., Pinto, J.A., et al. (2010) Breast Cancer Classification According to Immunohistochemistry Markers: Subtypes and Association With Clinicopathologic Variables in a Peruvian Hospital Database. *Clinical Breast Cancer*. **10** (4), 294–300.

Vassilev, L.T. (2006) Cell cycle synchronization at the G2/M phase border by reversible inhibition of CDK1. *Cell Cycle*. **5** (22), 2555–2556.

Vassilev, L.T., Tovar, C., Chen, S., Knezevic, D., et al. (2006) Selective small-molecule inhibitor reveals critical mitotic functions of human CDK1. *Proceedings of the National Academy of Sciences*. **103** (28), 10660–10665.

Velic, D., Couturier, A.M., Ferreira, M.T., Rodrigue, A., et al. (2015) DNA damage signalling and repair inhibitors: The long-sought-after achilles' heel of cancer. *Biomolecules*. **5** (4), 3204–3259.

Ventura-Bixenshpaner, H., Asraf, H., Chakraborty, M., Elkabets, M., et al. (2018) Enhanced ZnR/GPR39 Activity in Breast Cancer, an Alternative Trigger of Signaling Leading to Cell Growth. *Scientific Reports*. **8** (1), 1–15.

Veronesi, U., Boyle, P., Goldhirsch, A., Orecchia, R., et al. (2005) Breast cancer. *The Lancet*. **365** (9472), 1727–1741.

Verstraeten, S. V, Zago, M.P., MacKenzie, G.G., Keen, C.L., et al. (2004) Influence of zinc deficiency on cell-membrane fluidity in Jurkat, 3T3 and IMR-32 cells. *Biochemical Journal*. **378** (Pt 2), 579–587.

Vidarsson, G., Dekkers, G. & Rispens, T. (2014) IgG subclasses and allotypes: From structure to effector functions. *Frontiers in Immunology*. **5** (OCT), 1–17.

Vincent, B., Paitel, E., Frobert, Y., Lehmann, S., et al. (2000) Phorbol Ester-regulated Cleavage of Normal Prion Protein in HEK293 Human Cells and Murine Neurons. *The Journal of Biological Chemistry*. **275** (45), 35612–35616.

Vincent, B., Paitel, E., Saftig, P., Frobert, Y., et al. (2001) The disintegrins ADAM10 and TACE contribute to the constitutive and phorbol-esters-regulated normal cleavage of the cellular prion protein. *Journal of Biological Chemistry*. **276** (41), 37743–37746.

Vincent, B., Sunyach, C., Orzechowski, H., George-hyslop, P.S., et al. (2009) p53-Dependent Transcriptional Control of Cellular Prion by Presenilins. *The Journal of Neurosience*. **29** (20), 6752–6760.

Vivanco, I. & Sawyers, C.L. (2002) The phosphatidylinositol 3-Kinase–AKT pathway in human cancer. *Nature Reviews Cancer*. **2** (7), 489–501.

Van Vuuren, R.J., Visagie, M.H., Theron, A.E. & Joubert, A.M. (2015) Antimitotic drugs in the treatment of cancer. *Cancer Chemotherapy and Pharmacology*. **76** (6), 1101–1112.

Wakefield, J.G., Stephens, D. & Tavaré, J.M. (2003) A role for glycogen synthase kinase-3 in mitotic spindle dynamics and chromosome alignment. *Journal of Cell Science*. **116** (4), 637–646.

Wall, M.E. & Wani, M.C. (1996) Camptothecin and taxol: Discovery to clinic. *Medicinal Research Reviews*. **51**, 239–254.

Wang, F., Kim, B., Petris, M.J. & Eide, D.J. (2004) The Mammalian Zip5 Protein Is a Zinc Transporter That Localizes to the Basolateral Surface of Polarized Cells. *The Journal of Biological Chemistry*. **279** (49), 51433–51441.

Wastney, M.E., Aamodt, R.L., Rumble, W.F. & Henkin, R.I. (1986) Kinetic analysis of zinc metabolism and its regulation in normal humans. *American Journal of Physiology*. **251** (2 Pt 2), R398-408.

Watanabe, K., Hasegawa, K., Ohtake, H., Tohyama, C., et al. (1993) Inhibition of DNA synthesis by EDTA and its cancellation by zinc in primary cultures of adult rat hepatocytes. *Biomedical Research*. **14** (2), 99–110.

Wätjen, W., Haase, H., Biagioli, M. & Beyersmann, D. (2002) Induction of apoptosis in mammalian cells by cadmium and zinc. *Environmental Health Perspectives*. **110** (SUPPL. 5), 865–867.

Weaver, B.P., Zhang, Y., Hiscox, S., Guo, G.L., et al. (2010) Zip4 (Slc39a4) expression is activated in hepatocellular carcinomas and functions to repress apoptosis, enhance cell cycle and increase migration. *PloS one*. **5** (10), e13158.

Weber, A.M. & Ryan, A.J. (2015) ATM and ATR as therapeutic targets in cancer. *Pharmacology and Therapeutics*. **149**, 124–138.

Weber, T.S., Jaehnert, I., Schichor, C., Or-Guil, M., et al. (2014) Quantifying the Length and Variance of the Eukaryotic Cell Cycle Phases by a Stochastic Model and Dual Nucleoside Pulse Labelling. *PLOS Computational Biology*. **10** (7), 1–17.

Wei, Y. & Fu, D. (2006) Binding and transport of metal ions at the dimer interface of the Escherichia coli metal transporter YiiP. *Journal of Biological Chemistry*. **281** (33), 23492–23502.

Wenzlau, J.M., Juhl, K., Yu, L., Moua, O., et al. (2007) The cation efflux transporter ZnT8 (Slc30A8) is a major autoantigen in human type 1 diabetes. *Proceedings of the National Academy of Sciences*. **104** (43), 17040–17045.

Whitfield, M.L., Sherlock, G., Saldanha, A.J., Murray, J.I., et al. (2002) Identification of Genes Periodically Expressed in the Human Cell Cycle and Their Expression in Tumors. *Molecular Biology of the Cell*. **13** (6), 1977–2000.

Whitfield, M.L., Zheng, L.-X., Baldwin, A., Ohta, T., et al. (2000) Stem-Loop Binding Protein, the Protein That Binds the 3′ End of Histone mRNA, Is Cell Cycle Regulated by Both Translational and Posttranslational Mechanisms. *Molecular and Cellular Biology*. **20** (12), 4188–4198.

Wiener, J.R., Kerns, B.J.M., Harvey, E.L., Conaway, M.R., et al. (1994) Overexpression of the protein tyrosine phosphatase PTP1B in human breast cancer: Assocation with p185c-erbB-2protein expression. *Journal of the National Cancer Institute*. **86** (5), 372–378.

Williams, C. & Lin, C.-Y. (2013) Oestrogen receptors in breast cancer: basic mechanisms and clinical implications. *Ecancermedicalscience*. **7**, 370.

Wong, S.H.K., Shih, R.S.M., Schoene, N.W. & Lei, K.Y. (2008) Zinc-induced G2/M blockage is p53 and p21 dependent in normal human bronchial epithelial cells. *American journal of physiology. Cell physiology*. **294** (6), C1342-9.

Woodruff, G., Bouwkamp, C.G., Vrij, F.M. De, Lovenberg, T., et al. (2018) The Zinc Transporter SLC39A7 (ZIP7) Is Essential for Regulation of Cytosolic Zinc Levels.

Molecular Pharmacology. **94** (3), 1092–1100.

Wu, W., Graves, L.M., Jaspers, I., Devlin, R.B., et al. (1999) Activation of the EGF receptor signaling pathway in human airway epithelial cells exposed to metals. *The American journal of physiology*. **277** (5 Pt 1), L924-31.

Yamanaka, Y., Matsugano, S., Yoshikawa, Y. & Orino, K. (2016) Binding Analysis of Human Immunoglobulin G as a Zinc-Binding Protein. *Antibodies*. **5** (2), 13.

Yamasaki, S., Sakata-Sogawa, K., Hasegawa, A., Suzuki, T., et al. (2007) Zinc is a novel intracellular second messenger. *The Journal of cell biology*. **177** (4), 637–645.

Yamashita, S., Miyagi, C., Fukada, T., Kagara, N., et al. (2004) Zinc transporter LIVI controls epithelial-mesenchymal transition in zebrafish gastrula organizer. *Nature*. **429** (6989), 298–302.

Yang, M., Kroft, S.H. & Chitambar, C.R. (2007) Gene expression analysis of gallium-resistant and gallium-sensitive lymphoma cells reveals a role for metal-responsive transcription factor-1, metallothionein-2A, and zinc transporter-1 in modulating the antineoplastic activity of gallium nitrate. *Molecular Cancer Therapeutics*. **6** (2), 633–643.

Yde, C.W., Olsen, B.B., Meek, D., Watanabe, N., et al. (2008) The regulatory beta-subunit of protein kinase CK2 regulates cell-cycle progression at the onset of mitosis. *Oncogene*. **27** (37), 4986–4997.

Zalewski, P. (2011) Zinc in Mammalian Cell Cycle and Cell Death. In: Lothar Rink (ed.). *Zinc in Human Health*. IOS Press. pp. 63–93.

Zanin, S., Borgo, C., Girardi, C., O'Brien, S.E., et al. (2012) Effects of the CK2 Inhibitors CX-4945 and CX-5011 on Drug-Resistant Cells. *PLoS ONE*. **7** (11).

Zhang, T., Sui, D. & Hu, J. (2016) Structural insights of ZIP4 extracellular domain critical for optimal zinc transport. *Nature Communications*. **7** (May), 11979.

Zhao, L., Chen, W., Taylor, K.M., Cai, B., et al. (2007) LIV-1 suppression inhibits HeLa cell invasion by targeting ERK1/2-Snail/Slug pathway. *Biochem. Biophys. Res. Commun.* **363** (1), 82–88.

Zile, M.H. (1998) Vitamin A and embryonic development: an overview. *The Journal of Nutrition*. **128** (2), 455–458.

Ziliotto, S., Ogle, O. & Taylor, K.M. (2018) Targetting Zinc Signalling to prevent cancer. In: *Metal Ions in Life Sciences*. pp. 507–529.

Zou, J., Luo, H., Zeng, Q., Dong, Z., et al. (2011) Protein kinase CK2α is overexpressed in colorectal cancer and modulates cell proliferation and invasion via regulating EMT-related genes. *Journal of Translational Medicine*. **9** (1), 97.

Appendices

Appendix 1: buffers

PBS buffer:

- K_2HPO_4 (di-potassium hydrogen orthophosphate anhydrous) 8 mM
- KH_2PO_4 (potassium dihydrogen orthophosphate) 2 mM
- NaCl (sodium chloride) 250 mM

Permeabilisation buffer in PBS:

- BSA (bovine serum albumin)
- Saponin 0.4%

Lysis buffer:

- Tris Base pH 7.5 50 mM
- EGTA (ethylene glycol tetra-acetic acid) 5 mM
- NaCl (sodium chloride) 150 mM
- Triton X-100 1%
- Na_3VO_4 (sodium orthovanadate) 2 mM
- NaF (sodium fluoride) 50 mM
- Protease cocktail inhibitors 1:10

Running buffer for SDS-PAGE pH 8.3 (10X)

- Tris base 25 mM
- Glycine 192 mM
- SDS 0.1%
- Distilled H_20
- HCl (hydrogen chloride) to adjust pH to 7.6

Tris-buffered saline with Tween 20 (TBS-Tween) pH 7.6 (10X)

- Tris base 100 mM
- NaCl (sodium chloride) 1mM
- Tween 20 0.5%

Transfer buffer:

- Tris Base 120 mM
- Glycine 40 mM
- Distilled H_20
- Methanol 20%

Laemmli sample buffer (loading buffer 4X):

- Tris-HCl ph 6.8 120 mM
- Glycerol 20%
- SDS 4%
- DTT 100 mM
- Bromophenol blue

Ponceau S:

- Ponceau S 0.1% (w/v)
- 5% acetic acid

EndoFree® Plasmid Maxi kit:

Buffer	**Composition**
Buffer P1 (resuspension buffer)	50 mM Tris-Cl pH 8.0, 10 mM EDTA, 100 μg/ml RNase A
Buffer P2 (lysis buffer)	200 mM NaOH, 1% SDS (w/v)
Buffer P3 (neutralisation buffer)	3.0 M potassium acetate pH 5.5
Buffer ER	Proprietary formulation
Buffer QBT (equilibration buffer)	750 mM NaCl, 50 mM MOPS pH 7.0, 15% isopropanol (v/v), 0.15% Triton® X-100 (v/v)
Buffer QC (wash buffer)	1.0 M NaCl, 50 mM MOPS pH 7.0, 15% isopropanol (v/v)
Buffer QN (elution buffer)	1.25 M NaCl, 50 mM MOPS pH 7.0, 15% isopropanol (v/v)
Buffer TE	10 mM Tris-Cl pH 8.0, 1 mM EDTA

Appendix 2: ethics document

Nottingham Research Ethics Committee 2

Study title: Development of a molecular genetic classification of breast cancer

REC reference: C202313

Protocol number: N/A

Amendment number: 2 - To include a further local study

Amendment date: 27 April 2009